EPFL

Thèse n° 8480

Capturing the heterogeneity of alpha-synuclein pathology in synucleinopathies

Présentée le 17 juin 2022

Faculté des sciences de la vie
Laboratoire de neurobiologie moléculaire et neuroprotéomique
Programme doctoral en neurosciences

pour l'obtention du grade de Docteur ès Sciences

par

Melek Firat ALTAY

Acceptée sur proposition du jury

Prof. M. D. C. Sandi Perez, présidente du jury
Prof. H. Lashuel, directeur de thèse
Prof. M. G. Spillantini, rapporteuse
Prof. E. Bezard, rapporteur
Dr B. Schneider, rapporteur

École polytechnique fédérale de Lausanne

2022

Abstract (English)

Synucleinopathies such as Parkinson's disease, dementia with Lewy bodies and multiple system atrophy (MSA) are detrimental neurodegenerative diseases. Alpha-synuclein (aSyn), the main aggregating protein found in the pathological inclusions of these ailments, exists in numerous modified forms and conformations, leading to neuropathological heterogeneity in synucleinopathies. The functional, pathological and clinical implications of this heterogeneity remain unclear. Responding this knowledge gap requires the development of novel toolsets capable of capturing the biochemical and structural diversity of aSyn pathology in the brain and peripheral tissues.

To address this challenge, we describe in Chapter 2 the development and characterisation of antibodies that cover all three regions and post-translational modifications (PTMs) of aSyn. We assess these antibodies through a comprehensive validation pipeline, and select the best performing antibody subset to capture the neuropathological diversity of aSyn across Lewy body diseases (LBDs). We demonstrate that these antibodies could be used to achieve an in-depth characterization of the biochemical and morphological diversity of aSyn aggregates in the neuronal and *in vivo* models of aSyn seeding. Our results suggest that aSyn pathology is rich in Serine 129 phosphorylation (pS129) and in previously under-described PTMs, including nitration and phosphorylation at Tyrosine 39 (nY39, pY39) and C-terminal tyrosine phosphorylations (pY133, pY136) across neuronal and glial populations in LBDs. We also report that aSyn is hyperphosphorylated in the cellular and *in vivo* seeding models.

In Chapter 3, we demonstrate the power of our antibodies to achieve an unprecedented analysis of astrocytic aSyn pathology in LBDs. We characterise the biochemical properties, post-translational modifications and the aggregation state of astrocytic aSyn accumulations in the limbic regions across sporadic and familial LBDs. The astrocytic aSyn is revealed distinctively by antibodies against the late amino-terminus (N-terminus) and non-amyloid-beta component (NAC) region of aSyn, but not by the extreme N-terminal or carboxy-terminal (C-terminal) antibodies, suggesting that these aSyn species are truncated at both ends. The astrocytic aSyn accumulations are

negative for the key markers of Lewy bodies (aSyn pS129, Amytracker, p62- and ubiquitin-positivity and proteinase K resistance), and positive for aSyn nY39 and pY39. These findings suggest that the astrocytic accumulations may be composed of non-fibrillar, possibly oligomeric conformers of aSyn.

Chapter 4 focuses on deciphering the biochemical and morphological signatures of aSyn pathology in MSA. The antibodies described in Chapter 2 are applied to high and low pathology regions of MSA brains by immunohistochemistry (IHC). We also biochemically profile the aSyn species, and report an abundance of aSyn pS129-positive glial and neuronal inclusions that correspond to insoluble high molecular weight species by Western blot. We detect an enrichment of insoluble and truncated aSyn in the MSA cerebellum. By IHC, there is an enhancement of aSyn nY39, pY136 and of other aSyn PTMs.

Collectively, the new tools and findings described here may pave the way for future studies elucidating the role of these neuronal and glial aSyn proteoforms in disease pathogenesis and propagation in synucleinopathies.

Keywords: aggregation, alpha-synuclein, antibody development, astrocyte, dementia with Lewy bodies, multiple system atrophy, Parkinson’s disease, Parkinson’s disease with dementia, post-translational modifications, synucleinopathy

Résumé (français)

Les synucléinopathies, telles que la maladie de Parkinson, la démence avec des corps de Lewy et l'atrophie multisystématisée (MSA), sont des maladies neurodégénératives nuisibles. L'*alpha*-synucléine (aSyn), qui est la protéine qui compose majoritairement les inclusions pathologiques formées dans ces maladies, existe en tant que mélange complexe de formes et conformations modifiées, ce qui entraîne une hétérogénéité dans la neuropathologie des synucléinopathies. Les conséquences fonctionnelles, pathologiques et cliniques de cette hétérogénéité ne sont toujours pas comprises, et combler ce manque de connaissance requiert le développement de nouveaux outils capables de représenter la diversité biochimique et structurelle de la pathologie des aSyn dans le cerveau et les tissus périphériques.

Nous décrivons dans le chapitre 2 comment, pour relever ce défi, nous avons développé et caractérisé des anticorps pour parvenir à entièrement cibler les trois régions et les modifications post-traductionnelle (PTMs) de l'aSyn. Nous évaluons ces anticorps par un processus de validation exhaustif et sélectionnons les anticorps les plus performants pour capturer la diversité neuropathologique d'aSyn que l'on trouve dans les maladies à corps de Lewy (LBDs). Nous démontrons que ces anticorps peuvent être utilisés pour effectuer une caractérisation approfondie de la diversité biochimique et morphologique des agrégats d'aSyn dans des modèles neuronaux et *in vivo* de « seeding » et propagation d'aSyn. Nos résultats suggèrent que la pathologie d'aSyn est riche en phosphorylation de la sérine 129 (pS129) et en PTMs jusque-là très peu décrits, tels que la nitration et la phosphorylation de la tyrosine 39 (nY39, pY39) et les phosphorylations des Tyrosines au C-terminus (pY133, pY136) dans toute la population neuronale et gliale des tissus de LBDs. Nous rapportons aussi que l'aSyn est dans un état hyperphosphorylé dans les modèles cellulaires et *in vivo* de « seeding » et propagation.

Dans le chapitre 3, nous démontrons la puissance de notre ensemble d'anticorps pour parvenir à une analyse inédite de la pathologie d'aSyn astrocytaire dans les LBDs. Nous caractérisons les propriétés biochimiques, les modifications ainsi que l'état d'agrégation des accumulations d'aSyn astrocytaire dans le système limbique des

formes familiales et sporadiques de LBDs. Ces aSyn astrocytaires sont distinctement détectés par des anticorps contre les régions de la terminaison amine (N-terminus) et le composant non-amyloïde (NAC) de l'aSyn, et non par des anticorps contre l'extrémité du N-terminus ou la terminaison carboxyle (C-terminus). Ceci suggère que ces espèces d'aSyn sont tronquées aux deux extrémités. L'accumulation d'aSyn astrocytaire est négative aux marqueurs des corps de Lewy (aSyn pS129, Amytracker, positif à la p62 et l'ubiquitine et résistance à la protéinase K), et positive pour l'aSyn nY39 et pY39. Dans l'ensemble, ces résultats suggèrent que l'accumulation dans les astrocytes pourrait être composé d'aSyn non-fibrillaire, et potentiellement oligomérique.

Le chapitre 4 se concentre sur le décryptage des signatures biochimiques et morphologiques de la pathologie d'aSyn dans la MSA. Les anticorps décrits dans le chapitre 2 sont appliqués par immunohistochimie (IHC) à des régions de pathologie élevées et faible de cerveaux de patients avec MSA. Nous établissons également le profil biochimique des espèce d'aSyn, et nous rapportons une abondance d'inclusions gliales et neuronales positives à l'aSyn pS129 qui correspondent à des espèces insolubles de poids moléculaire élevé par Western Blot. Nous détectons un enrichissement d'aSyn insolubles et tronqués dans le cerebellum de patients MSA. Par IHC, nous trouvons un enrichissement d'aSyn nY39, pY136 et d'autres PTMs d'aSyn.

Ensemble, ces nouveaux outils et résultats décrits içi ouvrent la voie à de futurs études permettant d'élucider le rôle des formes protéiques d'aSyn neuronales et gliales dans la pathogénèse de ces maladies et la propagation des synucléinopathies.

Mots-clés: agrégation, alpha-synucléine, développement d'anticorps, astrocyte, démences avec des corps de Lewy, atrophie multisystématisée, maladie de Parkinson, démence de la maladie de Parkinson, modifications post-traductionnelles, synucléinopathies

Abstract (italiano)

Le sinucleinopatie come il morbo di Parkinson (PD), la demenza del morbo di Parkinson (PDD), la demenza da corpi di Lewy (DLB) e l'atrofia multisistemica (MSA), sono malattie neurodegenerative. L'alfa-sinucleina (aSyn), la principale proteina aggregante che si trova nelle inclusioni patologiche formate in queste malattie, si presenta come un aggregato complesso di diverse forme e conformazioni modificate, determinando una eterogeneità nella neuropatologia delle sinucleinopatie. Le implicazioni funzionali, patologiche e cliniche di questa eterogeneità rimangono poco chiare e colmare questa lacuna richiede lo sviluppo di nuovi strumenti in grado di catturare la diversità biochimica e strutturale della patologia delle aSyn nel cervello e nei tessuti periferici.

Per affrontare questo problema, nel Capitolo 2 descriviamo lo sviluppo e la caratterizzazione di anticorpi, allo scopo di trattare estensivamente tutte e tre le regioni e le modificazioni post-traduzionali (PTM) dell'aSyn. Valutiamo poi questi anticorpi attraverso una pipeline di convalida completa e selezioniamo il sottoinsieme di anticorpi più idonei a catturare e caratterizzare la varietà neuropatologica di aSyn rivelata da questo set di strumenti attraverso le malattie da corpo di Lewy (LBD). Infine, dimostriamo che questi anticorpi potrebbero essere utilizzati per ottenere una caratterizzazione approfondita della diversità biochimica e morfologica degli aggregati aSyn nei modelli neuronali e *in vivo* di *seeding* e diffusione della aSyn. I nostri risultati suggeriscono che la patologia aSyn è ricca di fosforilazione della serina 129 (pS129) e di PTM finora sotto-descritti, tra cui nitrazione e fosforilazione della tirosina 39 (nY39, pY39) e fosforilazioni della tirosina C-terminale (pY133, pY136) nelle popolazioni neuronali e gliali nelle LBD. Segnaliamo inoltre che la aSyn si trova in uno stato iperfosforilato nei modelli di *seeding* e diffusione cellulari e *in vivo*.

Nel Capitolo 3, dimostriamo la capacità del nostro set di strumenti anticorpali di ottenere un'analisi senza precedenti della patologia astrocitica aSyn nelle LBD. Caratterizziamo le proprietà biochimiche, le modificazioni e lo stato di aggregazione degli accumuli di aSyn astrocitici nelle regioni limbiche nelle forme sporadiche e familiari di LBD. Queste aSyn astrocitiche sono rivelate in modo distintivo da anticorpi

contro le regioni dell'ammino-terminale (N-terminale) e della componente non-beta-amiloide (NAC) della aSyn, ma non dagli anticorpi contro l'estremo N-terminale o carbossi-terminale (C-terminale). Ciò suggerisce che queste specie di aSyn sono troncate a entrambe le estremità. Gli accumuli di aSyn astrocitici sono negativi per i marcatori chiave dei corpi di Lewy (aSyn pS129, Amytracker, p62 e ubiquitina-positività e resistenza alla proteinasi K) e positivi per l'aSyn nY39 e pY39. Complessivamente, questi risultati suggeriscono che gli accumuli di aSyn astrocitici possono essere composti da conformeri non fibrillari e potenzialmente oligomerici di aSyn.

Il capitolo 4 si concentra sulla decifrazione delle firme biochimiche e morfologiche della patologia aSyn nella MSA. Gli anticorpi descritti nel Capitolo 2 vengono applicati alle regioni di alta e bassa patologia dei cervelli MSA mediante tecnica immunoistochimica (IHC). Profiliamo anche biochimicamente le specie di aSyn e riportiamo un'abbondanza di inclusioni gliali e neuronali positive all'aSyn pS129 che corrispondono a specie insolubili ad alto peso molecolare mediante Western blot. Rileviamo un arricchimento di aSyn insolubili e troncate nel cervelletto dei pazienti MSA. La tecnica IHC rivela un aumento di aSyn nY39, pY136, e di altre PTM di aSyn.

Complessivamente, i nuovi strumenti e le scoperte descritte potrebbero aprire la strada a studi futuri che chiariscano il ruolo di queste proteoforme di aSyn neuronali e gliali nella patogenesi della malattia e nella propagazione nelle sinucleinopatie.

Parole chiave: aggregazione, alfa-sinucleina, sviluppo di anticorpi, astrociti, demenza da corpi di Lewy, atrofia multisistemica, morbo di Parkinson, morbo di Parkinson con demenza, modificazioni post-traduzionali, sinucleinopatia

Contents

Abstract (English) 1

Résumé (français) 3

Abstract (italiano) 5

Contents 7

List of figures 9

List of tables 10

Abbreviations 11

CHAPTER 1 Introduction 15

1.1 Physiological and pathological properties of alpha-synuclein 16

1.2 Synucleinopathies 22

CHAPTER 2 Generation, validation and characterisation of alpha-synuclein antibodies as a novel toolset 61

2.1 Introduction 61

2.2 Results 67

2.3 Discussion 101

2.4 Materials and methods 105

2.5 Contributions of the authors 111

CHAPTER 3 Astrocytic aSyn pathology in Lewy body diseases 113

3.1 Introduction 114

3.2 Results 117

3.3 Discussion 132

3.4 Materials and methods 137

3.5 Contributions of the authors 140

CHAPTER 4 Capturing the aSyn proteoforms in MSA 141

4.1 Introduction 141

4.2 Results 143

4.3 Discussion *149*

4.4 Materials and methods *151*

4.5 Contributions of the authors *153*

CHAPTER 5 Conclusion 155

5.1 Achieved results and future development *155*

Acknowledgments 159

References 161

Curriculum vitae 205

List of figures

Figure 1. 1 16
Figure 1. 2 21
Figure 1. 3 28
Figure 1. 4 37

Figure 2. 1 64
Figure 2. 2 70
Figure 2. 3 73
Figure 2. 4 73
Figure 2. 5 76
Figure 2. 6 78
Figure 2. 7 82
Figure 2. 8 83
Figure 2. 9 85
Figure 2. 10 86
Figure 2. 11 89
Figure 2. 12 90
Figure 2. 13 93
Figure 2. 14 95
Figure 2. 15 96
Figure 2. 16 100

Figure 3. 1 119
Figure 3. 2 120
Figure 3. 3 121
Figure 3. 4 123
Figure 3. 5 125
Figure 3. 6 126
Figure 3. 7 127
Figure 3. 8 129
Figure 3. 9 131
Figure 3. 10 132
Figure 3. 11 133

Figure 4. 1 144
Figure 4. 2 145
Figure 4. 3 147
Figure 4. 4 149

List of tables

Table 1. 1 53

Table 2. 1 68
Table 2. 2 68
Table 2. 3 68
Table 2. 4 74
Table 2. 5 77
Table 2. 6 87
Table 2. 7 102

Table 3. 1 115
Table 3. 2 118

Table 4. 1 151

Abbreviations

3-NT	3-nitrotyrosine
AC	autoclave
AD	Alzheimer's disease
AEP	asparagine endopeptidase
AGE	advanced glycation end-product
aSyn	alpha-synuclein
BCA	bicinchoninic acid assay
BSA	bovine serum albumin
bSyn	beta-synuclein
CA	cornu ammonis
c-Abl	ABL proto-oncogene 1 non-receptor tyrosine kinase
CBD	corticobasal degeneration
CNS	central nervous system
COMT	catechol O-methyltransferase
cryo-EM	cryogenic electron microscopy
CSF	cerebrospinal fluid
CSLM	confocal scanning laser microscopy
C-terminal/Cter	carboxy terminal
DA	dopamine
DAB	3,3'-diaminobenzidine
DAT-SPECT	dopamine transporter single-photon emission computed tomography
DB	dot blot
DBS	deep brain stimulation
DIV	day *in vitro*
DLB	dementia with Lewy bodies
DLBD	diffuse Lewy body disease
DNA	deoxyribonucleic acid
DPX	Dibutylphthalate Polystyrene Xylene
E. coli	*Escherichia coli*
EDC	1-ethyl-3-(3-dimethyl aminopropyl) carbodiimide
EDS	excessive daytime sleepiness
ELISA	enzyme-linked immunosorbent assay
EM	electron microscopy
ER	endoplasmic reticulum
FA	formic acid
FBS	foetal bovine serum
FFPE	formalin-fixed paraffin-embedded
FL	full-length
FPLC	fast protein liquid chromatography
FTLD-TDP/C	frontotemporal lobar degeneration of TAR DNA-binding protein 43 type C
GCI	glial cytoplasmic inclusion
GFAP	glial fibrillary acidic protein
GIT	gastrointestinal tract
GNI	glial nuclear inclusion
gSyn	gamma-synuclein
H&E	haematoxylin and eosin
HDAT	human dopamine transporter

HMW	high molecular weight
HPLC	high performance liquid chromatography
HRP	horseradish peroxidase
HS	high-salt
Iba1	ionised calcium binding adaptor protein 1
ICC	immunocytochemistry
IDA	industrial denatured alcohol
IF	immunofluorescence
IHC	immunohistochemistry
ILBD	incidental Lewy body disease
IPTG	isopropyl-β-D-1-thiogalactopyranoside
KAT	lysine acetyltransferase
KLH	keyhole limpet hemocyanin
KO	knockout
LB	Lewy body
LBD	Lewy body disease
LBvAD	Lewy body variant of AD
LC-MS	liquid chromatography-mass spectrometry
LC-MS/MS	liquid chromatography with tandem mass spectrometry
LMU	Ludwig-Maximilians-Universitaet
LN	Lewy neurite
LRRK2	leucine rich repeat kinase 2
MAM	mitochondria-associated endoplasmic reticulum membrane
MAO-B	monoamine oxidase B
MAP	microtubule-associated protein
MBP	myelin basic protein
MMP3	matrix metalloproteinase-3
MPTP	1-methyl-4-phenyl-1,2,5,6-tetrahydropyridine
MRI	magnetic resonance imaging
mRNA	messenger ribonucleic acid
MSA	multiple system atrophy
MSA-C	cerebellar type multiple system atrophy
MSA-P	parkinsonian-type multiple system atrophy
MSC	mesenchymal stem cell
Mw	molecular weight
NAC	non-amyloid-beta component
NAC-P	non-amyloid-beta component protein
NAT	N-acetyl transferase
NBIA1	neurodegeneration with brain iron accumulation type 1
NBM	NeuroBiobank Muenchen
NCI	neuronal cytoplasmic inclusion
NEDD8	neural precursor cell expressed developmentally downregulated gene 8
NF	neurofilament
NFTD	neurofibrillary tangle-predominant dementia
NHS	N-hydroxy succinimide
NNI	neuronal nuclear inclusion
NO	nitric oxide
N-terminal/Nter	amino terminal
OBB	Oxford Brain Bank
O-GlcNAc	*O*-linked N-acetylglucosamine
OPCA	olivopontocerebellar atrophy

PAF	pure autonomic failure
PB	pale body
PBS	phosphate-buffered saline
PBS-T	phosphate-buffered saline-Tween
PD	Parkinson's disease
PDD	Parkinson's disease with dementia
PFA	paraformaldehyde
PFF	pre-formed fibril
PI	protease inhibitor
PIAS2	protein inhibitor of activated signal transducer and activator of transcription 2
PiD	Pick's disease
PK	proteinase K
PLA	proximity ligation assay
PMCA	protein misfolding cyclic amplification
PMSF	phenylmethylsulfonyl fluoride
PNS	peripheral nervous system
PSP	progressive supranuclear palsy
PTM	post-translational modification
QSBB	Queen Square Brain Bank
RBD	rapid eye movement sleep behaviour disorder
REM	rapid eye movement
ROS	reactive oxygen species
RT	room temperature
RT-QuIC	real-time quaking induced conversion
SB	slot blot
SDS	sodium dodecyl sulphate
SDS-PAGE	sodium dodecyl sulphate polyacrylamide gel electrophoresis
SIAH	seven in absentia homologue
SNAP	soluble N-ethylmaleimide-sensitive factor attachment protein
SNARE	soluble N-ethylmaleimide-sensitive factor attachment protein receptor
SND	striatonigral degeneration
SPR	surface plasmon resonance
STED	stimulated emission depletion
SUMO-1	small ubiquitin-like modifier-1
TBS	Tris-buffered saline
TBST	Tris-buffered saline-Tween
TCS	transcranial sonography
TH	tyrosine hydroxylase
ThT	thioflavin T
TPPP/p25	tubulin polymerisation promoting protein p25-alpha
Tx	Triton X-100
UCL	University College London
UPLC	ultra-performance liquid chromatography
USP9X/FAM	ubiquitin-specific protease 9X
USSLB	unified staging system for Lewy body disorders
VAMP2	vesicle associated membrane protein 2
WB	Western blot
WT	wild-type

CHAPTER 1 Introduction

Although Parkinson's disease (PD) was first described by James Parkinson as the 'shaking palsy' in 1817 (Parkinson, 2002), Lewy bodies (LBs), the key pathological hallmarks of the disease, were not discovered before the work by Friedrich Lewy in 1912, by Lafora in 1913 and Tretiakoff in 1919 (Engelhardt, 2017; Engelhardt and Gomes, 2017; Holdorff et al., 2013; Lees et al., 2008). In the 1960s, the discovery of dopamine deficit in PD patients (Barbeau et al., 1961), and the amelioration of parkinsonian symptoms after levodopa delivery gave rise to new therapeutic prospects (Birkmayer and Hornykiewicz, 1998; Cotzias et al., 1969), but the cellular and molecular mechanisms of Lewy pathology formation and disease progression were still unknown. In the 1990s, the non-amyloid-beta component (NAC) peptide was traced to the amyloid inclusions in Alzheimer's disease (AD) (Masliah et al., 1996; Ueda et al., 1993; Yoshimoto et al., 1995), suggesting that the NAC protein (NAC-P, the name given to alpha-synuclein at the time) and tau and/or amyloid-beta interactions may play an important role in neurodegenerative diseases. The research on PD and other synucleinopathies gained momentum following the identification of 1) a link between early-onset familial PD and mutations in the synuclein alpha (*SNCA)* gene encoding alpha-synuclein (aSyn) (Golbe et al., 1990; Krueger et al., 1998; Polymeropoulos et al., 1997, 1996), and the subsequent identification of 2) aSyn as the predominant aggregated protein within LBs in PD and dementia with Lewy bodies (DLB) (Baba et al., 1998; Irizarry et al., 1998; Spillantini et al., 1998b), and glial cytoplasmic inclusions (GCIs) in multiple system atrophy (MSA) (Arai et al., 1999; Spillantini et al., 1998a). aSyn became the central piece of basic and clinical research and a window to understand the cellular mechanisms of synucleinopathies to develop suitable therapeutic strategies. In this introductory chapter, we first describe the structural and functional properties of aSyn under physiological conditions, followed by an overview of the main findings on the mechanisms of aSyn aggregation and the role of aSyn post-translational modifications (PTMs) in the polymorphisms of aSyn conformers. Next, we discuss the symptoms, causes and micropathology of synucleinopathies, focusing on the composition and organisation of aSyn inclusions, and the key findings from human post-mortem studies on their PTM signatures. Lastly, we summarise the tools available to study the cellular and molecular mechanisms underlying synucleinopathies,

discussing briefly their advantages and limitations. We close this chapter by providing an overview of the primary objectives of this thesis, which focus on addressing these limitations, and on developing and validating novel tools to enable a more precise understanding of the sequence determinants of aSyn aggregation, pathology formation and maturation in PD and other synucleinopathies.

1.1 Physiological and pathological properties of alpha-synuclein

1.1.1 Alpha-synuclein structure, localisation and function

Synucleins were first described in *Torpedo californica* (Maroteaux et al., 1988) and in rat brains (Maroteaux and Scheller, 1991) before being identified in human brains in the early 1990s (Jakes et al., 1994; Ueda et al., 1994, 1993). Mapped to the long arm of chromosome 4 (Spillantini et al., 1995), aSyn is a physiologically soluble and heat-resistant monomeric protein that does not possess a stable secondary structure *per se* (Fauvet et al., 2012b; George et al., 1995; Gould et al., 2014; Theillet et al., 2016). It is composed of 140 amino acid residues that form the three domains of the protein (Figure 1. 1). The amphipathic amino-terminal (N-terminal) region is responsible for lipid binding and aSyn interactions with membranes (Clayton and George, 1999). The NAC region is hydrophobic (Han et al., 1995) with a high propensity to aggregate. The negatively charged carboxy-terminal (C-terminal) region enriched in acidic residues regulates many of the aSyn interactions with metals and other proteins (Brown, 2009; Lautenschlaeger et al., 2018; Payton et al., 2001). Although aSyn remains unfolded in aqueous solution, the seven repeat sequences made of 11-residues spanning across the N-terminus and the NAC regions of the protein fold into alpha-helices upon interaction with lipids or membranes (Davidson et al., 1998; George et al., 1995).

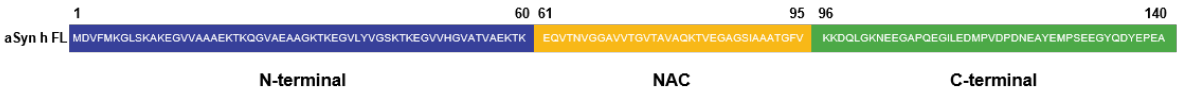

Figure 1. 1 The domains and amino acid sequence of alpha-synuclein. aSyn h FL = alpha-synuclein human full-length; C-terminal = carboxy-terminal; NAC = non-amyloid-beta component; N-terminal = amino-terminal

In the central nervous system (CNS), aSyn has been localised to the presynaptic terminals in the rodent brains and rat hippocampal culture (Hsu et al., 1998; Iwai et al.,

1995; Withers et al., 1997) as well as the neuronal somata and dendrites in rat brains (Andringa et al., 2003). Although predominantly in the neuronal soma in the developing human brains (Bayer et al., 1999), aSyn is increased in the synapses of adult human brains (Bayer et al., 1999). There is evidence that aSyn also localises to the nucleus (Schaser et al., 2019; Yu et al., 2007), the mitochondria (Cole et al., 2008; Devi et al., 2008; Li et al., 2007; Parihar et al., 2008; Robotta et al., 2014; Zhang et al., 2008; Zigoneanu et al., 2012) and the endoplasmic reticulum (ER) (Paillusson et al., 2017), particularly the mitochondria-associated ER membranes (MAMs) (Guardia-Laguarta et al., 2014), but the exact role and partners of aSyn in these cellular compartments is a topic of ongoing research.

Although not fully understood yet, a substantial portion of our knowledge on aSyn functions comes from studies run on aSyn knockout (KO) mice, where the ablation of the *SNCA* gene results in abnormalities in the lipid, dopamine (DA) and tyrosine hydroxylase (TH) metabolisms, as well as in mitochondrial functions: Absence of aSyn in mouse tissues and cell lines lead to dysregulated presynaptic DA recruitment and release (Abeliovich et al., 2000; Chadchankar et al., 2011; Chadchankar and Yavich, 2011; Yavich et al., 2004), alterations to the phospholipid composition and the electron transport chain functions of the mitochondria (Ellis et al., 2005), disruption to the astrocytic fatty acid uptake and trafficking (Castagnet et al., 2005), reduced palmitate uptake and arachidonic acid mass (Golovko et al., 2005, 2006a) but an increased mass of docosahexaenoic acid and neutral lipid (Barcelo-Coblijn et al., 2006; Golovko et al., 2006b). Triple KO mice for alpha-, beta- and gamma-synucleins show an overall shorter life span, neuronal dysfunction with age, synaptic protein content alterations, and a decline in the soluble N-ethylmaleimide-sensitive factor attachment protein (SNAP) receptor (SNARE) complex assembly (Burre et al., 2010; Greten-Harrison et al., 2010). aSyn has been proposed to chaperone the assembly of the SNARE complex by interacting with the SNARE protein vesicle associated membrane protein 2 (VAMP2) (Burre et al., 2010), thereby having an active part in repeated neurotransmitter release. In addition, *in vitro* studies have shown aSyn to have an inhibitory impact on TH i.e. the enzyme that converts tyrosine into levodopa (Perez et al., 2002), and that has a regulatory role on the human dopamine transporter (hDAT) activity of DA re-uptake from the synaptic cleft (Wersinger and Sidhu, 2003). It has also been associated with lipid rafts that in return mediate the synaptic localisation of aSyn

(Fortin et al., 2004) – a mechanism that is interrupted by mutations in aSyn such as the A30P point mutation. Furthermore, overexpression of aSyn in cultured mouse neurons leads to neurotransmitter release inhibition, dysregulated synaptic vesicle recycling, reduction in the synaptic vesicle recycling pool size and the synaptic vesicle density, and disruption of re-clustering of synaptic vesicles after endocytosis (Nemani et al., 2010). Put together, these reports suggest that aSyn has considerable roles in synaptic functions and dopamine metabolism in neurons.

1.1.2 aSyn expression and distribution

aSyn is expressed in the cerebral cortex, limbic region, midbrain, basal ganglia, cerebellum, olfactory region and the spinal cord in the CNS (Duda et al., 1999; Iwai et al., 1995; Uhlen et al., 2015), and in the Schwann cells of the peripheral nervous system (PNS) (Mori et al., 2002). It is also found enriched in the kidney, soft tissue, bone marrow, skin, blood and across the gastrointestinal tract (GIT) (Shin et al., 2000; Uhlen et al., 2015). On a cellular level, aSyn is abundantly expressed in the neurons of the CNS (Taguchi et al., 2016). Although some studies found aSyn to be expressed highly in oligodendrocytes during development (Djelloul et al., 2015; Richter-Landsberg et al., 2000), mature oligodendrocytes show a decreased level of aSyn. Likewise, it has been reported that astrocytes express aSyn (Castagnet et al., 2005) and beta-synuclein (bSyn) (Tanji et al., 2001), but how this expression varies depending on brain region and astrocyte subtype requires further investigation.

The synucleins are a family of vertebrate-specific proteins made of aSyn, bSyn and gamma-synuclein (gSyn). The gene that encodes for aSyn is *SNCA* (also referred to as *NACP* or *PARK1*) located on chromosome 4q21 (Chen et al., 1994; Spillantini et al., 1995). bSyn has 134 amino acid residues and has a molecular weight (Mw) of 14,288Da. It shows more than 60% overlap with that of aSyn, is highly expressed in the brain, and is located on chromosome 5q35 (Campion et al., 1995; Jakes et al., 1994; Spillantini et al., 1995). With 127 aa residues, gSyn is also a small protein with an Mw of 13,331Da, and is mapped to chromosome 10q23.2 (Ninkina et al., 1998).

The *SNCA* gene that encodes for aSyn has 6 exons (Spillantini et al., 1995; Touchman et al., 2001; Ueda et al., 1993). While aSyn-140 is the canonical form of aSyn with an

Mw of 14,460Da, the protein can be expressed as three other isoforms through alternative splicing: aSyn-126 with an Mw of 13,109Da; aSyn-112 with an Mw of 11,372Da and aSyn-98 with an Mw of 10,020Da (Beyer et al., 2008; Campion et al., 1995; McLean et al., 2012; Tagliafierro and Chiba-Falek, 2016; Ueda et al., 1994, 1993). The differential expression patterns or the functional roles of these isoforms in the brain and elsewhere are not well known. aSyn-140 and aSyn-112 are both expressed in the brain during development and adulthood, with aSyn-140 being the most predominantly expressed isoform across other bodily tissues but aSyn-112 and aSyn-98 remaining specific to brain regions (Beyer et al., 2008; Ueda et al., 1994). An increase in aSyn-112 and a decrease in aSyn-140 expression levels have been reported in DLB and AD cases (Beyer et al., 2004), and aSyn-126 expression is reported to decrease in DLB, AD and Lewy body variant of AD (LBvAD) prefrontal cortices (Beyer et al., 2006). Likewise, an increase in aSyn-98 has been reported in Lewy body disease (LBD), AD and MSA frontal cortices and PD cerebellum (Beyer et al., 2008, 2004; Cardo et al., 2014). These collectively suggest that expression patterns of the aSyn isoforms may be altered as part of, or as a response to, aSyn pathogenesis.

1.1.3 aSyn aggregation

A natively unfolded protein (Weinreb et al., 1996), aSyn is typically considered amyloidogenic i.e. under particular environmental conditions, it has a propensity to undergo conformational change, polymerise and form ordered fibrillar deposits of aSyn with a cross-beta sheet structure (Araki et al., 2019). These fibrils are made of beta-sheet stacks that run perpendicular to the fibrillar axis (Conway et al., 1998, 2000a, 2006; El-Agnaf et al., 1998; Roeters et al., 2017), and are characteristically stained with dyes including thioflavin or Congo red (Conway et al., 2000). Under certain conditions *in vitro*, including alterations in temperature, pH value, metal ions, organic solvents and salts (Munishkina et al., 2004, 2003; Uversky et al., 2002, 2001a, 2001b), the intermediate pre-molten globule state of aSyn is favoured over unfolded state. These monomeric intermediates have exposed hydrophobic surfaces, which interact with the hydrophobic surfaces of other monomeric intermediates, eventually forming oligomeric ‘nuclei’ for amyloidogenic aggregation (Ghosh et al., 2017). The soluble aSyn species are then recruited to these on-pathway species that are

thermodynamically more favourable, gradually leading to the formation of protofibrils, which eventually form stable amyloid fibrils (Cremades et al., 2012; Marvian et al., 2020; Uversky et al., 2001a). This fibrillisation process is influenced by several other factors, including protein concentration, mechanical agitation (Buell et al., 2014), lipid vesicles (Galvagnion et al., 2016), post-translational modifications, pH value and air-water interface (Campioni et al., 2014).

The aggregation process can take place via primary nucleation where aSyn aggregates from monomers spontaneously when there are no pre-existing fibrillar nuclei present (Fink, 2006). The process starts with a 'lag phase', during which the formation of aggregation-prone intermediates is assumed to take place. After the formation of these nuclei, the 'elongation phase' begins, where aSyn monomers rapidly self-assemble into amyloid fibrils. Finally comes the 'saturation phase', and this is when the fibrillar versus monomeric aSyn reach an equilibrium state. Next to primary nucleation, aSyn fibrils can be formed via secondary nucleation events (Buell et al., 2014; Gaspar et al., 2017; Ghosh et al., 2017), which involves the fragmentation of the pre-existing fibrils, thereby creating new surfaces for elongation by the recruitment of more monomeric aSyn species. Similarly, 'seeding' occurs with shortened lag phases when aSyn protofibrils or fibrils template the monomeric aggregation (Buell et al., 2014; Wood et al., 1999).

1.1.4 aSyn conformer heterogeneity

aSyn is a versatile protein that can take various conformations. Different aSyn oligomeric populations can exist side by side (Danzer et al., 2007), and aSyn oligomers can take annular, spherical or tubular shapes (Conway et al., 2000; Ding et al., 2002; Fredenburg et al., 2007; Lashuel et al., 2002). Several recent cryogenic electron microscopy (cryo-EM) studies have identified different polymorphs of aSyn wild-type (WT) (Guerrero-Ferreira et al., 2019, 2018; B. Li et al., 2018; Y. Li et al., 2018) (Figure 1. 2), as well as E46K (Boyer et al., 2020) and H50Q (Boyer et al., 2019) fibrils generated *in vitro*. Other studies on fibrils produced from recombinant monomers have reported polymorphs of aSyn fibrils with different proteinase K (PK) resistance patterns, electron microscopy morphologies and seeding capacity (Bousset et al., 2013; Landureau et al., 2021; Makky et al., 2016; Shrivastava et al., 2020).

Furthermore, different fibrillar end-products have been obtained via amplification methods (i.e. real-time quaking induced conversion (RT-QuIC) and protein misfolding cyclic amplification (PMCA)) from patient-derived brain and cerebrospinal fluid (CSF) materials (Burger et al., 2021; Candelise et al., 2019; Shahnawaz et al., 2020; Strohaeker et al., 2019; Tanudjojo et al., 2021; Van der Perren et al., 2020; Yoshinaga et al., 2020), bringing about the theory of aSyn 'strains' that may be responsible for the development of different types of synucleinopathies. It is important to note that the pre-formed fibrils (PFFs) generated *in vitro* by recombinant aSyn aggregation tend to differ from the PMCA or RT-QuIC fibrillar end-products (Strohaeker et al., 2019), and that these amplification methods may not always faithfully replicate the original seed structure (Lovestam et al., 2021). Likewise, the cryo-EM of MSA fibrils isolated directly from human brains shows an intricate structure composed of asymmetric protofibrils (Schweighauser et al., 2020), which are not replicated by *in vitro* preparations so far, collectively suggesting that the fibrillar compositions in human brain tissues may be more complex than what we can currently generate and model in cell-free conditions.

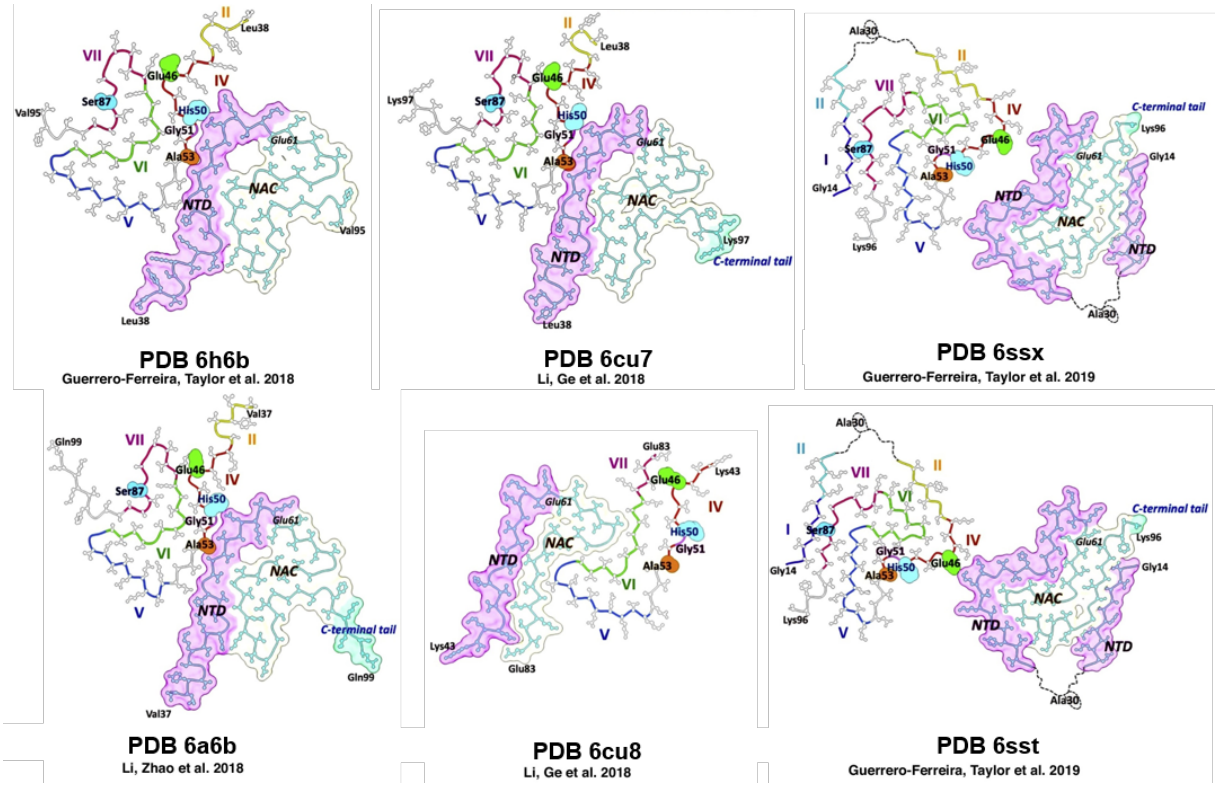

Figure 1. 2 The six polymorphs of aSyn human wild-type fibrils generated *in vitro* and resolved by cryo-EM. N-terminal region is shaded in pink, NAC region in white, and C-terminal in blue. Figure adapted from (Guerrero-Ferreira et al., 2020). NAC = non-amyloid-beta component; NTD = N-terminal domain

1.2 Synucleinopathies

Synucleinopathies are a subset of neurodegenerative diseases where aSyn is the main aggregating protein found in the pathological inclusions that serve as the hallmarks of these diseases (Arai et al., 1999; Baba et al., 1998; Dickson et al., 1999b; Irizarry et al., 1998; Spillantini et al., 1997, 1998a, 1998b). Synucleinopathies primarily include PD, DLB (Spillantini et al., 1998b, 1997) and MSA (Spillantini et al., 1998a). A subset of the synucleinopathies, namely PD, DLB, PD with dementia (PDD), incidental Lewy body disease (ILBD) and LBvAD, are referred to as LBDs due to the common LB pathology seen across them. Yet a small proportion of PD cases, such as those with certain PARK8/*LRRK2* (Gaig et al., 2007; Giasson et al., 2006) or *PARK2/Parkin* (Cornejo-Olivas et al., 2015; Hayashi et al., 2000) mutations, are found not to show any LB pathology. Although PDD, DLB, LBvAD, ILBD and pure autonomic failure (PAF) are also considered as part of the synucleinopathy family, we will be primarily focusing on PD as it is the most common type of LBD, and on MSA for simplicity and clarity.

1.2.1 Parkinson's disease

a) A brief introduction

First described by James Parkinson in 1817 as the 'shaking palsy' or *paralysis agitans* (Parkinson, 2002), PD is currently the second most frequent neurodegenerative disease worldwide after AD (Marti et al., 2003). PD shows a rising prevalence as a consequence of an increase in the ageing populations globally, combined with environmental influences, extended duration of the ailment, and the lack of a cure for the disease (Dorsey et al., 2018). This landscape generates considerable economic and social burdens (Kowal et al., 2013; Martinez-Martin et al., 2007; Whetten-Goldstein et al., 1997), urging for the development of effective treatment options in near future.

b) Aetiology of PD

PD is a complex disease with an aetiology involving both genetic and environmental factors. Less than 10% of the PD cases show a familial history of the disease, and to date, almost 30 chromosomal loci have been identified to have links with PD phenotype (Klein and Westenberger, 2012). Several studies have now shown that mutations in

the *SNCA* (also known as *PARK1* or *PARK4)* (Golbe et al., 1990; Polymeropoulos et al., 1997, 1996) and *LRRK2 (PARK8*) (Funayama et al., 2005; Paisan-Ruiz et al., 2005, 2004; Zimprich et al., 2004) genes result in autosomal-dominant monogenic PD; and mutations in *Parkin* (*PARK2)* (Foroud et al., 2003; Kann et al., 2002; Pramstaller et al., 2005)*, PINK1* (*PARK6*) (Hatano et al., 2004; Valente et al., 2004a, 2004b)*, DJ-1* (*PARK7*) (Bonifati et al., 2003a, 2003b) and *ATP13A2 (PARK9*) (Di Fonzo et al., 2007; Ramirez et al., 2006) genes are associated with autosomal-recessive PD. There are also a number of genetic risk factors, such as *GBA* mutations (Halperin et al., 2006; Kono et al., 2007; Tayebi et al., 2003; Varkonyi et al., 2003), which are identified to increase the chances of developing parkinsonian traits.

Out of these genes listed, *SNCA* is of particular interest as it encodes for aSyn protein (Jakes et al., 1994). The PD-linked mutations in this gene have been reported to result in the expression of aSyn with A30P (Krueger et al., 1998), E46K (Zarranz et al., 2004), H50Q (Appel-Cresswell et al., 2013; Proukakis et al., 2013), G51D (Lesage et al., 2013), A53T (Polymeropoulos et al., 1997), A53E (Pasanen et al., 2014) and most recently, T72M (Fevga et al., 2021) and E83Q (Kapasi et al., 2020) mutations. The cases that carry *SNCA* mutations tend to show an early onset of the disease, accompanied by an aggressive progression of symptoms (Golbe et al., 1990). There are also rare cases with familial PD due to *SNCA* duplication (Chartier-Harlin et al., 2004) or triplication (Singleton et al., 2003), with the more gene copies the individuals carry, the severer the symptoms and the earlier the disease onset.

LRRK2 gene mutations are also of interest as they represent the most frequent cases of familial parkinsonism (Schiesling et al., 2008). *LRRK2* encodes for the leucine rich repeat kinase 2 (LRRK2, also known as dardarin), a protein of 2527 residues and unknown function but with some role in neuritic maintenance and cytoskeletal re-organisation (Civiero et al., 2018; Haebig et al., 2013; MacLeod et al., 2006; Meixner et al., 2011). The common disease-causing mutations of this gene are R1441C (Zimprich et al., 2004), R1441G (Paisan-Ruiz et al., 2004; Vilas et al., 2019), G2019S (Bras et al., 2005; Gaig et al., 2006; Lesage et al., 2006; Ozelius et al., 2006) and I2020T (Funayama et al., 2002). LRRK2 and aSyn interactions have been reported (Guerreiro et al., 2013; Qing et al., 2009a, 2009b), and some studies showed LRRK2 localisation to LBs (Alegre-Abarrategui et al., 2008; Greggio et al., 2006; Guerreiro et

al., 2013; Qing et al., 2009b; Zhu et al., 2006a, 2006b), but this finding has been contested by others (Covy et al., 2006; Giasson et al., 2006; Rajput et al., 2006). Furthermore, the neuropathology of LRRK2 mutation cases are non-uniform, with several reports finding extensive neuronal loss in the substantia nigra but without any Lewy pathology (Agin-Liebes et al., 2020; Funayama et al., 2005; Gaig et al., 2007; Giasson et al., 2006; Henderson et al., 2019; Kalia et al., 2015; Marti-Masso et al., 2009; Takanashi et al., 2018; Vilas et al., 2019; Wszolek et al., 2004), whereas some other cases show LBs (Covy et al., 2009; Giasson et al., 2006; Henderson et al., 2019; Kalia et al., 2015; Mamais et al., 2018; Ross et al., 2006; Wszolek et al., 2004; Zimprich et al., 2004) and/or tau pathology (Covy et al., 2009; Giasson et al., 2006; Henderson et al., 2019; Rajput et al., 2006; Wszolek et al., 2004; Zimprich et al., 2004). It remains unclear if the type of LRRK2 mutation differentially influences the formation of Lewy pathology, and/or if the appropriate tools are yet to be used to reveal the previously undetected aSyn inclusions in the LB-negative LRRK2 cases.

The large majority i.e. 85-90% of the reported PD cases, on the other hand, are idiopathic with no family history of the disease (Gasser, 2007). Sporadic PD is believed to be triggered by a complex interaction of multiple environmental factors, ageing and potential genetic predispositions (Delamarre and Meissner, 2017). The role of environmental factors aligns well with the proposed peripheral aSyn aggregation initiation sites such as the olfactory and gastro-intestinal systems (Braak et al., 2002; Hawkes et al., 2009; Klingelhoefer and Reichmann, 2015), where exposure to external particles, contaminants and toxins is particularly high. Whilst ageing has been identified as the key risk factor for developing PD, the synergy of several other environmental aspects have been identified to increase the chances of developing parkinsonian traits, such as the use of the synthetic heroin 1-methyl-4-phenyl-1,2,5,6-tetrahydropyridine (MPTP) (Langston et al., 1983; Nonnekes et al., 2018), contact with agricultural pesticides and herbicides such as paraquat and rotenone (Hertzman et al., 1990; Liou et al., 1997; Tanner et al., 2011), exposure to metals such as manganese, copper, lead and mercury (Calne et al., 1994; Cook et al., 1974; Gorell et al., 2004; Pamphlett and Bishop, 2022; Willis et al., 2010), choices of lifestyle and diet (Gao et al., 2007), and experiences of head injuries (Doder et al., 1999; Nayernouri, 1985). In addition, rapid eye movement (REM) sleep behaviour disorder (RBD) is one pre-existing medical condition which has been found to show strong associations not only

with PD but also with DLB and MSA onset (Claassen et al., 2010; Iranzo et al., 2006; Schenck et al., 1996). Yet, the underlying reasons for the variability across RBD patients who do and do not develop PD and with differential intervals between RBD and PD onset, still requires further research. Likewise, larger studies to investigate the interaction between these genetic and environmental factors on a mechanistic level are essential to identify clear causal relationships between these and the pathogenesis of PD.

c) PD symptoms, diagnosis and treatment

Motor dysfunctions are the key clinical manifestations of PD, and the cardinal symptoms include resting and/or action tremor, slowness of movement (bradykinesia), instability in posture and rigidity (Gelb et al., 1999). However, the so-called non-motor symptoms of PD start showing years before the motor signs, and these may appear as olfactory deficits, gastrointestinal, sexual and urinary dysfunctions, mood disorders, cognitive deficits, fatigue and sleep disturbances (Gonera et al., 1997; Schapira et al., 2017; Shiba et al., 2000; Zis et al., 2015). These pre-motor symptoms tend not to be specific enough to allow for a differential diagnosis of PD, and by the time the patient starts showing cardinal manifestations of PD, almost half of the substantia nigra dopaminergic neurons are already lost (Fearnley and Lees, 1991). It is therefore crucial to pinpoint key biomarkers of the disease, and to develop sensitive tools that would allow for the early diagnosis of, and intervention to, the PD pathology.

Currently, no specific tests are available to diagnose PD conclusively. Instead, the diagnosis is carried out by a clinician based on the medical and family history of the patient combined with neurological and physical examination (Greffard et al., 2006; Hughes et al., 1992a). The diagnostic criteria for probable PD require the presence of at least two of the cardinal symptoms, bradykinesia, gait disturbance, resting tremor or rigidity (Larsen et al., 2009), which may then be supported by an optional dopamine transporter single-photon emission computed tomography (DAT-SPECT) and/or transcranial sonography (TCS) imaging (Alonso-Canovas et al., 2019; Mei et al., 2021; Suwijn et al., 2015; Tolosa et al., 2007). The clinical diagnosis is not a final one, and misdiagnosis may be revealed only after the neuropathological examination of the brain post-mortem (Hughes et al., 1992).

There is no permanent cure for PD, but several treatment options for the alleviation of symptoms are available. These involve pharmacological or surgical interventions and complementary therapies, such as speech therapy and physiotherapy. The gold standard of pharmacological intervention to lessen the motor symptoms since the 1960s is the levodopa administration (Rajput et al., 1990), although dopamine agonists (e.g. apomorphine, pramipexole, ropinirole, rotigotine, dihydroergocriptine) may be sought to enhance the levodopa treatment (Antonini et al., 2009; Latt et al., 2019). Other pharmacological treatment options include monoamine oxidase B (MAO-B) inhibitors (selegiline, rasagiline, safinamide) and catechol O-methyltransferase (COMT) inhibitors (entacapone, tolcapone), which are aimed at reducing the dopamine breakdown in the brain, and anticholinergics (benztropine, trihexyphenidyl), but these are less effective compared to levodopa, and come with several side effects (Connolly and Lang, 2014). Levodopa treatment likewise comes with its downsides: a) it requires continuous use for effectiveness; b) the patient may become less responsive over time; and c) there are side effects involved such as nausea, dizziness, sleep difficulties, hallucinations and dyskinesia. For advanced stage patients non-responsive to levodopa, the most promising surgical intervention to date is perhaps the deep brain stimulation (DBS) of the subthalamic nucleus by the implantation of electrodes (Benabid et al., 1987). However, this is an invasive option with added risks of infection and stroke, and may not be suitable for every PD patient. Furthermore, neither levodopa administration nor DBS can serve to slow down the disease progression and neurodegeneration. A better understanding of the cellular and molecular mechanisms of PD is necessary to develop more effective and long-lasting treatment options.

d) Micropathology of PD and other Lewy body diseases

One of the key hallmarks of PD and other LBDs on a cellular level is the presence of LBs (Gibb and Lees, 1988). These are round (5-25μm diameter), eosinophilic and highly organised inclusions that contain more than 200 components (Leverenz et al., 2008; Xia et al., 2008), the most predominant of all being aSyn (Mezey et al., 1998; Spillantini et al., 1997). First described by Friedrich Heinrich Lewy in 1912, these neuronal cytosolic inclusions were later associated with clinical parkinsonism (Greenfield and Bosanquet, 1953). The so-called ‘classical’ Lewy bodies refer to the

neuronal inclusions formed in the brainstem that characteristically have a circular appearance with a densely packed core and a looser halo (Lipkin, 1959; Sakamoto et al., 2002) and polychromatophilic properties (Greenfield and Bosanquet, 1953; Issidorides et al., 1990) (Figure 1. 3). As opposed to the orderly round shape of the brainstem LBs, the LBs formed in the cortical regions are less structured in morphology, and lack the 'halo' observed with the classical LB staining (Katsuse et al., 2003; Kosaka, 1978).

Next to the LBs detected in the cell bodies of neurons, the aSyn-positive Lewy neurites (LNs) and dots are observed in PD (Braak et al., 1999; Mori et al., 2008; Wakabayashi et al., 2013). aSyn accumulations in the oligodendrocytes (Arai et al., 1999; Hishikawa et al., 2001; Wakabayashi et al., 2000; Wakabayashi and Takahashi, 1996) and astrocytes (Braak et al., 2007b; Fathy et al., 2019; Hishikawa et al., 2001; Kovacs et al., 2014; Song et al., 2009; Sorrentino et al., 2019; Terada et al., 2003; Wakabayashi et al., 2000; Wakabayashi and Takahashi, 1996) have also been reported (for the full discussion on astrocytic aSyn in LBDs, see Chapter 3 on p.113). No data is available to date on aSyn accumulation in the microglia, but a link between aSyn pathogenesis and the activation of microglial cells as part of a neuroinflammatory response has been established in PD (Banati et al., 1998; McGeer et al., 1988; Mirza et al., 1999). The role aSyn aggregation plays in the astroglial-microglial interactions (Halliday and Stevens, 2011) and microglia-mediated neurodegeneration in PD is to be explored further.

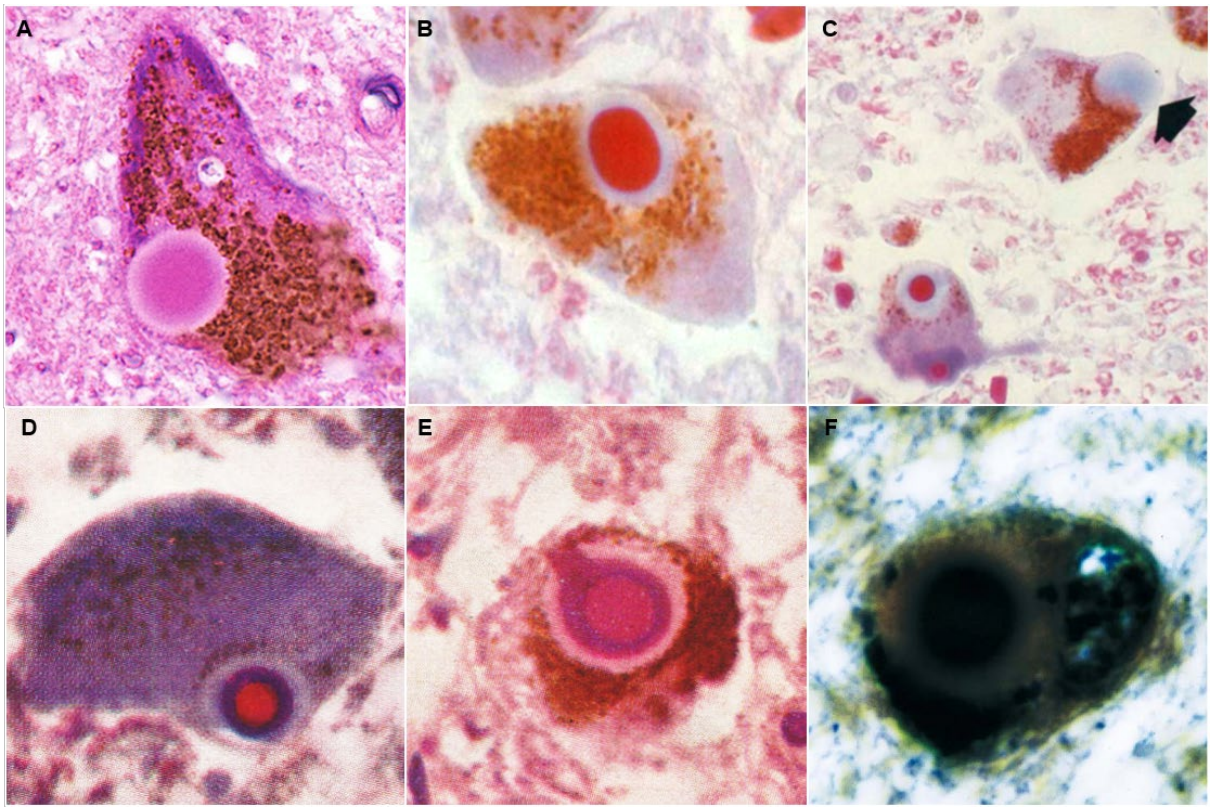

Figure 1. 3 Classical LBs revealed with different histological dyes, including (A) H&E, (B-C) Roque's chromotrope 2R-aniline blue, (D) Heidenhain's azan, (E) Lendrum's phloxine-tartrazine and (F) Bielschowsky staining. The arrow in C shows a LB without a central core. Image A adapted from (Kon et al., 2020); B-C from (Issidorides et al., 1990); D-E from (Greenfield and Bosanquet, 1953); and F from (Perkin, 1998). H&E = haematoxylin and eosin; LB = Lewy body

e) LB composition

An increasing number of immunohistochemistry (IHC), electron microscopy (EM) and proteomics-based studies are being run to show that LBs are composite structures made of multiple components (Wakabayashi et al., 2013). To date, there are only two papers that have looked at the contents of LBs via unbiased proteomics analyses (Leverenz et al., 2008; Xia et al., 2008), and there are already differences in the number and content of the components identified by each study. This may be due to the inclusion or exclusion of negative controls in the analysis as well as the different techniques followed in each study to isolate the LBs (i.e. laser capture microdissection versus sucrose density gradient enrichment), to analyse the components by mass spectrometry and to validate the hits. Regardless of these differences, the two studies converge on mapping out key categories for the components identified, and many of these have also been identified and localised to LBs by IHC (Wakabayashi et al.,

2007), which include structural and cytoskeletal proteins, aSyn-binding and synphilin-1-binding proteins, components involved in phosphorylation and signalling, cell cycle and apoptosis proteins, chaperones, cytosolic components, protein kinases, components of protein synthesis and degradation. Several EM-based studies have also demonstrated an accumulation of filaments, lipids and other vesicular structures, metal ions and several organelles including mitochondria, lysosomes and autophagosomes to be sequestered in the LBs (Adler et al., 2014; Duffy and Tennyson, 1965; Gai et al., 2000; Kosaka, 1978; Shahmoradian et al., 2019; Wakabayashi et al., 1998a; Watanabe et al., 1977). These findings altogether suggest that multiple cellular processes may be involved in the LB biogenesis and reveal the complexity of the LB composition.

f) LB formation, maturation, role and function

The mechanisms that trigger the LB formation, initiate the sequestration of all the organellar, fibrillar and vesicular components, and maintain LB maturation are still largely unknown. The large heterogeneity in the morphology and organisation of aSyn-positive inclusions (Kuusisto et al., 2003), has led the field to assume that these may correspond to different maturation stages, with pale bodies (PBs) being the key precursors to matured Lewy bodies (Hayashida et al., 1993). PBs are less eosinophilic, more irregular in structure and appear homogeneous in composition, but show considerable resemblance to LBs in terms of their components, which include dystrophic mitochondria, radiating filamentous structures and vacuoles (Gibb et al., 1991; Hayashida et al., 1993; Iranzo et al., 2014; Kuusisto et al., 2003; Takahashi et al., 1994). PBs and LBs show similar levels of abundance, and are often found to co-occur within the same neuron (Dale et al., 1992; Gibb et al., 1991). Despite such evidence, our understanding of a potential evolution of PBs into LBs is limited due to the unavailability of LB maturation models *in vitro* and *in vivo*.

Similarly, there is no consensus in the field on the role and function of LBs in relation to the advancement of LB diseases. On one hand, formation of LBs may result in the detriment of neuronal functions and contribute to neuronal apoptosis (Trojanowski et al., 1998). The LB load has also been shown to correlate with the severity of cognitive impairment (Hurtig et al., 2000; Mattila et al., 2000). On the other hand, LBs may be

formed to function as aggresomes in order to contain and discard the excess and toxic proteinaceous components within the neurons (Beyer et al., 2009; McNaught et al., 2002; Olanow et al., 2004). The conclusive understanding of the role of LBs in relation to neurodegeneration can only be obtained via faithful models that allow for temporal studies.

g) LB ultrastructure and organisation

EM studies of the last half century, combined with today's advanced imaging tools and super-resolution microscopy, have allowed for a deeper insight into the ultrastructural organisation of the LBs and the distribution of different aSyn species in LBs. Although Shahmoradian and colleagues recently proposed that many of the examined cortical LBs lacked aSyn fibrils (Shahmoradian et al., 2019), the vast majority of the preceding literature has converged on the understanding that aSyn accumulates within these LBs in fibrillar forms, and form a radiating pattern from the core of the inclusion outwards (Arima et al., 1998b; Baba et al., 1998; Spillantini et al., 1998b). By employing high-resolution confocal scanning laser microscopy (CSLM) and stimulated emission depletion (STED) microscopy, Moors and colleagues recently showed that LBs are organised in an onion-ring architecture, with full-length aSyn filaments and/or aSyn filaments phosphorylated at Serine 129 (aSyn pS129) arranged in the outer layers, and the C-terminally truncated aSyn fibrils captured along with lipids and organellar components within the core of the inclusions (Moors et al., 2021). This study 1) confirms the heterogeneity of aSyn fibrillar proteoforms co-existing within LBs, and 2) suggests that these different modified forms of aSyn fibrils may be arranged within the inclusions in a particular order.

h) LB distribution

To identify the affected brain regions in synucleinopathies, we rely on a) the aSyn-positive inclusion load, and on b) the regional neuronal loss. In terms of Lewy load within the CNS, the olfactory bulb, the spinal cord, the medulla (the dorsal vagal nucleus), pons (locus coeruleus), midbrain (substantia nigra pars compacta), basal forebrain, limbic regions (amygdala, hippocampus, hypothalamus) and the paralimbic cortex are all affected at late stages of PD (Braak et al., 2001, 1994, 2000, 2002, 2003b, 2007a; Dickson et al., 1994; Jellinger, 2003; Kingsbury et al., 2010; Kremer

and Bots, 1993; Tamura et al., 2012). Regarding the neuronal loss in PD brains, the deterioration of the dopaminergic neurons in the substantia nigra pars compacta is a key feature of PD (Damier et al., 1999; Fearnley and Lees, 1991). Degeneration is also observed in the neural populations of the dorsal vagal nucleus of the medulla, locus coeruleus and pedunculopontine nucleus of the pons, and the intralaminar thalamus in the forebrain (Gonzalez-Rodriguez et al., 2020).

Although some works have shown correlation between the LB load and severity of clinical symptoms across the PD patients (Hurtig et al., 2000; Mattila et al., 2000), there are other lines of evidence to suggest that the Lewy load does not fully correlate with the neuronal loss taking place in sporadic PD (Iacono et al., 2015). For instance, despite the high Lewy pathology in the lateral hypothalamus, neuronal cell death was found not to be predominant feature in this region in PD brains (Kremer and Bots, 1993). In some familial forms of PD particularly with various *LRRK2* mutations, furthermore, neurodegeneration in the substantia nigra seems to occur even in the absence of LBs (Agin-Liebes et al., 2020; Funayama et al., 2005; Gaig et al., 2007; Giasson et al., 2006; Henderson et al., 2019; Kalia et al., 2015; Marti-Masso et al., 2009; Takanashi et al., 2018; Vilas et al., 2019; Wszolek et al., 2004). Taken together, these observations suggest that LB load alone may not be sufficient to inform us on the affected brain regions and pathological progression routes.

1.2.2 Multiple system atrophy

a) A brief introduction

Multiple system atrophy has been described under several different titles for the large part of the 20th Century – it was first referred as *olivopontocerebellar atrophy* in 1900 by Dejerine and Thomas (Wenning et al., 1994), then as *postural hypotension* in 1925 by Bradbury and Eggleston (Bradbury and Eggleston, 1925), but also as *striopallidal-nigral degeneration* by van der Eecken in the same year (Wenning et al., 2004a), and later as *Shy-Drager syndrome* following the landmark publication by the authors in the same year (Shy and Drager, 1960). The term *multiple system atrophy* was finally coined in 1969 (Graham and Oppenheimer, 1969) to encompass a neuropathological condition that involved different combinations of cerebellar, parkinsonian and autonomic dysfunction symptoms. Only in 1989, the ubiquitin-positive GCIs or Papp-

Lantos inclusions (Papp et al., 1989) were identified as the common denominators of these collective of clinical conditions. Soon after the discovery of aSyn as the main protein component of LBs in PD and DLB (Spillantini et al., 1998b, 1997), aSyn was also mapped to MSA as the predominating constituent of GCIs and neuronal cytoplasmic inclusions (NCIs) (Dickson et al., 1999b; Spillantini et al., 1998a; Tu et al., 1998; Wakabayashi et al., 1998b). Despite such developments in deciphering the nature of this illness, MSA remains to be a comparatively less understood progressive synucleinopathy with debilitating and eventually fatal consequences for the patients.

b) Aetiology of MSA

Like PD, MSA is a neurodegenerative disease of unknown causes. There is sparse evidence on some environmental factors, such as exposure to metals and pesticides (Nee et al., 1991), as contributors to pathogenesis, but a causative link between environmental toxins and MSA has not been established clearly. Similarly, genetic contributors to disease onset are unclear. Although some reports point at genetic predispositions towards developing the disease (Federoff et al., 2016; Nirenberg et al., 2007; Soma et al., 2006), the familial cases of MSA are rare (Hara et al., 2007; Wullner et al., 2008), and no single mutation can be easily associated with the ailment. MSA is therefore still considered as sporadic.

c) Symptoms, diagnosis and treatment of MSA

MSA is a progressive disease that debilitates the patient over time. Based on the symptoms and affected brain regions, MSA is subdivided into two classifications i.e. parkinsonian-type MSA (MSA-P) and cerebellar-type MSA (MSA-C), with cases presenting a combination of symptoms from both referred to as mixed MSA (Gilman et al., 2008, 1999; May et al., 2007; Wenning et al., 1994). Regardless of classification, the key symptoms of MSA are orthostatic hypotension, urogenital dysfunction, postural instability, gait ataxia and parkinsonism (Gilman et al., 2008; Wenning et al., 1994). MSA-P, which corresponds to striatonigral degeneration (SND), is predominated by progressive signs of parkinsonism that are poorly responsive to levodopa treatment; whereas in MSA-C, sometimes called olivopontocerebellar atrophy (OPCA), cerebellar ataxia is a more prevalent characteristic (Gilman et al., 2008).

The overlapping features of PD, progressive supranuclear palsy (PSP) and MSA make differential clinical diagnosis a challenge (Kim et al., 2015; O'Sullivan et al., 2008; Schrag et al., 2008). However, compared to PD, MSA progresses more aggressively with a median survival time of 8-10 years (H.-J. Kim et al., 2011; Testa et al., 1996; Watanabe et al., 2002; Wenning et al., 1994, 2013), and poor response to dopaminergic replacement therapies combined with speech problems appearing early on as a symptom are key factors to point at probable MSA (Gilman et al., 1999; May et al., 2007; Wenning et al., 1994, 2004a). Magnetic resonance imaging (MRI) helps identify irregularities in the brainstem, striatum and the cerebellum, such as atrophy in the putamen and the pons, but is not fully sensitive to these alterations in all MSA patients (Schrag et al., 1998). A definite diagnosis of MSA necessitates post-mortem pathological examination of distribution and load of GCIs in the striatonigral, corticocerebellar and pyramidal systems (Papp and Lantos, 1994; Trojanowski and Revesz, 2007).

MSA is an aggressive disease for which no neuroprotective therapies are available (Bensimon et al., 2009; Holmberg et al., 2007). Although MSA-P patients initially respond to levodopa administration that may reduce parkinsonian symptoms, this response declines dramatically soon after the start of the treatment (Hughes et al., 1992b). Other therapeutic approaches to target genitourinary dysfunction (Beck et al., 1994) and sleep disordered breathing (Iranzo et al., 2000) are effective on alleviating the symptoms, but do not inhibit or slow down disease progression. Mesenchymal stem cell (MSC) therapy has shown promising clinical trial results (Dongmei et al., 2011; Lee et al., 2008, 2012), but would need to be examined and refined further in terms of safety administration before it can become a standard treatment approach for MSA.

d) Macropathology and micropathology of MSA

MSA subtypes show differential topographic distribution of aSyn pathology. In MSA-C, there is severe atrophy in the cerebellar white matter, the cerebellar peduncles and in the pontine base; whereas in MSA-P, there is degeneration in the putamen, caudate nucleus, substantia nigra and locus coeruleus regions (Ahmed et al., 2012). The aSyn pathology distribution in MSA mixed cases is similar to that seen both in MSA-C and MSA-P subtypes, i.e. the regions with the highest load of GCIs are the substantia nigra,

pons, locus coeruleus and the putamen. The Purkinje cells of the cerebellum, as well as the neuronal populations in the hypothalamus, caudal putamen, caudal nigra, medulla oblongata and the motor cortex are also impaired (Lantos, 1998).

In terms of the cell types affected, MSA shows striking differences to LBDs, in the sense that the large majority of the aSyn pathology is seen in the oligodendroglial cytoplasm, referred to as GCIs (formerly as Papp-Lantos inclusions). aSyn inclusions are also observed in the neuronal somata, but due to their morphological and compositional differences to LBs, these neuronal inclusions are referred to as NCIs. In addition, nuclear inclusions are observed both in the neurons and in oligodendrocytes, which are referred to as neuronal nuclear inclusions (NNIs) (Nishie et al., 2004; Wakabayashi et al., 2005) and glial nuclear inclusions (GNIs) (Wakabayashi et al., 1998a), respectively. Next to these inclusions, gliosis, neuroinflammation and neuronal loss are other microscopically observed phenomena.

The GCIs are the most frequent type of inclusions observed in MSA, and are therefore taken as the hallmark of the disease. The ultrastructural and immunohistochemical analysis of these inclusions suggest that GCIs are Gallyas silver staining-positive structures composed of aSyn filaments (Braak et al., 1999; Spillantini et al., 1998a) along with several other components, such as p62, 14-3-3, microtubule-associated proteins (MAPs), tubulin polymerisation promoting protein p25-alpha (TPPP/p25) and various other cytoskeletal proteins (Jellinger and Lantos, 2010). Several studies have found that the GCI load does not directly correspond to neuronal loss, and therefore may not be a prerequisite for the neurodegeneration observed in MSA (Papp and Lantos, 1994).

It is not yet clear why there is such a uniquely predominant oligodendroglial aSyn inclusion load in MSA pathology, as the data on aSyn expression in these cell types has been controversial. Compared to healthy controls, the overall aSyn protein levels are found to be increased in crude homogenates from pons as well as frontal and cerebellar white matters in MSA (Campbell et al., 2001). Whilst Miller and colleagues showed aSyn messenger ribonucleic acid (mRNA) expression to be lacking in the oligodendrocytes from healthy control and MSA brains (Miller et al., 2005), Asi and colleagues showed a trend for increased oligodendroglial and decreased neuronal

aSyn mRNA expression in MSA brains compared to controls (Asi et al., 2014). Further research into basal and pathological aSyn expression levels of oligodendrocytes may therefore help elucidate mechanisms involved in oligodendroglial aSyn accumulation in MSA.

e) Organisation, ultrastructure and composition of aSyn inclusions in MSA

The NCIs have been shown to be strongly argyrophilic, globular entities (Kato and Nakamura, 1990), which contain a mixture of organelles, vesicles and fibrillar structures. These fibrillar components appear to be granule-coated, arranged in bundles, randomly distributed or organised in parallel (Kato and Nakamura, 1990; Takeda et al., 1997). With granule coating, the fibrils appear to be 25-40nm wide (Takeda et al., 1997), whereas a smaller subset of non-coated fibrils appear to be 10nm wide (Kato and Nakamura, 1990). The GCIs are also largely fibrillar (30-50nm), with electron-dense granular and amorphous components (Abe et al., 1992; Gai et al., 1999; Pountney et al., 2004; Tu et al., 1998).

The NCIs are positive for ubiquitin (Arima et al., 1998; Papp and Lantos, 1992) and for 14-3-3 proteins (Kawamoto et al., 2002; Wakabayashi et al., 2005), but are found to be negative for neurofilaments, tau, alpha and beta tubulin, MAPs and actin (Dickson et al., 1999b; Kato and Nakamura, 1990; Takeda et al., 1997). The aSyn-positive GCIs isolated from MSA white matter via density gradient enrichment, on the other hand, are found positive not only for ubiquitin (Arima et al., 1998; Tamaoka et al., 1995), but also for 14-3-3 proteins (Giasson et al., 2003; Kawamoto et al., 2002; Wakabayashi et al., 2005), alpha- and beta-tubulin, alpha-crystallin B (Gai et al., 1999; Murayama et al., 1992; Pountney et al., 2005b; Tamaoka et al., 1995; Uryu et al., 2006), tau (Giasson et al., 2003), transferrin, MAP5 (Abe et al., 1992), heat shock proteins (Kawamoto et al., 2007; Uryu et al., 2006), neural precursor cell expressed developmentally downregulated gene 8 (NEDD8) (Mori et al., 2005) and also p62 (Kuusisto et al., 2001). More than 80% of both NCIs and GCIs in the pons show strong positivity for cytochrome c, Apaf-1 and activated caspase 9, suggesting a role for mitochondria-dependant apoptotic cell death in MSA (Kawamoto et al., 2016). Collectively, these findings suggest that the glial and neuronal inclusions found in MSA brains are composed of a multitude of components, which may be involved re-organisation and

maturation of these inclusions. On the other hand, we still do not fully understand the exact nature of the aSyn species present in these different types of inclusions. The mechanisms and key determinants of aSyn aggregation that may take part in sequestering these components to the pathological inclusions are also not well known.

1.2.3 aSyn modifications in synucleinopathies

PTMs refer to a number of reversible or irreversible chemical alterations that specific amino acid residues of a protein may undertake after its translation (Witze et al., 2007). Several different PTMs can take place simultaneously, crosstalk and play key roles in the properties and the functioning of the proteins in cellular processes, including signalling, localisation and protein degradation. Certain aSyn PTMs, such as phosphorylation at S129, ubiquitination and C-terminal truncations, have been considered to be markers of pathology formation in synucleinopathies. Growing evidence from cell-free, cellular and *in vivo* studies and also directly from human post-mortem studies point at aSyn PTMs to be not only markers but also key regulators of aSyn seeding and aggregation, inclusion formation and maturation in synucleinopathies. Here, we present the main findings primarily on human brain tissue-based studies on aSyn PTMs (Figure 1. 4) along with the current limitations and knowledge gaps to our understanding of the role of these modifications in relation to aSyn pathogenesis.

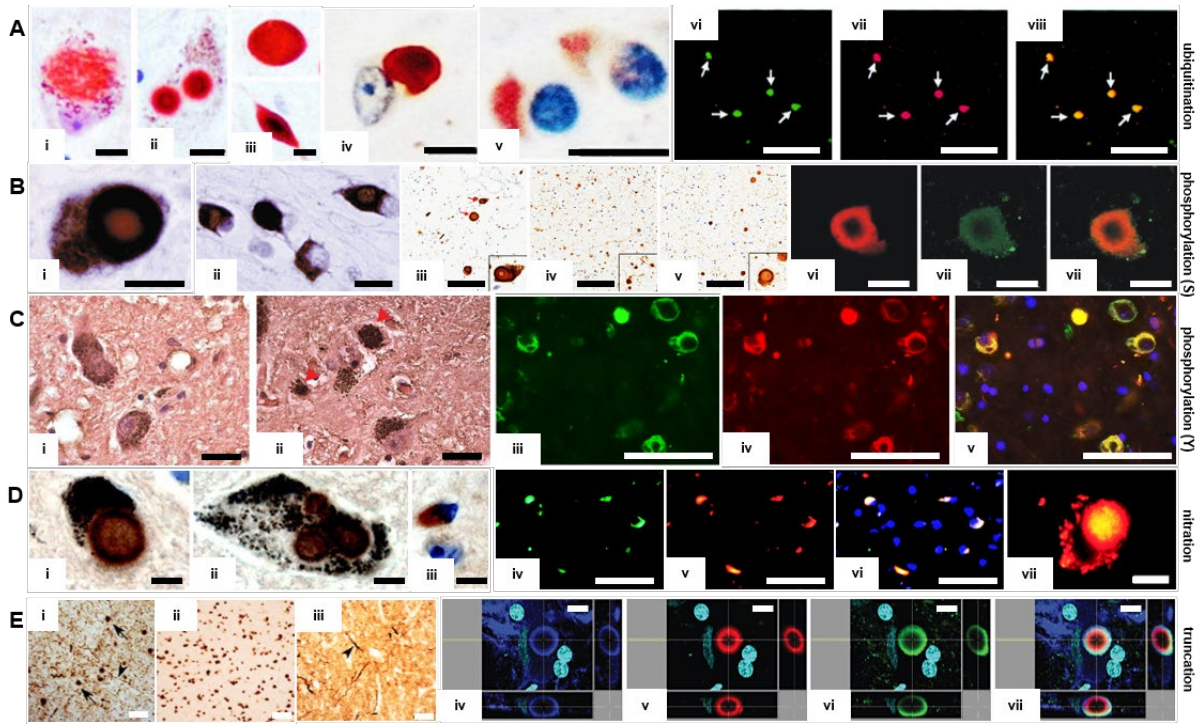

Figure 1. 4 **(A)** Ubiquitination detected in the (Ai) nigral PBs, (Aii) LBs and in the (Aiii) extrasomal inclusions of a PD case. Inclusions in the (Aiv) cingulate cortex of a DLB case, and in the striatum of an (Av) an MSA case, positive for ubiquitin. (Avi-viii) Double immunofluorescent labelling of the cingulate cortex of a DLB case shows co-localisation of total aSyn (green) and ubiquitin (red) in the cortical LBs. Scale bars 10μm (Ai-v) and 100μm (Avi-viii). Images Ai-iii adapted from (Kuusisto et al., 2003); images Aiv-v from (Kuusisto et al., 2001); and images Avi-viii from (Sampathu et al., 2003). **(B)** (Bi) Brainstem LBs of PD substantia nigra, and (Bii) GCIs of MSA pontine base stain positive for aSyn pS129. aSyn pS129 positivity in the (Biii) substantia nigra, (Biv) amygdala and (Bv) cingulate cortex of a DLB case. Total aSyn (red; Bvi) and aSyn pS87 (green; Bvii) show co-localisation in the (Bviii) cortical LB of a DLB brain. Scale bars 10μm (Bi-ii); 100μm (Biii-v) and 10μm (Bvi-viii). Images Bi-ii adapted from (Fujiwara et al., 2002); images Biii-v from (Sorrentino et al., 2019); and images Bvi-viii from (Paleologou et al., 2010). **(C)** IHC for aSyn pY39 in the (Ci) control versus (Cii) PD substantia nigra. The hippocampal CA2 region from an *SNCA* G51D case probed with total aSyn (green; Ciii) and aSyn pY125 (red; Civ) largely co-localise (DAPI in blue; Cv). Scale bar = 25μm (Ci-v). Images Ci-ii adapted from (Brahmachari et al., 2016); and images Ciii-v from (Kiely et al., 2013). **(D)** Nitration detected in the nigral LBs of (Di) DLB and (Dii) LBvAD, and in (Diii) the GCIs of MSA. Immunofluorescent double-labelling of GCIs in an MSA case with nitrated (green; Div) and total (red; Dv) aSyn antibodies show extensive co-localisation (blue= DAPI; Dvi). (Dvii) A cortical LB positive both for total and nitrated aSyn. Scale bars 10μm (Di-iii, Dvii) and 50μm (Div-vi). Images Di-vii adapted from (Giasson et al., 2000a). **(E)** The midfrontal cortices of (Ei) DLB, (Eii) MSA and (Eiii) *SNCA* A53T are positive for an antibody (EL101) specific to truncated aSyn at residue D119. Arrows show LBs and arrowheads the LNs. Immunofluorescent labelling of LBs from PD substantia nigra show positivity for TH (blue; Eiv), for C-terminally truncated aSyn (red; Ev) detected using a truncation-specific aSyn antibody, and for full-length aSyn (green; Evi), altogether displaying different compositional layers (DAPI in turquoise; Evii). Scale bars 100μm (Ei-iii) and 10μm (Eiv-vii). Images Ei-iii adapted from (Anderson et al., 2006); and images Eiv-vii from (Prasad et al., 2012). aSyn = alpha-synuclein; CA2 = cornu ammonis 2 region; DLB = dementia with Lewy bodies; GCI = glial cytoplasmic inclusion; IHC = immunohistochemistry; LB = Lewy body; LBvAD= Lewy body variant of Alzheimer's disease; LN= Lewy neurite; MSA= multiple system atrophy; PB= pale body; PD= Parkinson's disease; TH = tyrosine hydroxylase

a) aSyn ubiquitination

Prior to the description of aSyn as the predominant aggregating protein within LBs (Spillantini et al., 1998a, 1997), several histological approaches were used to interrogate the composition and ultrastructure of LBs and other pathological inclusions linked to neurodegenerative diseases (Greenfield and Bosanquet, 1953). Ubiquitin was identified as a common component of pathological aggregates in AD (Mori et al., 1987; Perry et al., 1987) and several other neurodegenerative diseases, including Pick's disease (PiD) and PSP (Manetto et al., 1988). This led to the discovery of ubiquitin in LBs and its use as a marker of LBs (Dickson et al., 1994, 1989), GCIs (Abe et al., 1992; Kato et al., 1991; Kobayashi et al., 1992; Matsuo et al., 1998; Murayama et al., 1992) and neuronal cytoplasmic inclusions (NCIs) (Arai et al., 1994; Arima et al., 1998a; Kato and Nakamura, 1990; Takeda et al., 1997) in PD, DLB and MSA. Although subsequent biochemical studies led to the description of several ubiquitinated proteins in LBs, the identity of these proteins and the role of ubiquitination in the biogenesis of pathological inclusions remained unclear. In 1995, for instance, Tamaoka and colleagues reported the presence of ubiquitinated alpha-crystallin B proteins in GCI-enriched fractions from MSA brains but not from neurologically healthy brain lysates (Tamaoka et al., 1995). Given the role of ubiquitination in regulating the degradation of proteins, it was initially hypothesized that the accumulation of ubiquitinated proteins might manifest an active attempt by the neurons to degrade aggregated proteins or prevent further aggregation (Tofaris et al., 2003).

The breakthrough identification of aSyn in LBs in 1997 (Spillantini et al., 1997) led subsequent IHC and biochemistry studies to show that the ubiquitin-positive LBs (Gai et al., 2000; Hasegawa et al., 2002), GCIs and NCIs (Arima et al., 1998a; Dickson et al., 1999b; Wakabayashi et al., 1998b) were also positive for aSyn. These observations combined with other data implicating impairment of the ubiquitin-proteasome system in PD (McNaught and Jenner, 2001) and other neurodegenerative diseases (Keck et al., 2003; Keller et al., 2000), led to the speculation that aSyn accumulating in pathological inclusions may be ubiquitinated, and that formation of these inclusions may reflect the failure to degrade these proteins. However, subsequent studies showed a lack of correlation between the accumulation of misfolded and ubiquitinated

aSyn aggregates and impairment of the ubiquitin proteasome system (Tofaris et al., 2003).

Two independent groups showed the co-localization of aSyn and ubiquitin biochemically in the GCI-enriched fractions (Dickson et al., 1999b; Gai et al., 1999). Subsequent biochemical studies demonstrated that some of the aSyn species phosphorylated at S129 in DLB and MSA brain lysates are also mono-, di- and tri-ubiquitinated (Hasegawa et al., 2002; Kuusisto et al., 2003; Sampathu et al., 2003; Tofaris et al., 2003). The majority of these biochemical and immunohistochemical studies relied on the use of antibodies against aSyn or ubiquitin. Therefore, it was not clear whether the synuclein species containing multiple ubiquitin molecules reflect the presence of a polyubiquitin chain or mono-ubiquitination at multiple residues. To establish whether aSyn is ubiquitinated and to identify the ubiquitination sites and pattern (mono- versus polyubiquitination) on aSyn, Anderson and colleagues performed unbiased mass spectrometry studies to map aSyn PTMs, and showed that aSyn in isolated LBs are mono-ubiquitinated at multiple lysine residues K12, K21, and K23 (Anderson et al., 2006). The same study identified aSyn as the major ubiquitinated protein within the LBs. A recent study by Schweighauser and colleagues has also identified ubiquitination of sarkosyl-insoluble aSyn at K80, and to a lower extent at K23 and K60 via mass spectrometry on MSA brains (Schweighauser et al., 2020).

Whether ubiquitination represents an early event that drives aSyn inclusion formation, or occurs post aSyn fibrillization was not clear. Spillantini and colleagues showed for the first time that a higher number of inclusions are detected using aSyn antibodies compared to ubiquitin antibodies both in PD and MSA (Spillantini et al., 1998a, 1998b). Kuusisto and colleagues reported that only PBs and LBs, but not punctate inclusions, were positive for p62 or ubiquitin after sequential IHC (Kuusisto et al., 2003). These observations are in line with a previous study by Gomez-Tortosa et al., which showed staining for aSyn and ubiquitin in the hippocampus, substantia nigra and the insular, cingulate, entorhinal, frontal and occipital cortices of DLB brains (Gomez-Tortosa et al., 2000). Interestingly, 2-10% more structures were found to be immunoreactive to aSyn compared to ubiquitin. Likewise, it has been shown that not all the inclusions positive for aSyn in DLB cingulate cortex and MSA cerebellum are positive for ubiquitin (Kuusisto et al., 2003; Sampathu et al., 2003).

A few studies have also reported an imperfect correlation between aSyn and ubiquitin immunoreactivity in pathological inclusions found in various synucleinopathies (Probst-Cousin et al., 1996; Sakamoto et al., 2005, 2002). This could be explained by the fact that ubiquitination or other common PTMs (e.g. C-terminal cleavage) interfere with the detection of aggregates by aSyn antibodies. Alternatively, it is plausible that ubiquitination may be a late event that occurs after aSyn misfolding and fibrillization. Under these conditions, it is likely that not all aSyn aggregates can be ubiquitinated. This hypothesis is consistent with subsequent studies demonstrating that 1) ubiquitination is not required for aSyn aggregation (Sampathu et al., 2003); 2) mono-ubiquitination of aSyn at different lysine residues inhibits the aggregation of monomeric aSyn *in vitro* (Hejjaoui et al., 2011); 3) the great majority of ubiquitinated aSyn is detected in the insoluble rather than soluble fractions (Hasegawa et al., 2002; Schweighauser et al., 2020; Tofaris et al., 2003); and 4) several E3 ubiquitin ligases accumulate with LBs in PD brains and were shown to interact and ubiquitinate aSyn *in vitro* and in cells (Lee et al., 2007; Liani et al., 2004; Rott et al., 2008). Some of these ubiquitin ligases, such as the seven in absentia homologue (SIAH) ligases SIAH-1 and SIAH-2 were shown to catalyse the mono-ubiquitination, but not the poly-ubiquitination of aSyn (Lee et al., 2007; Liani et al., 2004; Rott et al., 2008) at multiple lysine residues including, K12, K21 and K23 (Rott et al., 2008). The same residues were found mono-ubiquitinated in synucleinopathy brains (Anderson et al., 2006). Similarly, the ubiquitin-like proteins NEDD8 and Ubiquilin-2 were found to accumulate in GCIs of MSA brains as well as in the LBs of PD and DLB brains (Mori et al., 2012, 2005). Collectively, these observations suggest the involvement of the ubiquitin-proteasome system components in LB and GCI composition.

Intriguingly, ubiquitin-specific protease 9X (USP9X/FAM), a de-ubiquitinase that was reported to be involved in aSyn de-ubiquitination, was shown to be present in the LBs and LNs of PD midbrains and cingulate cortices, and also in the cortical LBs of diffuse Lewy body disease (DLBD) frontal cortices (Rott et al., 2011). Yet, biochemical analyses on brain homogenates from the same synucleinopathy cases revealed an overall decrease in USP9X levels and activity in PD and DLBD brains compared to healthy brains (Rott et al., 2011), suggesting that de-ubiquitination impairment of mono-ubiquitinated aSyn may play a role in aSyn pathogenesis.

Systematic immunohistochemical studies demonstrated close association and localization between the p62, ubiquitin, and aSyn in LBs of PD and DLB brains, and in GCIs of MSA brains (Kuusisto et al., 2003, 2001). Since then, p62 has also been recognized as a key component and marker of these aSyn inclusions. Ubiquitinated, p62-positive and aSyn pS129-positive filamentous cytoplasmic inclusions were also detected within the Schwann cells of MSA cases (Nakamura et al., 2015), suggesting a potential crosstalk between aSyn phosphorylation, ubiquitination and p62 recruitment to pathological aggregates, which could serve as a signal to target them for degradation by autophagy or other pathways. Whether the accumulation of ubiquitinated aSyn species in LBs, GCIs and NCIs represent a failed cellular response aimed at degrading aSyn aggregates, or a key determinant of aSyn inclusion formation and maturation remains unknown.

b) aSyn phosphorylation at Serine 129

aSyn pS129 was first identified by Fujiwara and colleagues (Fujiwara et al., 2002) using mass spectrometry following chemical cleavage of aSyn from insoluble fractions of DLB cerebral cortex. One of the two major peptide products was shown to be phosphorylated at Serine 129. This discovery inspired the generation of a rabbit polyclonal antibody against aSyn pS129, which was then used to demonstrate that LBs in the substantia nigra of PD brains and GCIs in the pons of MSA brains are immunoreactive for pS129. The first in-house aSyn pS129 rabbit polyclonal antibody was generated using synthetic peptides bearing phosphorylation at S129 (Fujiwara et al., 2002). It labelled LBs by IHC and recognized a band with an Mw similar to that of aSyn in the soluble and insoluble fractions from DLB brains by Western Blot (WB). Furthermore, the aSyn fibrils extracted from DLB brains were extensively and specifically decorated with gold particles when immunolabeled with the aSyn pS129 antibody, demonstrating that the aSyn fibrils in LBs and LNs bear this modification. In a subsequent study, the authors generated a mouse monoclonal antibody against aSyn pS129, i.e. psyn#64, and used it to screen a cohort of 157 brains that included not only PD and DLB but also AD, PSP, corticobasal degeneration (CBD), and neurofibrillary tangle-predominant dementia (NFTD), as well as clinically healthy control cases (Saito et al., 2003). In 25% of these cases, which included

neurodegenerative and control brains alike, positivity for aSyn pS129 was detected in the form of Lewy dots, threads and LB precursor neuronal inclusions.

Subsequent studies showed that aSyn pS129 species are also mono- and di-ubiquitinated, and these aSyn species are highly enriched in the insoluble fractions (Hasegawa et al., 2002), suggesting a potential crosstalk between aSyn phosphorylation and ubiquitination. Neumann and colleagues showed that the pS129-positive insoluble aSyn species in PD, DLB, MSA, and in neurodegeneration with brain iron accumulation type 1 (NBIA1) were also PK-resistant (Neumann et al., 2002). The large majority of the aSyn-positive GCIs, NCIs, dystrophic neurites, as well as NNIs and GNIs were then found to be aSyn pS129-positive (Nishie et al., 2004). Since then, studies in multiple laboratories have consistently shown that phosphorylation at S129 is a reliable marker of aSyn pathology and is one of the most common PTMs found in sporadic PD, PD with A53T mutation, and in MSA cases (Anderson et al., 2006). aSyn pS129 positivity within pathological inclusions has also been observed in idiopathic PD (Guerreiro et al., 2013; Landeck et al., 2016; Nishie et al., 2004; Vaikath et al., 2019), PD with LRRK2 G2019S mutation (Mamais et al., 2013), PD with aSyn G51D mutation (Kiely et al., 2013), PDD (Landeck et al., 2016), DLB (Colom-Cadena et al., 2017; Sano et al., 2017; Sorrentino et al., 2019; Takao et al., 2004; Vaikath et al., 2019) and MSA (Nishie et al., 2004). Combined with the close association of aSyn pS129 with aggregated, PK-resistant and insoluble forms of aSyn, these observations led to the emergence of aSyn pS129 antibodies as the primary tools to monitor and quantify aSyn pathology formation in the brain, peripheral tissues and disease models of synucleinopathies (Beach et al., 2010; Delic et al., 2018; Landeck et al., 2016; Lue et al., 2012; Mamais et al., 2013; Walker et al., 2013).

While aSyn pS129 immunoreactivity is constantly observed in aSyn pathologies and seems to correlate with increased aggregation and pathology formation, estimates of the amount of aSyn that is phosphorylated must be treated with a grain of salt. Although Fujiwara and colleagues reported that the vast majority (>90%) of aSyn within LBs from DLB brains is phosphorylated at S129 (Fujiwara et al., 2002), these findings have not been confirmed by other groups. Indeed, the method used by the authors to quantify the levels of aSyn could not have yielded an accurate assessment - it was based on an extrapolation of the aSyn pS129 levels in relation to the levels of total

aSyn proteins from DLB samples using aSyn LB509 for quantitative immunoblotting. The LB509 antibody has an epitope in the C-terminus of aSyn (115-122) and loses its binding capacity when aSyn is C-terminally truncated (Jakes et al., 1999), which is a common aSyn PTM detected both under physiological and pathological conditions in human brains (Anderson et al., 2006). Indeed, several reports have demonstrated the presence of significant amounts of C-terminally truncated forms of aSyn species lacking the pS129 epitope in pathological aSyn aggregates (Anderson et al., 2006; Baba et al., 1998; Campbell et al., 2001; Dickson et al., 1999; Gai et al., 1999; Kellie et al., 2015; Lewis et al., 2010; Moors et al., 2021; Ohrfelt et al., 2011; Tofaris et al., 2003; Tong et al., 2010). Therefore, aSyn pS129 antibodies alone may not allow for the accurate quantification of total aSyn levels or the capturing of aSyn pathology diversity. Furthermore, we recently showed that the presence of additional neighbouring modifications such as aSyn phosphorylation at Tyrosine 125 (aSyn pY125) or truncations at residues 133 or 135 abolish the immunoreactivity of most aSyn pS129 antibodies (Lashuel et al., 2022). Together, these observations suggest that aSyn pS129 antibodies detect aggregates composed of the full-length aSyn protein, but not aSyn aggregates composed of truncated aSyn species or aSyn bearing several C-terminal modifications (Anderson et al., 2006), such as phosphorylations and nitration or extreme C-terminal truncations (Chen et al., 2009; Giasson et al., 2000a; Kiely et al., 2013; Mahul-Mellier et al., 2018).

Despite these limitations and the fact that no other studies have attempted to quantify aSyn pS129 levels from PD and other synucleinopathies, there has been an increasing reliance on aSyn pS129 as the sole marker for aSyn pathology. There are several other caveats with this approach: 1) aSyn pS129 also occurs physiologically as part of aSyn metabolism (Anderson et al., 2006) and as part of aging (Muntane et al., 2012). The presence of aSyn pS129 species does not necessarily equate to presence of aSyn pathology. 2) aSyn S129 phosphorylation most likely occurs after the fibrillisation of the monomeric aSyn species, and is not required for aSyn aggregation (Mahul-Mellier et al., 2018). The mere dependence on aSyn pS129 signal may result in neglecting the less mature aSyn aggregates that are not yet phosphorylated at S129. 3) Several studies have highlighted the difficulties in generating aSyn pS129 antibodies and showed that, while being specific for aSyn pS129 versus non-modified aSyn, all aSyn pS129 antibodies cross-react with other proteins to different degrees (Delic et al., 2018;

Sacino et al., 2014a). Therefore, future studies should place greater emphasis on using well-validated aSyn pS129 antibodies and include other complementary experimental approaches to assess the aggregation state of the pS129-positive species. Furthermore, these results should always be compared to those obtained using multiple antibodies capable of capturing aSyn diversity.

c) aSyn phosphorylation at Serine 87

Although there are four serine and ten threonine putative phosphorylation sites in the human aSyn sequence, only phosphorylation at S129 and Serine 87 (aSyn pS87) out of these sites have been described to occur in the human brain. Serine 87 is of particular interest as it is a human-specific aSyn residue, and it is the only identified phosphorylation that is located in the NAC region of aSyn, playing key roles in the regulation aSyn aggregation (Giasson et al., 2001). Although an earlier publication assigned minimal roles to pS87 in synucleinopathies (Waxman and Giasson, 2008), we have shown, using in-house antibodies specific to this modification, the localization of aSyn pS87 species to LBs from DLB brains (Paleologou et al., 2010). Unfortunately, this modification has not been studied in-depth as: 1) robust and reliable tools to detect and quantify this PTM are limited; 2) aSyn pS87 is a human-specific modification, rendering it more challenging to model in cellular and animal studies; and 3) all biochemical studies suggest that this PTM is much less abundant than ubiquitination or aSyn S129 phosphorylation (Anderson et al., 2006).

d) aSyn phosphorylation at Tyrosines 39, 125, 133 and 136

There are four putative tyrosine phosphorylation sites in human aSyn, namely Tyrosine 39 (Y39), Tyrosine 125 (Y125), Tyrosine 133 (Y133), and Tyrosine 136 (Y133). The latter three sites are located in the C-terminal disordered domain and are near other residues that undergo phosphorylation and other types of PTMs (aSyn pS129, methionine oxidation and truncations at residues 115, 119, 122, 133, 135). In contrast, Y39 is in the N-terminus. Cryo-EM structures of aSyn fibrils derived from different aSyn proteins (Guerrero-Ferreira et al., 2019, 2018; B. Li et al., 2018; Y. Li et al., 2018) and from MSA brains (Schweighauser et al., 2020) show that Y39 occupies a position that is close to the core of the aSyn fibrils. Similar to aSyn pS87, there is a limited number of studies on aSyn tyrosine phosphorylations in synucleinopathies. To date, only two

studies have investigated the presence of aSyn phosphorylation at Y39 (aSyn pY39) in PD tissue (Brahmachari et al., 2016; Mahul-Mellier et al., 2014), and one recent study by Schweighauser et al. reported aSyn pY39 in the sarkosyl-insoluble fractions from the putamen of some MSA brains (Schweighauser et al., 2020). We previously showed that aSyn pY39 and pY125 species exist both in the cingulate cortices of PD and healthy control brains (Mahul-Mellier et al., 2014). We also showed that these modifications may be linked to the activity of ABL proto-oncogene 1 non-receptor tyrosine kinase (c-Abl), an enzyme with increased expression in PD brains (cingulate extracts). In another study, a significant increase in aSyn pY39 paralleled with a substantial increase in activated c-Abl (c-Abl pY245) levels was also observed in the substantia nigra and striatum lysates of PD patients compared to healthy controls (Brahmachari et al., 2016).

Our findings reported the existence of phosphorylated aSyn species at Y125 in neurologically healthy brains (Mahul-Mellier et al., 2014). This is in line with previous results by Chen and colleagues, who showed that aSyn pY125 is present in the cortex of young (i.e. <29 years old) human brains, but diminishes in aged (i.e. >70 years old) human brains as part of the aging process, and declines even further in DLB brains compared to age-matched neurologically healthy controls (Chen et al., 2009). On the other hand, a recent study argued that aSyn-positive pathological inclusions in PDD and DLB-AD brains are free of aSyn pY125 species (Fayyad et al., 2020). The authors did not detect aSyn pY125 species in sodium dodecyl sulphate (SDS)-urea-soluble fractions of healthy control, PD or DLB frontal cortices. These findings contradict a previous report showing enhanced aSyn pY125 signal overlapping with the aSyn pS129-positive species in the hippocampal cornu ammonis 2 (CA2) region of a *SNCA* G51D mutation case (Kiely et al., 2015, 2013). Although several studies have reported phosphorylation of aSyn at Y133 (aSyn pY133) and at Y136 (aSyn pY136) in cell cultures (Chen et al., 2009; Kleinknecht et al., 2016) and *in vitro* (Negro et al., 2002), to the best of our knowledge, there has been only one study to show aSyn pY133 in DLB tissues by IHC, and aSyn pY136 by IHC and WB (Sano et al., 2021). No other targeted or systematic investigation exists to assess aSyn phosphorylated at Y133 or Y136 in human brains or pathological aSyn inclusions.

e) aSyn nitration

Several lines of evidence showed strong links between the formation of reactive oxygen species (ROS), oxidative stress, neurodegeneration and the pathogenesis of neurodegenerative diseases, including PD (Jenner and Olanow, 1996), DLB (Lyras et al., 2002) and AD (Markesbery, 1997; Sultana et al., 2006). Furthermore, elevated levels of several markers of oxidative and nitrosative stress, activated microglia and pro-inflammatory cytokines are commonly observed in the brains of PD patients (Dexter et al., 1989; Alam et al., 1997; Floor et al., 1998; Hirsch et al., 1998; Giasson et al., 2000; Wullner et al., 2003). Dopaminergic neurons in the substantia nigra are highly susceptible to oxidative and nitrosative stress due to the high oxygen consumption of this brain region together with the auto-oxidation of dopamine. It has been proposed that nitric oxide (NO) is one of the key species contributing to the neuronal loss in PD substantia nigra (Przedborski and Dawson, 2001), and that this toxic role may be mediated by the activity of the peroxynitrite (Beckman et al., 1990). To determine the extent of peroxynitrite-induced tyrosine nitration, and to evaluate the degree of NO-triggered oxidative damage (Beckman et al., 1992; Ischiropoulos et al., 1992), several antibodies that allow the detection of nitrotyrosine were developed (Beckman et al., 1994). Using an antibody against 3-nitrotyrosine (3-NT), Duda et al. showed that nitrated species were localized to the pathological inclusions in synucleinopathies, including LBs in PD midbrain, LBs and LNs in DLB and LBvAD cingulate cortex and mesencephalon, LB-like inclusions in NBIA1 insular cortex and globus pallidus, and the GCIs and NCIs in MSA cerebellum (Duda et al., 2000a).

There are four tyrosine residues within the human aSyn sequence, i.e. Y39, Y125, Y133, and Y136, which can be subjected to nitration. To determine whether tyrosine nitration takes place specifically on aSyn, Giasson and colleagues developed mouse monoclonal antibodies that were raised against nitrated human recombinant aSyn protein (Giasson et al., 2000a). The specificity of these antibodies to nitrated aSyn species was validated via enzyme-linked immunosorbent assay (ELISA) and WB screening using non-modified aSyn and nitrated aSyn, nitrated bSyn and other nitrated proteins. Then, using human recombinant aSyn nitrated at one or multiple tyrosine residues and also full-length or truncated aSyn, the authors identified antibodies that recognize either N-terminally (nSyn14) or C-terminally nitrated aSyn (nSyn12 and

nSyn24). These antibodies were used for IHC, WB and EM-immunogold labelling to show that nitrated aSyn fibrillar species exist within pathological lesions of PD, DLB, LBvAD and MSA, and that nitration at these residues represents disease-specific modifications. Similarly, aSyn nitrated species have been detected in cases with PiD frontal cortices both by WB and IHC using a nitrated pan-aSyn antibody (Dalfo et al., 2006). Not all of the aSyn lesions, such as PBs and aSyn-positive neurites, which are thought to represent earlier inclusion forms that precede the mature LB formation (Dale et al., 1992; Hayashida et al., 1993; Mahul-Mellier et al., 2020), were shown to be positive for 3-NT. The enhancement of nitrated aSyn species level in the dopaminergic neurons from aged primates was also reported (McCormack et al., 2012). These observations suggest that nitration may represent a post-fibrillization event and is not required for aSyn aggregation (Gomez-Tortosa et al., 2002). Further studies to assess the role of C- versus N-terminal aSyn nitrations in pathology formation and maturation in PD, DLB and MSA are yet to be run.

f) aSyn truncation

Truncation is one of the most prevalent aSyn PTMs found under physiological and pathological conditions in the human brain. The presence of truncated species of aSyn was described for the first time by WB in DLB (Baba et al., 1998) and MSA (Gai et al., 1999). In the later studies, the use of antibodies with epitopes against the NAC region of aSyn that would allow for the biochemical detection of full-length as well as C- and/or N-terminally truncated variants of aSyn then allowed for a better detection of this PTM (Campbell et al., 2001; Culvenor et al., 1999).

A small subset of N-terminally (Muntane et al., 2012) and C-terminally (Anderson et al., 2006; Campbell et al., 2001; Li et al., 2005; Muntane et al., 2012) truncated aSyn species have been reported to be present in healthy human brains, suggesting that this PTM may have a physiological role. Yet, an increasing number of studies show that cleaved and detergent-insoluble aSyn fragments are enhanced in PD (Anderson et al., 2006; Baba et al., 1998; Campbell et al., 2001; Culvenor et al., 1999; Dufty et al., 2007; Kellie et al., 2015, p. 201; Killinger et al., 2018; Lewis et al., 2010; Li et al., 2005; Liu et al., 2005; Moors et al., 2021; Ohrfelt et al., 2011; Prasad et al., 2012; Tong et al., 2010; Zhang et al., 2017), DLB (Anderson et al., 2006; Baba et al., 1998;

Culvenor et al., 1999; Liu et al., 2005; Muntane et al., 2012; Ohrfelt et al., 2011; Waxman et al., 2008; Zhang et al., 2017) and MSA (Anderson et al., 2006; Campbell et al., 2001; Dickson et al., 1999b; Gai et al., 1999; Tong et al., 2010) brains. Altogether, these findings indicate that aggregation of truncated aSyn species may be closely associated with pathogenesis and disease progression in synucleinopathies.

A large number of reports point at an increased level of various aSyn species C-terminally truncated between residues 100-140 in LBD brains (Anderson et al., 2006; Campbell et al., 2001; Kellie et al., 2015, p. 201; Lewis et al., 2010; Ohrfelt et al., 2011; Tofaris et al., 2003) and specifically in LBs (Baba et al., 1998; Moors et al., 2021; Prasad et al., 2012). The detergent-insoluble aSyn bands with an Mw of 12kDa are biochemically profiled in PD, DLB (Anderson et al., 2006; Baba et al., 1998; Bhattacharjee et al., 2019; Campbell et al., 2001; Culvenor et al., 1999; Dufty et al., 2007; Killinger et al., 2018; Lewis et al., 2010; Li et al., 2005; Liu et al., 2005; Muntane et al., 2012; Ohrfelt et al., 2011; Prasad et al., 2012; Tong et al., 2010; Waxman et al., 2008; Zhang et al., 2017) and MSA (Anderson et al., 2006; Campbell et al., 2001; Dickson et al., 1999b; Duda et al., 2000b; Gai et al., 1999; Tong et al., 2010) brain homogenates,. This 12kDa band is revealed only by N-terminal or NAC region aSyn antibodies, but not by C-terminal aSyn antibodies with epitopes after residue 116. Similarly, aSyn bands at 10kDa (Anderson et al., 2006; Baba et al., 1998; Campbell et al., 2001; Dickson et al., 1999b; Killinger et al., 2018; Li et al., 2005; Liu et al., 2005; Zhang et al., 2017) and 8kDa (Bhattacharjee et al., 2019; Culvenor et al., 1999; Dickson et al., 1999b; Killinger et al., 2018; Li et al., 2005; Liu et al., 2005; Ohrfelt et al., 2011) have also been revealed biochemically using synucleinopathy brains. These data suggest that aSyn aggregates are not made of a homogenous population of aSyn fibrils, but of a mixture of full-length and truncated aSyn species.

The antibody-based studies allowed for the detection of cleaved aSyn fragments, but not for the precise mapping of the cleavage sites. For a more accurate understanding of these cleaved aSyn populations in human brain, mass spectrometry-based studies were carried by Anderson and colleagues, who have shown that the C-terminally truncated species in LBs include aSyn truncated at Aspartic acids 115, 119, 135 (D115, D119, D135), Asparagine 122 (N122) and Tyrosine 133 (Y133) (Anderson et al., 2006). Likewise, around twenty different aSyn proteoforms, all N-terminally acetylated, were

found both in the PD and control cingulate cortices by liquid chromatography with tandem mass spectrometry (LC-MS/MS) (Bhattacharjee et al., 2019). An enrichment of aSyn fragments in the detergent-insoluble fractions of PD cases, such as aSyn truncated at D119 and aSyn truncated in the NAC region at residues 65, 66 or 68 as well as full-length aSyn monomers and dimers, was also reported (Bhattacharjee et al., 2019). Collectively, the most abundant aSyn species found in PD and DLB brain tissues as well as the PD appendix analysed by LC-MS/MS appear to be the 1-119 and 1-122 fragments of aSyn (Anderson et al., 2006; Bhattacharjee et al., 2019; Kellie et al., 2015; Killinger et al., 2018; Ohrfelt et al., 2011).

In addition to mass spectrometry analyses, the use of antibodies specific to truncated aSyn allowed for the visualisation of these aSyn fragments by IHC and immunofluorescence (IF) (Anderson et al., 2006; Lewis et al., 2010; Moors et al., 2021; Prasad et al., 2012). A particular assembly of the different aSyn species within the pathological lesions was revealed using truncation-specific antibodies and confocal or STED microscopy, where the C-terminally truncated aSyn species at residues 119 and 122 remain within the inner layers of the LBs, PBs and LNs, with the S129-phosphorylated and full-length aSyn species surrounding these species on the outer layers (Moors et al., 2021; Prasad et al., 2012). Together, these data suggest that a particular packing of differentially fragmented aSyn species may be taking place as the Lewy inclusions mature over time, where the more truncated the aSyn species, the closer it is located within the core of inclusions.

Mass spectrometry studies have also revealed several aSyn species with N-terminal truncations in the LBD brains and appendices (Bhattacharjee et al., 2019; Kellie et al., 2015; Killinger et al., 2018; Muntane et al., 2012). Specifically, the aSyn species truncated at residues 5 and 39 were identified in the PD frontal cortex (Kellie et al., 2015), and aSyn species truncated at residues 47 and 50 in the PD cingulate cortex (Bhattacharjee et al., 2019) by mass spectrometry. Interestingly, the top-down mass spectrometry analysis revealed aSyn fragments 18-140 and 19-140 in the PD appendix (Killinger et al., 2018). Yet the full spectrum of N-terminally cleaved aSyn fragments in brain and other CNS regions of synucleinopathies, and the role of these aSyn N-terminal truncations under physiological and pathological circumstances still need to be explored further.

A number of proteases have been linked to aSyn cleavage at different sites so far. Dufty and colleagues, for instance, detected calpain-1-cleaved aSyn species in around 70% of LNs and LBs in DLB, and in around 90% of LNs and LBs in PD cases (Dufty et al., 2007). Wang and colleagues mapped caspase-1 enzymatic activity to aSyn D121 *in vivo*, and showed co-localization of aSyn and caspase-1 within LBs (Wang et al., 2016). Similarly, Choi and colleagues showed aSyn to be a substrate of matrix metalloproteinase-3 (MMP3) *in vitro* (Choi et al., 2011), and aSyn and MMP3 to be co-localising in LBs of PD brains. Recently a significant increase of aSyn truncated after Asparagine 103 (N103) has been detected in the soluble and insoluble fractions of PD substantia nigra and cortex, compared to controls (Zhang et al., 2017). In this report, the formation of 1-103 truncated species was linked to the asparagine endopeptidase (AEP) activity via *in vivo* models. In addition, an increase in the protein levels of kallikrein-6 in the putamen and the cerebellar white matter; an increase of calpain-1 activity in the putamen and cerebellar white matter; and an increase of cathepsin-D in the pons and cerebellar white matter in MSA tissue has been reported (Kiely et al., 2019), suggesting the involvement of these proteases in the cleavage of aSyn species. Collectively, these suggest that multiple proteases are involved in the processing of aSyn not only under physiological but also pathological conditions. Failure to clear truncated species generated under physiological conditions may eventually lead to their aggregation, which could trigger the formation of pathological inclusions of PD, DLB and MSA brains.

g) aSyn SUMOylation

aSyn SUMOylation is one of the least explored PTMs in the literature - to our knowledge, only two papers have investigated aSyn SUMOylation state in the inclusions formed in MSA (Pountney et al., 2005; Wong et al., 2013). By IHC, Pountey and colleagues and a subsequent study by Wong et al. reported strong punctate localization of small ubiquitin-like modifier-1 (SUMO-1) in the aSyn-positive GCIs from MSA patients (Pountney et al., 2005; Wong et al., 2013). There is some evidence for the localization of SUMO-1 in LBs (Kim et al., 2011), and for the enhancement of the protein inhibitor of activated signal transducer and activator of transcription 2 (PIAS2), i.e. the E3 SUMO-protein ligase, in PD brains compared to control tissues (Rott et al.,

2017). However, additional histological and biochemical studies are needed to explore this modification further in human tissue.

h) aSyn acetylation

N-terminal acetylation of a protein occurs when an acetyl group is transferred to the alpha-amino group of the first amino acid in the N-terminus (Varland et al., 2015). This is an irreversible modification facilitated by N-acetyl transferases (NATs) (Ree et al., 2018). Lysine acetylation, on the other hand, is reversible, and is catalysed by lysine acetyltransferases (KATs) (Allis et al., 2007; Drazic et al., 2016; Glozak et al., 2005). The N-terminal acetylation of aSyn may be important in maintaining an alpha-helical conformation that facilitates the membrane binding of the protein (Bartels et al., 2014; Dikiy and Eliezer, 2014; Fauvet et al., 2012a; Theillet et al., 2016; Trexler and Rhoades, 2012), and has been reported in the mouse brain homogenates (Burre et al., 2013), in human erythrocytes (Bartels et al., 2011; Fauvet et al., 2012b) and in PD, PDD, DLB and healthy control brains by mass spectrometry (Anderson et al., 2006; Kellie et al., 2015; Ohrfelt et al., 2011). The lysine acetylation, on the other hand, has only been reported by a recent study by Schweighauser and colleagues by mass spectrometry analysis of MSA putamen, where aSyn is acetylated at K21, K23, K32, K34, K45, K58, K60, K80 and K96 (Schweighauser et al., 2020). Interestingly, the lysine residues reported to by acetylated in the mouse brains are K6 and K10 (de Oliveira et al., 2017). Further research into the physiological and pathological roles of aSyn lysine acetylation is needed, but these efforts are limited by the lack of site-specific antibodies for this modification.

i) aSyn glycation

The lysine, arginine or histidine residues of proteins may undergo glycation reactions with reducing sugars (Bidasee et al., 2004; Thornalley, 2008). LBs have been shown to be positive for advanced glycation end-products (AGEs) by IHC (Castellani et al., 1996; Muench et al., 2000), and AGE expression to be increased in DLB brains by biochemical analyses (Dalfo et al., 2005). Similarly, Vicente Miranda and colleagues have shown by WB that the aSyn from LBDs are glycated (Vicente Miranda et al., 2017). Yet, further research is needed to understand the role of glycation in aSyn pathogenesis.

j) aSyn O-GlcNAcylation

O-GlcNAcylation occurs by the transfer of *O*-linked N-acetylglucosamine (*O*-GlcNAc) to the serine or threonine residues of proteins (Hart et al., 2011, 2007; Yang and Qian, 2017). By mass spectrometry, sites of aSyn *O*-GlcNAcylation have been identified on rodent brain lysates at T64 and T72 (Alfaro et al., 2012; Wang et al., 2010) and on human erythrocytes at S87 (Wang et al., 2009). The *O*-GlcNAcylation at T72 (Marotta et al., 2015), at S87 (Lewis et al., 2017) and a combination of several threonine and serine sites (Levine et al., 2019) by synthetic chemistry have been reported to prevent the aggregation of aSyn. No direct evidence has so far been presented, however, on the existence of this aSyn modification in synucleinopathies, and for its relevance to disease pathogenesis.

1.2.4 Pathology spreading and staging in LBDs

In the last two decades, several lines of evidence have been presented to support the hypothesis that 1) aSyn pathology may initiate in the periphery, and gradually spread to and within the brain; and that 2) this spreading occurs in a cell-to-cell manner in a prion-like fashion, where misfolded aSyn acts as a template for seeding that allows the endogenous monomeric aSyn to aggregate. This has led to the development of different approaches for the staging patterns of PD, the most well-known being the Braak staging. Here, we review the literature on aSyn pathology in the periphery, the Braak and other staging approaches on LBDs and MSA, and state the evidence to support or refute these approaches.

a) The ‘dual hit’ theory

The pre-motor symptoms of sporadic PD and DLB involving anosmia (Haehner et al., 2009), constipation (Abbott et al., 2001) and sleep problems including excessive daytime sleepiness (EDS) and RBD (Abbott et al., 2005; Iranzo et al., 2006), combined with the studies to show a lower risk of developing PD in patients undertaking vagotomy (Liu et al., 2017; Svensson et al., 2015), has led to a new line of research investigating the origins of aSyn pathology in the periphery. Consequently, the ‘dual hit’ theory was born, suggesting that the aSyn aggregation initiates in the gut and/or

the olfactory system, from where it spreads to the brain (Braak et al., 2003a; Hawkes et al., 2009, 2007). This hypothesis has gained support from the subsequently increasing number of studies that reported aSyn-positive structures in the human GIT with an abundance of aSyn pS129 species in the colon, small intestine and the appendix, the stomach, oesophagus and the salivary gland (Beach et al., 2010; Corbille et al., 2017; Killinger et al., 2018; Ruffmann et al., 2018; Stokholm et al., 2016) (for all the articles to report on aSyn in the GIT, see Table 1. 1). Furthermore, the alterations in the gut microbiome (Engen et al., 2017; Heintz-Buschart et al., 2018; Hopfner et al., 2017; Li et al., 2017; Lin et al., 2018; Petrov et al., 2017; Qian et al., 2018; Tan et al., 2018; Wan et al., 2019), bowel inflammation and increased intestinal permeability (Clairembault et al., 2015; Devos et al., 2013; Engen et al., 2017; Forsyth et al., 2011; Schwiertz et al., 2018) have been widely reported in the PD and MSA patients. These data gave birth to the hypothesis that aSyn misfolding may first initiate in response to an environmental toxin or pathogen in the enteric nerve cells or the olfactory bulb, and spread to the central nervous system by trans-synaptic transmission (Hawkes et al., 2007). It is important to note that the large majority of the studies looking at aSyn in the GIT relied heavily or only on aSyn pS129 positivity as an indicator of aggregation (Table 1. 1). The exact characteristics, including the PTM signature and aggregation state, of these aSyn species in the GIT therefore require more comprehensive assessments.

Table 1. 1 A summary of the articles to report on aSyn in the GIT, the approaches they have followed to characterise aSyn aggregation, and the GIT tissues they have looked at. aSyn = alpha-synuclein; GIT = gastrointestinal tract; LB = Lewy body; PK = proteinase K; PLA = proximity ligation assay; PMCA = protein misfolding cyclic amplification assay; ub = ubiquitin

	main approaches							GIT tissues						
article	**A**	**B**	**C**	**D**	**E**	**F**	**G**	**a**	**b**	**c**	**d**	**e**	**f**	**g**
Adler et al., 2014														
Adler et al., 2016														
Aldecoa et al., 2015														
Annerino et al., 2012														
Antunes et al., 2016														
Barrenschee et al., 2017														
Beach et al., 2013														
Beach et al., 2016														
Beach et al., 2010														
Beach et al., 2018														
Boettner et al., 2012														
Boettner et al., 2015														
Braak et al., 2006														
Calderon-Garciduenas et al., 2017														
Carletti et al., 2017														
Cersosimo et al., 2011														
Chandra et al., 2017														
Chung et al., 2016														
Clairembault et al., 2015														
Corbille et al., 2016a														
Corbille et al., 2016b														
Corbille et al., 2017														
Del Tredici et al., 2010														
Del Tredici and Duda, 2011														
Desmet et al., 2017														
Fenyi et al., 2019														
Fernandez-Arcos et al., 2018														
Folgoas et al., 2013														
Forsyth et al., 2011														
Gao et al., 2015														
Gelpi et al., 2014														
Gold et al., 2013														
Grathwohl et al., 2019														
Gray et al., 2014														
Hilton et al., 2014														
Iranzo et al., 2018														
Ito et al., 2014														
Killinger et al., 2018														
Kim et al., 2017														
Lebouvier et al., 2010														
Lebouvier et al., 2008														
Leclair-Visonneau et al., 2019														
Lee et al., 2018														
Ma et al., 2019														
Masuda et al., 2014														
Mu et al., 2015														
Ohlsson and Englund, 2019														
Pouclet et al., 2012a														
Pouclet et al., 2012b														
Pouclet et al., 2012c														
Punsoni et al., 2019														
Rouaud et al., 2017														
Ruffmann et al., 2018														
Sanchez-Ferro et al., 2015														
Shannon et al., 2012a														
Shannon et al., 2012b														
Sharrad et al., 2013														
Shin et al., 2017														
Shin et al., 2018														
Shin et al., 2019														
Skorvanek et al., 2018														
Sprenger et al., 2015														
Stewart et al., 2014														
Stokholm et al., 2016														
Stolzenberg et al., 2017														
Vilas et al., 2016														
Visanji et al., 2015														
Xuan et al., 2016														
Yan et al., 2018														

A = amyloid dye binding
B = solubility
C = LB markers (ub, p62)
D = PK resistance
E = PLA
F = PMCA
G = aSyn pS129

+
-

a= salivary glands
b= oesophagus
c= stomach
d= small intestine
e= appendix
f= colon
g= other GIT tissue

+
-

b) Staging of synucleinopathies and the prion-like spreading of aSyn

In parallel to the findings of aSyn pathology in the gastro-intestinal and olfactory tracts, Braak and colleagues immunohistochemically studied different brain regions of a subset of ILBD and PD patients with variable clinical symptoms and deciphered that, in line with the progression of the clinical symptoms, aSyn pathology progresses in the brain following specific pathways (Braak et al., 2003). This has led to the Braak staging of PD, where stages 1-2 show pathology in a restricted number of regions, including the olfactory bulb and the vagal nerve, but no corresponding clinical motor symptoms; stages 3-4 show increasing pathology in the substantia nigra pars compacta, locus coeruleus and other brainstem regions, which correspond to the presence of clinical motor symptoms; and stages 5-6 where pathology has advanced to the neocortex and the basal forebrain, which correlates with increasing cognitive dysfunction (Braak et al., 2003a, 2003b, 2002; Del Tredici et al., 2002; Del Tredici and Braak, 2012; Muller et al., 2005).

On a cellular level, this spread of pathological aSyn has been believed to be in a prion-like manner, which gained significant ground after a) longitudinal studies showing that transplanted neurons developed aSyn-positive inclusions decades after the PD patients received a graft (Kordower et al., 2008; Li et al., 2008); b) lentiviral-based rodent and non-human primate models showing the diffusion of aSyn pathology spreading after targeted overexpression of the protein (Eslamboli et al., 2007; Helwig et al., 2016; Kirik et al., 2003, 2002; Lauwers et al., 2006; Lo Bianco et al., 2002; St Martin et al., 2007; Ulusoy et al., 2015, 2013; Yamada et al., 2004) and the spread of aSyn pathology from host to graft cells in these models (Angot et al., 2012; Desplats et al., 2009; Hansen et al., 2011; Kordower et al., 2011); and c) recombinant PFFs (Abdelmotilib et al., 2017; Breid et al., 2016; Holmqvist et al., 2014; Luk et al., 2012a, 2012b; Masuda-Suzukake et al., 2014, 2013; Osterberg et al., 2015; Paumier et al., 2015; Peelaerts et al., 2015; Rey et al., 2016, 2013; Reyes et al., 2014; Sacino et al., 2014b, 2013) and patient-derived aggregates injected to animal models (Bernis et al., 2015; Holmqvist et al., 2014; Masuda-Suzukake et al., 2013; Prusiner et al., 2015; Recasens et al., 2014; Thomzig et al., 2021; Ulusoy et al., 2017; Watts et al., 2013) inducing the formation and spreading of aSyn aggregation overtime within the brain, from the periphery to the central nervous system, and vice versa. According to the

prion theory, the misfolded aSyn species are released from the donor cell and taken up by the healthy recipient cell where they then act as seeds to initiate nucleation and aggregation of the endogenous, natively unfolded aSyn (Angot et al., 2010; Angot and Brundin, 2009), allowing for the cell-to-cell transmission and propagation of aSyn pathology.

Next to the ILBD and PD staging proposed by Braak and colleagues (Braak et al., 2003a, 2003b, 2002; Del Tredici et al., 2002; Del Tredici and Braak, 2012; Muller et al., 2005), other staging approaches have been postulated. Namely, McKeith and colleagues put forward a diagnostic and staging approach for DLB cases, allowing the disease severity and progression to be categorised as brainstem-predominant, limbic and neocortical (McKeith et al., 2017, 2005, 1996), which was later on refined by Leverenz and colleagues (Leverenz et al., 2008). Marui et al. proposed four groups of severity (stages I-IV) for DLB cases based on a semi-quantitative assessment of Lewy load in the amygdala, limbic cortex and neocortex (Marui et al., 2002). Deramecourt and colleagues, on the other hand, sought to stage the DLB progression to 10 steps based on the biochemical profiles of the insoluble aSyn density in the entorhinal, cingulate, temporal, frontal and parietal cortices (Deramecourt et al., 2006). An improved staging approach by the BrainNet Europe was taken to increase the inter-observer agreeability and thus reduce variability, and to combine the McKeith and Braak staging (Alafuzoff et al., 2009). Likewise, Beach and colleagues proposed the unified staging system for Lewy body disorders (USSLB) in order to allow for the classification of a larger percentage of subjects showing Lewy pathology (Beach et al., 2009). This approach consisted of the categorisation of cases into stages referred to as olfactory bulb only, brainstem-predominant, limbic-predominant, brainstem and limbic, and neocortical (Adler et al., 2019; Adler and Beach, 2016; Beach et al., 2009), and intended to incorporate not only ILBD, PD and DLB, but also AD with LBs into the staging process. Another approach by Horsager and colleagues proposed to take PD in two subtypes: the ‘body-first’ subtype, in which the aSyn pathology originates in the periphery and spreads to the CNS; and the ‘brain-first’ subtype, where aSyn pathology first forms in the brain and spreads to the PNS (Horsager et al., 2020). With MSA, on the other hand, differential progression patterns are observed with MSA-P, MSA-C and MSA mixed cases (Halliday et al., 2011), rendering the staging of this disease complex. The current staging approaches are based on the symptomatology of the cases (Geser

et al., 2006; Seppi et al., 2005; Wenning et al., 2004) but corresponding neuropathological examination is needed to understand the disease progression pathways in correlation to clinical data.

Several succeeding studies to Braak staging examining LB distribution in large cohorts have shown a positive correlation between Lewy pathology load and symptom severity, in agreement with the Braak staging model (Hurtig et al., 2000; Mattila et al., 2000; Saito et al., 2004). However, a considerable percentage of PD cases do not support the Braak model of progression - the symptoms and prognoses of PD patients are heterogeneous, and depending on the age of onset and the presence of other co-morbidities, these differences can be drastic (Alafuzoff et al., 2009; Beach et al., 2009; Coughlin et al., 2019; Halliday and McCann, 2010; Kalaitzakis et al., 2008; Parkkinen et al., 2008). Kalaitzakis et al. have reported, for instance, 47% of 71 PD cases studied do not fit with the spreading model predicted by Braak, with a small subset of these cases not showing any pathology in the dorsal vagal nucleus despite neurodegeneration in the substantia nigra and the cortex (Kalaitzakis et al., 2008). Remarkably, Parkkinen et al. showed that 55% of the 226 aSyn-positive cases, pathologically fitting to Braak stages V-VI, did not show the expected corresponding clinical symptoms of dementia (Parkkinen et al., 2008). Contrastingly, cases that did not present any clinical motor symptoms of PD were retrospectively found to show advanced Lewy pathology (Parkkinen et al., 2001). Furthermore, Lewy pathology load has shown to be not necessarily an indicator of disease progression routes, but a feature of normal ageing (Forno, 1969; Perry et al., 1990) and/or other neuropsychiatric comorbidities (Jellinger, 2004; Woodard, 1962). Moreover, the Braak staging studies are based on immunohistochemical screening using a C-terminal antibody with an epitope against the 116-131 residues of aSyn. Yet, mounting evidence shows that aSyn is heavily modified particularly in the C-terminal region in pathology as described above, which may render the C-terminal antibodies inefficient to capture the full range of aSyn pathology. This caution, combined with the lack of studies on the PTM characterisation of the aSyn pathologies in relation to Braak staging deem it necessary to re-visit the staging of PD and other LBDs to have a better grasp of how these diseases progress, and therefore how they could be interfered with.

1.3.2 Epilogue: Tools for research on synucleinopathies

Earlier studies on synucleinopathies using histological dyes (e.g. haematoxylin and eosin, silver stain) combined with typical markers of amyloids (thioflavin, Congo red or Amytracker) and inclusion formation (ubiquitin- and p62-positivity) have helped shed light on the morphologies and topographical distribution of different types of pathologies in these neurodegenerative diseases. Yet our knowledge specific to the aSyn species within these inclusions predominantly come from IHC, IF and/or high-resolution microscopy studies that rely on the use of aSyn antibodies. Very few studies have looked at cryo-EM-based ultrastructural (Schweighauser et al., 2020) and proteome (Leverenz et al., 2007; Xia et al., 2008) characteristics of the aSyn-positive inclusions isolated directly from the human brain, and these have not yet systematically covered all the various neuronal and glial inclusion types encountered across different synucleinopathies. The biochemical profiling of the aSyn species isolated from post-mortem tissues (e.g. by sequential extraction, sucrose density centrifugation followed by downstream applications including WB and filter trap) is another means to understand the sequence, molecular and conformational properties of aSyn species, and also depends on the utilisation of reliable aSyn antibodies. Yet the vast majority of human post-mortem studies do not account for the PTMs or structural diversity of aSyn aggregates due to the limited availability of antibodies to target these different species. This necessitates the development, validation and application of a widened range of tools to re-visit, capture and characterise aSyn in all its pathological diversity across synucleinopathies.

1.3.3 Thesis objectives

The main objectives of this thesis are a) development and validation of a novel and comprehensive antibody toolset against different proteoforms of aSyn; and b) systematic and extensive profiling of the aSyn pathology across different brain regions and types of synucleinopathies. To fulfil these objectives, Chapter 2 focuses on the generation, validation and characterisation processes of aSyn antibodies using a recombinant library of aSyn proteins and aSyn KO neurons and mouse brain tissues. These antibodies are then used to screen the pathological diversity across LBDs, and for the first time the distribution of all key aSyn PTMs. We also describe briefly the aSyn PTMs in the neuronal and *in vivo* fibrillar seeding models. In Chapter 3, we focus

on the astrocytic aSyn pathology revealed in the LBD tissues, and describe the biochemical properties of these astrocytic accumulations. Finally, in Chapter 4, we specifically look at MSA brain tissues by immunohistochemical and biochemical approaches to describe the aSyn proteoforms in this specific type of synucleinopathy.

CHAPTER 2 Generation, validation and characterisation of alpha-synuclein antibodies as a novel toolset[1]

The abnormal aggregation and accumulation of aSyn in the brain is a defining hallmark of synucleinopathies. An increasing number of studies show that aSyn in pathological aggregates exists as a complex mixture of various post-translationally modified forms and conformations. The distribution of these different species changes during disease progression and varies among the different synucleinopathies. Current approaches for detecting aSyn in human tissues and disease models rely on a limited set of antibodies that have not been thoroughly assessed for their ability to capture the diversity of aSyn proteoforms and aggregation states, and thus are unlikely to provide an accurate evaluation of aSyn pathology in the brain. To address these challenges, we developed, validated, and characterized an expanded set of antibodies that target different sequences and PTMs along the entire length of aSyn, and recognize all conformations of the protein (monomers, oligomers and fibrils). We demonstrate that the use of multiple antibodies targeting different regions on aSyn is necessary to reveal the heterogeneity of aSyn pathology in human LBD brains, and in neuronal and animal models of aSyn aggregation and inclusion formation. We also present, for the first time, the profiling of aSyn pathology using antibodies against all its key post-translationally modified forms across sporadic and familial LBDs. The antibody validation pipeline we describe here paves the way for a more systematic investigation of the diversity of aSyn pathology in the human brain and peripheral tissues, and in cellular and animal models of synucleinopathies.

2.1 Introduction

Synucleinopathies are a subgroup of neurodegenerative diseases primarily including PD, DLB and MSA (Baba et al., 1998; Spillantini et al., 1998a, 1998b). Mounting evidence points to the aggregation and accumulation of the presynaptic protein aSyn

[1] The work presented in this chapter is part of the following publication in preparation:
Altay M.F., Kumar S.T., Burtscher J., Jagannath S., Miki Y., Parkkinen L., Holton J.L. and Lashuel H.A. (2022) Development and validation of an expanded antibody toolset that enables capturing alpha-synuclein pathological diversity in Lewy body diseases.

as critical processes in the pathophysiology of synucleinopathies: 1) Fibrillar and aggregated forms of aSyn are enriched in pathological inclusions that are the defining features of PD, DLB and MSA, including LBs, LNs, GCIs and NCIs (Baba et al., 1998; Spillantini et al., 1998b, 1998a); 2) mutations and duplications of the aSyn-encoding gene *SNCA* have been shown to cause familial forms of PD (Appel-Cresswell et al., 2013; Chartier-Harlin et al., 2004; Kapasi et al., 2020; Kiely et al., 2013; Krueger et al., 1998; Lesage et al., 2013; Pasanen et al., 2014; Polymeropoulos et al., 1997, 1996; Proukakis et al., 2013; Singleton et al., 2003; Spira et al., 2001; Zarranz et al., 2004); and 3) inoculation of recombinant aSyn fibrils or PD and MSA brain-derived aSyn aggregates is sufficient to induce LB-like inclusion formation in cellular and animal models (Kumar et al., 2021; Luk et al., 2012b, 2009; Mahul-Mellier et al., 2020, 2018; Tarutani et al., 2016; Volpicelli-Daley et al., 2014), and to induce the spreading of LB-like intracellular pathology in brain regions and along the gut-brain axis (Arotcarena et al., 2020; Dehay and Bezard, 2019; Recasens et al., 2014; Rey et al., 2016, 2013).

Despite aSyn being the common denominator of synucleinopathy brain pathology, increasing evidence suggests that aSyn within these inclusions exists as a mixture of different post-translationally modified and aggregated forms or strains of the protein (Anderson et al., 2006; Schweighauser et al., 2020; Shahmoradian et al., 2019). The morphology (Kuusisto et al., 2003), composition (Leverenz et al., 2007; Wakabayashi et al., 2013; Xia et al., 2008), structure (Shahmoradian et al., 2019; Strohaeker et al., 2019) and distribution (Alafuzoff et al., 2009) of the aSyn inclusions show considerable diversity (Figure 2. 1A) depending not only on the type of synucleinopathy but also on the cell type, the brain region and the individual patient concerned. At the fibril level, the recent cryo-EM studies of fibrils generated from full-length, truncated and modified recombinant and semisynthetic aSyn monomers *in vitro* revealed that aSyn is capable of forming fibrils of variable morphologies and conformations (Guerrero-Ferreira et al., 2019; B. Li et al., 2018) (Figure 2. 1B). Likewise, recent cryo-EM studies of fibrils isolated from MSA and DLB brains (Schweighauser et al., 2020) show polymorphism and suggest the presence of significant biochemical and structural heterogeneity in aSyn-related pathologies.

In the field of aSyn research, the detection, quantification and monitoring of aSyn pathology in LBs, GCIs and NCIs have largely depended on the use of antibodies

targeting different sequences, modifications or conformations of aSyn (Covell et al., 2017; Dhillon et al., 2017; Duda et al., 2002; Fayyad et al., 2020b; Giasson et al., 2000b; Henderson et al., 2020; Kovacs et al., 2012; Vaikath et al., 2015; Waxman et al., 2008). aSyn accumulating within the neuronal and glial inclusions is subjected to different types of PTMs at multiple residues (Figure 2. 1C), including phosphorylation, ubiquitination, nitration, acetylation and N- and C-terminal truncations. Of these modifications, aSyn pS129 has been described as the most common aSyn PTM in pathological aSyn aggregates, and aSyn pS129 levels have been reported to increase by multiple folds in PD, DLB and MSA brains (Anderson et al., 2006; Fujiwara et al., 2002). These observations have led to the emergence of aSyn pS129 as a key marker of aSyn pathology. Several antibodies against aSyn pS129 have been developed as the primary tools for assessing aSyn pathology formation and spreading in the central nervous system and peripheral tissues. However, the extent to which these antibodies capture the full spectrum of aSyn pathology has not been systematically investigated. Furthermore, recent findings support a potentially protective effect of aSyn pS129 (Ghanem et al., 2022), and therefore the absence of this modification does not necessarily indicate the absence of aSyn pathology.

Several immunohistochemical and mass spectrometry studies on the distribution of aSyn species in LBs and GCIs revealed the presence of various aSyn proteoforms that are cleaved at different residues within the C-terminal region of the protein (e.g. 1-115, 1-119, 1-122, 1-133, 1-135) (Anderson et al., 2006; Baba et al., 1998; Campbell et al., 2001; Dickson et al., 1999a; Gai et al., 1999; Kellie et al., 2015; Lewis et al., 2010; Moors et al., 2019; Ohrfelt et al., 2011; Tofaris et al., 2003; Tong et al., 2010), and of other aSyn C-terminal modifications, including phosphorylation and/or nitration at Y125, Y133 and Y136 (Chen et al., 2009; John E. Duda et al., 2000; Giasson et al., 2000a; Mahul-Mellier et al., 2014) (Figure 2. 1C). Interestingly, the most abundant C-terminally truncated species, i.e. aSyn 1-119 and 1-122 (Anderson et al., 2006; Bhattacharjee et al., 2019; Kellie et al., 2015; Killinger et al., 2018; Ohrfelt et al., 2011), lack the epitope for aSyn pS129 antibodies. Furthermore, the occurrence of several modifications in close proximity to S129 suggests that they may interfere with the immunoreactivity of several aSyn C-terminal or pS129 antibodies (Lashuel et al., 2022; Mahul-Mellier et al., 2018).

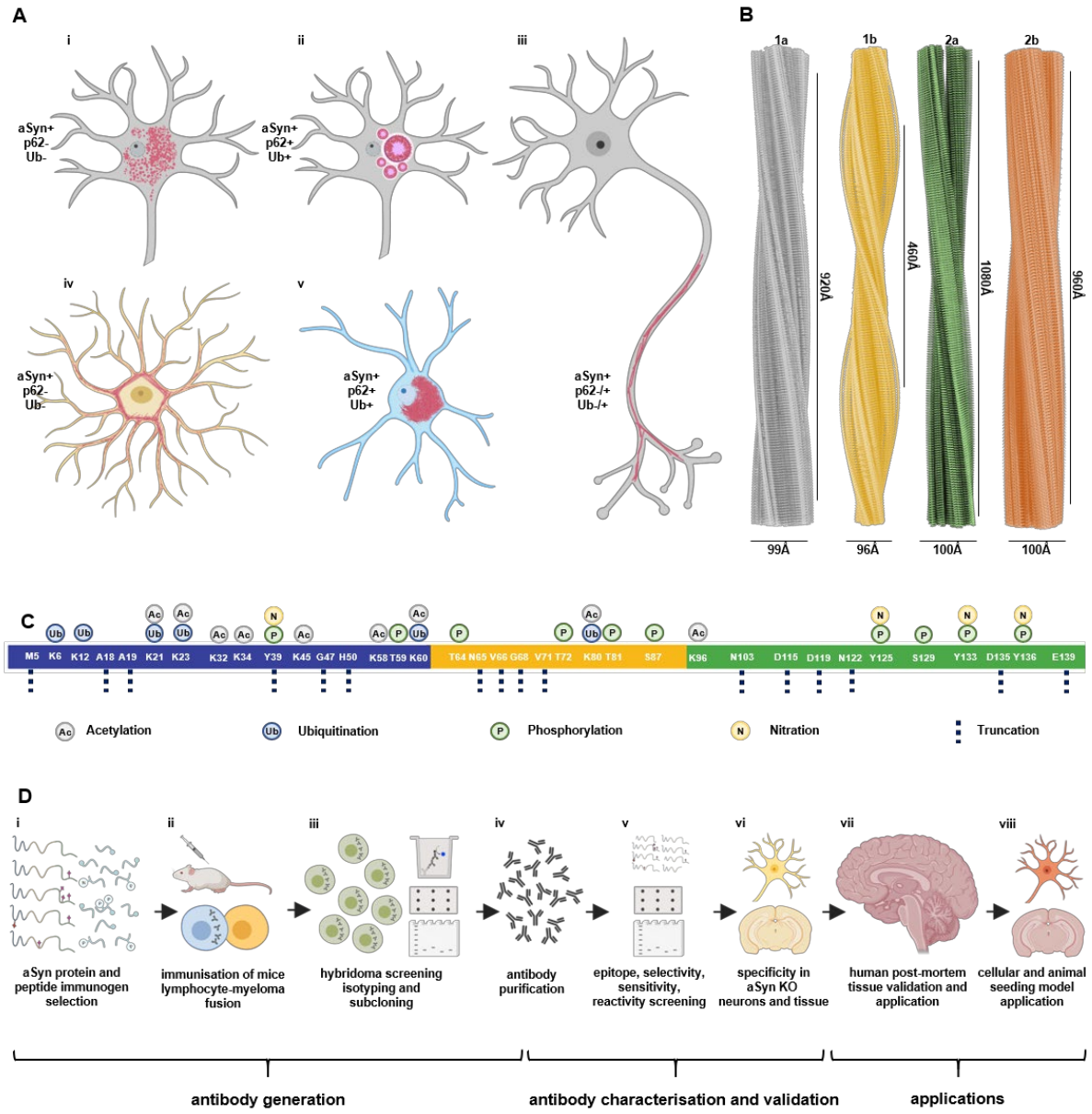

Figure 2. 1 **(A)** Diversity of aSyn pathology in synucleinopathies with **(Ai)** granular/ punctate cytoplasmic inclusions in the neurons; **(Aii)** classical LBs in the neuronal soma; **(Aiii)** LNs in the neuronal processes; **(Aiv)** astrocytic aSyn accumulations; **(Av)** oligodendroglial cytoplasmic inclusions. These pathological structures show differences in their positivity to aggregation markers, including ubiquitin (Ub) and p62. Schematic created with BioRender.com (agreement no: *QW23G6FJ76*). **(B)** Cryo-EM three-dimensional reconstructions of the recombinant full-length aSyn PFFs to show the polymorphism of aSyn fibrils generated *in vitro* (Guerrero-Ferreira et al., 2019; B. Li et al., 2018). Four distinct polymorphs were identified based on the protofilament fold and inter-protofilament interfaces: Polymorph 1a 'rod' (PDB-6CU7, EMD-7618); polymorph 1b 'twister' (PDB-6CU8, EMD-7619); polymorph 2a (PDB-6SSX, EMD-10307); and polymorph 2b (PDB-6SST, EMD-10305). **(C)** aSyn PTMs identified in synucleinopathy brain tissues, which include acetylation, ubiquitination, phosphorylation, nitration and truncation across the whole sequence of the protein. **(D)** A schematic representation of the steps followed for the generation, characterisation, validation and application of the novel aSyn monoclonal mouse antibodies. These involved (**Di**) antibody design via the selection of immunogens comprising of aSyn recombinant proteins and peptides; (**Dii**) immunisation of the mice followed by lymphocyte-myeloma fusion; (**Diii**) screening of the hybridomas via ELISA, DB and WB, isotyping and

subcloning, and (**Div**) acquisition of purified antibodies. These antibodies were then (**Dv**) characterised using a library of aSyn recombinant proteins for their epitopes, conformational selectivity, sensitivity, specificity and reactivity via DB and WB. The antibody specificity was then further validated on (**Dvi**) aSyn KO mouse primary hippocampal and cortical neurons, and in aSyn KO mouse amygdala tissues. (**Dvii**) The antibodies were validated on human brain tissues of different LBDs. (**Dviii**) The mouse aSyn-reactive antibodies were applied to neuronal seeding model and PFF-injected mouse brain tissues to profile the newly formed aggregates. Schematic created with BioRender.com (agreement no: *FN23G6E1SR*). aSyn = alpha-synuclein; DB = dot blot; cryo-EM = cryogenic electron microscopy; ELISA = enzyme-linked immunoassay; KO = knockout; LB = Lewy body; LBD = Lewy body disease; LN = Lewy neurite; PFFs = pre-formed fibrils; PTM = post-translational modification; Ub = ubiquitin; WB = Western blot

Interestingly, a large part of the immunohistochemistry and biochemistry studies on human brain samples, including the PD staging work by Braak and colleagues (Braak et al., 2001, 2003b, 2002), has relied primarily on the use of antibodies with epitopes against the C-terminal region of aSyn. Yet, these most commonly used antibodies are less likely to capture truncated forms of aSyn, aggregated but not yet phosphorylated aSyn, or aggregated aSyn bearing multiple C-terminal modifications (Anderson et al., 2006; Chen et al., 2009; Giasson et al., 2000a; Kiely et al., 2013; Mahul-Mellier et al., 2014). Reliance on a single or a restricted number of antibodies in human post-mortem, cellular and *in vivo* studies thus may significantly underestimate the amount, and under-represent the diversity, of aSyn pathology. Furthermore, the cellular environment dramatically influences the kinetics of aSyn aggregation, fibril polymorphism and PTMs (Peng et al., 2018). It is likely that the aSyn aggregates formed in the different types of synucleinopathies, or at different stages of disease progression, possess distinct biochemical and structural signatures that expose amino acid sequences and antibody epitopes differentially. Therefore, it is crucial to use multiple, well-characterized and validated antibodies to elucidate the biochemical and structural features underlying the pathological heterogeneity of aSyn in different synucleinopathies (Baba et al., 1998; Covell et al., 2017; Dhillon et al., 2017; Duda et al., 2000b; Giasson et al., 2000b). If successfully deciphered, these differences could be exploited to develop novel approaches to identify disease-specific biomarkers for PD and other synucleinopathies. They will also improve our currently insufficient understanding of the association of aSyn pathology and disease progression (Jellinger, 2009; Milber et al., 2012; Steiner et al., 2018).

Towards this goal, we sought to develop an antibody toolbox that would enable capturing the diversity of soluble, aggregated and post-translationally modified forms of aSyn, thus making it possible to profile the full heterogeneity of aSyn pathology in post-mortem LBD brains. First, a combination of peptides and WT or site-specifically modified aSyn proteins were designed and used as immunogens to identify antibodies targeting different epitopes and modifications along the sequence of aSyn. The newly generated antibodies were complemented with a selection of pre-existing antibodies, and these were then systematically characterised with regards to their a) epitopes and species reactivity; b) sensitivities to aSyn PTMs neighbouring their epitopes; and c) conformational selectivity, using a library of recombinant aSyn monomers, oligomers and fibrils (Figure 2. 1D). We validated their specificity to aSyn by employing aSyn KO mouse neurons and brain tissues. The antibodies were then titrated for use on post-mortem synucleinopathy tissues. We selected a subset of antibodies that would allow the full coverage of the N-terminus, NAC and C-terminus regions of aSyn as well as the post-translationally modified aSyn forms. The antibodies were next used to profile the pathological diversity in sporadic and familial LBDs. The use of this expanded toolbox revealed distinct and heterogeneously modified aSyn pathologies rich in pS129, but also in N-terminal nitration at Tyrosine 39 (Y39) and in N- and C-terminal tyrosine phosphorylations, scattered both to neurons and glial cells. To the best of our knowledge, this is the first study to employ antibodies targeting all disease-associated PTMs to profile aSyn brain pathology in the same set of cases. Finally, we used these validated antibodies to assess the dispersion of differentially modified aSyn aggregates in seeding-based cellular and animal models. Altogether, our results highlight the critical importance of re-visiting human tissues and cellular/tissue samples from model organisms using toolsets that capture the diversity of aSyn species. This is a necessary first step towards understanding the relationship between aSyn pathology formation, neurodegeneration, disease symptomatology and disease progression.

2.2 Results

2.2.1 Design, development and generation of aSyn mouse monoclonal antibodies

To generate antibodies that capture the biochemical and structural diversity of aSyn, we employed a collection of human aSyn proteoforms as antigens. These included large peptide fragments and proteins spanning the three regions and pathology-associated PTMs of aSyn (Table 2. 1). The C-terminal region of aSyn was extensively covered by using antigen sequences encompassing aSyn residues 108-120, 113-127 and 108-140, to ensure that all the disease-associated C-terminal truncations are targeted. To increase the likelihood of generating antibodies with epitopes in the N-terminal and/or the NAC region of the protein, human aSyn full-length (1-140) and aSyn 1-119 recombinant proteins and aSyn 1-20 peptide were employed as immunogens. For the generation of aSyn pS129 antibodies, we initiated two programmes – one with human aSyn 124-135 peptide phosphorylated at S129 (aSyn 124-135 pS129), and another one with human aSyn 120-135 peptide doubly phosphorylated at Y125 and S129 (aSyn 120-135 pY125/pS129). This way, we sought to develop phospho-specific antibodies that would detect aSyn pS129 even in the presence of neighbouring PTMs. Lastly, the mice were immunised with aSyn 34-45 peptide nitrated at Y39 (aSyn 34-45 nY39) to produce monoclonal antibodies against this N-terminal PTM, for which there are no validated antibodies currently available. Following the immunisation of the BALB/c mice, test bleeds, hybridoma supernatants and subclones were analysed via ELISA, WB and slot/dot blot (DB) against a selected library of aSyn proteins (Table 2. 2) to determine the strongest and the most specific antibody response. Details of the monoclonal antibody generation process are provided in the 2.4 Materials and Methods section. A total of 12 aSyn mouse monoclonal antibodies were obtained (Table 2. 3), the purity of which was validated by SDS-PAGE/Coomassie staining and WB.

Table 2. 1 A list of all the programmes initialised to generate monoclonal antibodies against aSyn.

programme	immunogen	protein or peptide origin	carrier	antigen sequence
LASH-EGT403	UniProtKB - P37840 (SYUA_HUMAN) **1-20**	Eurogentec	KLH	MDVFMKGLSK AKEGVVAAAE
LASH-EGT404	UniProtKB - P37840 (SYUA_HUMAN) **1-140**	Eurogentec	n/a	recombinant aSyn human FL (1-140)
LASH-EGT405	UniProtKB - P37840 (SYUA_HUMAN) **113-127**	Eurogentec	KLH	LEDMPVDP DNEAYEM
LASH-EGT406	UniProtKB - P37840 (SYUA_HUMAN) **108-120**	Eurogentec	KLH	PQE GILEDMPVDP
LASH-EGT407	UniProtKB - P37840 (SYUA_HUMAN) **124-135 pS129**	Eurogentec	KLH	AYEMP(pS)E EGYQD
LASH-EGT408	UniProtKB - P37840 (SYUA_HUMAN) **108-140**	Lashuel Laboratory	n/a	PQE GILEDMPVDP DNEAYEMPSE EGYQDYEPEA
LASH-EGT409	UniProtKB - P37840 (SYUA_HUMAN) **120-135 pY125/pS129**	Eurogentec	KLH	P DNEA(pY)EM P(pS)E EGYQD
LASH-EGT410	UniProtKB - P37840 (SYUA_HUMAN) **1-119**	Lashuel Laboratory	n/a	recombinant aSyn human 1-119
LASH-EGT416	UniProtKB - P37840 (SYUA_HUMAN) **34-45 nY39**	Eurogentec	KLH	KEGVL(nY)VGSKTK

aSyn = alpha-synuclein; FL = full-length

Table 2. 2 A list of all aSyn proteins and peptides included in this study.

protein/ peptide	Mw/ Da	protein/ peptide	Mw/ Da	protein/ peptide	Mw/ Da	protein/ peptide	Mw/ Da
aSyn 1-11	1,227	aSyn h 1-133	13,627	aSyn h FL	14,460	aSyn h pS129	14,540
aSyn h 1-101	10,062	aSyn h 1-135	13,871	bSyn h FL	14,288	aSyn h pY125/pY133/pY136	14,745
aSyn h 1-110	11,045	aSyn h 5-140	13,968	aSyn h Y39F	14,444	aSyn m 1-120	12,222
aSyn h 1-114	11,457	aSyn h 39-140	10,600	aSyn h Y133/136F nY39	14,490	aSyn m Δ120-125	13,881
aSyn h 1-115	11,572	aSyn h 65-140	7,872	aSyn h nY39	14,522	aSyn m Δ133-135	14,079
aSyn h 1-119	12,015	aSyn h 71-140	7,374	aSyn h nY125	14,522	aSyn m 20-140	12,551
aSyn h 1-120	12,112	aSyn h Δ111-115	13,933	aSyn h pY39	14,540	aSyn m FL	14,485
aSyn h 1-122	12,341	aSyn h Δ111-115/133-135	13,526	aSyn h pS87	14,540	aSyn m E114A	14,427
aSyn h 1-123	12,470	aSyn h Δ120-125	13,770	aSyn h pY125	14,540	aSyn m D115A	14,441
aSyn h 1-124	12,541	aSyn h Δ133-135	14,054	aSyn h pY125/S129	14,620	aSyn m pS129	14,580

aSyn = alpha-synuclein; bSyn = beta-synuclein; Da = dalton; FL = full-length; h = human; m = mouse; Mw = molecular weight

Table 2. 3 A list of all the purified antibodies after finalisation of the monoclonal antibody generation programmes.

antibody full name	antibody short name	epitope	species/ clonality	isotype	reactivity	concentration	amount
LASH-EGT403 6D10-F10	LASH-EGT403	1-5	mouse monoclonal	IgG1 K	human, mouse	1.1mg/mL	56.2mg
LASH-EGT410 5B10-A12	5B10-A12	1-10	mouse monoclonal	IgG1 K	human, mouse	1.4mg/mL	56.2mg
LASH-EGT406 2F10-E12	2F10-E12	110-115	mouse monoclonal	IgG1 K	human, mouse	1.8mg/mL	79.7mg
LASH-EGT405 7H10-E12	7H10-E12	115-125	mouse monoclonal	IgG1 K	human	1.6mg/mL	38.4mg
LASH-EGT408 4E9-C12	4E9-C12	121-132	mouse monoclonal	IgG1 K	human	1.2mg/mL	35.5mg
LASH-EGT405 2C4-B12	2C4-B12	123-125	mouse monoclonal	IgG1 K	human	1.0mg/mL	28.7mg
LASH-EGT408 4E9-G10	4E9-G10	120-125	mouse monoclonal	IgG1 K	human	0.9mg/mL	26.5mg
LASH-EGT410 6B2-D12	6B2-D12	126-132	mouse monoclonal	IgG1 K	human, mouse	1.2mg/mL	37.2mg
LASH-EGT410 1F10-B12	1F10-B12	121-125	mouse monoclonal	IgG1 K	human	1.2mg/mL	36.7mg
LASH-EGT406 6A3-E9	6A3-E9	aS-120	mouse monoclonal	IgG1 K	human	1.0mg/mL	23.0mg
LASH-EGT416 5E1-G8	5E1-G8	nY39	mouse monoclonal	IgG1 K	human, mouse	1.3mg/mL	52.2mg
LASH-EGT416 5E1-C10	5E1-C10	nY39	mouse monoclonal	IgG1 K	human, mouse	1.3mg/mL	53.1mg

2.2.2 Characterisation of aSyn antibodies using recombinant synuclein proteins and peptides

a) Epitope mapping and sequential specificity

Using aSyn and beta-synuclein (bSyn) recombinant protein standards (Table 2. 2), we first sought to assess the sequential specificity of our novel monoclonal aSyn antibodies and narrow down their epitopes by DB (Figure 2. 2A) and WB (Figure 2. 3). The two antibodies, LASH-EGT403 and 5B10-A12, targeted the N-terminus of aSyn, i.e. residues 1-5 and 1-10, respectively. All the other novel monoclonal antibodies were mapped to the C-terminal region spanning residues 110-132, and showed staggered coverage of this region of the protein (Figure 2. 2B; Table 2. 3). The epitopes of these seven antibodies were mapped to residues 110-115 (2F10-E12), 115-125 (7H10-E12), 120-125 (4E9-G10), 121-125 (1F10-B12), 121-132 (4E9-C12), 123-125 (2C4-B12) and 126-132 (6B2-D12). The results of the epitope mapping of all the novel monoclonal antibodies are summarised in Figure 2. 2B (antibodies marked with *).

The newly produced monoclonal antibodies alone were not sufficient to achieve full coverage of the aSyn sequence. Therefore, we expanded the antibody set to include in-house polyclonal aSyn antibodies (Figure 2. 2B, antibodies marked with **), as well as a number of commercially available and frequently used aSyn antibodies (Figure 2. 2B, antibodies marked with ***). It is worth noting that, of these commercial antibodies, LASH-BL 34-45, LASH-BL 80-96, LASH-BL 117-122, LASH-BL A15127A (120-122) as well as LASH-BL pY39 were developed jointly with Biolegend (Figure 2. 2B, antibodies marked with *°*). The epitopes and sequential specificities of all these antibodies were validated by DB and WB (Figure 2. 2A-B; Figure 2. 3). We mapped the epitope of the homemade polyclonal LASH-EGTNter antibody to aSyn residues 1-20. For all the commercial antibodies, the epitopes we identified were similar to those reported in the literature (Figure 2. 2A-B; Figure 2. 3).

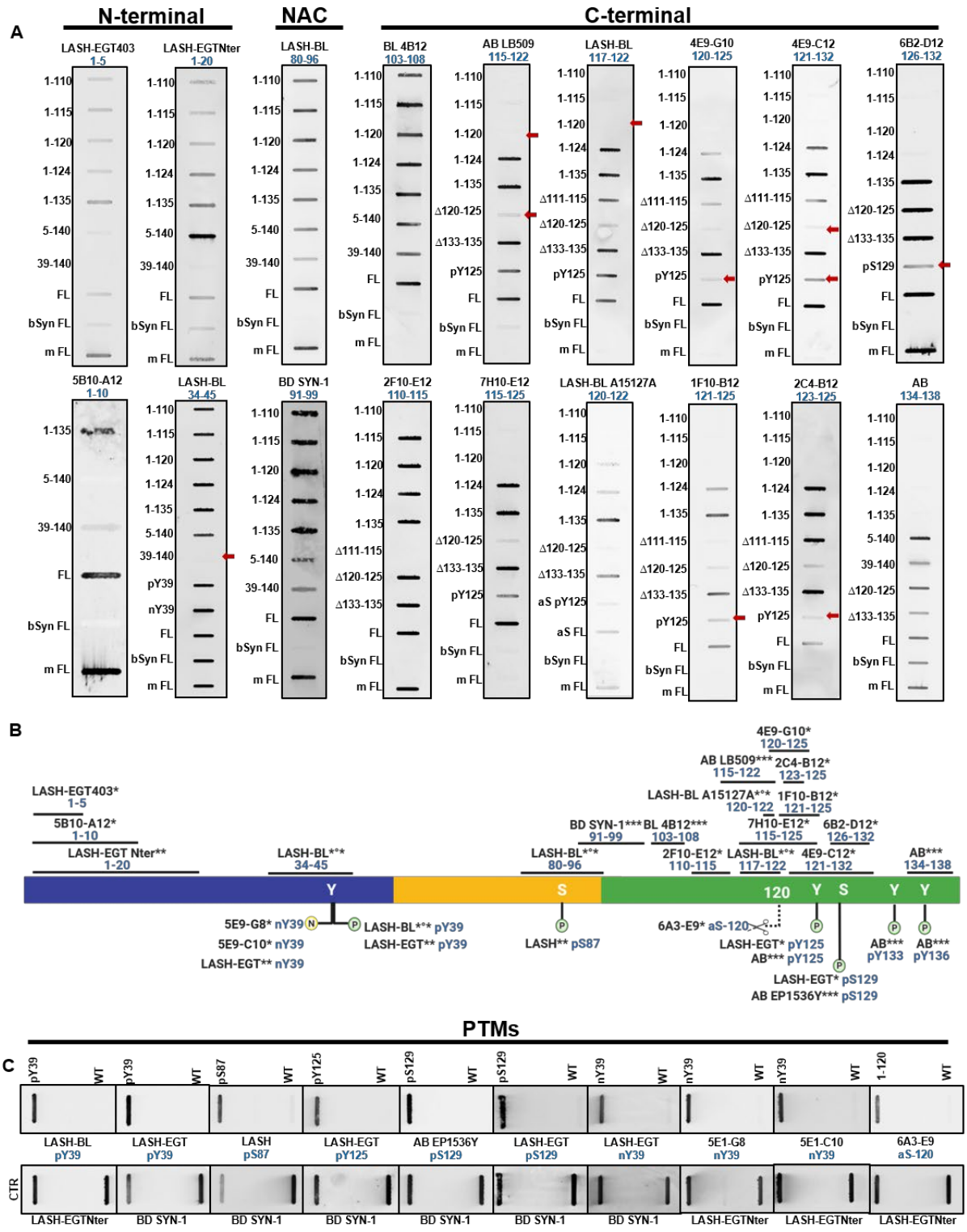

Figure 2. 2 Validation and epitope mapping of aSyn antibodies. **(A)** DB validation of the novel monoclonal, in-house polyclonal and commercially available aSyn antibodies against the N-terminal, non-amyloid component (NAC) and the C-terminal regions of aSyn for epitope mapping, specificity and species reactivity using a selected library of aSyn and bSyn recombinant proteins under native conditions. Protein loading control was run via Ponceau S staining. All loaded proteins represent human aSyn forms except for human bSyn and mouse aSyn full-length (m FL) proteins. **(B)** A schematic to represent the novel monoclonal (marked with *), in-house polyclonal (marked with **) and pre-existing commercial aSyn antibodies (marked with ***) included in this study. The commercial antibodies

developed jointly with Biolegend are marked with *°*. The epitope information of each antibody is indicated in blue. Schematic created with BioRender.com (agreement no: *JR23G6G5LA*). **(C)** Validation of the aSyn PTM antibodies via DB screening. aSyn = alpha-synuclein; bSyn = beta-synuclein; DB = dot blot; FL = full-length; m = mouse; PTM = post-translational modification

In addition to the antibodies against non-modified aSyn, we also generated novel monoclonal antibodies that target specific aSyn PTMs. Three aSyn PTM antibodies were developed, two of which were mapped to aSyn nY39 (5E9-G8 and 5E9-C10), and one to aSyn truncated at residue 120 (6A3-E9) by DB and WB (Figure 2. 2B-C; Figure 2. 4A). Amongst the monoclonal antibodies against aSyn nY39, we observed that 5E1-G8 was weakly positive to aSyn WT and aSyn nY39 by WB (Figure 2. 4A, red arrow) but not by DB (Figure 2. 2C). On the other hand, the other monoclonal antibody 5E1-C10 was positive only for aSyn nY39 both by DB and WB (Figure 2. 2C; Figure 2. 4A). The specificity of 6A3-E9 was further validated via supplementary DB, WB and surface plasmon resonance (SPR) analyses (Figure 2. 4B-D), all of which showed that it only detects human aSyn cleaved at residue 120. We complemented our battery of antibodies against the aSyn PTMs with the previously generated in-house polyclonal antibodies against aSyn nY39 (LASH-EGT nY39), aSyn pY39 (LASH-EGT pY39), aSyn pS87 (LASH pS87), aSyn pY125 (LASH-EGT pY125), aSyn pS129 (LASH-EGT pS129), with the monoclonal aSyn pY39 antibody generated in collaboration with Biolegend (LASH-BL pY39) and with the commercially available aSyn pS129 antibody AB EP1536Y, which were also screened and validated in parallel to the novel monoclonal aSyn PTM antibodies. These antibodies were found to be specific to their targeted modifications by DB and WB (Figure 2. 2B-C; Figure 2. 4A). Altogether, this selection provided us with 18 aSyn non-modified and 10 aSyn PTM antibodies to work with.

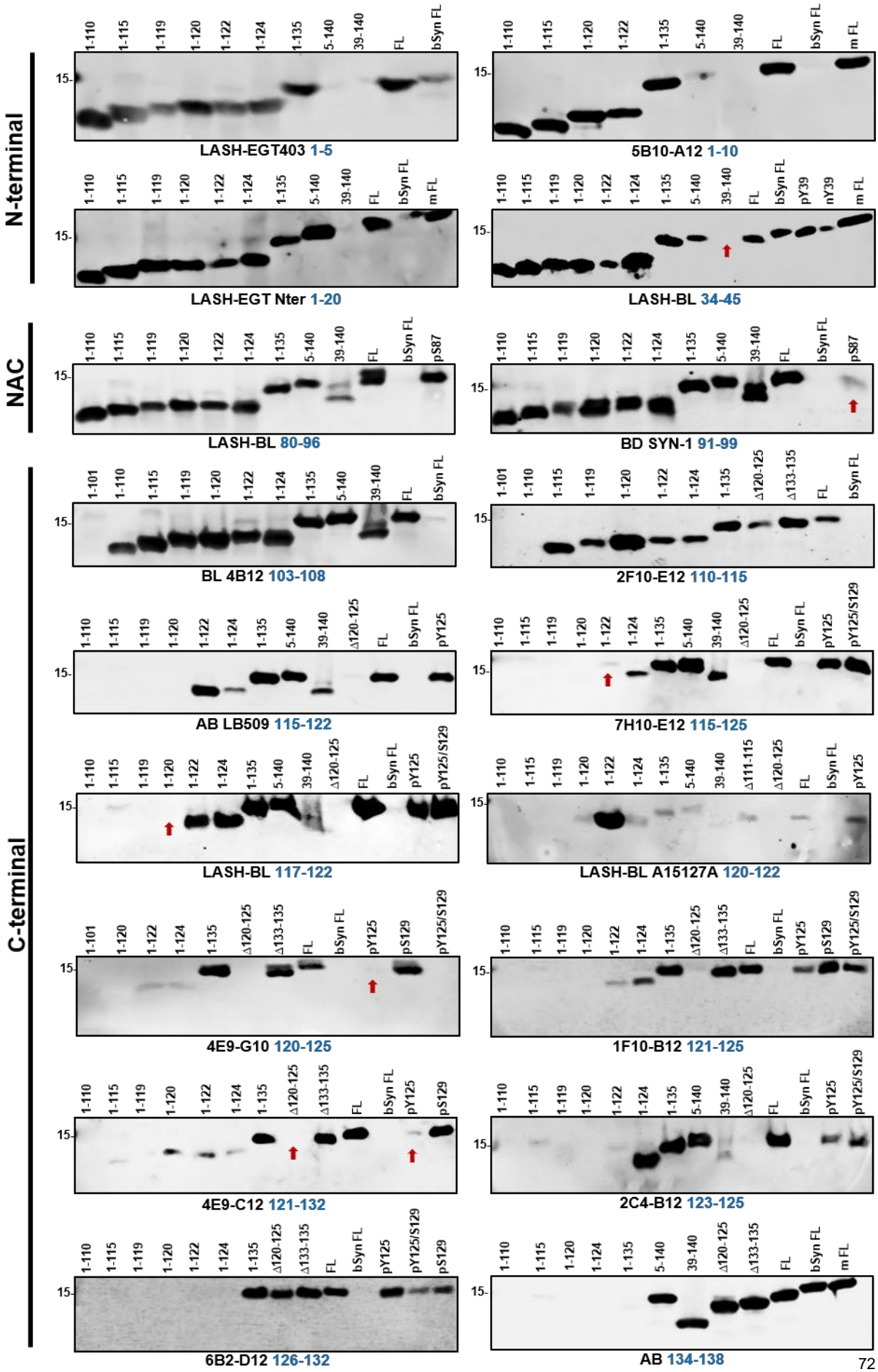
N-terminal
NAC
C-terminal
LASH-EGT403 1-5
5B10-A12 1-10
LASH-EGT Nter 1-20
LASH-BL 34-45
LASH-BL 80-96
BD SYN-1 91-99
BL 4B12 103-108
2F10-E12 110-115
AB LB509 115-122
7H10-E12 115-125
LASH-BL 117-122
LASH-BL A15127A 120-122
4E9-G10 120-125
1F10-B12 121-125
4E9-C12 121-132
2C4-B12 123-125
6B2-D12 126-132
AB 134-138

Figure 2. 3 Validation and epitope mapping of aSyn antibodies. WB validation of the novel monoclonal, in-house polyclonal and commercially available aSyn antibodies against the N-terminal, non-amyloid component (NAC) and the C-terminal regions of aSyn for epitope mapping, specificity and species reactivity using a selected library of aSyn recombinant proteins under denatured conditions. Protein loading control was run via re-blotting the membranes with complementary aSyn antibodies. All loaded proteins represent human alpha-synuclein (aSyn) forms except for human beta-synuclein (bSyn) and mouse aSyn full-length (m FL) proteins. aSyn = alpha-synuclein; bSyn = beta-synuclein; FL = full-length; m = mouse; WB = Western blot

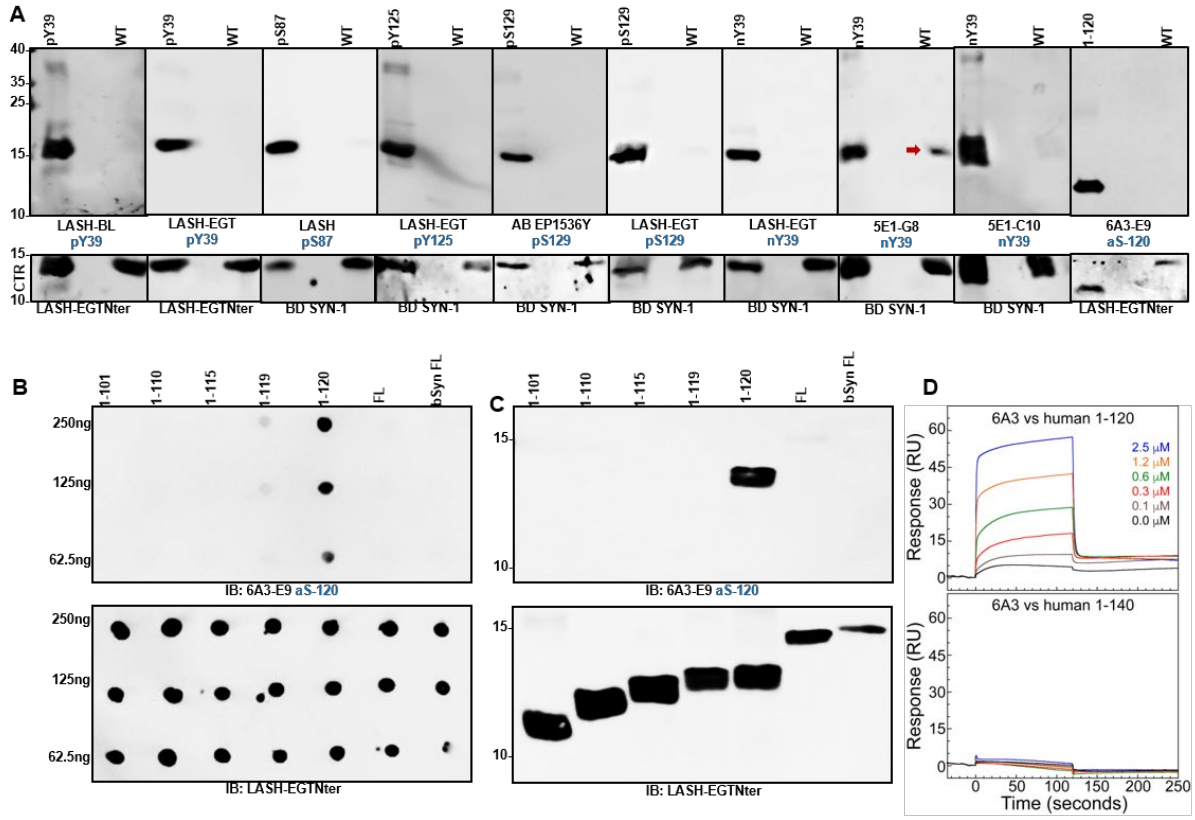

Figure 2. 4 Validation of the aSyn PTM antibodies via DB, WB and SPR using human recombinant aSyn standards. In-house and commercial aSyn PTM antibodies were validated by (A) WB screening. Further (B) DB and (C) WB analyses on 6A3-E9 showed that this antibody is specific to human aSyn truncated at residue 120. (D) SPR sensograms showed the binding responses of immobilised antibody 6A3-E9 against varying concentrations of aSyn human 1-120 (top) or aSyn human full-length (bottom). aSyn = alpha-synuclein; DB = dot blot; PTM = post-translational modification; SPR = surface plasmon resonance; WB = Western blot; WT = wild-type

b) Sensitivity to neighbouring aSyn PTMs

We have recently shown that the aSyn pS129 antibody binding could be affected by the presence of aSyn PTMs neighbouring S129 (Lashuel et al., 2022), and hypothesised that sensitivity to neighbouring PTMs could also be applicable to other

C-terminal as well as N-terminal or NAC region antibodies. Therefore, we investigated the reactivity of the non-modified aSyn antibodies in the presence of PTMs nearby their epitopes by DB and WB, and the results are summarised in Table 2. 4. We note that a large number of the aSyn C-terminal antibodies (i.e. 8 out of 12) showed sensitivity to the presence of aSyn pY125 and/or truncations across residues ~119-125 (Table 2. 4). In the presence of aSyn pY125, for instance, antibody 4E9-G10 (120-125) failed to produce a positive result both by DB and WB (Figure 2. 2A; Figure 2. 3, red arrow). This finding is in line with the mapped epitope of this antibody (Figure 2. 2B), which covers Y125. Therefore, phosphorylation of this residue may hinder the antibody recognition. Similarly, the antibody 4E9-C12 (121-132) generated a weaker signal by DB and WB when aSyn pY125 was present or if residues 120-125 were absent (Figure 2. 2A; Figure 2. 3, red arrows). Interestingly, the antibodies 1F10-B12 (121-125) and 2C4-B12 (123-125) were sensitive to this modification only by DB (Figure 2. 2A, red arrows), but were not noticeably affected by the presence of aSyn pY125 under the denaturing conditions of WB (Figure 2. 3). The 6B2-D12 (126-132) positive signal was weakened in the presence of aSyn pS129, especially by DB (Figure 2. 2A, red arrow). The positive signals revealed by AB LB509 (115-122), 7H10-E12 (115-125) and LASH-BL 117-122 were all affected by C-terminal truncations roughly between residues 119-125 (Figure 2. 2A; Figure 2. 3, red arrows), but less so by the presence of aSyn pY125. We expanded the same analysis to the NAC region and N-terminal antibodies. Of the two antibodies with epitopes in the NAC region, the BD SYN-1 (91-99) signal appeared to be weaker when aSyn is phosphorylated at Serine 87 (Figure 2. 3, red arrow), whereas this modification did not have an impact on the positivity of LASH-BL 80-96. The LASH-BL 34-45 antibody showed no sensitivity to the presence of nY39 or pY39, but lost all positive signal with the N-terminal truncation at residue 39 (Figure 2. 2A; Figure 2. 3, red arrows). Collectively, our results highlight that the antibody sensitivities to the presence of PTMs should always be considered before aSyn antibodies are selected for prospective experimental studies.

Table 2. 4 Characterisation of non-modified aSyn antibodies using recombinant synuclein proteins and peptides. aSyn = alpha-synuclein; bSyn = beta-synuclein; DB = dot blot; f = fibril; hu = human; m = monomer; mus = mouse; o = oligomer; PTM = post-translational modification; WB = Western blot

antibody	epitope	species reactivity	bSyn detection	neighbouring PTM sensitivity	conformational selectivity	
					WB	DB
LASH-EGT403	1-5	hu, mus	yes	-	m/ o/ f	m/ o/ f
5B10-A12	1-10	hu, mus	-	truncation at ~5	m/ o/ f	m/ o/ f
LASH-EGTNter	1-20	hu, mus	yes	-	m/ o/ f	m/ o/ f
LASH-BL 34-45	34-45	hu, mus	yes	truncation at ~39	m/ f	m/ o/ f
LASH-BL 80-96	80-96	hu, mus	-	-	m/ o/ f	m/ o/ f
BD SYN-1	91-99	hu, mus	-	pS87	m/ o/ f	m/ o/ f
BL 4B12	103-108	hu	-	-	m/ o/ f	m/ o/ f
2F10-E12	110-115	hu, mus	-	-	m/ o/ f	m/ o/ f
AB LB509	115-122	hu	-	truncation at ~119-122	m/ o/ f	m/ o/ f
7H10-E12	115-125	hu	-	truncation at ~119-125	m/ o/ f	m/ o/ f
LASH-BL 117-122	117-122	hu	-	truncation at ~119-122	m/ o/ f	m/ o/ f
LASH-BL A15127A	120-122	hu	-	pY125	m/ o/ f	m/ o/ f
4E9-G10	120-125	hu	-	pY125	m/ o/ f	m/ o/ f
1F10-B12	121-125	hu	-	pY125 (DB only)	m/ o/ f	m/ o/ f
4E9-C12	121-132	hu	-	truncation at ~125, pY125	m/ o/ f	m/ o/ f
2C4-B12	123-125	hu	-	pY125 (DB only)	m/ o/ f	m/ o/ f
6B2-D12	126-132	hu, mus	-	pS129 (DB only)	m/ o/ f	m/ o/ f
AB 134-138	134-138	hu, mus	yes	-	m/ o/ f	m/ o/ f

aSyn = alpha-synuclein; bSyn = beta-synuclein; DB = dot blot; f = fibril; hu = human; m = monomer; mus = mouse; o = oligomer; PTM = post-translational modification; WB = Western blot

c) Species reactivity

Next, we assessed the reactivity of the full antibody panel to human and mouse aSyn. All N-terminal and NAC-region antibodies, including LASH-EGT403 (1-5), 5B10-A12 (1-10), LASH-EGTNter (1-20), LASH-BL (34-45), LASH-BL (80-96) and BD SYN-1 (91-99) were identified as both human- and mouse-reactive (Figure 2. 2A). The large majority of the C-terminal antibodies, on the other hand, detected only human aSyn proteins, with the exception of 2F10-E12 (110-115), 6B2-D12 (126-132) and Abcam (134-138) antibodies that were reactive to both human and mouse aSyn (Figure 2. 2A). These findings are consistent with the sequence differences between human and mouse aSyn in the C-terminus, particularly across the region covering residues 115-125 (Figure 2. 5A). Interestingly, the N-terminal antibodies LASH-EGT403 (1-5), LASH-EGTNter (1-20), LASH-BL (34-45) and the extreme C-terminal antibody AB (134-138) showed reactivity also to bSyn, whereas the N-terminal antibody 5B10-A12 (1-10), the NAC-region antibodies and the rest of the C-terminal antibodies were negative to bSyn (Figure 2. 2A; Figure 2. 3). These results are consistent with the sequence similarities and differences between aSyn and bSyn (Figure 2. 5B). All antibodies used in this study are listed in Table 2. 5.

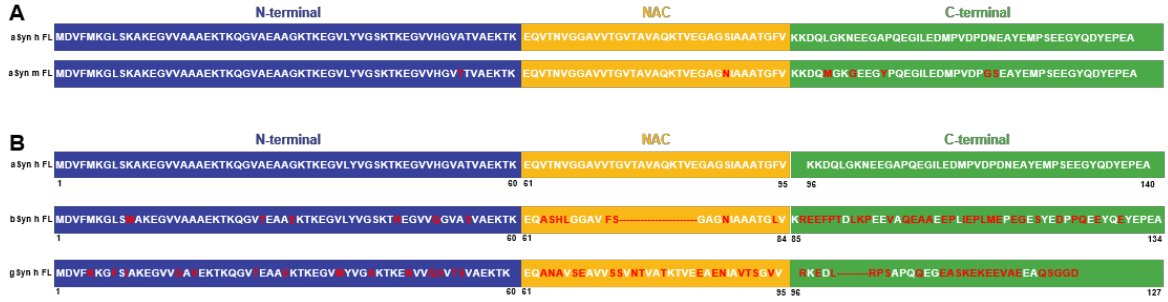

Figure 2. 5 Amino acid sequences of aSyn, of its mouse orthologue and its protein homologues. **(A)** The amino acid sequence of aSyn human and its mouse orthologue. The residue differences between the two proteins are highlighted in red. **(B)** The synuclein family comprises three homologous proteins – alpha (aSyn), beta (bSyn) and gamma synuclein (gSyn). Only alpha- and beta-synuclein were included in this study. The sequence differences are highlighted in red.

d) Conformational selectivity

aSyn exists in different conformations in healthy and diseased human tissues (Covell et al., 2017; Gai et al., 2003; Kovacs et al., 2012; Roberts et al., 2015; Spillantini et al., 1998a, 1998b). Therefore, we sought to determine the selectivity of the antibodies against non-modified aSyn towards the different aSyn conformations. To this end, DB and WB analyses were run on purified recombinant aSyn WT monomers, oligomers and fibrils (Figure 2. 6A-B; Table 2. 4), which were prepared and characterized as described previously (Kumar et al., 2020b). Electron microscopy (EM) analysis revealed that monomers, oligomers and fibrils of aSyn exhibit morphological differences (Figure 2. 6A). Interestingly, all antibodies were strongly positive for all conformations of aSyn both by DB and WB except for LASH-BL 34-45, which was positive for aSyn monomers, oligomers and fibrils by DB, but lost its positivity to high-molecular weight (HMW) aSyn oligomers under denatured conditions (Figure 2. 6B, red arrow). These results suggest that the vast majority of the selected antibodies are capable of recognizing all conformations and aggregation states of aSyn.

Table 2. 5 A list of all the primary and secondary antibodies used in this study.

primary antibodies						
antibody name	**epitope**	**species/ clonality**	**reactivity**	**concentration (mg/mL)**	**company**	**catalogue #**
LASH-EGT403	aSyn 1-5	mus mc	h, m	1.12	-	-
5B10-A12	aSyn 1-10	mus mc	h, m	1.40	-	-
LASH-EGTNter	aSyn 1-20	rab pc	h, m	1.34	-	-
LASH-BL 34-45	aSyn 34-45	mus mc	h, m	1.00	Biolegend	849102
LASH-BL 80-96	aSyn 80-96	mus mc	h, m	1.00	Biolegend	848302
BD SYN-1	aSyn 91-99	mus mc	h, m	0.25	BD Transduction	BD610787
BL 4B12	aSyn 103-108	mus mc	h	1.00	Biolegend	807801
2F10-E12	aSyn 110-115	mus mc	h, m	1.81	-	-
AB LB509	aSyn 115-122	mus mc	h	1.00	Abcam	ab27766
7H10-E12	aSyn 115-125	mus mc	h	1.60	-	-
LASH-BL 117-122	aSyn 117-122	mus mc	h	1.53	Biolegend	848601
LASH-BL A15127A	aSyn 120-122	mus mc	h	5.19	Biolegend	848401
4E9-G10	aSyn 120-125	mus mc	h	0.89	-	-
1F10-B12	aSyn 121-125	mus mc	h	1.23	-	-
4E9-C12	aSyn 121-132	mus mc	h	1.18	-	-
2C4-B12	aSyn 123-125	mus mc	h	0.96	-	-
6B2-D12	aSyn 126-132	mus mc	h, m	1.24	-	-
AB 134-138	aSyn 134-138	rab pc	h, m	1.00	Abcam	ab131508
LASH-BL pY39	aSyn pY39	mus mc	h	1.00	Biolegend	849201
LASH-EGT pY39	aSyn pY39	rab pc	h, m	0.50	-	-
LASH pS87	aSyn pS87	rab pc	h	0.40	-	-
LASH-EGT pY125	aSyn pY125	rab pc	h	0.20	-	-
AB pY125	aSyn pY125	rab pc	h	0.50	Abcam	ab10789
AB EP1536Y	aSyn pS129	rab mc	h, m	2.68	Abcam	ab51253
LASH-EGT pS129	aSyn pS129	rab pc	h, m	0.10	-	-
BL 81A	aSyn pS129	mus mc	h, m	1.00	Biolegend	825701
BL 81A biotin	aSyn pS129	mus mc	h, m	0.50	Biolegend	824704
AB MJF-R13	aSyn pS129	rab mc	h, m	4.20	Abcam	ab168381
AB pY133	aSyn pY133	rab pc	h, m	1.50	Abcam	ab194910
AB pY136	aSyn pY136	rab pc	h, m	1.00	Abcam	ab131491
LASH-EGT nY39	aSyn nY39	rab pc	h, m	0.53	-	-
5E1-G8	aSyn nY39	mus mc	h, m	1.31	-	-
5E1-C10	aSyn nY39	mus mc	h, m	1.27	-	-
6A3-E9	aSyn-120	mus mc	h	0.96	-	-
AB β-actin AC-15	β-actin	mus mc	h, m	1.00	Abcam	ab6276
AB anti-MAP2	MAP2	ch pc	m, r	na	Abcam	ab5392

secondary antibodies			
antibody name	**concentration (mg/mL)**	**company**	**catalogue #**
DAPI 461	2.00	ThermoFisher	D1306
goat anti-mouse Alexa Fluor 488	2.00	ThermoFisher	A-11029
donkey anti-rabbit Alexa Fluor 488	2.00	ThermoFisher	A-21206
goat anti-chicken Alexa Fluor 568	2.00	ThermoFisher	A-11041
donkey anti-rabbit Alexa Fluor 568	2.00	ThermoFisher	A-10042
donkey anti-mouse Alexa Fluor 647	2.00	ThermoFisher	A-31571
donkey anti-rabbit Alexa Fluor 647	2.00	ThermoFisher	A-31573
IRDye 680RD goat anti-mouse	-	Li-Cor	926-68070
IRDye 800CW goat anti-rabbit	-	Li-Cor	926-32211

aSyn = alpha-synuclein; ch = chicken; h = human; mc = monoclonal; mus or m = mouse; pc = polyclonal rab or r = rabbit

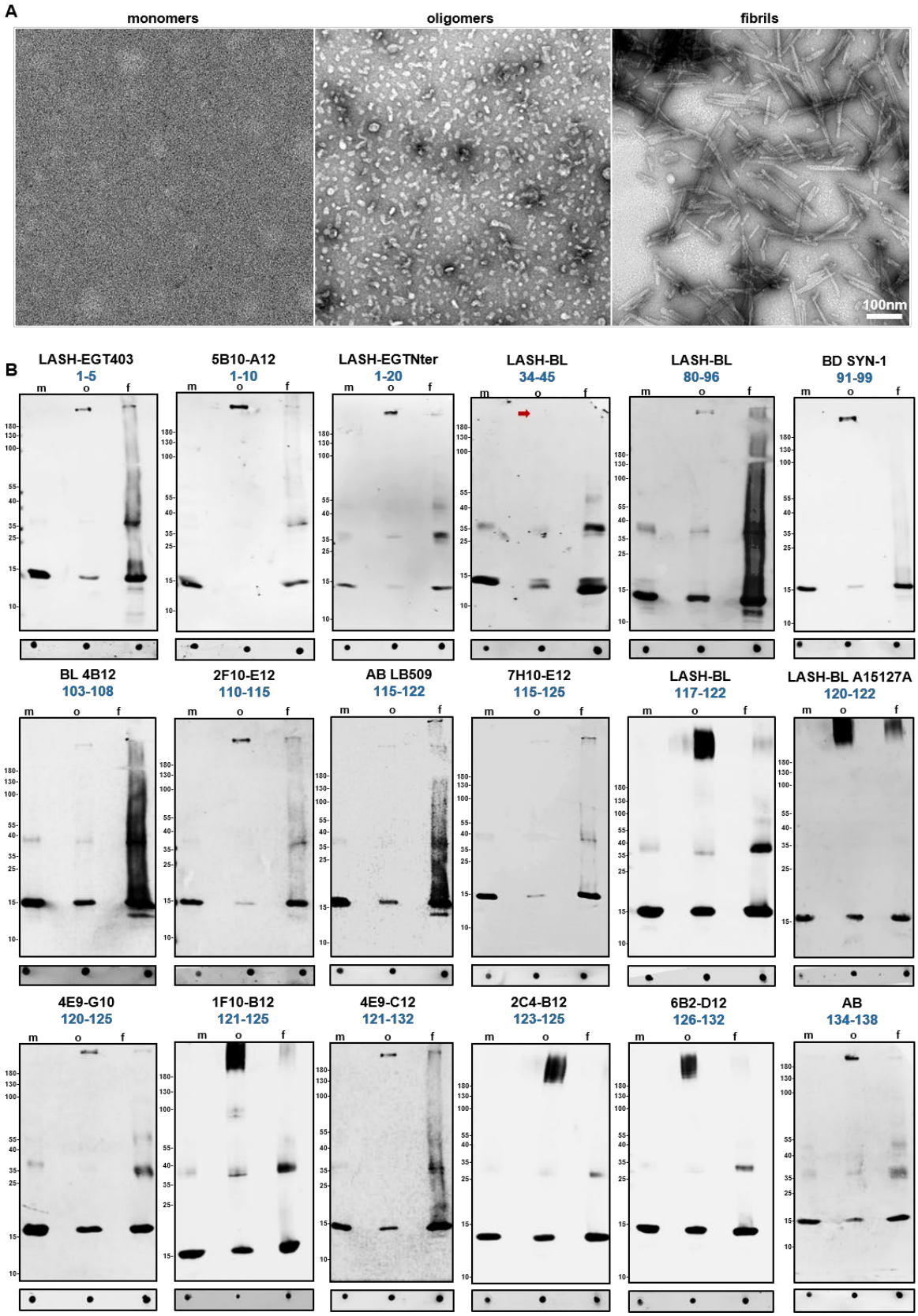

Figure 2. 6 Selectivity of aSyn antibodies over aSyn conformations. **(A)** Representative EM images of aSyn human WT monomers, oligomers and fibrils. **(B)** DB and WB characterisation of the novel monoclonal, in-house polyclonal

and commercially available aSyn antibodies to determine their conformational selectivity using aSyn human WT recombinant monomers, oligomers and pre-formed fibrils. aSyn = alpha-synuclein; DB = dot blot; EM = electron microscopy; f = fibrils; m = monomers; o = oligomers; WB = Western blot; WT = wild-type

2.2.3 Validation of antibodies using aSyn knockout mouse primary neurons and brain tissues

a) aSyn KO mouse primary neurons

To validate the specificity of the antibodies to aSyn species, we assessed their immunoreactivity using aSyn KO mouse primary neurons. We first determined the minimal working concentration for each of the mouse-reactive antibodies on WT naïve and PFF-seeded hippocampal neurons by immunocytochemistry (ICC). This approach allowed us to work on aSyn KO neurons with appropriate antibody concentrations that otherwise permit the detection of endogenous aSyn, exogenously added aSyn fibrils and the newly formed aSyn aggregates in WT neurons, based on a well-characterised neuronal seeding model (Mahul-Mellier et al., 2020, 2018; Volpicelli-Daley et al., 2014). For the antibodies that are human-reactive only, we opted for the recommended dilutions by the suppliers when such information was available, and if not, we aimed at a final antibody concentration of 2-5µg/mL for ICC. We then screened the antibodies using aSyn KO hippocampal and cortical neurons.

By ICC, we observed that LASH-EGT403 (1-5), 5B10-A12 (1-10), BD SYN-1 (91-99), 2F10-E12 (110-115), AB LB509 (115-122), 4E9-G10 (120-125), 4E9-C12 (121-132) and 6B2-D12 (126-132) antibodies showed no non-specific background in hippocampal (Figure 2. 7A) and cortical (Figure 2. 7B) aSyn KO neurons. The LASH-EGTNter (1-20), LASH-BL (34-45) and AB (134-138) antibodies showed positivity, possibly for bSyn protein, both in hippocampal and cortical aSyn KO neurons (Figure 2. 7A-B, blue arrows), an observation consistent with DB and WB results on recombinant bSyn reactivity using these antibodies (Table 2. 4; Figure 2. 2A; Figure 2. 3). Collectively, all of these antibodies showed specificity by ICC on aSyn KO hippocampal and cortical neurons. The cytoplasmic and/or nuclear signals detected in hippocampal and cortical aSyn KO neurons with BL 4B12 (103-108), 7H10-E12 (115-125), LASH-BL (117-122), LASH-BL A15127A (120-122), 1F10-B12 (121-125) and 2C4-B12 (123-125), on the other hand, were deemed to be non-specific background

(Figure 2. 7A-B, red arrows). Interestingly, the LASH-BL 80-96 antibody revealed a weak, non-specific cytoplasmic signal in the hippocampal (Figure 2. 7A, red arrow) but not in cortical aSyn KO neurons (Figure 2. 7B). The specificity of the aSyn PTM antibodies was screened also by ICC. The LASH-BL pY39, LASH-EGT pY39, LASH-EGT pY125, AB EP1536Y pS129, LASH-EGT pS129, LASH-EGT nY39 and 6A3-E9 antibodies were negative by ICC (Figure 2. 8A-B), suggesting that these antibodies are specific and show no cross-reactivity. In contrast, the monoclonal aSyn nY39 antibodies 5E1-G8 and 5E1-C10 showed strong positivity both in the hippocampal and cortical aSyn KO neurons, and mild nuclear positivity was observed with LASH pS87 (Figure 2. 8A-B, red arrows).

We used a similar approach to investigate the specificity of the aSyn antibodies in neuronal lysates by WB. For the WB, sequential extraction was run on aSyn KO hippocampal and cortical neurons, and then the soluble and insoluble fractions were profiled using the battery of aSyn antibodies. aSyn mouse or human recombinant standards were used as positive controls. Of the human-reactive non-modified aSyn antibodies, faint non-specific bands were present mainly in the HMW regions of the soluble and/or insoluble fractions of BL 4B12 (103-108), AB LB509 (115-122), LASH-BL A15127A (120-122), 4E9-G10 (120-125) (Figure 2. 9A, red arrows), but not in the region to which monomeric aSyn migrates, at 15kDa. Non-specific bands were not observed with the human-reactive 7H10-E12 (115-125), LASH-BL (117-122), 1F10-B12 (121-125), 4E9-C12 (121-132) and 2C4-B12 (123-125) antibodies (Figure 2. 9A). The human- and mouse-reactive non-modified aSyn antibodies i.e. LASH-EGT403 (1-5), 5B10-A12 (1-10), LASH-EGTNter (1-20), LASH-BL (34-45), LASH-BL (80-96), BD SYN-1 (91-99), 2F10-E12 (110-115), 6B2-D12 (126-132) and AB (134-138), did not detect any non-specific bands at 15kDa in the phosphate buffered saline(PBS)-treated soluble or insoluble fractions (Figure 2. 9A), with AB (134-138) possibly detecting bSyn in the PBS-treated soluble neuronal fractions (Figure 2. 9A, blue arrows). On the other hand, LASH-EGT403, 5B10-A12, LASH-EGTNter, LASH-BL 34-45, LASH-BL 80-96, 2F10-E12, 6B2-D12 and AB 134-138 showed non-specific bands in the HMW regions in the soluble and/or insoluble fractions (Figure 2. 9A, red arrows). The aSyn PTM antibodies did not reveal any non-specificity, except for LASH-BL pY39, LASH-EGT pY39, 5E1-G8 nY39 and 5E1-C10 nY39 that detected a few non-specific bands

between 35-180kDa, and LASH-EGT pS129 which detected both HMW bands and bands around 15kDa in the insoluble fractions (Figure 2. 9B, red arrows).

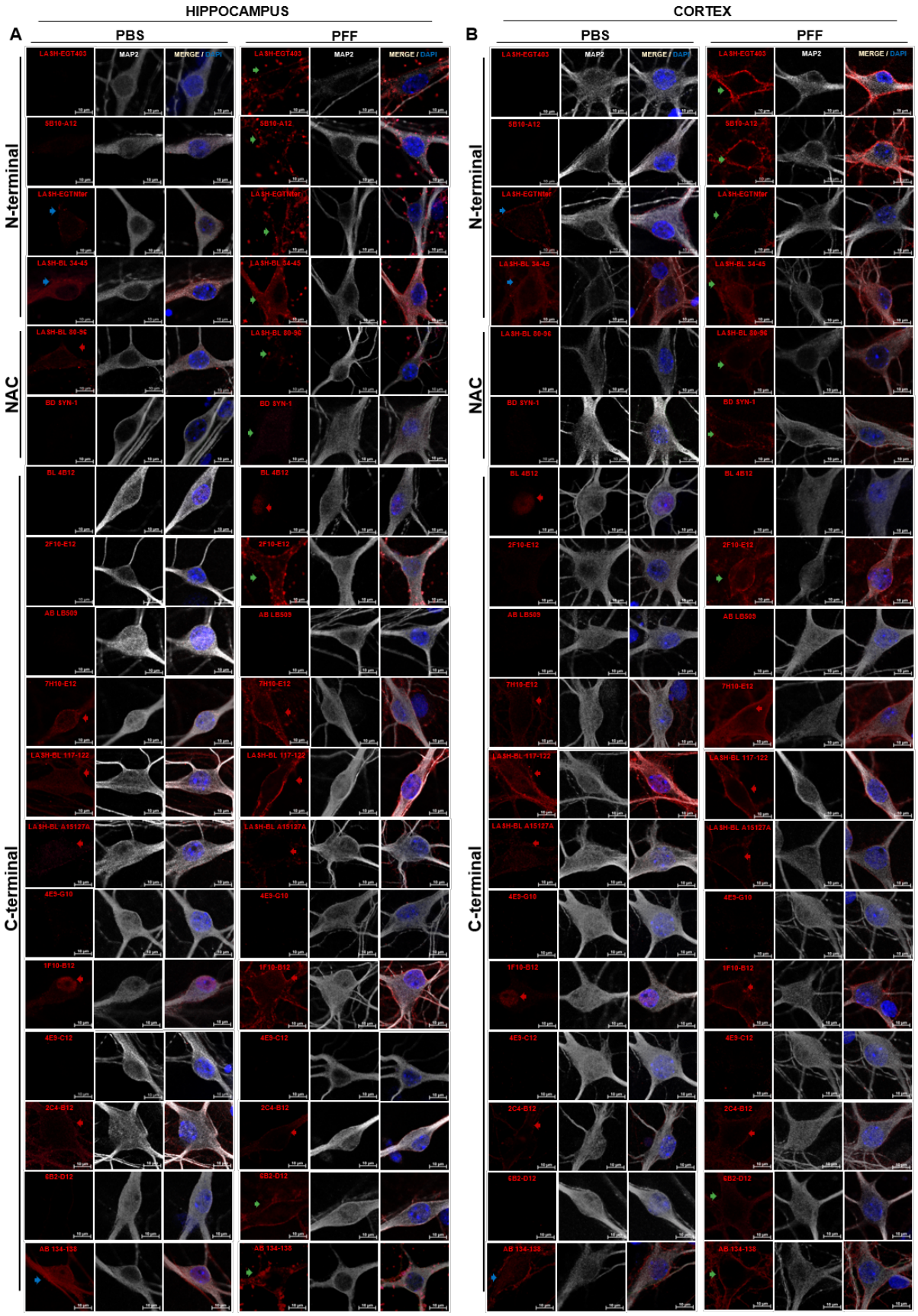

Figure 2. 7 Specificity validation of non-modified aSyn antibodies on aSyn KO hippocampal and cortical neurons by ICC. PBS- and PFF-treated aSyn KO **(A)** hippocampal and **(B)** cortical neurons were immunostained to validate the specificity of the antibodies with epitopes against the N-terminus, NAC region and C-terminus of aSyn. Blue

arrows indicate bSyn positivity in PBS-treated neurons, green arrows indicate positivity to aSyn mouse WT fibrils in PFF-treated neurons, and red arrows indicate non-specific background both in PBS- and PFF-treated neurons. aSyn = alpha-synuclein; bSyn = beta-synuclein; ICC= immunocytochemistry; KO = knockout; MAP2 = microtubule associated protein 2; PBS = phosphate buffered saline; PFF = pre-formed fibril; WT = wild-type

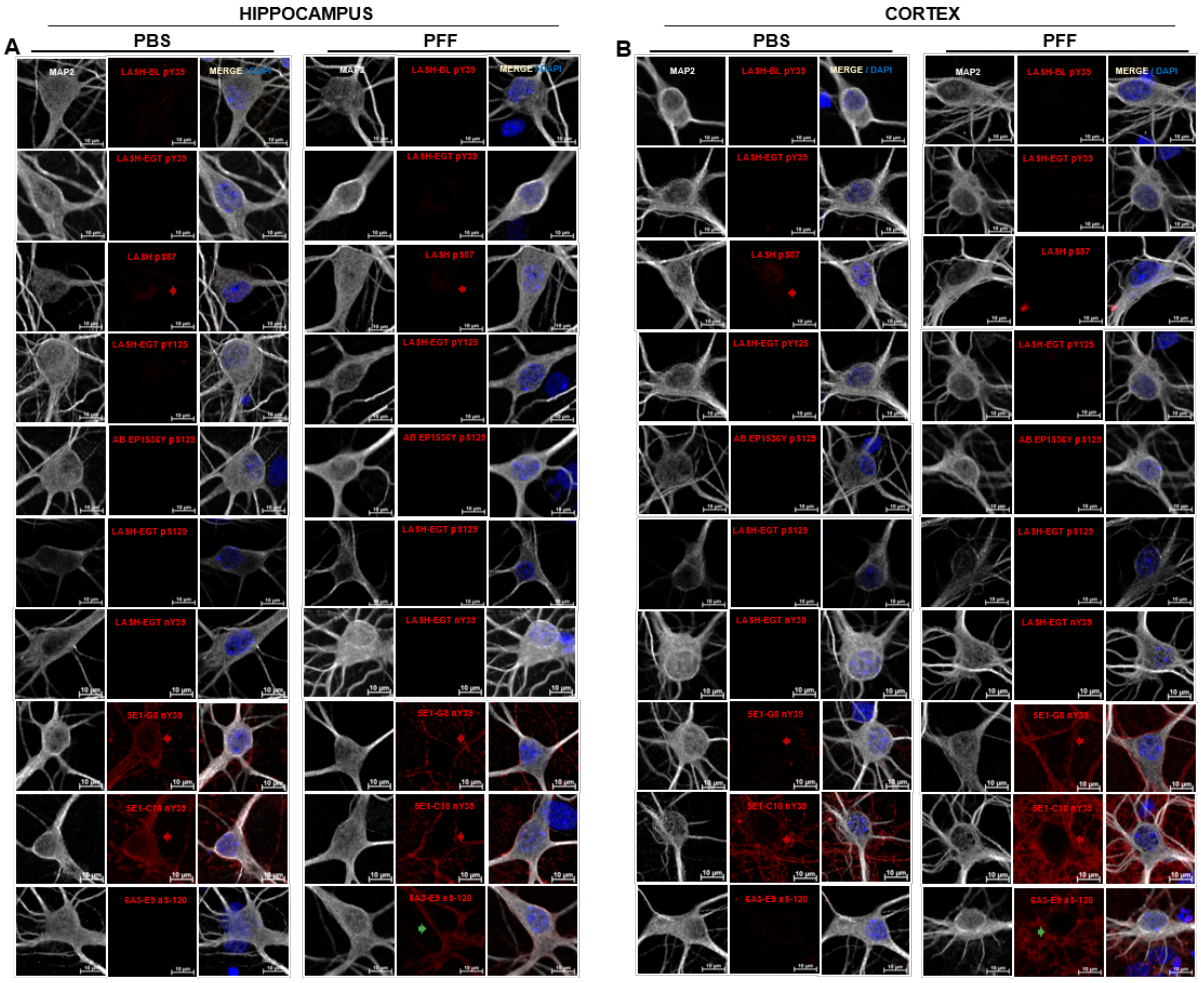

Figure 2. 8 Specificity validation of aSyn PTM antibodies on aSyn KO hippocampal and cortical neurons by ICC. PBS- and PFF-treated aSyn KO **(A)** hippocampal and **(B)** cortical neurons were immunostained to validate the specificity of the antibodies with epitopes against the PTMs of aSyn. Green arrows indicate positivity to aSyn mouse WT fibrils in PFF-treated neurons, and red arrows indicate non-specific background both in PBS- and PFF-treated neurons. aSyn = alpha-synuclein; bSyn = beta-synuclein; ICC = immunocytochemistry; KO = knockout; MAP2 = microtubule associated protein 2; PBS = phosphate buffered saline; PFF = pre-formed fibril; PTM = post-translational modification; WT = wild-type

b) aSyn KO mouse brain tissues

Next, we validated the specificity of the non-modified and PTM aSyn antibodies on aSyn KO mouse amygdala tissue, a brain region previously shown to be particularly

affected by aSyn pathology (Burtscher et al., 2019). By immunofluorescence (IF), we observed no background with any of the antibodies against non-modified aSyn (Figure 2. 10A). With the aSyn PTM antibodies, on the other hand, we observed non-specific punctate cytoplasmic positivity with LASH pS87, LASH-EGT pY125, LASH-EGT pS129 and mild diffuse background with 5E1-G8 and 5E9-C10 nY39 antibodies (Figure 2. 10B, red arrows). A summary of the findings on aSyn KO neurons and mouse tissue for each antibody is presented in Table 2. 6.

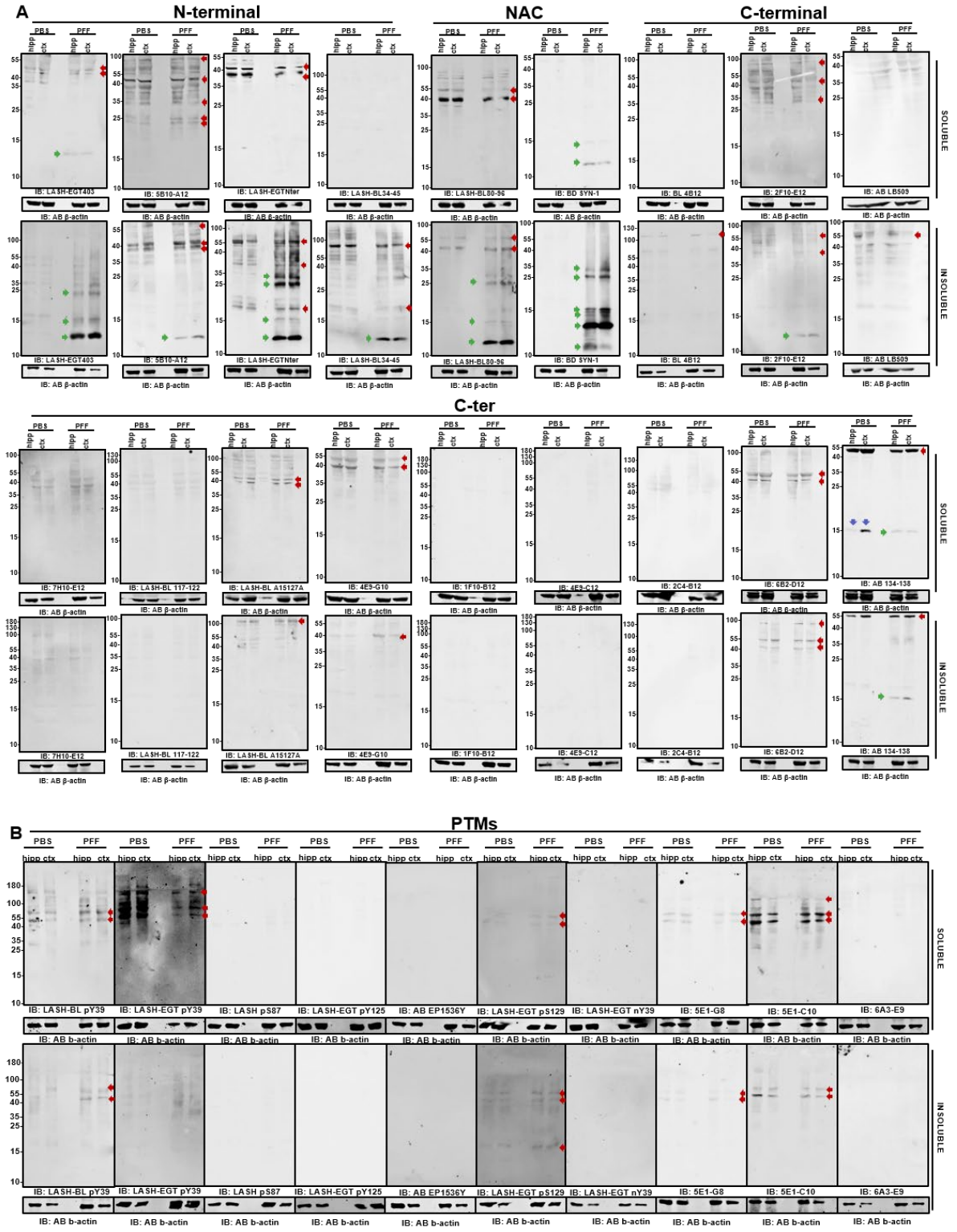

Figure 2. 9 Specificity validation of aSyn antibodies on aSyn KO hippocampal and cortical neurons by WB. PBS- and PFF-treated aSyn KO hippocampal and cortical neurons were separated to soluble and insoluble fractions by sequential extraction, and stained using **(A)** non-modified and **(B)** aSyn PTM antibodies for specificity validation. Green arrows indicate bands specific to aSyn mouse WT fibrils, blue arrows indicate bSyn-specific bands, and red arrows indicate non-specific background. aSyn = alpha-synuclein; bSyn = beta-synuclein; KO = knockout; PBS = phosphate buffered saline; PFF = pre-formed fibril; PTM = post-translational modification; WB = Western blot; WT = wild-type

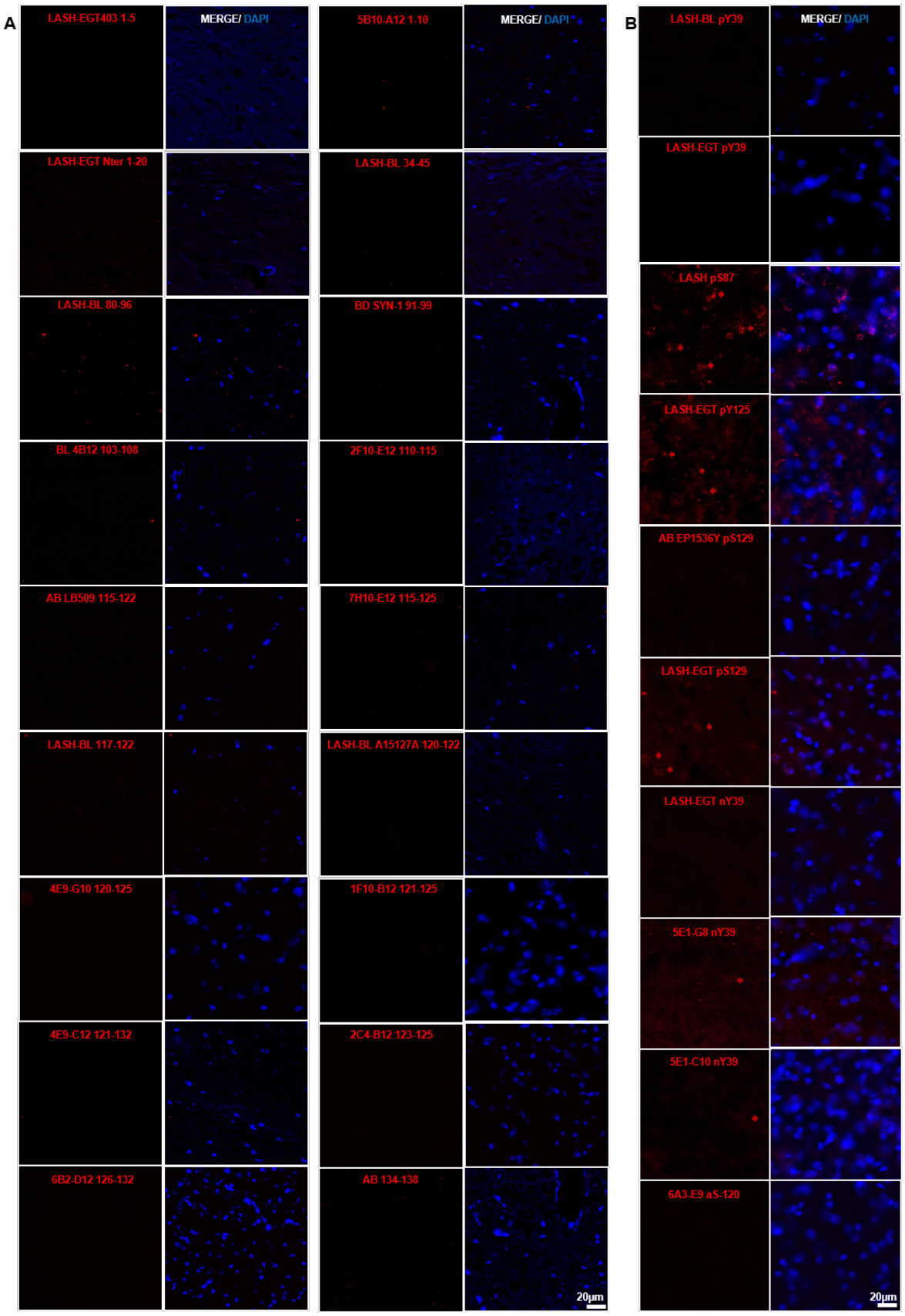

Figure 2. 10 Specificity validation of aSyn antibodies on aSyn KO mouse brain tissue by IF. The in-house and commercial antibodies against **(A)** non-modified aSyn and against **(B)** aSyn PTMs were screened for their specificity

using aSyn KO mouse amygdala sections. Red arrows indicate non-specific background. aSyn = alpha-synuclein; IF = immunofluorescence; KO = knockout; PTM = post-translational modification

Table 2. 6 Specificity summary of aSyn antibodies on aSyn KO mouse neuronal culture and brain tissues. aSyn = alpha-synuclein; KO = knockout

antibody name	epitope	reactivity	specificity aSyn KO neurons - ICC	specificity aSyn KO neurons – WB		specificity aSyn KO tissue – IHC
				15kDa	35-180kDa	
LASH-EGT403	1-5	h, m	specific	specific	non-specific bands	specific
5B10-A12	1-10	h, m	specific	specific	non-specific bands	specific
LASH-EGTNter	1-20	h, m	specific (bSyn-positive)	specific	non-specific bands	specific
LASH-BL 34-45	34-45	h, m	specific (bSyn-positive)	specific	non-specific bands	specific
LASH-BL 80-96	80-96	h, m	non-specific in hipp aSyn KO only	specific	non-specific bands	specific
BD SYN-1	91-99	h, m	specific	specific	specific	specific
BL 4B12	103-108	h	mild nuclear positivity	specific	non-specific bands	specific
2F10-E12	110-115	h, m	specific	specific	non-specific bands	specific
AB LB509	115-122	h	specific	specific	non-specific bands	specific
7H10-E12	115-125	h	non-specific	specific	specific	specific
LASH-BL 117-122	117-122	h	non-specific	specific	specific	specific
LASH-BL A15127A	120-122	h	non-specific	specific	non-specific bands	specific
4E9-G10	120-125	h	specific	specific	non-specific bands	specific
1F10-B12	121-125	h	non-specific	specific	specific	specific
4E9-C12	121-132	h	specific	specific	specific	specific
2C4-B12	123-125	h	non-specific	specific	specific	specific
6B2-D12	126-132	h, m	specific	specific	non-specific bands	specific
AB 134-138	134-138	h, m	specific (bSyn-positive)	specific (bSyn-positive)	non-specific bands	specific
LASH-BL pY39	pY39	h	specific	specific	non-specific bands	specific
LASH-EGT pY39	pY39	h, m	specific	specific	non-specific bands	specific
LASH pS87	pS87	h	mild nuclear positivity	specific	specific	punctate cytoplasmic
LASH-EGT pY125	pY125	h	specific	specific	specific	punctate cytoplasmic
AB pY125	pY125	h	specific	specific	specific	specific
AB EP1536Y	pS129	h, m	specific	specific	specific	specific
LASH-EGT pS129	pS129	h, m	specific	non-specific	non-specific bands	punctate cytoplasmic
AB pY133	pY133	h, m	specific	specific	specific	specific
AB pY136	pY136	h, m	specific	specific	specific	specific
LASH-EGT nY39	nY39	h, m	specific	specific	specific	specific
5E1-G8	nY39	h, m	non-specific	specific	non-specific bands	mild diffuse background
5E1-C10	nY39	h, m	non-specific	specific	non-specific bands	mild diffuse background
6A3-E9	aSyn-120	h	specific	specific	specific	specific

aSyn = alpha-synuclein; bSyn = beta-synuclein; ICC = immunocytochemistry; IHC = immunohistochemistry; KO = knockout; WB = Western blot

2.2.4 Antibody validation and application in human post-mortem brain tissues

Following the characterisation and validation of the antibodies using recombinant aSyn proteins, aSyn KO mouse primary neurons and brain tissues, we sought to apply these tools for human post-mortem brain tissue studies. The antibodies were first titrated for immunohistochemistry (IHC) by comparing different pre-treatment conditions and antibody dilutions. All of the non-modified aSyn antibodies (18) revealed mild to extensive staining of aSyn pathology in the PD cingulate cortex (Figure 2. 11A) except for the LASH-EGT403 (1-5) and 6B2-D12 (126-132) antibodies, which were rarely immunoreactive to LBs and did not detect LNs. Amongst the three PTM antibodies against aSyn nY39, we observed positivity only with the LASH-EGT nY39 polyclonal antibody, which detected cortical LBs and LNs. The 5E1-G8 and 5E1-C10 nY39 monoclonal antibodies, on the other hand, were negative on PD tissue by IHC. With regards to aSyn phosphorylation, some LBs but also thin neurites were positive for aSyn pY39, detected both by the monoclonal LASH-BL pY39 and by the polyclonal LASH-EGT pY39 antibodies. Likewise, extensive LB and LN pathology was revealed both by the commercial AB EP1536Y and the homemade LASH-EGT pS129 antibodies. On the contrary, the LASH pS87 and LASH-EGT pY125 antibodies showed little to no reactivity in the PD cingulate cortex. The truncation-specific antibody 6A3-E9 (aSyn-120) detected exclusively the LBs without producing signal in the neurites (Figure 2. 11A).

Interestingly, triple immunolabelling using aSyn N-terminal, C-terminal and PTM antibodies revealed that the cortical LBs were equally detected by all antibodies (Figure 2. 11B; Figure 2. 12). Yet, some of the LNs and Lewy dots were selectively revealed by the LASH-BL 34-45 antibody, and not by the AB 134-138 or the 81A pS129 antibodies (Figure 2. 11B, arrows), suggesting that a portion of neuritic pathology is non-phosphorylated and may be cleaved in the extreme C-terminus. Overall, these results support our hypothesis that capturing the diversity of aSyn species in pathological aggregates requires the use of multiple antibodies targeting different domains and disease-relevant PTMs.

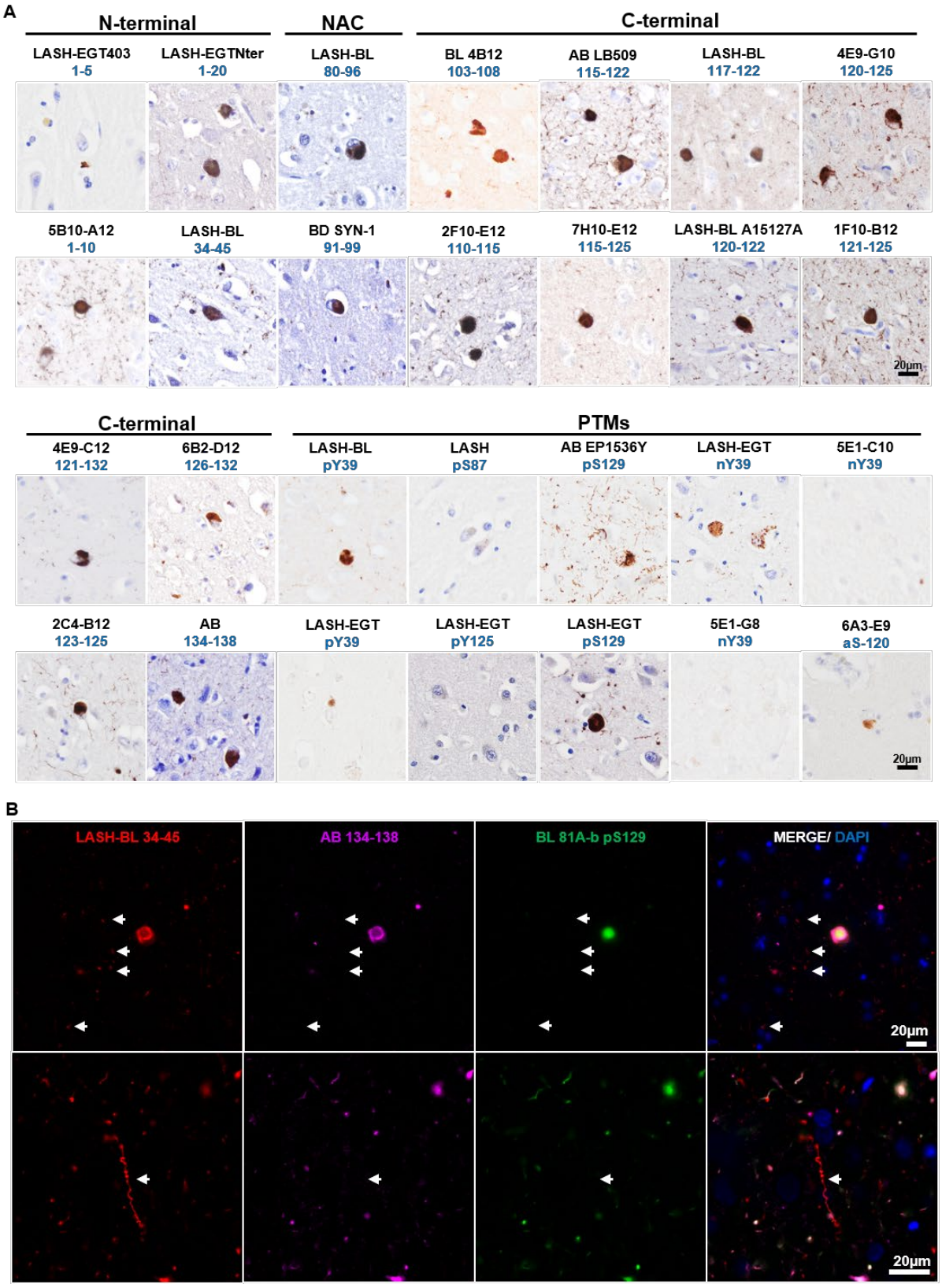

Figure 2. 11 Application and validation of the aSyn antibodies on PD tissue. **(A)** The in-house monoclonal, polyclonal and commercial aSyn antibodies were titrated for IHC on the PD cingulate cortex. **(B)** Triple labelling of PD cingulate cortex by IF using an aSyn N-terminal (LASH-BL 34-45), a C-terminal (AB 134-138) and a pS129 (BL 81A-biotin) antibody. aSyn = alpha-synuclein; IF = immunofluorescence; IHC = immunohistochemistry; PD = Parkinson's disease

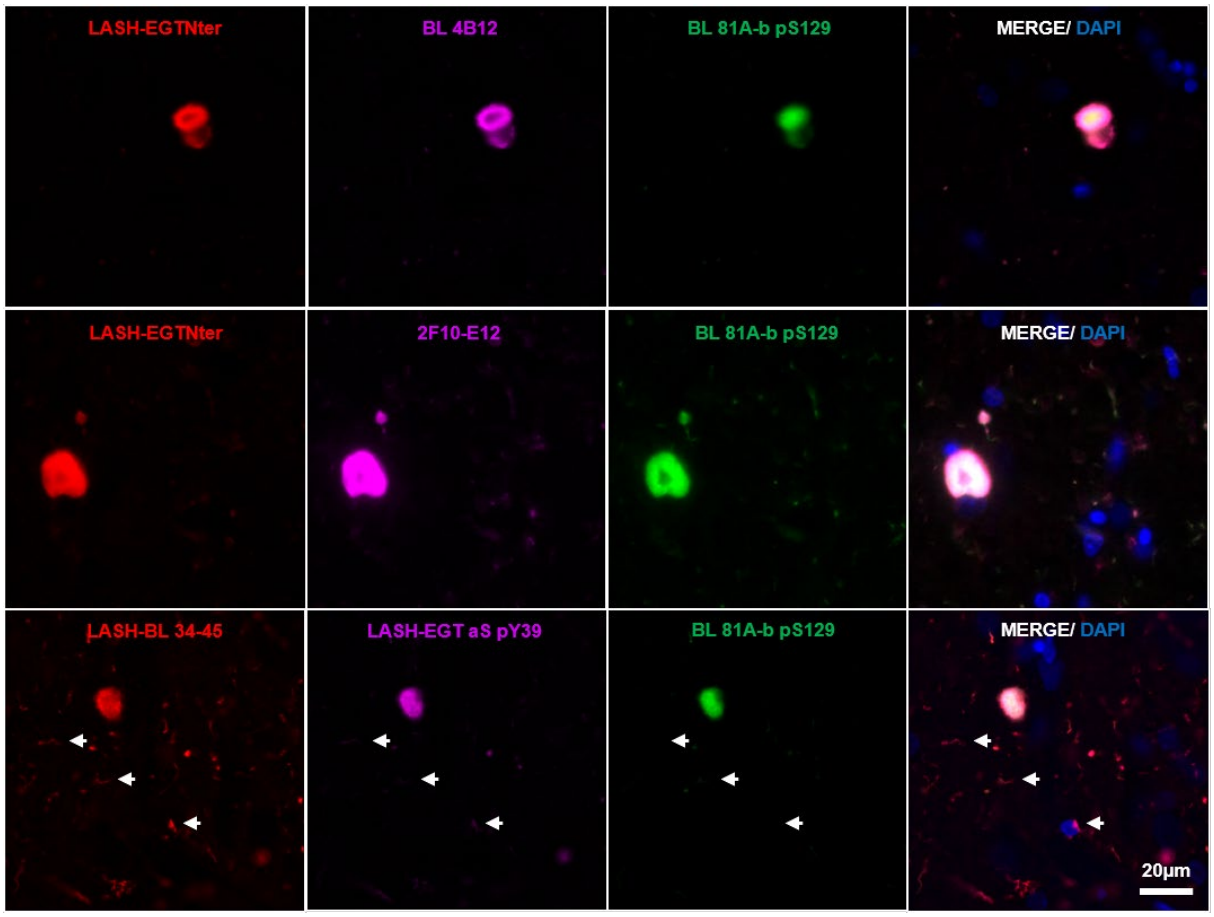

Figure 2. 12 IF labelling of PD cingulate cortex using the aSyn N-terminal LASH-EGTNter 1-20 or LASH-BL 34-45, aSyn C-terminal BL 4B12 103-108 or AB 134-138, and aSyn pS129 BL 81A-biotin antibodies. aSyn = alpha-synuclein; IF = immunofluorescence; IHC = immunohistochemistry; PD = Parkinson's disease

2.2.5 A selected panel of aSyn antibodies reveal the morphological diversity of human pathology

aSyn exists in heterogeneous conformations and proteoforms in human tissues (Anderson et al., 2006; John E Duda et al., 2000; John E. Duda et al., 2000; Fujiwara et al., 2002; Giasson et al., 2000b; Kuusisto et al., 2003); yet, profiling of the same set of synucleinopathy tissues systematically for a full range of aSyn PTMs to capture pathological diversity, has not been performed previously. Therefore, we sought to characterize aSyn pathology across different types of LBDs using our battery of antibodies.

For this, we selected the best performing aSyn antibody subset that would allow for the maximal coverage of the aSyn sequence and PTMs. This subset included two antibodies against the N-terminus (LASH-EGTNter 1-20 and LASH-BL 34-45), two antibodies against the NAC region (LASH-BL 80-96 and BD SYN-1 91-99), and two antibodies against the C-terminus (i.e. 2F10-E12 110-115 and AB 134-138) of aSyn. Two additional antibodies were incorporated to cover the aSyn serine phosphorylations: AB EP1536Y pS129, as this antibody has been the most specific to aSyn pS129 species in our hands and in the literature (Delic et al., 2018), and LASH pS87. For the N-terminal tyrosine phosphorylation modification, we opted for the monoclonal LASH-BL pY39 antibody. For the C-terminal phosphorylation at Y125, we switched to the polyclonal aSyn pY125 antibody from Abcam as our homemade LASH-EGT pY125 antibody revealed no positivity in the PD cingulate cortex (Figure 2. 11A) and showed high background when applied to aSyn KO mouse brain tissues (Figure 2. 10B). To cover all possible C-terminal tyrosine phosphorylation modifications, we also included the polyclonal aSyn pY133 and pY136 antibodies from Abcam. To the best of our knowledge, these two C-terminal tyrosine phosphorylations have not been explored in post-mortem tissues, with the exception of one recent study (Sano et al., 2021). The specificities of these three Abcam antibodies were validated in hippocampal and cortical aSyn KO neurons by ICC and WB (Figure 2. 13A-C; Table 2. 6). Finally, we added 6A3-E9 against aSyn 1-120 and LASH-EGT nY39 to our selection. The final antibody subset chosen for further human tissue screening is presented in Figure 2. 14A.

The specificity of this antibody selection to aSyn species in human brain tissue was validated directly using post-mortem materials of cases with neurodegenerative diseases that are not classified as synucleinopathies. The frontal cortices of progressive supranuclear palsy (PSP) and corticobasal degeneration (CBD), and the hippocampi of Alzheimer's disease (AD), Pick's disease (PiD) and frontotemporal lobar degeneration of TAR DNA-binding protein 43 type C (FTLD-TDP/C) cases were immunostained. Rare aSyn-positive inclusions were revealed by the LASH-EGTNter antibody in the CBD frontal cortex (Figure 2. 15, arrow), whereas the other non-modified aSyn antibodies did not show any immunoreactivity. With regards to the aSyn PTM antibodies, LASH-EGT nY39 and 6A3-E9 aSyn-120 were negative in all cases stained (Figure 2. 15). AB EP1536Y (pS129) detected neuritic aSyn and AB pY133

extracellular aSyn structures in AD hippocampi (Figure 2. 15, arrows). AB pY136 showed rare neuronal cytoplasmic positivity in the FTLD-TDP/C hippocampus, and LASH-BL pY39 scarce diffuse cytoplasmic positivity in PSP and extracellular aSyn in CBD frontal cortices (Figure 2. 15, arrows). Interestingly, both the LASH pS87 and AB pY125 antibodies revealed sparse granular cytoplasmic structures in the FTLD-TDP/C, AD and PiD hippocampi ((Figure 2. 15, arrows). These results suggest that the positive structures are genuine aSyn species that are found co-existing in brain tissues of patients with neuropathologies not classified as synucleinopathies.

The selected aSyn antibodies were then used to immunohistochemically analyse the substantia nigra of sporadic (PD n=5, PDD n=2, DLB n=1) and familial (*SNCA* G51D n=3, *SNCA* H50Q n=1, *SNCA* duplication n=1) LBDs. Across these diseases, moderate to dense staining of LBs and LNs was observed with LASH-EGTNter (1-20) antibody, which was also positive for Lewy dots, thin threads, pale bodies (PBs), extracellular aSyn structures and coiled body-like oligodendroglial inclusions, but negative for astroglial structures (Figure 2. 14B). The AB 134-138 antibody labelled LBs, LNs, PBs and extracellular aSyn, and the 2F10-E12 (110-115) antibody densely labelled classical LBs, dystrophic neurites and thin threads, coiled body-like oligodendroglial inclusions but not any astrocytes. In contrast, the LASH-BL 34-45, LASH-BL 80-96 and BD SYN-1 antibodies showed very similar profiles, revealing LBs, dystrophic neurites and thin threads, coiled body-like oligodendroglial inclusions but also distinctively the punctate neuronal cytoplasmic and punctate astroglial accumulations (Figure 2. 14B). Similar punctate astroglial structures were also picked up by the N-terminal PTM antibodies LASH-EGT nY9 and LASH-BL pY39. Additionally, LASH-EGT nY39 revealed punctate cytoplasmic neuronal accumulations, PBs, thin threads and extracellular aSyn accumulations, and LASH-BL pY39 thin threads, extracellular aSyn structures, coiled body-like oligodendrocytes and some LBs. With the same set of aSyn PTM antibodies in the cingulate cortex of these LB disorders, we again observed a similar phenomenon where LASH-BL pY39 and LASH-EGT nY39 antibodies picked up star-shaped glial structures (Figure 2. 14C).

Both in the substantia nigra and the cingulate cortex, the most abundant aSyn PTM we observed was aSyn pS129, and the AB EP1536Y antibody against this modification labelled LBs, PBs, diffuse neuronal cytoplasmic aSyn, neurites and dots extensively

(Figure 2. 14B-C). In contrast, LASH pS87 together with AB pY125 revealed the scantiest structures across the LBDs. LASH pS87 antibody unveiled very rare granular cytoplasmic bodies in the neurons, dystrophic neurites and PBs in the substantia nigra (Figure 2. 14B), but no glial accumulations or thin threads (Figure 2. 14B-C). Similarly, AB pY125 labelled only very rare granular cytoplasmic aSyn structures and rare PBs in the substantia nigra, without staining any neurites or LBs in either of the two regions looked at (Figure 2. 14B-C). The other C-terminal tyrosine phosphorylation antibody AB pY133 detected some LBs with multiple centres, PBs and rare thin threads, whereas AB pY136 moderately picked up LBs, neurites, dots and thin threads. The truncation-specific 6A3-E9 antibody (aSyn-120), on the contrary, stained PBs, neuronal nuclear thread-like and extracellular aSyn structures, but no neurites. Altogether, our set of antibodies was able to uncover large heterogeneity of aSyn pathology in LBDs that is distributed both in neuronal and glial cells that cannot be discerned in its entirety when only individual antibodies are used. We further observed the cell-specific occurrence of different aSyn modifications, and report co-existence of differentially modified aSyn species, including several combinations that have not been previously described systematically, such as aSyn nY39, pY133 and pY136.

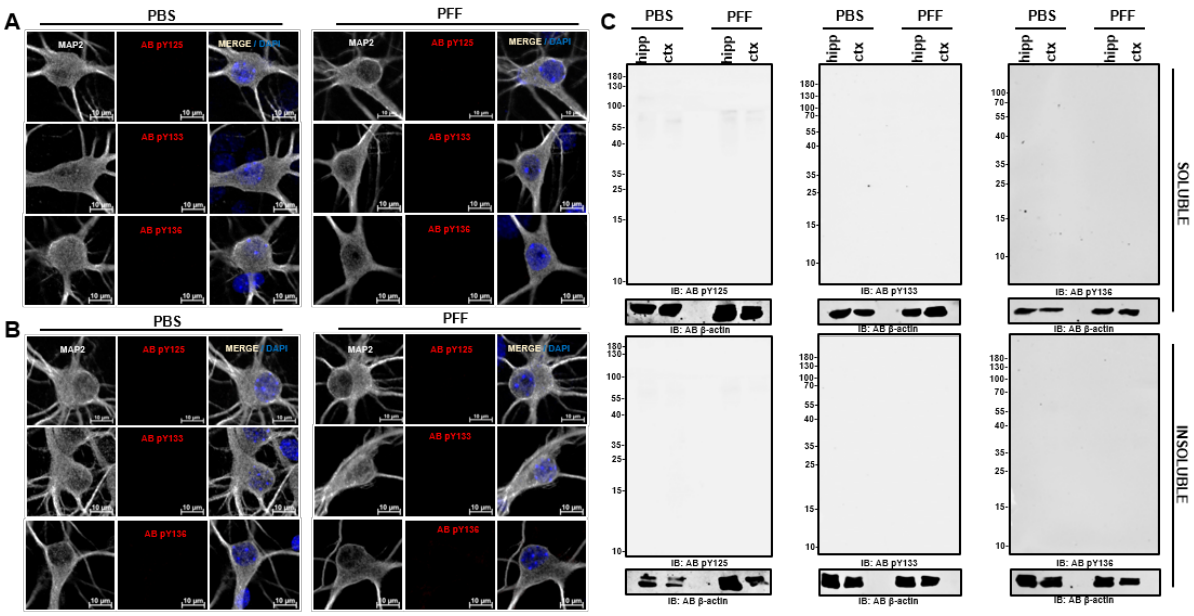

Figure 2. 13 Specificity validation of the aSyn antibodies against C-terminal tyrosine phosphorylations on aSyn KO hippocampal and cortical neurons by ICC and WB. PBS- and PFF-treated aSyn KO **(A)** hippocampal and **(B)** cortical neurons were immunostained to validate the specificity of the Abcam antibodies with epitopes against aSyn pY125, pY133 and pY136. **(C)** PBS- and PFF-treated aSyn KO hippocampal and cortical neurons were separated to soluble and insoluble fractions by sequential extraction, and stained using Abcam pY125, pY133 and pY136 antibodies for

specificity validation. aSyn = alpha-synuclein; ICC = immunocytochemistry; KO = knockout; MAP2 = microtubule associated protein 2; PBS = phosphate buffered saline; PFF = pre-formed fibril; WB = Western blot

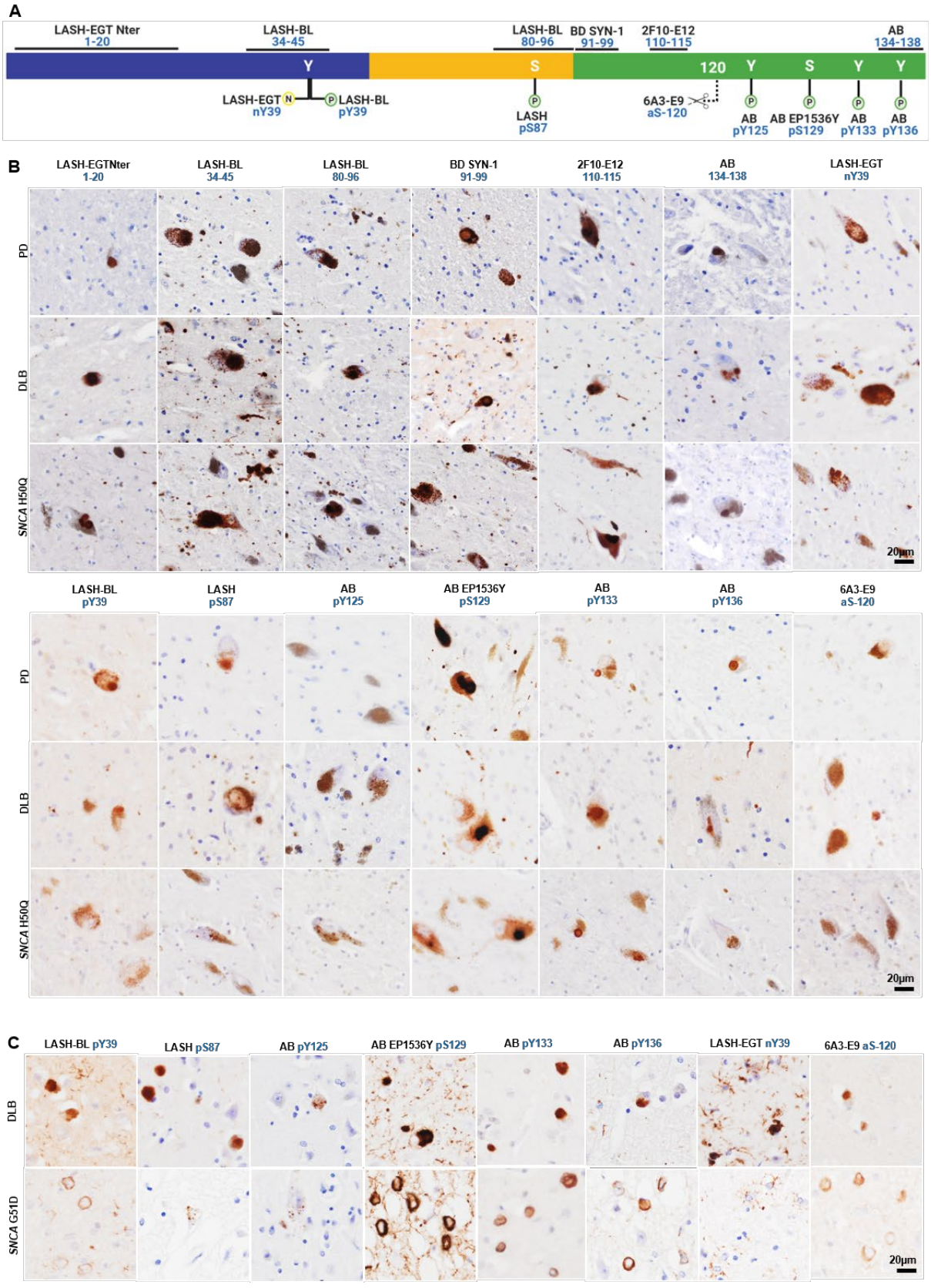

Figure 2. 14 A selected panel of aSyn antibodies reveal the broad diversity of human pathology in the substantia nigra of LBDs. **(A)** An outline to show the epitopes of the aSyn antibody selection used for IHC studies on LBD tissues. Schematic created with BioRender.com (agreement no: *NU23G6E7KK*). **(B)** Representative images from the substantia nigra of sporadic (PD, DLB) and familial (*SNCA* H50Q) LBDs screened with the selection of aSyn non-modified and aSyn PTM antibodies. **(C)** Representative images from the cingulate cortex of sporadic (DLB) and familial (*SNCA* G51D) LBDs screened with the selected aSyn PTM antibodies. aSyn = alpha-synuclein; DLB = dementia with Lewy bodies; IHC = immunohistochemistry; LBD = Lewy body disease; PD = Parkinson's disease; PTM = post-translational modification

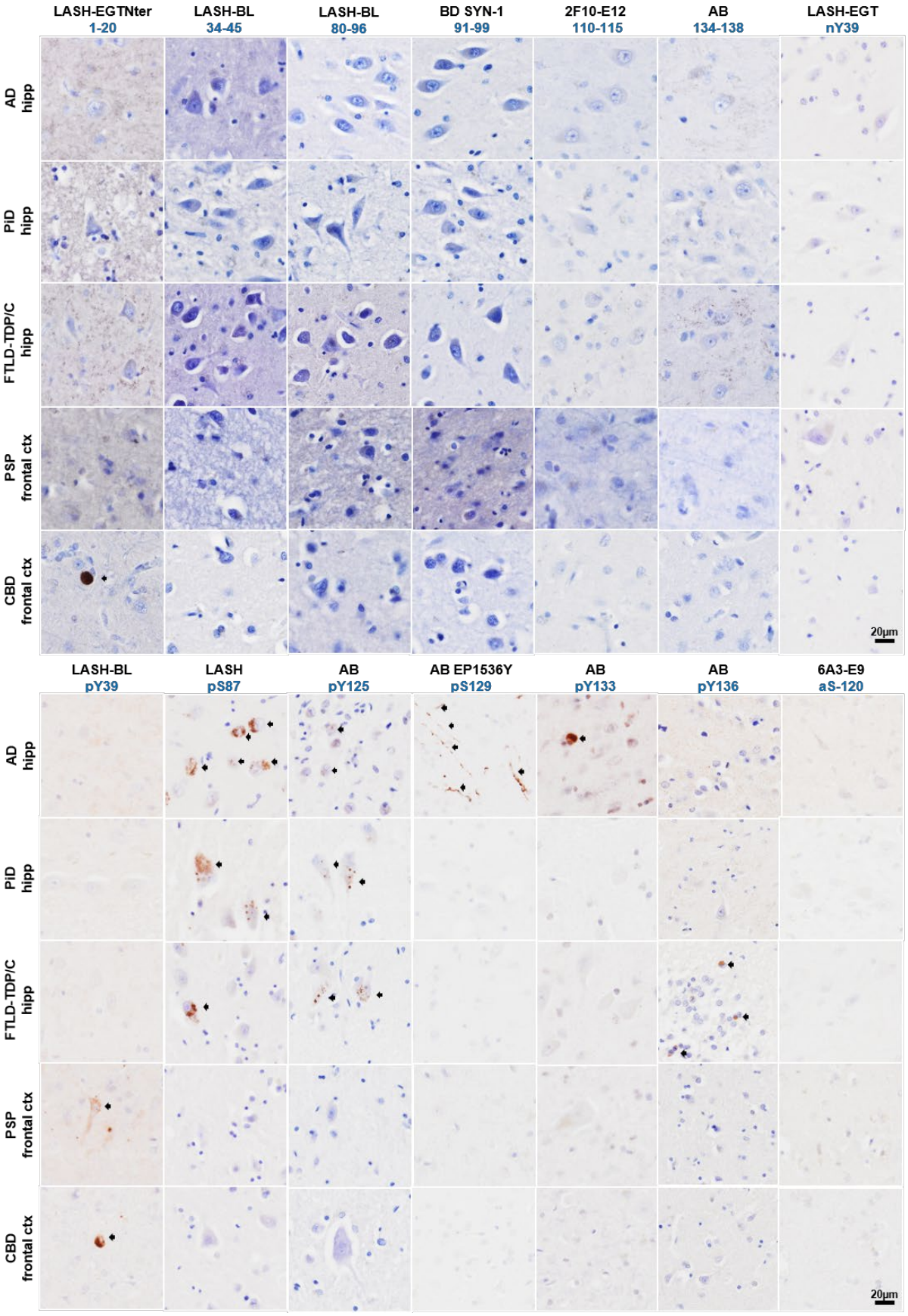

Figure 2. 15 Specificity validation of aSyn antibodies on post-mortem human tissues via IHC. The frontal cortices of PSP and CBD, and the hippocampi of AD, PiD and FTLD-TDP type C were stained using the selection of aSyn

non-modified and PTM antibodies. No cross-reactivity was observed. Arrows indicate aSyn-positive structures detected on each tissue. AD = Alzheimer's disease; aSyn = alpha-synuclein; CBD = corticobasal degeneration; ctx = cortex; FTLD-TDP/C = frontotemporal lobar degeneration of TAR DNA-binding protein 43 type C; hipp = hippocampus; IHC = immunohistochemistry; PiD = Pick's disease; PSP = posterior supranuclear palsy

2.2.6 Biochemical and morphological diversity of aSyn aggregates in cellular and animal models of aSyn seeding

aSyn antibodies are essential for the characterisation of preclinical models. Seeding-based cellular and animal models using aSyn PFFs have emerged as the most common tools to investigate mechanisms and pathways of aSyn pathology formation (Kumar et al., 2021; Luk et al., 2012b, 2009; Mahul-Mellier et al., 2020, 2018; Volpicelli-Daley et al., 2014, 2011). In the majority of the studies using these models, monitoring, quantification and characterisation of aSyn are based on the detection of aSyn pS129 species. However, no study has systematically assessed the occurrence of other disease-associated PTMs in these models, with the exception of some C-terminal cleaved aSyn species (Elfarrash et al., 2019; Luk et al., 2012b, 2009; Mahul-Mellier et al., 2020, 2018; Volpicelli-Daley et al., 2011). Therefore, our knowledge about the role of PTMs in regulating aSyn seeding and LB formation in these models remains incomplete.

To address this knowledge gap and characterize the diversity of aSyn species in these PFF models, we first sought to determine the ability of our antibodies to detect exogenously added PFFs in aSyn KO hippocampal and cortical neurons, by ICC (Figure 2. 7; Figure 2. 8) and WB (Figure 2. 9) 14 hours after treatment. All of the 9 non-modified and mouse aSyn-reactive antibodies i.e. the N-terminal LASH-EGT403 (1-5), 5B10-A12 (1-10), LASH-EGTNter (1-20) and LASH-BL 34-45; the NAC-region LASH-BL 80-96, BD SYN-1 (91-99); and the C-terminal 2F10-E12 (110-115), 6B2-D12 (126-132) and AB 134-138 antibodies detected exogenous fibrils in the PFF-treated hippocampal (Figure 2. 7A) and cortical (Figure 2. 7B) aSyn KO neurons by ICC. By WB, bands specific to exogenously added fibrils were revealed between 10kDa-35kDa by these antibodies (Figure 2. 9A, green arrows) except for the 6B2-D12 (126-132) antibody, which failed to detect any bands in the PFF-added neuronal fractions. With the aSyn PTM antibodies, no positivity was detected in the PFF-treated hippocampal

or cortical aSyn KO neurons using the aSyn pY39, pS129, pY133 or pY136 antibodies by ICC (Figure 2. 8A-B; Figure 2. 13A-B) or by WB (Figure 2. 9A; Figure 2. 13C). Similarly, no positivity was revealed with the LASH-EGT nY39 antibody in the hippocampal or cortical aSyn KO neurons by ICC (Figure 2. 8A-B) or WB (Figure 2. 9B). On the contrary, the monoclonal nY39 antibodies 5E1-G8 and 5E1-C10 were positive both in the PFF-treated and control (PBS-treated) aSyn KO neurons, signals which we presumed to be non-specific by ICC (Figure 2. 8A-B, red arrows). Intriguingly, 6A3-E9 antibody against aSyn-120 showed no background in PBS-treated control neurons (Figure 2. 8A-B) but showed positivity to PFF-treated hippocampal and cortical aSyn KO neurons by ICC (Figure 2. 8A-B, green arrows), and so we cannot rule out the possibility that this antibody may be reactive to aSyn full-length mouse fibrils. By WB, on the other hand, no bands were revealed in the PFF-treated aSyn KO hippocampal and cortical soluble and insoluble fractions (Figure 2. 9B). Collectively, these results confirm the specificity of our antibodies, and suggest that the internalised PFFs do not undergo any type of PTMs, except for N- and C-terminal cleavages, in the absence of seeding.

Finally, the mouse aSyn-reactive antibodies (Table 2. 5) were used to characterize the PTM profile of newly formed aSyn aggregates in the neuronal seeding model (Mahul-Mellier et al., 2020, 2020; Volpicelli-Daley et al., 2014, 2011), and in the PFF-injected *in vivo* model (Burtscher et al., 2019; Luk et al., 2012b; Masuda-Suzukake et al., 2013) of aSyn. Whilst all the non-modified aSyn antibodies detected the endogenous aSyn in PFF-treated or control (PBS-treated) WT hippocampal neurons by ICC, the 5B10-A12 (1-10), LASH-EGTNter (1-20), LASH-BL 34-45 and AB 134-138 antibodies showed almost complete overlap with the aSyn pS129-positive inclusions in the PFF-treated neurons (Figure 2. 16A, arrows), suggesting that these could be useful and alternative tools to aSyn pS129 for monitoring the aSyn aggregation in cell culture, especially if the cross-reactivity of the pS129 antibodies may confound the results. A similar pattern of overlap with the aSyn-positive inclusions, specifically for 5B10-A12 (1-10), LASH-EGTNter (1-20), 2F10-E12 (110-115) and AB 134-138 antibodies (Figure 2. 16C, arrows), was also observed in the amygdala of WT mice that had been injected with PFFs in the striatum. The amygdala has previously been reported to be particularly prone to develop early and substantial aSyn pathology in this model (Burtscher et al., 2019). We speculate that this staining pattern may be due to the preferential exposure

of epitopes in the extreme N- and C-terminal aSyn, whereas the hydrophobic NAC region is less accessible and buried in the core of the newly formed aggregates.

With the aSyn nY39 antibodies, we did not see any positivity in the neurons or in mouse tissue (Figure 2. 16B-C), except for diffuse cytoplasmic staining with the 5E1-G8 and 5E1-C10, which we also observed in aSyn KO neurons and therefore deemed non-specific (Figure 2. 8A-B). With the N-terminal tyrosine phosphorylation at Y39, on the other hand, both in the PFF-treated neurons and in the PFF-injected mouse amygdala, we detected punctate structures in close proximity to, and partially overlapping with, the aSyn pS129-positive inclusions (Figure 2. 16B-C, arrowheads). We noted similar punctate positivity also with aSyn pY133 and pY136 antibodies in the neuronal seeding model (Figure 2. 16B, arrowheads), which again partially overlapped with the aSyn pS129-positive accumulations. Altogether, these data suggest that aSyn may become hyperphosphorylated during the aggregation and inclusion maturation processes. Further research is needed to decipher the mechanism of formation and fate of these puncta structures, which are not detectable by the aSyn pS129 antibodies. These results illustrate the power of the antibodies we have presented in this study to investigate the role of PTMs in regulating aSyn seeding and inclusion formation, and to capture the morphological and biochemical diversity of aSyn aggregates in the cellular and *in vivo* models of aSyn seeding.

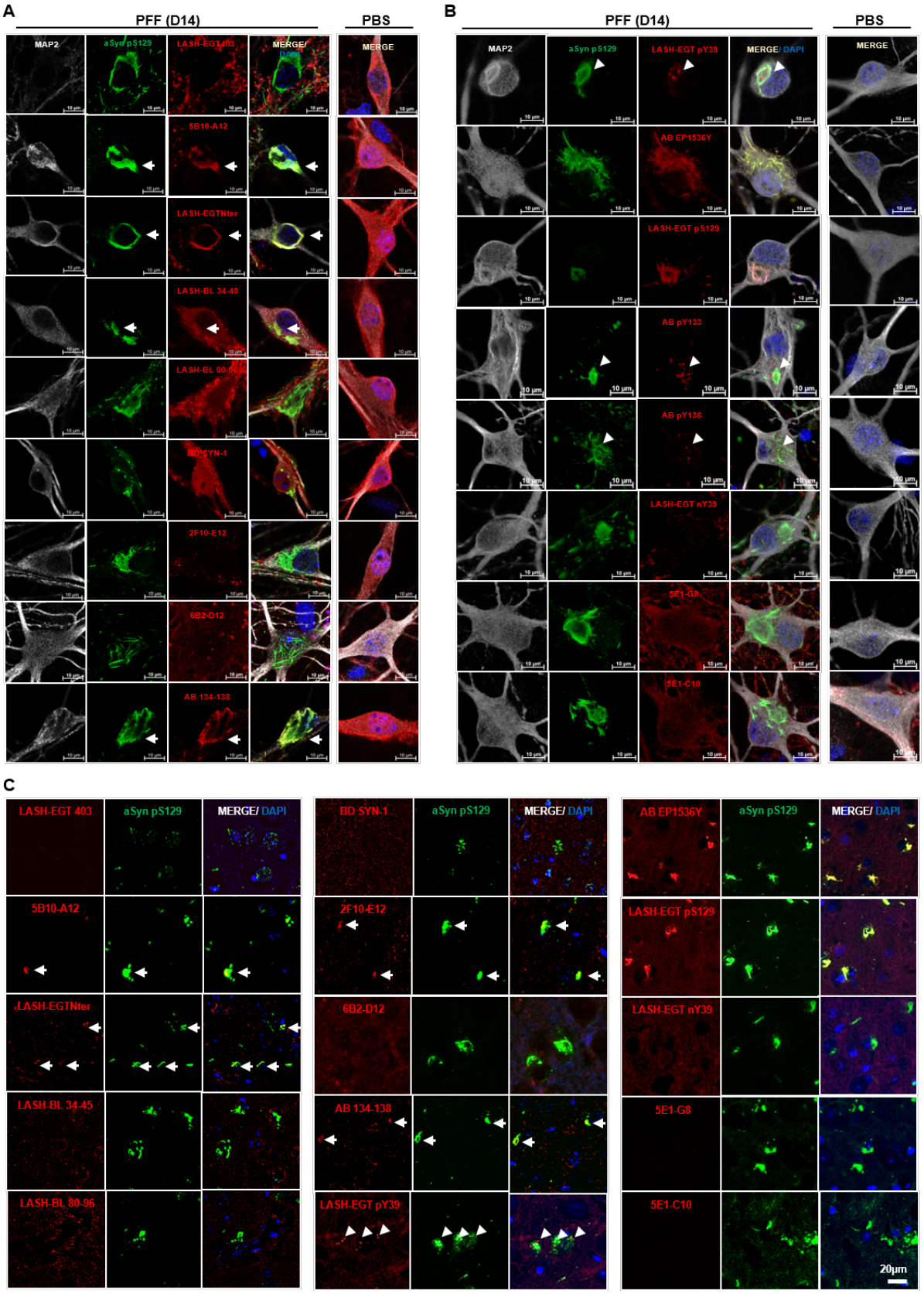

Figure 2. 16 Application of the aSyn antibodies to the cellular and animal seeding models to profile the newly formed aSyn aggregates. WT hippocampal neurons were seeded with PFFs for 14 days, and the newly formed aggregates monitored by ICC using the mouse-reactive **(A)** non-modified aSyn and **(B)** aSyn PTM antibodies in parallel to aSyn pS129 antibodies BL 81A or AB MJF-R13. **(C)** The same type of screening was run in PFF-injected mouse

amygdala tissues by IHC. The non-modified aSyn antibody signals overlapping with the aSyn pS129-positive aggregates are marked with an arrow. The punctate positivity shown by aSyn pY39, pY133 and pY136 antibodies in close proximity to aSyn pS129-positive aggregates are shown by arrowheads. Note the non-specific diffuse positivity revealed by the two monoclonal nY39 antibodies 5E1-G8 and 5E1-C10 in the WT hippocampal neurons as also revealed in the aSyn KO neurons using these two antibodies (Supplementary Figure 5). aSyn = alpha-synuclein; ICC = immunocytochemistry; IHC – immunohistochemistry; KO = knockout; PFFs = pre-formed fibrils; PTM = post-translational modification; WT = wild-type

2.3 Discussion

Previous studies focusing on the development and application of multiple antibodies have been instrumental in the understanding of aSyn heterogeneity in LBDs and MSA (Almandoz-Gil et al., 2017; Covell et al., 2017; Croisier et al., 2006; Dhillon et al., 2017; Duda et al., 2002, 2000b; Fagerqvist et al., 2013; Galvin et al., 2000; Giasson et al., 2000a, 2000b; Henderson et al., 2020; Vaikath et al., 2015; Waxman et al., 2008). On the other hand, no reports are yet available that characterise and validate aSyn non-modified and PTM antibodies in a single study, followed by pathology profiling on the same set of LBD cases. In this study, we presented the development, validation and characterization of 12 novel monoclonal antibodies against different regions and PTMs of aSyn. These were complemented with pre-existing in-house and commercial antibodies to guarantee a more comprehensive coverage of the aSyn biochemical and structural diversity. In total, 31 antibodies were thoroughly characterised using a stringent validation pipeline (Figure 2. 1D), leading to the selection of 14 of them for profiling the diversity of aSyn pathology in LBDs (Table 2. 7). Although all of the antibodies targeting non-modified aSyn sequences efficiently detected LBs, considerable differences particularly in the revelation of astroglial aSyn accumulations, punctate neuronal cytoplasmic inclusions and a subset of LNs and dots were observed in the substantia nigra and cingulate cortex of LBDs. This finding suggests differential capacities of the individual antibodies to uncover specific aspects of aSyn pathology with important implications for disease staging and characterisation of disease subtypes. Specifically, our results indicate that the use of single antibodies or inappropriate antibody combinations may result in profound underrating of the aSyn pathological load and diversity.

Table 2. 7 A summary of the pathology detection patterns of aSyn non-modified and PTM antibodies on LBD substantia nigra. aSyn = alpha-synuclein; LB = Lewy body; LBD = Lewy body disease; LN = Lewy neurite; PB = pale body; PTM = post-translational modification; - absent; + mild; ++ moderate; +++ frequent

antibody	NEURONAL						GLIAL		EXTRACELLULAR
	LBs	PBs	granular cytoplasmic	LNs	thin threads & dots	nuclear thread-like	astroglial	coiled body-like oligodendroglial	
LASH-EGTNter 1-20	++	++	-	++	++	-	-	+	+
LASH-BL 34-45	+++	+	+++	+++	+++	-	+++	+	+
LASH-BL 80-96	++	+	++	++	++	-	++	+	+
BD SYN-1 91-99	++	+	++	++	++	-	++	+	+
2F10-E12 110-115	+++	++	-	+++	+++	-	-	++	+
AB 134-138	++	++	-	++	++	-	-	-	+
LASH-BL pY39	+	-	-/+	+	+	-	+	+	+
LASH pS87	+	+	+	+	-	-	-	-	+
AB pY125	-	+	+	-	-	-	-	-	-
AB EP1536Y pS129	+++	++	-	+++	+++	-	-	+	+
AB pY133	+	+	-	+	+	-	-	-	+
AB pY136	++	-	-	++	+	-	-	-	+
LASH-EGT nY39	+	+	++	+	+	-	++	-	++
6A3-E9 aSyn-120	-	+	-	-	-	+	-	-	++

aSyn = alpha-synuclein; LB = Lewy body; LN = Lewy neurite; PB = pale body; - absent; + mild; ++ moderate; +++ frequent

LBs are mature inclusions composed of a mixture of full-length and N- and C-terminally truncated aSyn species (Bhattacharjee et al., 2019; Moors et al., 2021; Prasad et al., 2012). This makes LBs more likely to be detected by aSyn antibodies regardless of their sequential epitopes. Yet, the other types of aSyn accumulations may be difficult to detect using single antibodies. These may include less mature and poorly characterised manifestations of aSyn pathology, such as granular/punctate neuronal inclusions, astroglial aSyn accumulations, and a subset of LNs, which could be composed of homogenous aSyn proteoforms. The availability of the expanded toolbox

presented herein enables us to perform systematic profiling of aSyn species and pathology at a single cell level by ICC/IHC, which is not possible by biochemical methods such as WB. With this work, we identified antibodies that were able to detect specific aSyn species and inclusions in distinct cell types. This paves the way for future elucidation of the sequence, cell type or cell environment determinants of aSyn pathology formation and multiple cellular and molecular processes linked to neurodegeneration.

Our pioneering study allowed for the investigation of the most prominent disease-associated phosphorylation, nitration and truncation PTMs of aSyn at the same time on the same set of LBD cases. This was enabled by the combined use of a total of 6 non-modified aSyn antibodies against all three regions of the protein and 8 different aSyn PTM antibodies that were used to screen a subset of LB disorders. Our results revealed a wide range of aSyn inclusion types at differing densities. We confirm that aSyn pS129 is the most abundant disease-related modification of aSyn in the substantia nigra, an observation consistent with previous publications reporting similar results on aSyn pS129 enrichment in diseased brains by mass spectrometry analyses (Anderson et al., 2006; Fujiwara et al., 2002). Uniquely, we report here that LB disorders are also rich in N-terminal nitration at Y39. Nitrated aSyn in post-mortem human studies has been previously reported (Duda et al., 2000) but the site-specific N-terminal nitration at Y39 was not investigated due to the lack of an antibody targeting this modification specifically. Similarly, only a handful of studies so far have investigated the N-terminal (Chen et al., 2009; Mahul-Mellier et al., 2014) and C-terminal (Sano et al., 2021) tyrosine phosphorylations. Here we describe the widespread co-presence of these modifications across LB disorders scattered to neurons and glia. Our study was limited in deciphering the distribution of ubiquitinated or acetylated aSyn species due to the lack of antibodies against this particular modification of the protein, and future efforts to develop appropriate tools to fill in this gap will provide an even more complete picture of aSyn pathology heterogeneity.

The neuronal seeding model of aSyn aggregation and LB-like inclusion formation has been well characterised, and the occurrences of the phosphorylation at Serine 129 and C-terminal truncations have been described by several groups (Mahul-Mellier et al., 2020, 2018; Volpicelli-Daley et al., 2014, 2011). Here, we show that the neuronal aSyn

inclusions are hyperphosphorylated, and report for the first time the formation of punctate intracellular structures that are positive for N- or C-terminal tyrosine phosphorylations (pY39, pY133, pY136), which are not revealed by the aSyn pS129 antibodies. These findings illustrate the power of using multiple antibodies to gain insight into the role of PTMs in regulating the formation of different types of aSyn aggregates. Prospective studies to decipher the cellular mechanisms modulating these modifications, and the role of these PTMs in aSyn aggregation, aggregate maturation and aSyn-mediated toxicity may be of crucial translational value.

In summary, we highlight the limitations of relying on individual antibodies for aSyn pathology characterisation, and provide a selected, well-characterised toolset of antibodies for an extensive evaluation of aSyn pathology diversity. Clearly, not every study design will justify the use of the complete set used here. However, the provided characterizations of the individual antibodies, including their capacities to uncover specific features of aSyn pathology, will enable the choice of appropriate antibodies for specific studies based on solid rationales, a possibility that did not exist before. On the other hand, re-visiting the staging studies of PD and other LBDs based on aSyn pathology would greatly benefit from using a good selection of several well-suited antibodies described here to possibly resolve inconsistencies observed when correlating pathology with symptomatology (Jellinger, 2009; Milber et al., 2012; Parkkinen et al., 2008, 2007; Steiner et al., 2018).

The scope of this work primarily covered sporadic and familial LBDs, and thus studying MSA pathology using this toolset in upcoming studies may shed light onto our understanding of this synucleinopathy type. Finally, we believe that future research aimed at re-visiting 1) PD and other LBD staging in the central nervous system using large cohorts, and 2) aSyn aggregation in the periphery using this validated antibody set would open new avenues in our comprehension of aSyn pathology spreading routes, and help identify novel therapeutic targets to interfere with these mechanisms.

2.4 Materials and methods

2.4.1 Generation of aSyn monoclonal antibodies

A combination of aSyn human recombinant proteins and peptides against different forms and modifications of aSyn were used for the immunisation of BALB/c mice (Table 2. 1). These were solubilised in PBS and, where appropriate, conjugated to the carrier protein keyhole limpet hemocyanin (KLH). Following pre-immune serum collection, BALB/c mice were subcutaneously injected with the immunogen-complete Freund's adjuvant mixture on Day 0, and with immunogen-incomplete Freund's adjuvant on Day 21 and Day 42. Test bleeds were run on Days 35 and 56, and antibody response was evaluated by ELISA, WB and DB. Animals with strong immunoreactivities were euthanised and their splenocytes surgically harvested.

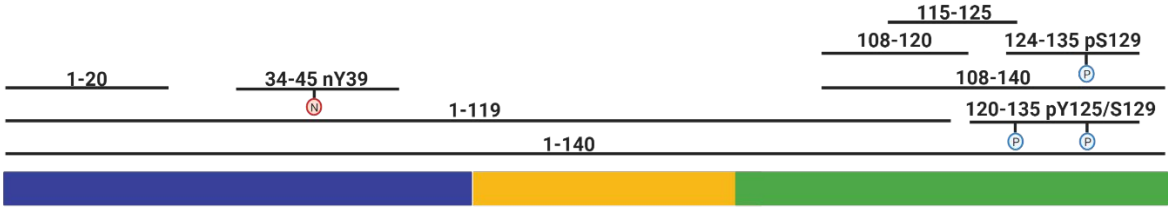

aSyn human proteins and peptides used for BALB/c mouse immunisation.

Hybridoma technology was used for the production of monoclonal antibodies, where the antibody-producing lymphocytes were fused with Sp2/0-Ag14 (ATCC #CRL-8287) mouse myeloma cells using polyethylene glycol at a 5:1 ratio. The hybridomas were grown in hypoxanthine-aminopterin-thymidine selective media to eliminate unfused myeloma cells. Supernatants of 6 to 44 clones per programme were tested by ELISA, DB and WB against a selected library of aSyn proteins (Table 2. 2) to determine the clones with the strongest and the most specific results. Selected clones were further sub-cultured for several rounds to maintain stability, subjected to serial dilution to ensure monoclonality, and screened by ELISA, DB and WB for the identification of positive and specific clones. Isotyping and *in vitro* production of antibodies were carried out with the selected subclones, on an Akta 25 fast protein liquid chromatography (FPLC) system using a 25mL protein G sepharose column (Cytiva) according to the instructions of the manufacturer. Briefly, the resin was equilibrated using 10 column volumes of buffer A (20mM phosphate buffer pH7.2) before loading the filtrated sample on the column. Following a wash step of 10 CV with buffer A, antibodies were eluted

using an isocratic elution with buffer B (100mM glycine pH2.7), and were immediately pH-neutralised with 1M Tris buffer pH8.0 upon their harvest in fractionation tubes. Buffer exchange was performed against 10mM PBS using a 30kDa dialysis membrane, and the harvested antibodies were stored at -70 °C. Antibody concentrations were determined using absorbance reading at 280nm, and purity was determined by size exclusion chromatography. An average of 45mg from each of the 12 antibodies were obtained.

2.4.2 Expression and purification of aSyn monomers

The expression and purification of human and mouse aSyn were carried out as described (Fauvet et al., 2012b). Briefly, pT7-7 plasmids encoding variants of mouse and human aSyn were used to transform BL21(DE3) chemically competent *E. coli* and let to grow on an agar dish with ampicillin. One colony was transferred to 400mL of Luria broth (LB) media with ampicillin at 100µg/mL and left to grow at 37 °C on shaker (at 180RPM) for 16h. The small culture was then used to inoculate a large culture of 6L LB media with ampicillin at 100µg/mL. At an optic density (OD_{600}) of 0.5-0.6, isopropyl β-D-1-thiogalactopyranoside was added at a final concentration of 1mM to induce aSyn expression. The large culture was left to grow further for 4h on shaker, centrifuged at 4,000*g* for 15min at 4 °C. The pellet was re-suspended on ice in lysis buffer (10mL p/L of culture) containing 20mM Tris pH8.0, 0.3mM phenylmethylsulfonyl fluoride (PMSF) protease inhibitor and cOmplete, mini, EDTA-free protease inhibitor cocktail tablet (Roche #4693159001; one tablet per 10mL lysis buffer). Cells were lysed by sonication (59s-pulse and 59s-no pulse over 5min at 60% amplitude). The lysate was centrifuged at 4 °C for 30min at 20,000*g*, the supernatant boiled for 5-15min at 100 °C, and the centrifugation step repeated. Supernatant was filtered using a 0.22µm syringe filter, and purified via anion exchange chromatography and reverse-phase high performance liquid chromatography (HPLC). The quality control of the proteins was run via analysis by liquid chromatography-mass spectrometry (LC-MS), ultra-performance liquid chromatography (UPLC) and SDS-PAGE separation and Coomassie staining. aSyn nY39, pY39, pS87, pY125 and pS129 protein standards were prepared using semi-synthesis as previously described (Hejjaoui et al., 2012).

2.4.3 aSyn oligomer generation

Generation of aSyn oligomers was carried out as previously described (Kumar et al., 2020b). Briefly, aSyn human WT monomers were dissolved in PBS for a final concentration of 12mg/mL, and was supplemented with benzonase at 1uL/mL. The solution was incubated in low-protein binding tubes at 37 °C for 5h at 900rpm, centrifuged for 10min at 12,000*g* at 4 °C, and 5mL of supernatant was run through a PBS-equilibrated Hiload 26/600 Superdex 200pg column. Eluted fractions were screened via SDS-PAGE. Oligomeric fractions were characterised by EM, circular dichroism (CD) before being collected, snap frozen and stored at -20 °C.

2.4.4 Generation of aSyn pre-formed fibrils *in vitro*

Lyophilised human or mouse aSyn WT monomers were re-suspended in PBS, and the pH was adjusted to 7.5. The protein solution was passed through filters with 100kDa cut-off to remove any spontaneously formed aggregates. Protein concentration was measured via ultraviolet absorption at 280nm and/or by bicinchoninic acid (BCA) assay. Monomers in solution were left on an orbital shaker (at 1000RPM) for 5 days at 37 °C. For application to cellular seeding models, the fibrils were sonicated to achieve a median fibril length of 50-100nm. The final fibril prep was characterised for the monomer-to-fibril ratio by sedimentation and filtration assays as described in (Kumar et al., 2020a), for amyloid formation by ThT assay, and for fibril length quantification by electron microscopy analysis.

2.4.5 Dot blot/slot blot and Western blot analysis using aSyn recombinant proteins

For the dot blot/slot blot analysis, aSyn proteins were diluted in PBS and blotted on a nitrocellulose membrane of 0.22µm in 50µL volume corresponding to 250ng of protein loading. For the WB analysis, aSyn proteins were diluted in PBS and Laemmli buffer 4X (50% glycerol, 1M Tris at pH 6.8, 20% β-mercaptoethanol, 10% SDS and 0.1% bromophenol blue), loaded onto a 4-16% Tricine gel in 10µL volume corresponding to 100ng of protein loading and transferred onto a nitrocellulose membrane of pore size 0.22µm using a semi-dry transfer system (BioRad) for 45min at 0.5A and 25V. Where appropriate, Ponceau S staining (2% Ponceau S in 5% acetic acid) was applied as

protein loading control. The membranes were blocked overnight at 4 °C in Odyssey blocking buffer (Li-Cor). They were incubated with primary antibodies diluted in PBS for 2h at RT, washed three times for 10min in PBS with 0.01% Tween-20 (PBS-T), incubated in dark with secondary antibodies diluted in PBS and washed three times for 10min in PBS-T. For the primary and secondary antibody details, see Table 2. 5. The membranes were imaged at 700nm and/or 800nm using the Li-Cor Odyssey CLx imaging system, and the images processed using Image Studio 5.2.

2.4.6 Surface plasmon resonance (Biacore)

SPR data were collected on a Biacore 8 K device (GE Healthcare). Antibody (6A3) was immobilized on a CM5 biosensor chip (GE Healthcare) at 10–20 µg/mL concentration in 10 mM acetate solution (GE Healthcare) at pH 4.5 to reach a final surface ligand density of around 2000–4000 response units (RUs). In short, the whole immobilization procedure using solutions of 1-ethyl-3-(3-dimethyl aminopropyl) carbodiimide (EDC) and N-hydroxy succinimide (NHS) mixture, antibody sample and ethanolamine, was carried out at a flow rate of 10 µL/min into the flow cells of the Biacore chip. Firstly, the carboxyl groups on the sensorchip surface were activated by injecting 200 µL of 1:1 (v/v) mixture of EDC/NHS (included in the amine coupling kit, Cytiva Life Sciences) into both flow cells 1 and 2 and followed by the injection of antibodies overflow cell 2 for 180 s. The remaining activated groups in both the flow cells were blocked by injecting 129 µL of 1 M ethanolamine-HCl pH 8.5. The sensor chip coated with antibodies were equilibrated with PBS buffer before the initiation of the binding assays. Serial dilutions of analytes such as α-syn monomers (human WT 1-20 or human WT 1-140) at a concentration ranging between 2.5 µM to 0.1 µM in PBS buffer were injected into both flow cells at a flow rate of 30 µL/min at 25 °C. Each sample cycle has the contact time (association phase) of 120 s and is followed by a dissociation time of 600 s. After every injection cycle, surface regeneration of the Biacore chips was performed using 10 mM glycine (pH 3.0).

2.4.7 Mouse primary neuronal culture and seeding assay

Primary hippocampal and cortical neurons were collected from P0 pups of WT (C57BL/6JRccHsd, Harlan) or aSyn KO (C57BL/6J OlaHsd, Harlan) mice, according to the dissection procedure described elsewhere (Steiner et al., 2002). Following the

plating in poly-L-lysine-coated plates (300,000 cells/mL), the neurons were left to mature at 37 °C with 5% CO_2. WT neurons were treated with 70nM aSyn mouse WT PFFs on day *in vitro* (DIV)7 and left to incubate for 14 days; and aSyn KO neurons on DIV20 and left to incubate for 24h, as described (Mahul-Mellier et al., 2020, 2018; Volpicelli-Daley et al., 2014, 2011).

2.4.8 Immunocytochemistry and confocal imaging

Mouse primary neurons were washed twice in PBS, fixed with 4% PFA for 20min at RT and stained as described elsewhere (Mahul-Mellier et al., 2015). The antibodies used for ICC are detailed in Table 2. 5. Imaging was carried out on a confocal laser-scanning microscope (LSM 700, Carl Zeiss, Germany) and image analysis on Zen Digital Imaging software (RRID: SCR_013672).

2.4.9 Cell lysis, sequential extraction and Western blotting

Mouse primary neurons were washed in PBS twice on ice and extracted in Tris-buffered saline (TBS; 50mM Tris and 150mM NaCl at pH7.5) with 1% Triton X-100 and with protease inhibitor (PI) cocktail (1:100), 1mM phenylmethane sulfonyl fluoride (PMSF), phosphatase inhibitor cocktails 2 and 3 (1:100), as described previously (Mahul-Mellier et al., 2020, 2018; Volpicelli-Daley et al., 2014, 2011). The cells were lysed via sonication (1s intermittent pulse 10 times at 20% amplitude) using a small probe (Sonic Vibra Cell, Blanc Labo, Switzerland). The lysate was incubated for 30min on ice and centrifuged at 100,000*g* for 30min at 4 °C. The supernatant i.e. the 'soluble' fraction, was collected and diluted in 4X Laemmli buffer (50% glycerol, 1M Tris at pH 6.8, 20% β-mercaptoethanol, 10% SDS and 0.1% bromophenol blue). As the wash step, the pellet was re-suspended in lysis buffer, sonicated and centrifuged as described above. Supernatant was discarded and the pellet re-suspended in TBS with 2% sodium dodecyl sulphate supplemented with protease and phosphatase inhibitors as described above. The re-suspension, i.e. the 'insoluble fraction', was sonicated (1s intermittent pulse 15 times at 20% amplitude) and diluted in 4X Laemmli buffer. Protein concentration was determined by BCA assay separately for the soluble and the insoluble fractions.

The soluble and insoluble fractions were separated on a 16% Tricine gel (ThermoFisher), transferred onto a nitrocellulose membrane of pore size 0.22µm using

a semi-dry transfer system (BioRad) for 45min at 0.5A and 25V. The membranes were blocked overnight at 4 °C in Odyssey blocking buffer (Li-Cor), and washed three times for 10min in PBS with 0.01% Tween-20 (PBS-T). Membranes were incubated with primary antibodies diluted in PBS for 2h at RT, washed three times for 10min in PBS-T, incubated in dark with secondary antibodies diluted in PBS and washed three times for 10min in PBS-T. For the antibody details, see Table 2. 5. The membranes were imaged at 700nm and/or 800nm using the Li-Cor Odyssey CLx imaging system, and the images processed using Image Studio 5.2.

2.4.10 Animals and intra-striatal stereotaxic injection procedure

All animal experimentation was performed in compliance with the European Communities Council Directive of 24 November 1986 (86/609EEC) and with approval of the Cantonal Veterinary Authorities (Vaud, Switzerland) and the Swiss Federal Veterinary Office (authorisation number VD2067.2). C57BL/6JRj male mice (Janvier Labs) at 3 months of age were stereotaxically injected with aSyn mouse WT PFFs (5mg in 2mL PBS) in the right dorsal striatum. 6 months post-injection, the animals were sacrificed by intracardiac perfusion with heparinized sodium chloride (NaCl; 0.9%), and fixed with 4% paraformaldehyde (PFA) in PBS overnight, and paraffin-embedded for immunohistochemical studies. For the antibody validation studies, naïve adult aSyn KO mice (C57BL/6J OlaHsd, Harlan) were sacrificed and brain sections were prepared in the same way as for PFF-injected WT animals.

2.4.11 Immunofluorescent double-labelling of mouse tissue and imaging

WT and aSyn KO mouse paraffin-embedded brain sections were cut coronally to 4µm and dewaxed. Epitope retrieval was carried out in 10mM trisodium citrate buffer at pH6.0 for 20min at 95 °C. Tissue blocking was run by incubation in 3% bovine serum albumin (BSA) and 0.1% Triton X-100 in PBS for 1h at RT. Sections were then incubated with the primary antibody solution overnight at 4 °C, and with the secondary antibody solution for 60min at RT (Table 2. 5). Slides were mounted using an aqueous mounting medium, and tiled imaging was carried out on the Olympus VS120 microscope.

2.4.12 Human brain tissue samples

Post-mortem human brains were collected in accordance with the London Multicentre Research Ethics Committee-approved protocol, and upon the written informed consent from donors. The samples were stored under the licence approved by the Human Tissue Authority (no. 12198). The ethical approval for research was given by the NRES Committee London Central. The cases were selected from the Queen Square Brain Bank (QSBB), UCL Institute of Neurology in London, UK.

2.4.13 Immunohistochemistry of human brain samples and imaging

5 PD, 2 PDD, 1 DLB, 1 *SNCA* H50Q, 3 *SNCA* G51D mutation and 1 *SNCA* duplication brain were used for the immunohistochemical studies. Formalin-fixed paraffin-embedded (FFPE) sections were cut sequentially to 8µm of thickness, de-paraffinised, and treated with methanol and hydrogen peroxide at 1:50 ratio in order to quench the endogenous peroxidase. For epitope retrieval, the sections were treated for 10min with 98% formic acid and 10min with citrate buffer under pressure-cooking. After the blocking in 10% non-fat milk in TBS-Tween (TBST), sections were incubated in primary antibody solution for 1h at RT, washed three times for 5min in TBST, incubated in secondary antibody solution for 30min at RT and washed three times for 5min in TBST. For the antibody details, see Table 2. 5. Avidin-biotin complex was applied according to the manufacturer's instructions, and colour development was run using di-aminobenzidine/ hydrogen peroxide for 2-5min. Counterstaining was run using Mayer's haematoxylin (TCS Biosciences).

2.5 Contributions of the authors

Hilal A. Lashuel conceived and conceptualised the study. Hilal A. Lashuel and Melek Firat Altay designed the experiments. Senthil T. Kumar ran the SPR experiment. Johannes Burtscher provided the aSyn KO and PFF-seeded WT mouse brain tissues for IHC. Somanath Jagannath generated and characterised the aSyn oligomers. Janice L. Holton selected the human cases. Laura Parkkinen contributed to the optimisation of the IHC assays on human cases. Janice H. Holton, Yasuo Miki and Laura Parkkinen contributed to the analysis of the human data. Melek Firat Altay performed all other experiments involved in the study and wrote the chapter.

CHAPTER 3 Astrocytic aSyn pathology in Lewy body diseases[2]

aSyn is a pre-synaptic monomeric protein that can form aggregates in neurons in PD, PDD and DLB, and in oligodendrocytes in MSA. Although the accumulation of aSyn in astrocytes has previously been described in PD, PDD and DLB, the biochemical properties of aSyn in this type of pathology and its topographical distribution have not been studied in detail. Here, we present a systematic investigation of aSyn astrocytic pathology, using an expanded toolset of antibodies covering the entire sequence and PTMs of aSyn in LBDs, including sporadic PD, PDD, DLB, familial PD with *SNCA* G51D mutation and *SNCA* duplication, and in MSA. Astrocytic aSyn was mainly detected in the limbic cortical regions of LBDs, but were absent in key pathological regions of MSA. These astrocytic aSyn accumulations were detected only with a subset of aSyn antibodies with epitopes against the mid N-terminal and NAC regions, but not with the extreme N- or C-terminal antibodies. The astroglial accumulations were negative to canonical aSyn aggregation markers, including p62, ubiquitin and aSyn pS129, but positive for phosphorylated and nitrated forms of aSyn at Tyrosine 39 (Y39), and mostly not resistant to PK. Our findings suggest that astrocytic aSyn accumulations are a major part of aSyn pathology in LBDs, and possess a distinct sequence and PTM signature that is characterized by both N- and C-terminal truncations and modifications at Y39. To the best of our knowledge, this is the first description of aSyn accumulation made solely from N-and C-terminally cleaved aSyn species and the first report demonstrating that astrocytic aSyn exists as a mixture of Y39 phosphorylated and nitrated species. These observations underscore the critical importance of systematic characterization of aSyn in different cell types as a necessary step to capturing the diversity of aSyn species and pathology in the brain. Our findings combined with further studies on the role of astrocytic pathology in the progression of LBDs can pave the way towards identifying novel disease mechanisms and therapeutic targets.

---

[2] The work presented in this chapter is part of the following publication in preparation:

Altay M.F., Liu A.K.L., Holton J.L., Parkkinen L., Lashuel H.A. (2022) Prominent astrocytic alpha-synuclein pathology with unique post-translational modification signatures unveiled across Lewy body disorders.

3.1 Introduction

PD, PDD, DLB and MSA are age-related neurodegenerative diseases that are characterized by the abnormal accumulation and aggregation of aSyn. Hence, they are collectively referred to as synucleinopathies. PD, PDD and DLB typically involve the accumulation of aSyn in the neuronal soma and processes as LBs and LNs, respectively (Baba et al., 1998; Spillantini et al., 1998b, 1997). MSA, on the other hand, is primarily characterized by the inclusion formation mainly in the oligodendrocytes called GCIs (Spillantini et al., 1998a).

In the early 2000s, several studies reported the presence of aSyn-positive astrocytes in LBDs (Hishikawa et al., 2001; Shoji et al., 2000; Takeda et al., 2000; Terada et al., 2003; Wakabayashi et al., 2000) (Table 3. 1). Yet, despite the increasing number of publications aimed at dissecting the molecular and structural features of aSyn pathology, very little is known about the biochemical properties and distribution of aSyn species associated with the astrocytes, how they form, and what role they may have in the pathogenesis of PD and other synucleinopathies. Only a limited number of studies (13) have been published, using a limited number of antibodies, on the characterization of aSyn astrocytic pathology and its relationship to aSyn neuronal pathology, disease stage or duration (Braak et al., 2007b; Fathy et al., 2019; Hishikawa et al., 2001; Kovacs et al., 2014, 2012; Nakamura et al., 2016; Shoji et al., 2000; Song et al., 2009; Sorrentino et al., 2019; Takeda et al., 2000; Terada et al., 2003, 2000; Wakabayashi et al., 2000).

Table 3. 1 The studies since 2000 investigating the astrocytic aSyn pathology in human disease brains.

study	aSyn antibody	aSyn epitope	disorder	anatomical regions detected	characteristics
Shoji et al 2000	MDV	1-15	DLBD	cerebral cortex, basal ganglia	star-like
			PD	cerebral cortex	dot-like
Takeda et al 2000	anti-NAC	61-75	LBD	neocortex, hippocampus, brainstem	star-like negative for ubiquitin
Terada et al 2000	Chemicon	unknown	DLB	temporal, insular, cingulate and fronto-orbital cortices, amygdala, hippocampus	star-like positive with GB and GFAP double staining negative for aSyn, ubiquitin or tau
Wakabashi et al 2000	NACP-1	unknown	PD	midbrain	circular or coil-like, argyrophilic
	NACP-3	121-140			positive with GB staining
	NACP-5	114-131			which of the aSyn antibodies detect astrocytic aSyn not specified
Hishikawa et al 2001	FL140	61-95	PD	striatum, substantia nigra, pons, medulla, cerebellum, spinal cord	circular or coil-like, argyrophilic distribution of glial accumulations not exclusive to astrocytic aSyn – refers to astrocytic and oligodendroglial aSyn distribution combined
Terada et al 2003	EQV1	61-76	DLBD	temporal, cingulate, fronto-orbital, parietal, insular cortices, amygdala, basal ganglia	star-like, argyrophilic positive with GB staining not resistant to PK
Braak et al 2007	SYN-1	91-99	PD	amygdala, thalamus, septum, striatum, claustrum and cerebral cortex	star-like negative for ubiquitin, p62 negative with modified Gallyas or Campbell-Switzer staining
Song et al 2009	SYN-1	91-99	PD	pons	cytoplasmic staining
	Abcam	unknown			
Kovacs et al 2012	5G4	44-57 // agg-aSyn	DLB	amygdala, cingulate cortex	star-like
Kovacs et al 2014	5G4	44-57 // agg-aSyn	PD, DLB	entorhinal and temporal cortices, amygdala, striatum, hippocampus	star-like (cortex and amygdala) granular cytoplasmic (striatum)
Nakamura et al 2016	Wako	pS129	MSA	medulla, pons, midbrain, spinal cord, lateral ventricles	granular, non-fibrillar negative for ubiquitin, p62
	Abcam EP1536Y	pS129			negative with GB staining
Fathy et al 2019	SYN-1	91-99	ILBD, PD, PDD, DLB	insula	thin, fuzzy projections with some star-like accumulations; cytoplasmic aSyn in GFAP-positive astrocytes form a mesh-like structure
Sorrentino et al 2019	3H11	43–63	DLB, AD/ALB	amygdala	star-like, granular
	5G4	44–57 // agg-aSyn			

AD/ALB = Alzheimer's disease with amygdala restricted Lewy bodies; aSyn = alpha-synuclein; agg-aSyn = aggregated alpha-synuclein; DLB = dementia with Lewy bodies; DLBD = diffuse Lewy body disease; GB = Gallyas-Braak; GFAP = glial fibrillary acidic protein; ILBD = incidental Lewy body disease; LBD = Lewy body disease; PD = Parkinson's disease; PDD = Parkinson's disease with dementia; PK = proteinase K

One of the key reasons for the scarcity of data on astrocytic aSyn is that only a few of the aSyn antibodies appear to reveal these species. Although previous studies have reported that the astrocytic aSyn is detected by antibodies with epitopes against the NAC region of aSyn (Braak et al., 2007b; Kovacs et al., 2012; Sorrentino et al., 2019), they did not define the sequence properties of aSyn or identify the molecular

determinants underpinning their observations. These astrocytic aSyn species are not revealed by the classical inclusion markers such as positivity for ubiquitin (Braak et al., 2007b; Kovacs et al., 2014; Nakamura et al., 2016; Takeda et al., 2000; Terada et al., 2000) and p62 (Braak et al., 2007b; Kovacs et al., 2014; Nakamura et al., 2016; Takeda et al., 2000; Terada et al., 2000), and their PTM profile and aggregation states have not been systematically investigated beyond two studies that assessed S129 phosphorylation status (Nakamura et al., 2016; Sorrentino et al., 2019). Furthermore, the majority of the antibodies used to characterise and diagnose aSyn pathology are directed at the C-terminal domain of the protein, which could lead to the under-reporting of aSyn astrocytic pathology. The lack of appropriate tools and techniques that allow for the selective isolation and characterization of the astrocytic aSyn presents major challenges to defining their biochemical properties and relationship to other aSyn brain pathologies.

To address these challenges, we assessed aSyn astrocytic pathology using an expanded set of antibodies that target epitopes throughout the entire sequence of the protein and for the first time against all key aSyn PTMs (8 PTMs). To further characterize the aggregation state of aSyn species in the astroglia, we used antibodies against known markers of LBs (ubiquitin, p62), aSyn aggregate-specific antibodies, the amyloid-specific dye Amytracker, and investigated their resistance to proteolysis by PK. With the aim of shedding light on the biochemical properties of astrocytic aSyn pathology across different regions and synucleinopathies, we extended our studies to several limbic brain regions, including the entorhinal cortex, hippocampus, cingulate cortex, insula and amygdala of PD, PDD and DLB; and the pons, putamen, cerebellum, frontal cortex and occipital cortex of MSA.

Our studies show that astrocytic aSyn accumulations occur extensively in the limbic and cortical areas of LB disease cases. These aSyn species are post-translationally modified at Tyrosine 39 and cleaved at both the N- and C-termini of the protein, as evidenced by the fact that they are detected with antibodies targeting epitopes approximately between residues 34-99. In addition to presenting new insight into the sequence, aggregation state and biochemical properties of astrocytic aSyn, our work provides a validated toolset that should enable a more systematic re-assessment of the role of astrocytic aSyn pathology in the development and progression of

synucleinopathies. Our findings also emphasise the importance of using an expanded set of appropriate and validated detection tools capable of capturing the diversity of aSyn species to map and characterize aSyn pathology in astrocytes and other cell types.

3.2 Results

3.2.1 Mapping the astrocytic aSyn proteoform in LBDs

We have previously shown that the use of antibodies against different regions and post-translational modifications of aSyn enables revealing the pathological diversity across synucleinopathies (see Chapter 2 on p.61). Therefore, we sought to use an expanded antibody tool box to characterize the aSyn astrocytic pathology. A complete list of the antibodies used in this study and their epitopes is shown in Table 3. 2. DLB entorhinal cortex was stained using two antibodies against the N-terminal (epitopes 1-20 and 34-45), two against the NAC region (epitopes 80-96 and 91-99) and two against the C-terminal regions (epitopes 110-115 and 134-138) of aSyn (Figure 3. 1A). The same sections were also screened for aSyn PTMs, including Serine (at Ser87 and Ser129) and Tyrosine (at Tyr39, Tyr125, Tyr133 and Tyr136) phosphorylations, N-terminal nitration at Tyr39 (nY39) and C-terminal truncation at residue 120 (Figure 3. 1B). Whilst all the antibodies against non-modified aSyn were able to detect LBs and LNs, only the N-terminal antibody LASH-BL 34-45 and the two NAC region antibodies LASH-BL 80-96 and BD SYN-1 (epitope 91-99) were able to reveal the star-like astroglial aSyn structures (Figure 3. 1A). We confirmed the specificity of these three antibodies to aSyn by pre-adsorption treatment, after which the positivity to LBs and star-like structures was lost (Figure 3. 2). Strikingly, only the two antibodies against the aSyn PTMs in the N-terminal region of the protein, i.e. pY39 and nY39, but not the antibodies targeting the C-terminal aSyn PTMs, were positive for these astroglial structures (Figure 3. 1B).

Table 3. 2 The primary and secondary antibodies included in this study.

primary antibodies							
antibody	**epitope**	**species/ clonality**	**company / catalogue #**	**IHC: antigen retrieval**	**IHC: dilution**	**IF: dilution***	**SB: dilution**
LASH-EGTNter	aSyn 1-20	rab pc	na	AC+FA	1:15,000	na	1:1,000
LASH-BL 34-45	aSyn 34-45	mus mc	Biolegend #849101	FA	1:30,000	1:10,000	na
LASH-BL 80-96	aSyn 80-96	mus mc	Biolegend #848302	FA	1:20,000	na	na
BD SYN-1	aSyn 91-99	mus mc	BD #BD610787	FA	1:5,000	na	1:2,000
BL 4B12	aSyn 103-108	mus mc	Biolegend #807801	AC+FA	1:100,000	na	na
2F10-E12	aSyn 110-115	mus mc	na	AC+FA	1:10,000	na	na
AB 134-138	aSyn 134-138	rab pc	Abcam #ab131508	AC+FA	1:25,000	na	na
LASH-EGT pY39	aSyn pY39	rab pc	na	AC+FA	1:500	na	na
LASH-BL pY39	aSyn pY39	mus mc	Biolegend #849201	AC+FA	1:2,000	1:500	1:1,000
LASH pS87	aSyn pS87	rab pc	na	FA	1:600	na	na
AB pY125	aSyn pY125	rab pc	Abcam #ab10789	FA	1:500	na	na
AB EP1536Y	aSyn pS129	rab mc	Abcam #ab51253	AC+FA	1:60,000	1:10,000	na
AB pY133	aSyn pY133	rab pc	Abcam #ab194910	AC+FA	1:400	na	na
AB pY136	aSyn pY136	rab pc	Abcam #ab131491	FA	1:100	na	na
LASH-EGT nY39	aSyn nY39	rab pc	na	FA	1:1,000	1:500	1:200
6A3-E9	aSyn-120	mus mc	na	AC+FA	1:2,500	na	na
5G4	44-57 // agg-aSyn	mus mc	Merck-Millipore #MABN389	AC+FA	1:5,000	na	na
SYNO4	agg-aSyn	mus mc	na	FA	1:5,000	na	na
Merck-MP anti-GFAP	GFAP	ck pc	Merck-Millipore #AB5541	na	na	1:500	na
Merck-MP EP79 anti-NF	NF	rab mc	Merck-Millipore #302R-1	na	na	1:500	na
AB anti-Iba1	Iba1	goat pc	Abcam #ab5076	na	na	1:80	na
Merck-MP anti-MBP	MBP	rab pc	Merck-Millipore #AB5864	na	na	1:2,000	na
AB EPR8830 recomb anti-Ub	ubiquitin	rab mc	Abcam #ab134953	na	na	1:800	na
Proteintech anti-p62	p62	rab pc	Proteintech #18420-1-AP	na	na	1:200	na
*AC+FA pre-treatment was applied for IF studies for all antibodies.							

secondary antibodies				
antibody	**dilution**	**company**	**catalogue #**	**application**
donkey anti-chicken 488	1:400	Jackson ImmunoResearch	703-545-155	IF
goat anti-chicken 568	1:400	ThermoFisher	A-11041	IF
donkey anti-goat 488	1:1,000	ThermoFisher	A-11055	IF
donkey anti-rabbit 568	1:1,000	ThermoFisher	A-10042	IF
donkey anti-mouse 568	1:1,000	ThermoFisher	A-10037	IF
donkey anti-mouse 647	1:1,000	ThermoFisher	A-31571	IF
IRDye goat anti-mouse 680	1:20,000	Li-Cor	926-68070	SB
IRDye goat anti-rabbit 800	1:20,000	Li-Cor	926-32211	SB

AC = autoclave; agg-aSyn = aggregated alpha-synucleina; aSyn = alpha-synuclein; FA = formic acid; GFAP = glial fibrillary acidic protein; Iba1 = ionised calcium binding adaptor protein 1; IF = immunofluorescence; IHC = immunohistochemistry; MBP = myelin basic protein; mc = monoclonal; mus = mouse; na = not applicable; NF = neurofilament; pc = polyclonal; rab = rabbit; SB = slot blot

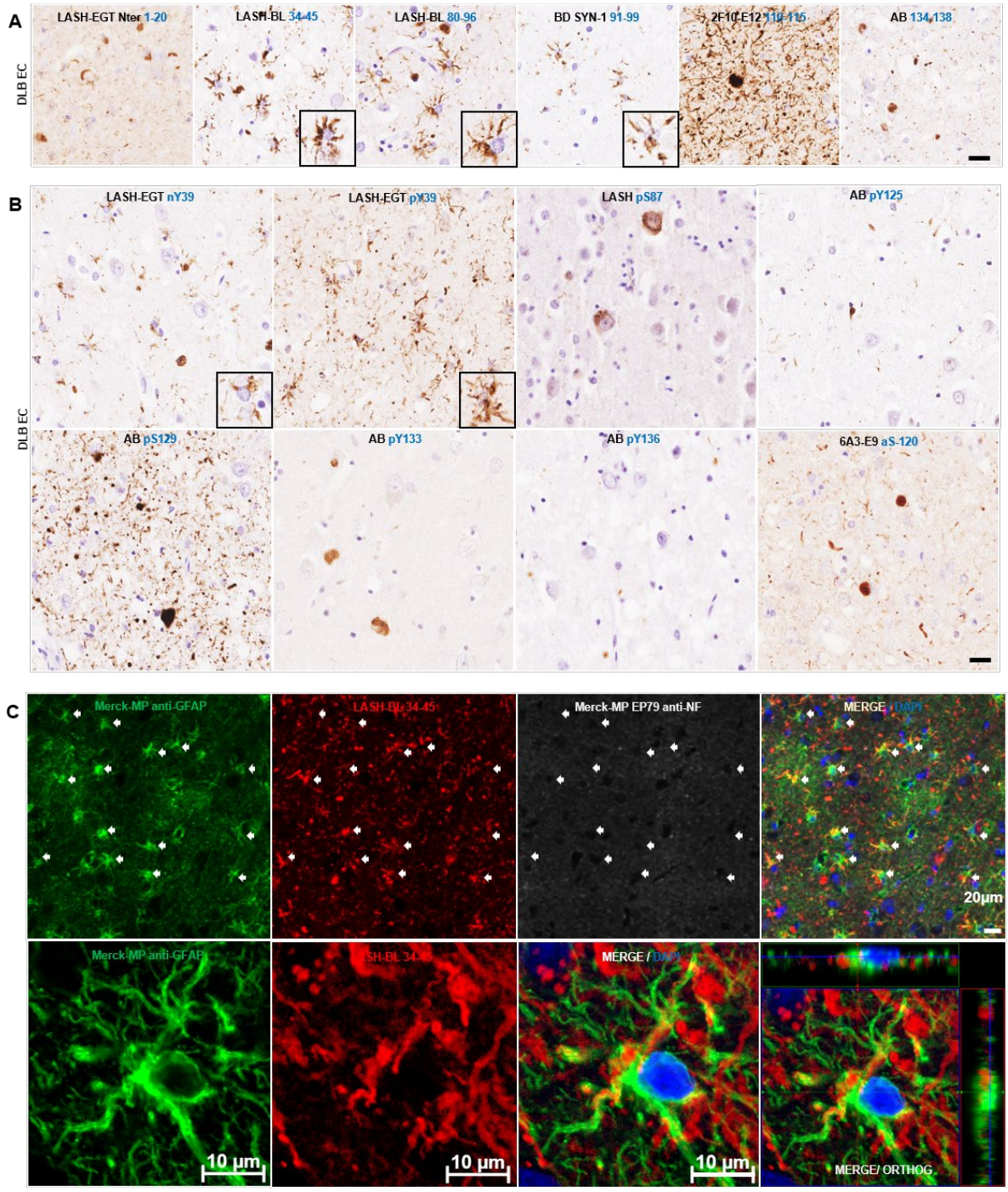

Figure 3. 1 The star-like astrocytic aSyn accumulations in the entorhinal cortex of a DLB patient. (A) The EC of DLB brains were immunohistochemically stained using aSyn antibodies with epitopes against the N-terminus (LASH-EGTNter 1-20 and LASH-BL 34-45), the NAC region (LASH-BL 80-96 and BD SYN-1 91-99) and the C-terminus (2F10-E12 110-115 and AB 134-138) of aSyn. The extreme N-terminal antibody LASH-EGTNter as well as the C-terminal antibodies 2F10-E12 and AB 134-138 showed neuronal pathology in the soma and neurites. The late N-terminal antibody LASH-BL 34-45 as well as the two NAC region antibodies LASH-BL 80-96 and BD SYN-1 were positive for LBs and LNs, but also distinctively detected star-shaped glial aSyn species (insets). (B) The aSyn PTM antibodies against phosphorylation and nitration at Tyrosine 39 (Y39) were also reactive to the star-like astroglial pattern (insets). (C) Star-like aSyn species are associated with the GFAP-positive astrocytes in the DLB brains as shown by IF using antibodies for astrocytic and neuronal markers GFAP and NF, and LASH-BL 34-45 antibody against aSyn. The star-like aSyn species (arrows) appeared in and around the GFAP-positive astrocytes, and not

the LNs. Images on the upper panel taken using Olympus slide scanner at 40x magnification, and the lower panel on Zeiss LSM700 confocal microscope. Scale bar for Figure 1A-B is 20µm for the main images and 40µm for the insets. aSyn = alpha-synuclein; DLB = dementia with Lewy bodies; EC = entorhinal cortex; GFAP = glial fibrillary acidic protein; IF = immunofluorescence; LB = Lewy body; LN = Lewy neurite; NAC = non-amyloid-beta component; NF = neurofilament; PTM = post-translational modification

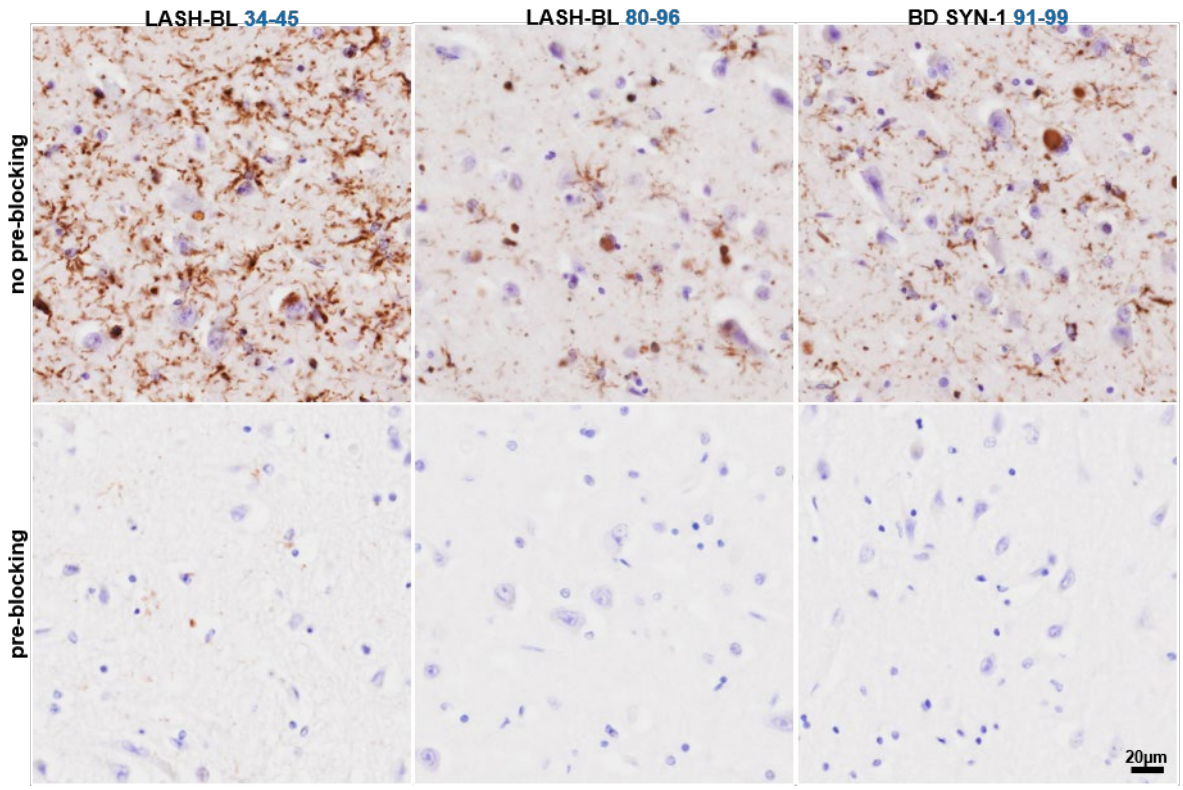

Figure 3. 2 Specificity validation of the aSyn antibodies LASH-BL 34-45, LASH-BL 80-96 and BD SYN-1 by pre-adsorption followed by IHC on DLB cingulate cortex. aSyn = alpha-synuclein; DLB = dementia with Lewy bodies; IHC = immunohistochemistry

To validate that these structures represent aSyn in the astrocytes, we performed immunofluorescent labelling. DLB cingulate cortex was stained using LASH-BL 34-45, the best performing antibody to reveal the star-like aSyn accumulations by immunohistochemistry (Figure 3. 1A), and glial fibrillary acidic protein (GFAP) and neurofilament (NF) antibodies i.e. the standard markers for astrocytes and neurons, respectively. The cortical LBs were positive for NF and LASH-BL 34-45, and negative for GFAP (Figure 3. 3A). The GFAP-positive astrocytes, on the other hand, were also positive for LASH-BL 34-45, and negative for NF by confocal imaging (Figure 3. 1C). The oligodendroglia and the microglia in the white matter, marked with myelin basic protein (MBP) and ionised calcium binding adaptor protein 1 (Iba1) respectively, were

negative to aSyn (Figure 3. 3B). Microglial positivity to aSyn was observed in the grey matter as rare events and did not show a star-like morphology (Figure 3. 3B). Collectively, these observations demonstrate that the star-like structures revealed by immunohistochemistry using the late N-terminal and NAC region aSyn antibodies represent aSyn accumulations in and around the astrocytes. These findings also suggest that the extreme N- and C-terminal regions of aSyn are either masked by heavy modifications, bound to other molecules or are cleaved, and thus explain why astrocytic aSyn cannot be detected with antibodies targeting these regions.

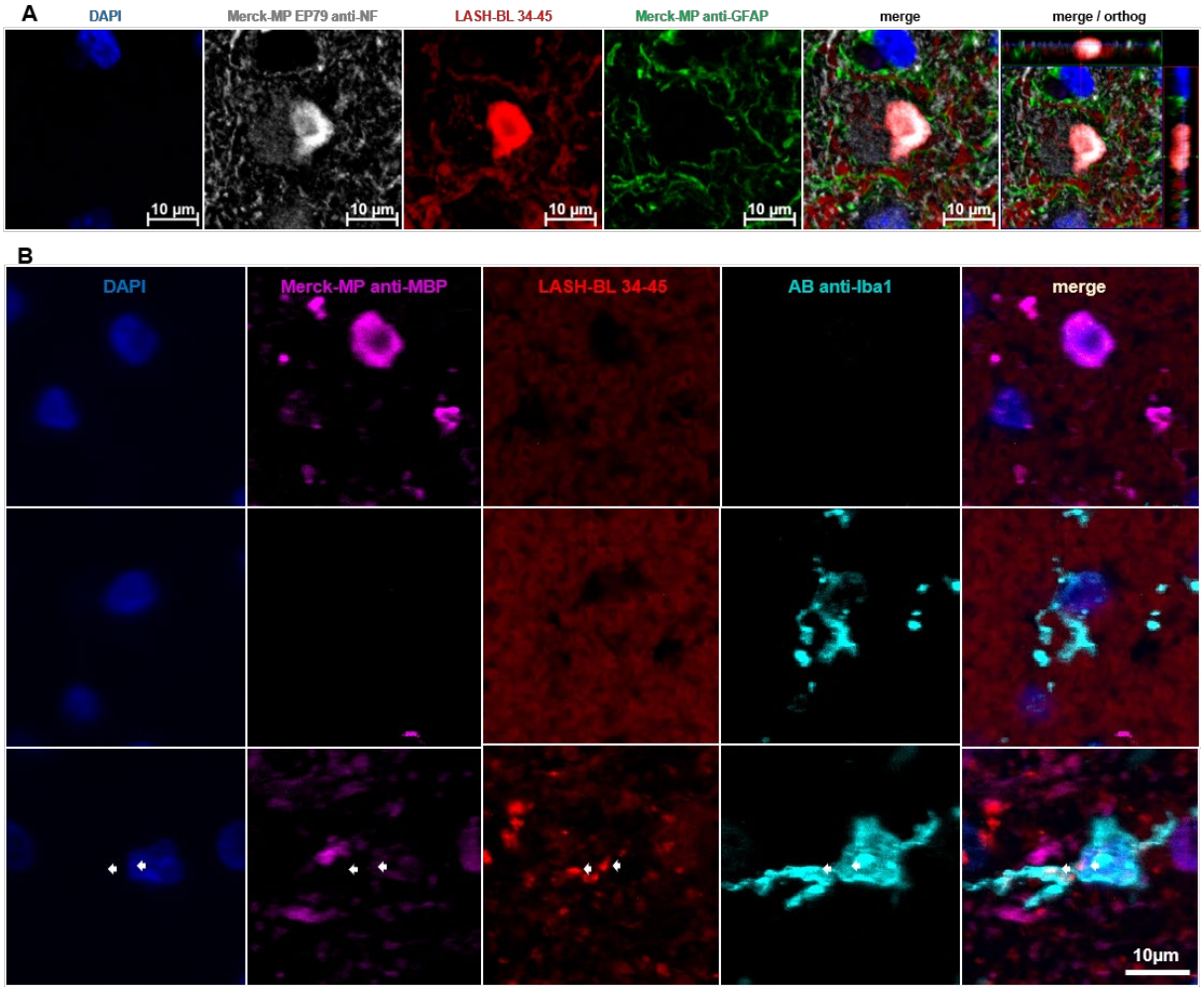

Figure 3. 3 (A) A representative image of a cortical LB positive for NF and LASH-BL 34-45, and negative for GFAP. Image from DLB cingulate cortex, taken using Zeiss LSM700 confocal microscope. (B) The oligodendrocytes and microglial cells, marked by anti-MBP and anti-Iba1 antibodies, respectively, were negative for aSyn in the white matter (upper two panels). Punctate aSyn positivity was detected in the microglial cells in the grey matter (lower panel) as rare events. Images taken from DLB cingulate cortex using Olympus slide scanner at 40x magnification. aSyn = alpha-synuclein; DLB = dementia with Lewy body; GFAP = glial fibrillary acidic protein; Iba1 = ionised calcium binding adaptor protein 1; MBP = myelin basic protein; LB = Lewy body; NF = neurofilament

3.2.2 Astrocytic aSyn is modified at Tyrosine 39

As shown in Figure 3. 1B, our data show for the first time that astrocytic aSyn accumulations contain a mixture of aSyn species that are phosphorylated or nitrated at Tyrosine 39 (Y39). To corroborate our findings, we first validated the specificity of the aSyn pY39 and nY39 antibodies. The antibodies were incubated with aSyn recombinant protein bearing either pY39 or nY39 before using them to detect site-specifically nitrated and phosphorylated recombinant aSyn by slot blot (SB). The positive signal for aSyn nY39 and for aSyn pY39 recombinant proteins were lost after the pre-blocking of LASH-EGT nY39 and LASH-BL pY39 antibodies, respectively (Figure 3. 4A). The same pre-blocking protocol was then repeated, and the pre-blocked antibody solutions applied onto DLB cingulate cortex tissues. Similarly, following the pre-blocking of the antibodies, the positivity for aSyn nY39 and pY39-positive species, including that for the astroglial structures, was abolished (Figure 3. 4B). Next, we immunofluorescently co-labelled the cingulate sections with GFAP and aSyn pY39 or nY39 antibodies. Consistent with our observations by brightfield microscopy (Figure 3. 1B), GFAP-positive astrocytes showed star-like aSyn inclusions positive for nY39 (Figure 3. 4C).

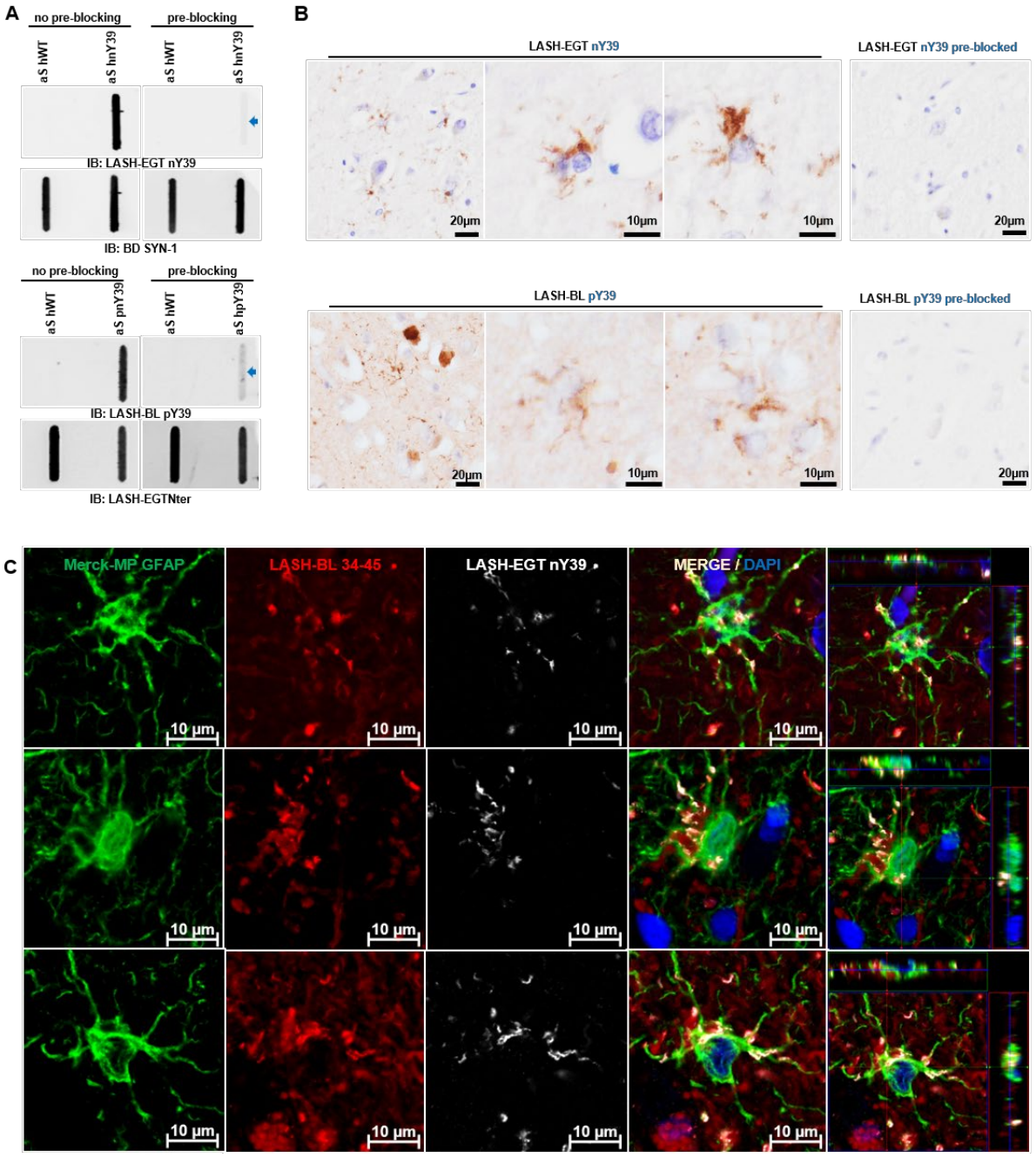

Figure 3. 4 Astrocytic aSyn is modified at Tyrosine 39. (A) The specificity of the aSyn PTM antibodies against phosphorylation and nitration at Y39 were validated via antibody pre-blocking overnight followed by SB analysis. (B) The signal for astrocytic aSyn phosphorylated and nitrated at Y39 was lost with the antibody pre-blocking in the DLB cingulate cortex. (C) The GFAP- and aSyn-positive astrocytes in the cingulate cortex of DLB were positive for aSyn nY39. aSyn = alpha-synuclein; DLB = dementia with Lewy bodies; GFAP = glial fibrillary acidic protein; PTM = post-translational modification; SB = slot blot

3.2.3 Astrocytic aSyn accumulations occur across LBDs and may be truncated in the N- and C-termini

Having established that the star-like aSyn structures are astrocytic in DLB brains, we then sought to explore if the astrocytic aSyn exhibits similar biochemical and staining properties across other LBDs. We screened, using the same set of antibodies against non-modified aSyn, the cingulate cortices of sporadic and familial PD, PDD and DLB cases. The astrocytic aSyn accumulations were observed widely across these LB diseases (Figure 3. 5A; Figure 3. 6). These sections were double-labelled with aSyn LASH-BL 34-45 antibody and GFAP, which revealed that GFAP-positive astrocytes are positive to the aSyn accumulations in these cases (Figure 3. 7). The pons, putamen, cerebellum, frontal cortex and occipital cortex of MSA cases were stained using these aSyn antibodies, but we failed to detect astroglial pathology in the MSA brains.

To determine if the astrocytic aSyn species are also N-terminally and/or C-terminally truncated, and to more precisely map their sequence, we stained the same cingulate sections using BL 4B12 antibody, which targets residues 103-108. Interestingly, the astroglial structures were not detected using this antibody in any of the LBD cases in the cingulate cortex (Figure 3. 6B). Our results suggest that astrocytic aSyn may be truncated in the N-terminus between residues 21-33, and in the C-terminus between residues 100-102 (Figure 3. 5C).

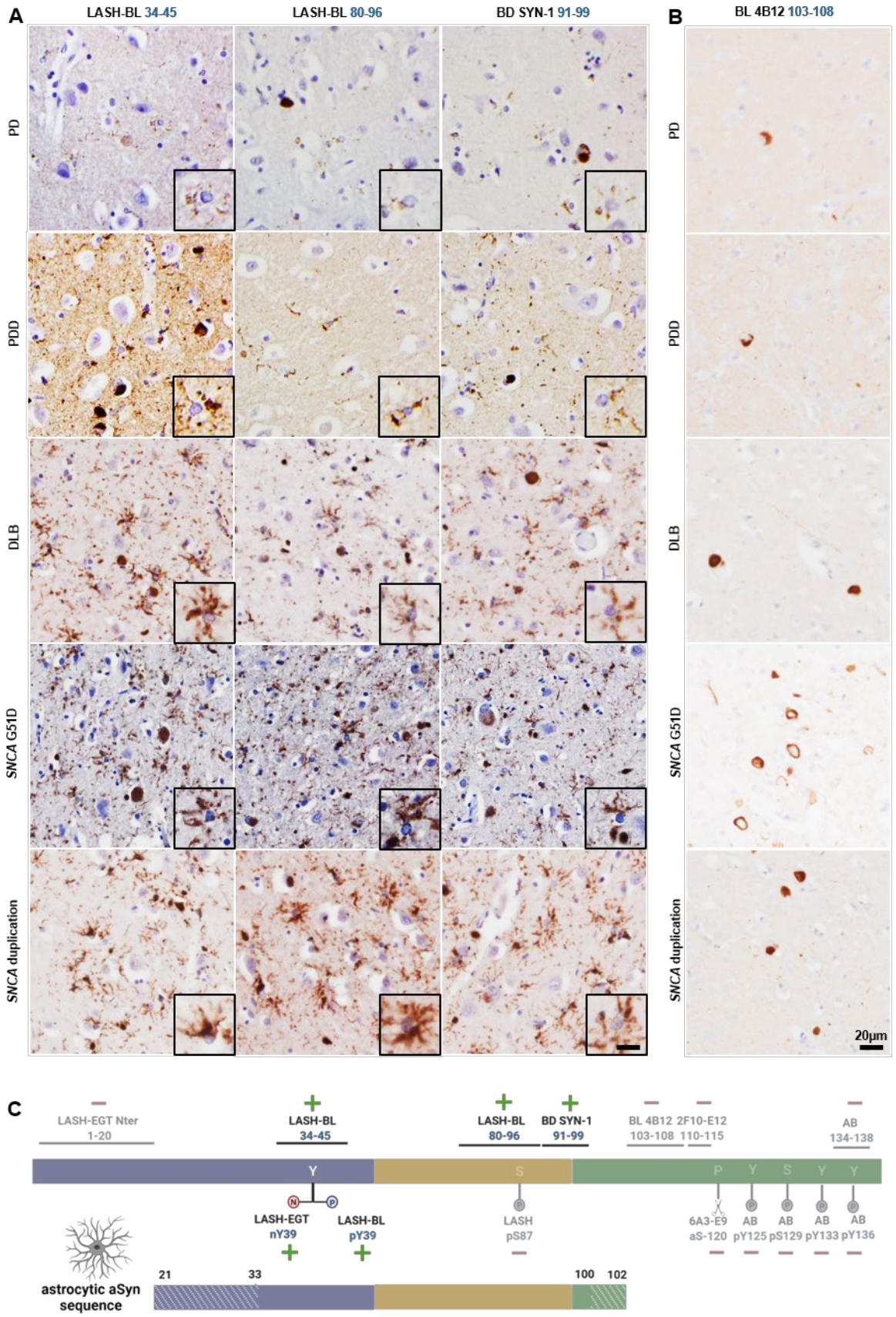

Figure 3. 5 Astrocytic aSyn accumulations occur across LBDs, and may be truncated in the N- and C-termini. (A) PD, PDD, DLB, *SNCA* G51D mutation and *SNCA* duplication cingulate cortices were immunohistochemically stained using the three aSyn antibodies LASH-BL 34-45, LASH-BL 80-96 and BD SYN-1, and astrocytic

accumulations (insets) were revealed across these LBDs. (B) To further map the C-terminal truncation region of the astrocytic aSyn, the same cingulate cortex sections were stained using the C-terminal BL 4B12 antibody with an epitope 103-108 of aSyn. Neuronal inclusions were revealed, but the astrocytic aSyn was not detected, suggesting that the aSyn species associated with the astrocytes are truncated at residues 21-33 in the N-terminus, and at residues 100-102 in the C-terminus. (C) A summary to show the antibodies that are positive and negative for astrocytic aSyn, and their epitopes. The areas in stripes denote the potential truncation regions in the N- and C-termini. Schematic created with BioRender.com (agreement no: *DJ23GJF70T*). Scale bar for Figure 3A is 20µm for the main images and 40µm for the insets. aSyn = alpha-synuclein; DLB = dementia with Lewy bodies; LB = Lewy body; LBD = Lewy body disease; PD = Parkinson's disease; PDD = Parkinson's disease with dementia

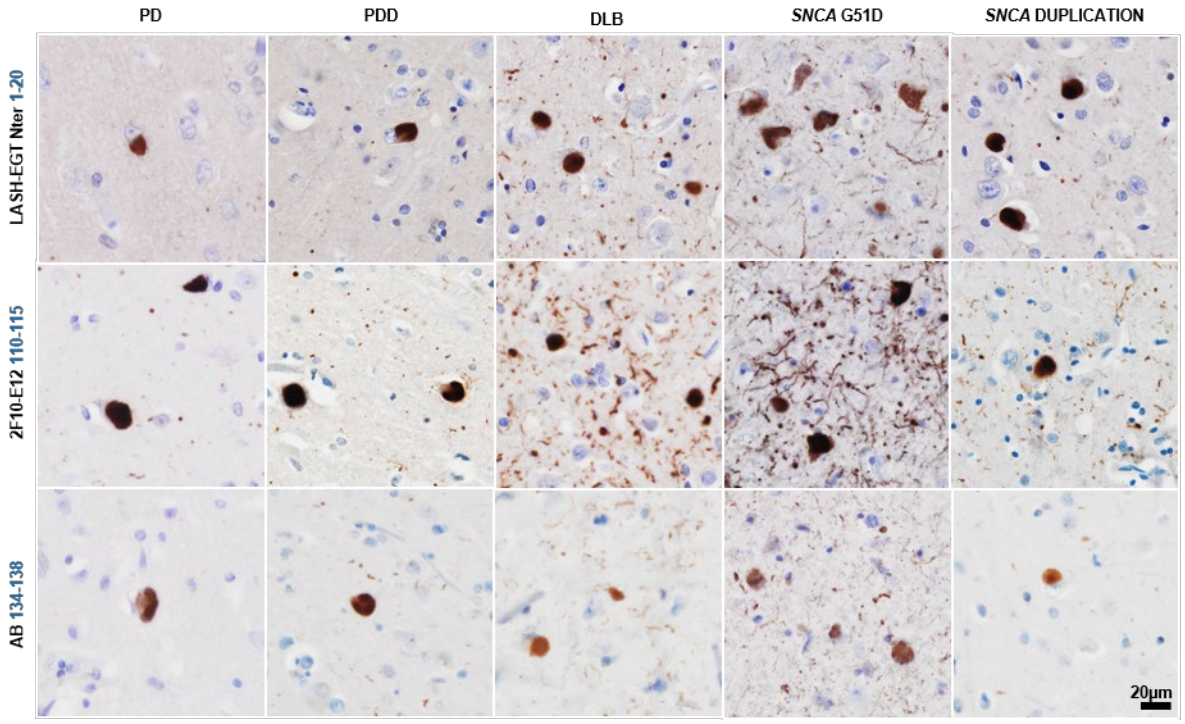

Figure 3. 6 The cingulate cortex of sporadic PD, PDD, DLB, *SNCA* G51D mutation and *SNCA* duplication cases immunostained using antibodies against the N-terminal (LASH-EGTNter) and C-terminal (2F10-E12 and AB 134-138) of aSyn. Astrocytic aSyn was not detected using these antibodies. aSyn = alpha-synuclein; DLB = dementia with Lewy bodies; PD = Parkinson's disease; PDD = Parkinson's disease with dementia

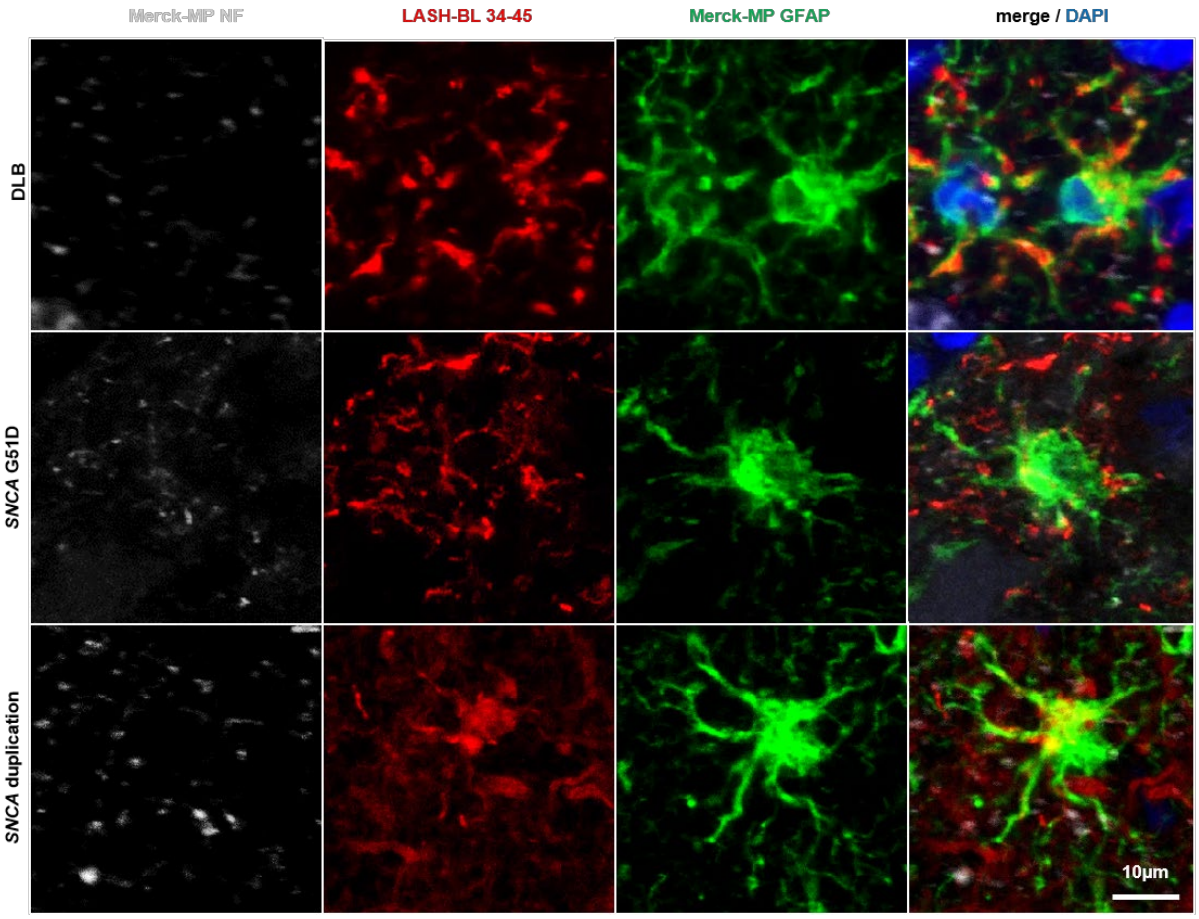

Figure 3. 7 Representative IF images of GFAP-positive astrocytes from DLB, *SNCA G51D* mutation and *SNCA* duplication cingulate cortices, showing positivity for aSyn detected using LASH-BL 34-45 antibody. Images taken using Olympus slide scanner at 40x magnification. aSyn = alpha-synuclein; DLB = dementia with Lewy body; GFAP = glial fibrillary acidic protein; IF = immunofluorescence; NF = neurofilament

3.2.4 Astrocytic aSyn accumulations are not immunoreactive for the classical Lewy pathology markers

To investigate the nature and aggregation state of aSyn in these accumulations, the astrocytic aSyn species were screened for the canonical markers of aSyn aggregation and inclusion formation. DLB cingulate cortex was triple labelled with LASH-BL 34-45 and GFAP, and either with antibodies against p62, ubiquitin, aSyn pS129 or with the amyloid dye Amytracker. In line with our brightfield microscopy results (Figure 3. 1B), the cortical LBs and LNs showed strong positivity to aSyn pS129, whereas the astrocytes positive for LASH-BL 34-45 remained negative for aSyn pS129 (Figure 3. 8A). Similarly, whereas the cortical LBs were positive for ubiquitin and p62, the aSyn-positive astrocytes were negative for these LB markers (Figure 3. 8B-C). In contrast,

astrocytic aSyn accumulations showed only partial positivity to amyloid dye Amytracker, which also labelled the cortical LBs (Figure 3. 8D). Considering that several of the key lysine residues, found to be ubiquitinated in LBs (Anderson et al., 2006), reside in the N-terminal domain of the protein (i.e. K12, K21 and K23), and that p62 is a monoubiquitin- and polyubiquitin-binding protein (Cavey et al., 2004; Lee and Weihl, 2017; Raasi et al., 2005), the absence of ubiquitin and p62 positivity in the astrocytic aSyn is in line with our observations that the aSyn species in the astroglia are N-terminally truncated between residues 21-33.

One of the characteristics of aggregated aSyn in LB diseases is their resistance to PK digestion (Neumann et al., 2004; Tanji et al., 2010). To further characterize the aggregation state of aSyn in astrocytes, we treated the DLB cingulate cortex tissues with PK, and observed that the large majority of the astrocytic aSyn signal disappeared after PK treatment (Figure 3. 8E). Next, we profiled the astrocytic aSyn using two antibodies, 5G4 and SYNO4, that show preferential binding to aggregated aSyn (Kovacs et al., 2014, 2012; Kumar et al., 2020b; Vaikath et al., 2015). Interestingly, the star-shaped astrocytic aSyn accumulations were revealed by the 5G4 antibody, but not by the SYNO4 antibody (Figure 3. 8F). Altogether, these observations suggest that aSyn species that accumulate in the astrocytes may not possess the amyloid-like properties of aSyn fibrils found in LBs and LNs, but could still represent a mixture of soluble and non-amyloidogenic aggregates i.e. oligomers. Unfortunately, the lack of oligomer-specific antibodies and our inability to isolate and interrogate astrocytic aSyn make it difficult to more precisely determine the exact aggregation state of aSyn in the astrocytes.

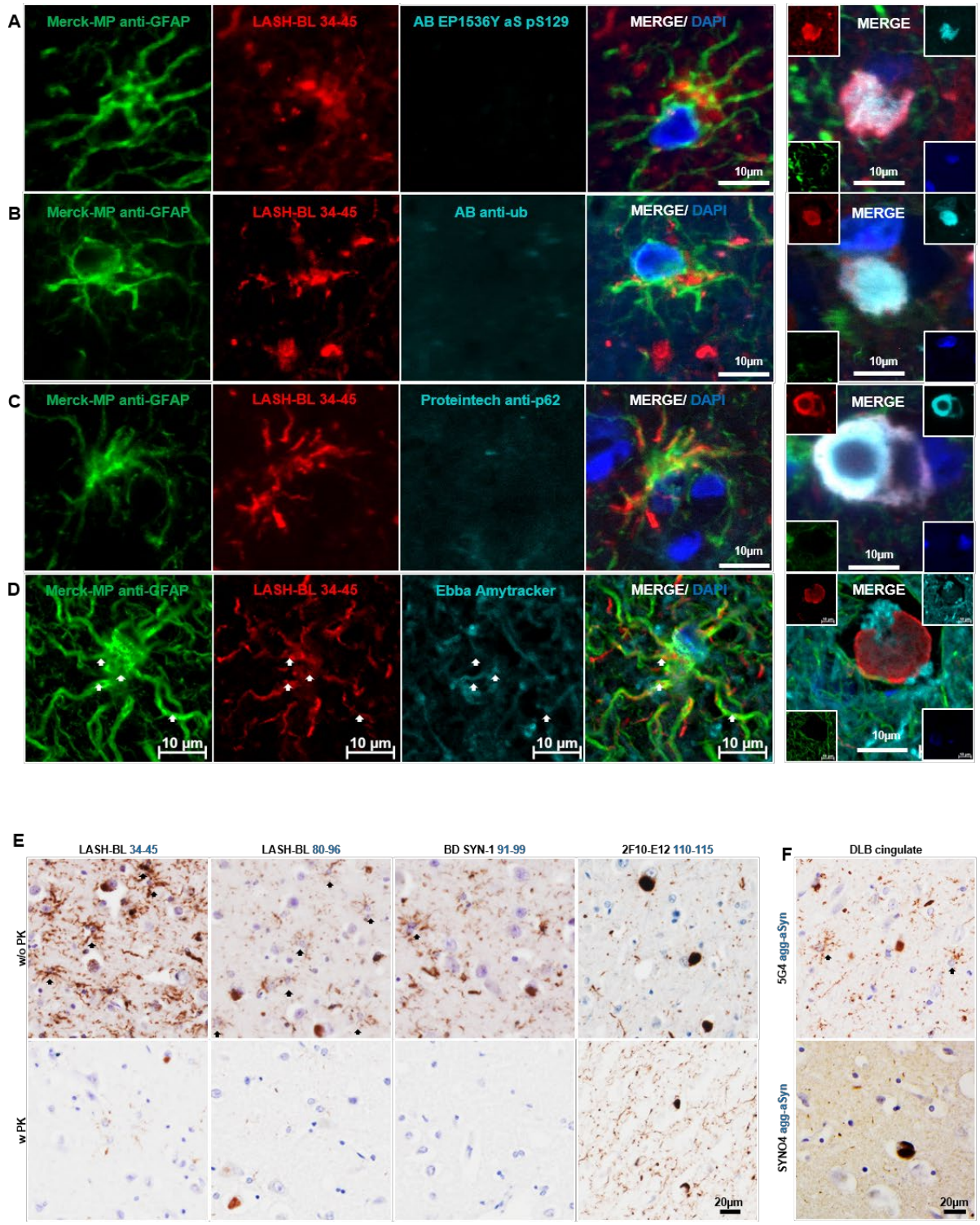

Figure 3. 8 Astrocytic aSyn is free of classical inclusion markers. (A-C) The GFAP-positive astrocytic accumulations in DLB cingulate cortex were negative to aSyn pS129 (AB EP1536Y), ubiquitin and p62. (D) These astrocytic species showed partial overlap with the amyloid marker Amytracker (arrows). Images of cortical LBs are included as positive controls for aSyn pS129, ubiquitin, p62 and Amytracker reactivity. Images for Figure 4A-C taken using Olympus slide scanner at 40x magnification, and for Figure 4D on Zeiss LSM700 confocal microscope. (E) The astrocytic aSyn signal (arrows) was largely abolished after PK treatment in DLB cingulate cortex. The 2F10-E12 staining was included as a positive control to show the PK resistance of LBs and LNs. (F) The star-shaped astrocytic aSyn accumulations were revealed by the 5G4 antibody, but not by the SYNO4 antibody in the DLB cingulate

cortex. agg-aSyn = aggregated alpha-synuclein; aSyn = alpha-synuclein; DLB = dementia with Lewy bodies; GFAP = glial fibrillary acidic protein; LB = Lewy body; LN = Lewy neurite; PK = proteinase K

3.2.5 Astrocytic aSyn accumulations occur in several limbic regions of LBDs

After having observed the frequent occurrence of astrocytic aSyn in the cingulate cortices of LBDs (Figure 3. 5A), we expanded our screening of astrocytic aSyn species in other limbic brain regions. We observed that the astrocytic aSyn accumulations were also prominently present in the entorhinal cortex, the insula, the amygdala and the CA2-CA4 of the hippocampus (Figure 3. 9A; Figure 3. 10) of LBDs. Interestingly, we identified different morphologies of astrocytic aSyn accumulations. The majority of the astrocytic aSyn accumulations appeared in soma-sparing star-like forms typically labelling the ramified processes of astrocytes (Figure 3. 9B). In the hippocampal subregions, the astrocytic aSyn accumulations were predominantly in the soma and did not exhibit a star-shaped morphology (Figure 3. 9C). Altogether, our findings demonstrate that astrocytic aSyn is a prominent pathological feature of LB diseases, and presents itself in a number of brain regions.

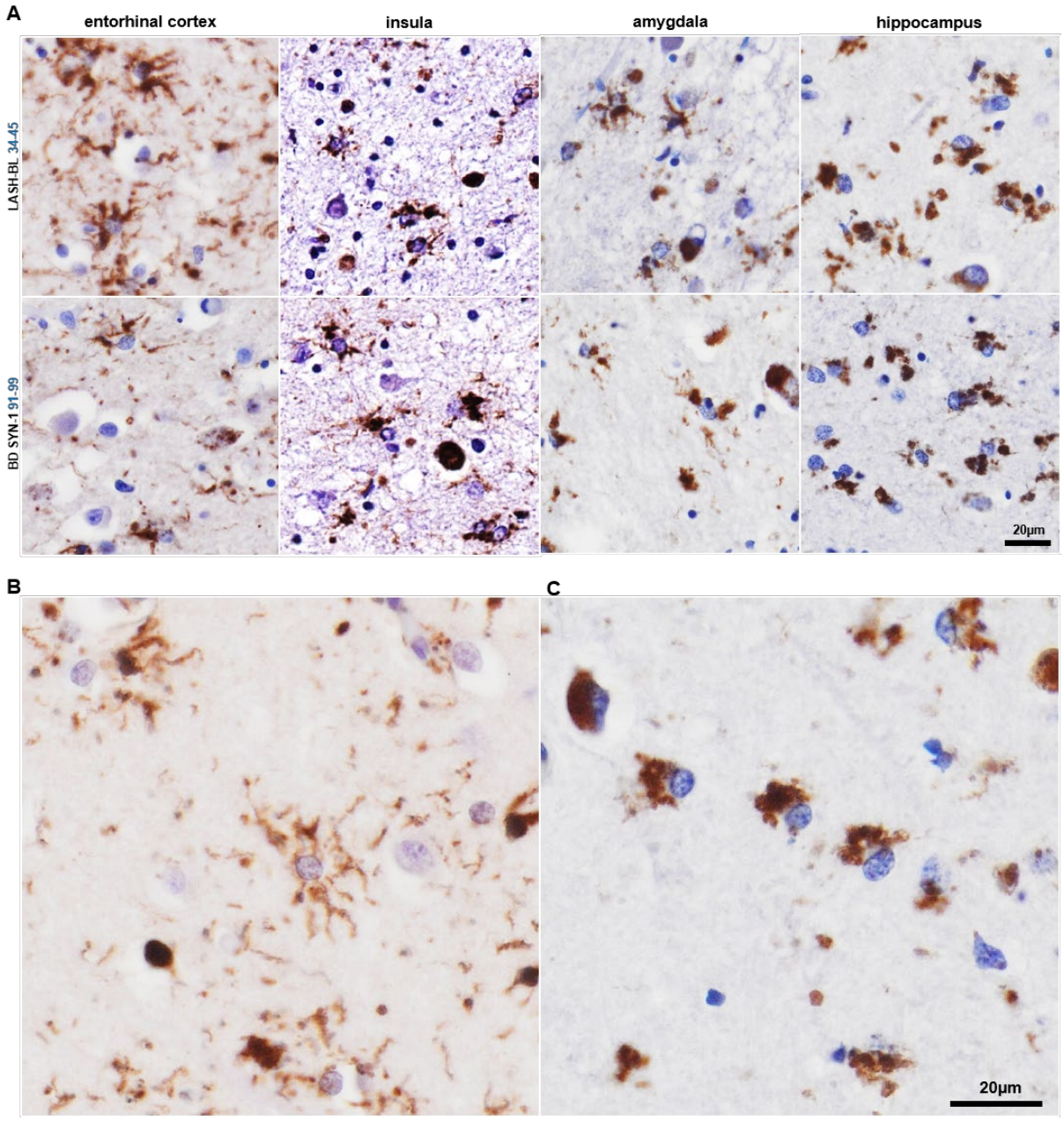

Figure 3. 9 Astrocytic aSyn accumulations occur in several limbic regions of LB disease brains. (A) The astrocytic aSyn accumulations were encountered in the EC (*SNCA* G51D), insula (PDD), amygdala (DLB) and hippocampal CA4 (*SNCA* duplication) regions of LBDs. (B) The astrocytic accumulations showed morphological diversity, with the majority showing a star shape and labelling the ramified processes (cingulate cortex). (C) Some of the astrocytic aSyn appeared as cytoplasmic accumulations (CA4). Figure 5B-C images from a *SNCA* duplication brain stained with the LASH-BL 34-45 antibody. aSyn = alpha-synuclein; CA4 = cornu ammonis 4; DLB= dementia with Lewy bodies; EC = entorhinal cortex; LB = Lewy body; LBD = Lewy body disease; PD = Parkinson's disease; PDD = Parkinson's disease with dementia.

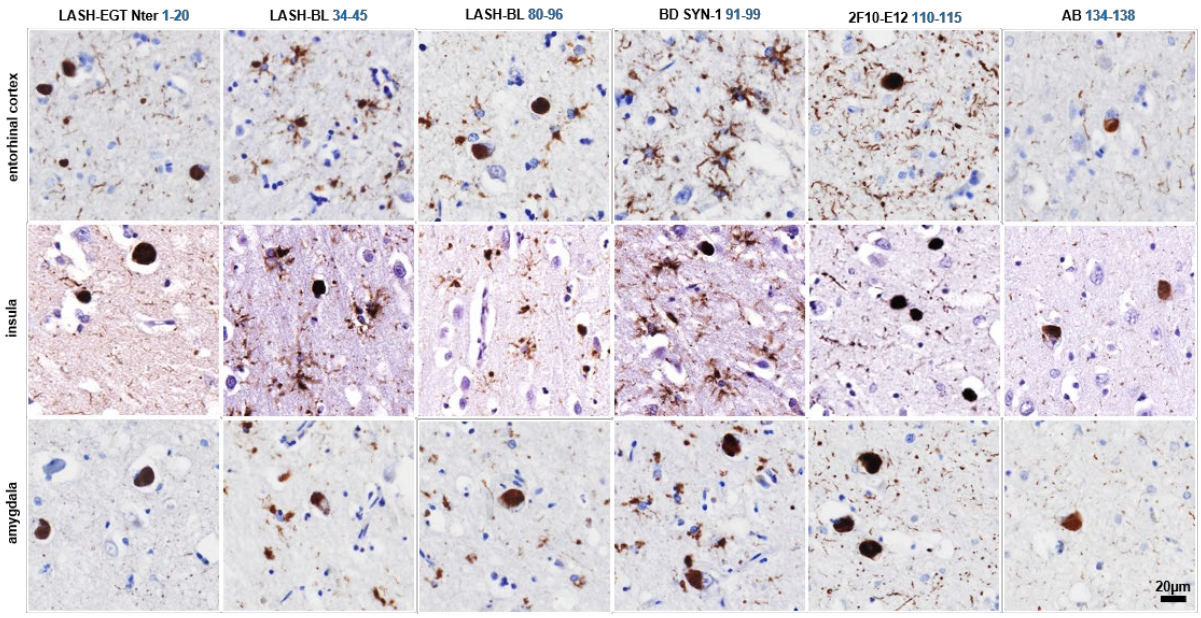

Figure 3. 10 Representative images from the *SNCA* duplication EC, insula and amygdala immunostained using antibodies against the N-terminal, NAC and C-terminal regions of aSyn. The astrocytic aSyn detected only by LASH-BL34-45, LASH-BL80-96 and BD SYN-1 (91-99) antibodies. Similar staining patterns were observed in the same regions from PD, PDD, DLB and *SNCA* G51D cases stained with the same antibody set. aSyn = alpha-synuclein; DLB = dementia with Lewy bodies; EC = entorhinal cortex; PD = Parkinson's disease; PDD = Parkinson's disease with dementia

3.3 Discussion

Astrocytic aSyn pathology is a relatively less explored aspect of neuropathology in synucleinopathies. In this study, we systematically characterised the biochemical properties and aggregation state of astrocytic aSyn accumulations using an expanded tool box of aSyn antibodies across the Lewy body diseases. Our results demonstrate that the astrocytic aSyn accumulations are widely present in several brain regions of PD, PDD and DLB cases, are negative for ubiquitin, p62 and aSyn pS129, but show positivity to other aSyn PTMs, including nitration and phosphorylation at Y39. Furthermore, only a subset of antibodies against non-modified aSyn are able to reveal astrocytic aSyn in brain tissues. These are antibodies that targeted the NAC (80-96 and 91-99) and the late N-terminal (34-45) regions of the protein. This is in line with the previous studies that reported astrocytic positivity only, or primarily with NAC region aSyn antibodies (Braak et al., 2007; Fathy et al., 2019; Hishikawa et al., 2001; Kovacs et al., 2014, 2012; Song et al., 2009; Sorrentino et al., 2019; Takeda et al., 2000; Terada et al., 2003) (Figure 3. 11). However, our studies allow for the more precise mapping, to the extent possible using antibodies, of the putative cleavage sites and

demonstrate conclusively that the majority of astrocytic aSyn are both N- and C-terminally truncated. In addition, we demonstrate for the first time that astrocytic aSyn exists as a mixture of non-amyloid species that are phosphorylated or nitrated at Y39.

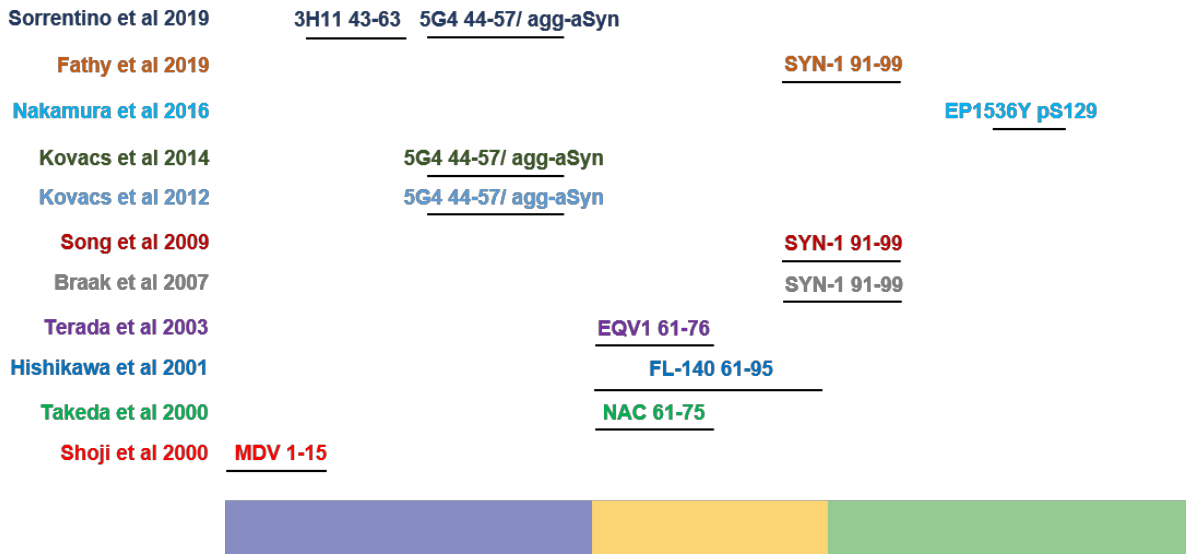

Figure 3. 11 A representation of the aSyn sequence, the publications that have reported aSyn positivity in the astrocytes, and the antibodies they have used. aSyn = alpha-synuclein; agg-aSyn = aggregated alpha-synuclein

The fact that we were not able to detect astrocytic aSyn species with three antibodies targeting the C-terminal region of the protein spanning residues 103 to 138 strongly suggests that the astrocytic aSyn may be C-terminally truncated somewhere between residues 100-102. Similarly, the astrocytic aSyn species were detected by an antibody targeting residues 34-45 (LASH-BL 34-45), but not an antibody targeting the first N-terminal 20 amino acids (LASH-EGTNter 1-20). These results suggest that the N-terminal truncation of astrocytic aSyn is likely to occur between residues 21-33. Although an initial study (Shoji et al., 2000) reported the detection of astrocytic aSyn using an antibody with an N-terminal epitope (MDV, 1-15), subsequent studies showed that N-terminal antibodies covering aSyn residues 1-21 (Sorrentino et al., 2019; Takeda et al., 2000; Terada et al., 2003) did not detect astrocytic aSyn. Altogether, these data demonstrate that the great majority of aSyn in astrocytes are subjected to both N- and C-terminal cleavage at approximately residues 21-33 and 100-102, respectively. These results are supported by our findings that astrocytic aSyn inclusions were immunoreactive for only aSyn PTMs in the mid-N-terminal region. However, we cannot rule out the possibility that the extreme N- and C-terminal

sequences are masked by aSyn interactions with other proteins, especially since both termini serve as hubs for regulating aSyn membranes/lipids and protein interactions. If this is the case, it would suggest that aSyn conformations and interactome in astrocytes are distinct from those in neurons, where aSyn is detectable using both N- and C-terminal-targeting antibodies. Whether truncated aSyn species are cleaved in the neurons, in the astrocytes or in the extracellular space is an important gap of knowledge that should be addressed and could shed new light into the role of PTMs in regulating the function/dysfunction of aSyn and mechanisms of aSyn trafficking between neurons and glia in the disease brains.

Very little is known about the aggregation state of the astrocytic aSyn species. Kovacs and colleagues (Kovacs et al., 2014, 2012) were the first to show positivity for astrocytes with the 5G4 antibody, reported to be specific for oligomeric and fibrillar forms of aSyn (Kovacs et al., 2012; Kumar et al., 2020b). Similar astrocytic positivity using 5G4 was also detected by Sorrentino and colleagues (Sorrentino et al., 2019), but there has not been any studies to validate these findings using multiple aggregated aSyn antibodies and define the aggregation state of aSyn in astrocytes. Similarly, only two studies have assessed the ultrastructure of astrocytic aSyn by EM (Kovacs et al., 2014; Nakamura et al., 2016). Nakamura et al. described the aSyn pS129-positive subpial astrocytic processes in the MSA brains as non-filamentous (Nakamura et al., 2016), and Kovacs and colleagues reported that the astrocytic accumulations of LB diseases are beta-sheet-rich oligomers (Kovacs et al., 2014).

In this study, we investigated the aggregation state of aSyn in astrocytes using multiple approaches, including aSyn conformational/ aggregate-specific antibodies (5G4 and SYNO4), amyloid dyes and limited proteolysis (PK resistance). In line with Kovacs and colleagues (Kovacs et al., 2014), the astrocytic inclusions of LB diseases were revealed by 5G4, but were not detected with SYNO4. We also report that the majority of the astrocytic aSyn did not show resistance to PK digestion, and were only partially positive to the amyloid dye Amytracker. These findings, combined with our observation that astrocytic aSyn accumulations are not positive for the canonical markers of LBs, including ubiquitin, p62, and the most common pathology-associated aSyn PTM, pS129 (Anderson et al., 2006; Fujiwara et al., 2002), suggest that aSyn accumulations

in astrocytes possess a distinct PTM and sequence signature, and may be composed primarily of oligomers or other non-fibrillar forms of the protein.

We speculate that the lack of aSyn phosphorylation at S129 is because the astrocytic aSyn species are truncated in the C-terminus, and no longer carry the binding site for the aSyn pS129 antibodies. Likewise, these aSyn accumulations are cleaved in the N-terminus, the domain where aSyn is found to be ubiquitinated in disease brains (Anderson et al., 2006). Given that aSyn pS129 has been reported to be important for priming aSyn ubiquitination (Hasegawa et al., 2002), the absence of pS129 could explain the absence of ubiquitination at other lysine residues in the protein. One final possibility is that both of these aSyn PTMs are linked to the formation of aSyn pathology (Anderson et al., 2006; Fujiwara et al., 2002; Hasegawa et al., 2002), and their absence suggests that the astrocytic aSyn species exist in non-aggregated forms. The fact that astrocytic aSyn is cleaved and non-fibrillar at the same time is surprising given that removal of the solubilising N- and C-terminal domains is expected to increase the hydrophobicity and aggregation propensity of the protein (Bodles et al., 2000; Crowther et al., 1998; Eliezer et al., 2001; Giasson et al., 2001; Han et al., 1995; Volpicelli-Daley et al., 2011). Therefore, more extensive investigations of astrocytic aSyn conformations and aggregation state are needed. These studies could shed novel insights into the function(s) of aSyn in astrocytes and the role of astrocytic pathology in the pathogenesis of LB diseases. Furthermore, understanding what keeps these truncated aSyn species from forming fibrils in astrocytes could shed light on novel mechanisms for regulating aSyn aggregation.

These observations raise important questions about the origins and mechanisms involved in the astrocytic uptake, processing, degradation and/or release of aSyn. Cell culture studies have shown that astrocytes take up (Braidy et al., 2013; Cavaliere et al., 2017; Hua et al., 2019; H.-J. Lee et al., 2010b; Lindstrom et al., 2017; Loria et al., 2017; Rostami et al., 2017), degrade (Hua et al., 2019; Lindstrom et al., 2017; Loria et al., 2017; Rostami et al., 2017), and/or release (Cavaliere et al., 2017; Loria et al., 2017; Rostami et al., 2017) aSyn. Yet, a consensus has not been reached on whether or not the astrocytic uptake and processing of aSyn may have cytoprotective (Hua et al., 2019; Lindstrom et al., 2017; Loria et al., 2017) or cytotoxic (Braidy et al., 2013; Cavaliere et al., 2017; H.-J. Lee et al., 2010b; Lindstrom et al., 2017; Rostami et al.,

2017) consequences. Kovacs and colleagues have shown that the astrocytic aSyn is localised in the endo-lysosomal compartments in the disease brains (Kovacs et al., 2014). Similarly, cell model-based research has shown that glial-glial and glial-neuronal oligomeric aSyn transfer can occur in lysosomal vesicles via direct transfer or tunnelling nanotubes (Cavaliere et al., 2017; Loria et al., 2017; Rostami et al., 2017). The fact that the great majority, if not all, of astrocytic aSyn across different LBDs is truncated suggests differential processing of aSyn in the astrocytes that may reflect its astrocytic functions, or a cellular response to aSyn species originating neurons or other glial cells. Altogether, a precise understanding of the astrocytic involvement in the cell-to-cell propagation of misfolded aSyn is needed to grasp the pathology spreading pathways in LB diseases.

Astrocytes are the most populous type of glial cells in the brain, with crucial functions in neuronal survival, synaptic maintenance, glucose metabolism, water homeostasis and in immune response (Sofroniew and Vinters, 2010). Insults may activate astrocytes (Wilhelmsson et al., 2006), which can in turn signal the microglia (Farina et al., 2007; H.-J. Lee et al., 2010a; Zhang et al., 2005) and act as key determinants of microglial activation and neuroinflammation in disease progression (Yamanaka et al., 2008). Furthermore, aSyn aggregates have been reported to activate both astrocytes (Chavarria et al., 2018; Chou et al., 2021; Fellner et al., 2013; Klegeris et al., 2006; H.-J. Lee et al., 2010b) and microglia (Fellner et al., 2013; E.-J. Lee et al., 2010) into giving an inflammatory response. Nitrated aSyn in particular has been reported to induce microglial activation (Reynolds et al., 2009, 2008a, 2008b; Thomas et al., 2007), which may then attain neurotoxic characteristics (Reynolds et al., 2009, 2008b). We found astrocytic aSyn to be nitrated at Y39, and speculate that this specific aSyn PTM may play a key role in the astrocytic signalling of microglia and neuroinflammation in LB diseases. Further studies to investigate the mechanisms of astrocytic activation of microglia, and the involvement of aSyn nY39 taken up and/or released by astrocytes within this context may further explain the interaction of neuroinflammation and neurodegeneration in LBDs.

To our knowledge, this is the first study that examined the post-translational modifications profile (serine and tyrosine phosphorylations, tyrosine nitration and N- and C-terminal truncations) of astrocytic aSyn inclusions in Lewy body diseases.

Although this hypothesis cannot be validated by biochemical profiling due to technical limitations to the isolation of astrocytic accumulations from the rest of the aSyn pathology, the failure of 4 different N- and C-terminal antibodies to detect astrocytic aSyn species strongly supports our conclusions on the biochemical properties of aSyn in astrocytic pathology. Furthermore, this is the first study reporting on aSyn brain pathological species that is composed primarily of truncated aSyn species. Previous studies have also shown high abundance of N- and C-terminally truncated aSyn species in the human brain (Anderson et al., 2006; Bhattacharjee et al., 2019; Kellie et al., 2015; Moors et al., 2021; Ohrfelt et al., 2011) and appendix (Killinger et al., 2018); however, in many of these studies the full-length protein remains highly abundant as the dominant species, as evidenced by the fact that antibodies against phosphorylated aSyn at S129 remain the primary tools used to monitor and quantify aSyn pathology in human brains and in animal models of synucleinopathies. The co-occurrence of N- and C-terminal truncation in the astrocytic aSyn without fibrillisation is particularly important, as the NAC region alone is known to be prone to aggregation by itself (Giasson et al., 2001). Which cell-specific mechanisms may prevent aSyn from forming aggregates in the astrocytes can have implications for understanding the cellular determinants of aSyn pathology formation and therapeutic applications.

Our findings raise several important questions that should be addressed in future studies to clarify 1) if these truncated species of aSyn become cleaved after internalisation by the astrocytes, or are internalised after being cleaved; 2) why these astrocytic aSyn inclusions appear in abundance in LBDs but are spared in MSA; 3) the precise nature of the aggregation state of aSyn in these astrocytes; and 4) the occurrence of astrocytic pathology in relation to LB disease staging and progression. The expanded toolset that we present here should facilitate these studies and advance our understanding of the function of astrocytic aSyn in health and disease.

3.4 Materials and methods

3.4.1 Antibodies

The primary and secondary antibodies used in this study are detailed in Table 3. 2.

3.4.2 Human brain tissue samples

Post-mortem human brains stored at QSBB, University College London (UCL) Institute of Neurology, and Oxford Brain Bank (OBB), Nuffield Department of Clinical Neurosciences in University of Oxford, were collected in accordance with approved protocols by the London Multicentre Research Ethics Committee and the Ethics Committee of the University of Oxford (ref 15/SC/0639). All participants had given prior written informed consent for the brain donation. Both brain banks comply with the requirements of the Human Tissue Act 2004 and the Codes of Practice set by the Human Tissue Authority (licence numbers 12198 for QSBB and 12217 for OBB). 3 cases of sporadic PD, MSA and familial PD with *SNCA* G51D mutation, 2 cases with PDD, 1 case with DLB and 1 case with PD with *SNCA* duplication were derived from QSBB, and 2 cases with sporadic PD, 2 cases with PDD and 2 cases with DLB from OBB were used in this study.

3.4.3 Immunohistochemistry with 3,3'-diaminobenzidine revelation and imaging

FFPE sections were dewaxed in xylene and rehydrated through decreasing concentrations of industrial denatured alcohol (IDA). Antigen retrieval was carried out for the appropriate antibody (Table 3. 2). Autoclaving (AC) was run at 121°C for 10 minutes in citrate buffer (pH6.0). For formic acid (FA) pre-treatment, tissues were incubated in 80-100% FA for 15 minutes (except for 5 minutes with 5G4) at RT. For PK pre-treatment, tissues were incubated at 37°C for 5 minutes in 20µg/mL of PK diluted in TE-$CaCl_2$ buffer (50mM Tris-base, 1mM EDTA, 5mM $CaCl_2$, 0.5% Triton X-100, adjusted to pH8.0). Next, the sections were incubated for 30 minutes in 3% hydrogen peroxide in PBS for quenching the endogenous peroxidase activity. Sections were briefly rinsed in distilled water and PBS, blocked in 10% foetal bovine serum (FBS) for 30 minutes at RT, and left at 4°C overnight for incubation with the primary antibodies. Subsequently, the sections were washed in PBS-T (3x 5 minutes) and incubated in the secondary antibody-horseradish peroxidase (HRP) complex as part of REAL EnVision detection system (Dako #K5007) for 1h at RT. Sections were rinsed in PBS-T (3x 5 minutes) before visualisation with 3,3'-diaminobenzidine (DAB), and counterstained with Mayer's haematoxylin. Finally, they were dehydrated in increasing concentrations of IDA, cleared in xylene (3x 5 minutes) and mounted using

Dibutylphthalate Polystyrene Xylene (DPX). Imaging of the slides was carried out on the Olympus VS120 microscope.

3.4.4 Immunofluorescent labelling of human brain tissues and imaging

After the blocking in 10% FBS in PBS-T for 60 minutes at RT, sections were washed in PBS for 5 minutes and incubated for 1 minute in TrueBlack lipofuscin autofluorescence quencher (Biotium #23007) in 70% ethanol. The sections were washed in PBS (3x 5 minutes) and incubated in primary antibodies overnight at 4°C. They were rinsed in PBS (3x 5minutes) and incubated in secondary antibodies for 1h at RT in dark. Amytracker 680 (Ebba Biotech) was applied according to the manufacturer's instructions, at a dilution of 1:1,000, and the tissue washed in PBS (3x 5 minutes). The slides were mounted using an aqueous mounting medium with DAPI (Vector Laboratories #H-1500-10). Tiled imaging was carried out on the Olympus VS120 microscope. Confocal imaging was carried out on a confocal laser-scanning microscope (LSM 700, Carl Zeiss, Germany), and image analysis on Zen Digital Imaging software (RRID: SCR_013672).

3.4.5 Recombinant aSyn generation, antibody pre-adsorption and slot blot analysis

aSyn expression and purification was performed as described (Fauvet et al., 2012b). In brief, aSyn human WT-encoding pT7-7 plasmids were used to transform BL21(DE3) chemically competent *E. coli*, which were then grown on an agar dish supplemented with ampicillin. A single colony was transferred to Luria broth media with ampicillin at 100µg/mL, the small culture was left to grow at 37 °C on shaker (at 180RPM) for 16h, and was then used to inoculate a large culture of 6L Luria broth media supplemented with ampicillin at 100µg/mL. aSyn expression was induced at an optic density of 0.5-0.6A, using IPTG at a final concentration of 1mM. The culture was grown for another 4h on shaker, centrifuged at 4,000*g* for 15min at 4 °C, and the pellet collected. The lysis buffer of 20mM Tris pH8.0, 0.3uM PMSF protease inhibitor and cOmplete, mini, EDTA-free protease inhibitor cocktail tablet (Roche #4693159001; one tablet per 10mL lysis buffer) was used to re-suspend the pellet (10mL p/L of culture) on ice. Cell lysis was carried out by sonication (59s-pulse and 59s-no pulse over 5min at 60%

amplitude), and the lysate was spun down for 30min at 20,000*g* and 4 °C. The supernatant was collected and boiled for 15min at 100 °C, and the centrifugation repeated before the supernatant was filtered via a 0.22µm syringe filter. The purification was performed by anion exchange chromatography and reverse-phase HPLC. The protein quality control was carried out by LC-MS, UPLC, and SDS-PAGE separation and Coomassie staining. The preparation of the aSyn nY39 and pY39 proteins involved the use of a semi-synthetic approach as described previously (Hejjaoui et al., 2012).

For the antibody pre-adsorption, 5-fold of recombinant aSyn protein, or just PBS as control, was added to the IHC-optimised antibody solution in PBS (see Table 3. 2 for the IHC dilutions). The mixture was incubated overnight at 4 °C on a wheel, and the probing protocol, adapted from (Kumar et al., 2020b), was carried out for the slot blot analysis. 200ng of aSyn proteins diluted in PBS to 100µL were blotted on 0.22µm nitrocellulose membranes, which were blocked at 4 °C overnight in Odyssey blocking buffer (Li-Cor). After the incubation with primary antibodies diluted in PBS for 2h at RT, the membranes were washed x3 for 10 minutes in PBS-T, incubated with the secondary antibodies diluted in PBS in the dark, and washed x3 for 10 minutes in PBS-T. For the SB dilutions of the primary and secondary antibodies, see Table 3. 2. Imaging was carried out at 700nm and 800nm using Li-Cor Odyssey CLx, and the image processing using Image Studio 5.2.

3.5 Contributions of the authors

Hilal A. Lashuel and Laura Parkkinen conceived and conceptualised the study. Hilal A. Lashuel, Laura Parkkinen and Melek Firat Altay designed the experiments. Janice L. Holton selected the cases originating the Queen Square Brain Bank, and Laura Parkkinen those originating the Oxford Brain Bank. Janice L. Holton contributed to, and Laura Parkkinen and Melek Firat Altay finalised the determination of optimal IHC conditions for the aSyn antibodies (Figure 3. 1A-B). Laura Parkkinen and Alan K.L. Liu provided the PD, PDD and DLB images for Figure 3. 5A and for Figure 3. 8F (SYNO4), and contributed to the analysis and interpretation of neuropathological data. Melek Firat Altay performed all other experiments and wrote the chapter.

CHAPTER 4 Capturing the aSyn proteoforms in MSA

MSA is a progressive neurodegenerative disorder with no effective disease-modifying therapies. Although aSyn has been described as the main aggregating protein in the glial and neuronal inclusions, the pathological hallmarks of MSA, our current knowledge of the aSyn proteoforms present in MSA tissue is limited. This knowledge gap has significant implications for understanding the role of aSyn in the pathogenesis of MSA and developing diagnostics for distinguishing MSA from PD and other neurodegenerative diseases. To fill in this knowledge gap, we used an expanded validated antibody tools set (15) to immunohistochemically and biochemically map the PTMs of aSyn in the MSA prefrontal and occipital cortices and cerebellum. Our results show that, in addition to an enrichment of phosphorylation at Serine 129 (S129) and C-terminal truncation, aggregated aSyn species are also positive for nitration and phosphorylation at Tyrosine 39 (Y39) and C-terminal phosphorylations at Tyrosine 133 (Y133) and Tyrosine 136 (Y136). Some of these aSyn PTMs, namely aSyn nY39, pY133 and pY136, are reported to be present in MSA pathology for the first time. These findings should be replicated in larger cohorts and could pave the way for a better understanding of the role of aSyn modifications in the development, maturation and spreading of aSyn pathology or cellular responses to aSyn pathology in MSA.

4.1 Introduction

MSA is a rare sporadic type of synucleinopathy characterised by the loss of neurons in the substantia nigra, striatum, inferior olivary nucleus of the medulla, pons and cerebellum (Lantos, 1998). It is a fatal, adult-onset neurodegenerative disease that leads to autonomic nervous system failure, ataxia and parkinsonism (Fanciulli and Wenning, 2015). The prognosis is poor, with a progressive decline in the quality of life and an average of 8 years of life expectancy post-diagnosis (Bower et al., 1997). Currently, no cure is available to treat MSA, and the present medications are aimed at providing symptomatic relief only, thus underscoring the importance of understanding the underlying disease mechanisms and the development of effective therapies (Lopez-Cuina et al., 2018).

Soon after aSyn was described as the main aggregating protein in the LBs of PD and DLB (Baba et al., 1998; Irizarry et al., 1998; Spillantini et al., 1998b), it was also identified within the proteinaceous accumulations in GCIs of MSA (Spillantini et al., 1998a), which led to re-classifying MSA as a synucleinopathy, a group of neurodegenerative diseases that are characterized by the accumulation of aggregated forms of aSyn. Why aSyn accumulations take place primarily in the oligodendrocytes, and why the aSyn pathology appears to be far more aggressive in this disease type compared to LBDs remains unknown. Furthermore, the overlying clinical characteristics of MSA with several other neurodegenerative diseases frequently result in the misdiagnosis of MSA as PD, DLB or PSP, and vice versa (Kim et al., 2015; Koga et al., 2015), necessitating the need for identifying biomarkers to help with early and accurate diagnosis. Mounting evidence from human post-mortem studies (Anderson et al., 2006; Bhattacharjee et al., 2019; Duda et al., 2000a; Fujiwara et al., 2002; Hasegawa et al., 2002; Schweighauser et al., 2020), from cellular and *in vivo* models (Chen et al., 2009; Mahul-Mellier et al., 2018, 2014; Volpicelli-Daley et al., 2011) point to key roles of PTMs as master regulators of aSyn aggregation, inclusion maturation and spreading mechanisms. Differential PTM signature of aSyn aggregates in the CNS, PNS and body fluids identified in MSA patients may help towards establishing MSA-specific biomarkers.

We hypothesised that the aSyn PTMs detected directly in MSA brain tissues may provide clues on the biochemical determinants of aSyn aggregation and pathology in MSA and help identify unique pathological signatures that distinguish MSA from other neurodegenerative diseases. With this aim in mind, we focused our efforts to immunohistochemically profile the regions of high and low pathology (prefrontal cortex and occipital cortex, respectively) from 3 MSA and 3 healthy control cases, using a well-characterised set of aSyn antibodies (15 in total) against all three regions and described modifications of aSyn (Figure 4. 1A). In parallel, the cerebellar samples were sequentially extracted and biochemically profiled to better determine the aSyn proteoforms present in MSA brains. We found an abundance of aSyn pS129-positive, but also interestingly aSyn nY39-, pY39-, pY133- and pY136-positive glial and neuronal inclusions. Our results may pave the way for further insight on the role of aSyn PTM profile on the aggressiveness of aSyn strains that are specific to MSA.

Replication and validation of the findings reported herein with additional cases is currently underway both in our laboratory and by our collaborators.

4.2 Results

Towards deciphering the spectrum of aSyn PTMs in the MSA brains, we sought to profile aSyn species in the brain by IHC and biochemistry. For the immunohistochemical studies, three MSA and three healthy control cases were selected, with one region of high pathology (prefrontal cortex) and one region of low pathology (occipital cortex). The selection of antibodies (Figure 4. 1A) was based on extensive characterisation as described in Chapter 2 (p.61). In the prefrontal cortex, antibodies targeting multiple non-modified regions throughout the sequence of aSyn (epitopes 1-20, 34-45, 80-96, 91-99, 103-108, 110-115 and 134-138) revealed similar staining patterns as previously observed in terms of the detection of GCIs and NCIs. Interestingly, the 2F10-E12 antibody (epitope 110-115) revealed extensive neuritic pathology that is not captured by other non-modified aSyn antibodies (Figure 4. 1B). Next, we performed staining in the same regions using aSyn antibodies that target multiple aSyn PTMs. As has previously been reported, the most prominent modification detected was aSyn pS129 (Figure 4. 1C). In addition, we observed that the frontal cortex of the MSA cases were abundantly positive for aSyn nY39, pY39 and aSyn pY136 (Figure 4. 1C). Moderate positivity for aSyn pY133 and aSyn truncated at residue 120 were also observed in the GCIs. On the other hand, the GCIs or NCIs appeared negative for aSyn pS87 and aSyn pY125 (Figure 4. 1C). In the occipital cortex i.e. the region of low aSyn pathology, fewer inclusions were revealed by these non-modified aSyn antibodies (Figure 4. 2A) compared to prefrontal cortex. Nonetheless, these inclusions still showed rare positivity for aSyn pS129 as well as aSyn nY39, pY39, pY133 and pY136 (Figure 4. 2B), but were negative for aSyn pS87, pY125 and aSyn 1-120. To the best of our knowledge, this is the first study to report the presence of aSyn pY133 and pY136 in MSA, and the co-existence of multiple tyrosine phosphorylations, N-terminal nitration and phosphorylation at S129 in the same disease tissues.

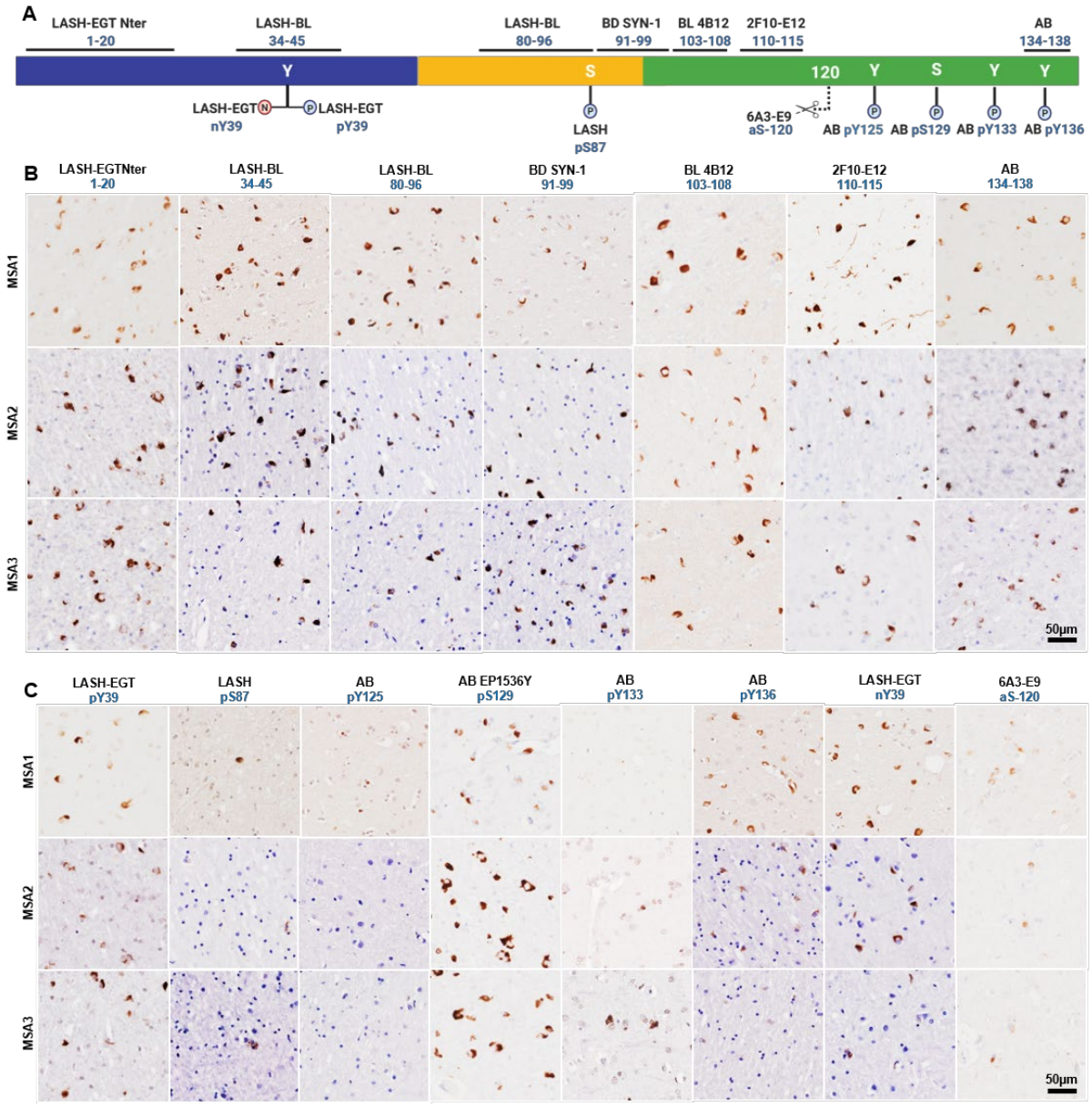

Figure 4. 1 The screening of MSA frontal cortex using a selection of aSyn antibodies against different regions and modifications of the protein. (**A**) The schematic of the antibodies employed for the IHC studies, and their epitopes. Schematic created with BioRender.com (agreement no: *DI23K01SXD*). The prefrontal cortex of three MSA cases were immunohistochemically stained using (**B**) aSyn non-modified and (**C**) aSyn PTM antibodies. aSyn = alpha-synuclein; IHC = immunohistochemistry; MSA = multiple system atrophy; PTM = post-translational modification

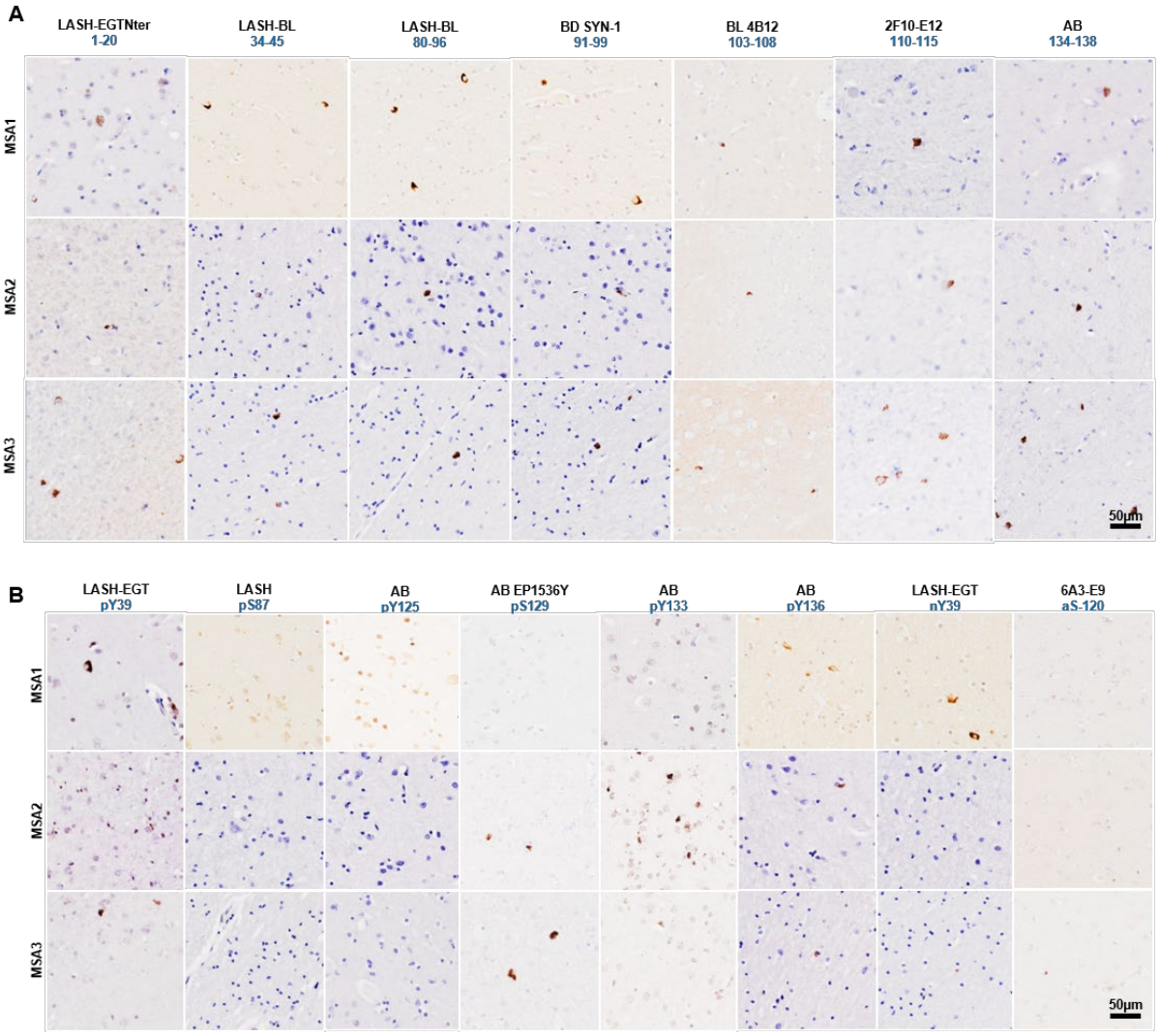

Figure 4. 2 The occipital cortex of three MSA cases were immunohistochemically stained using (**A**) aSyn non-modified and (**B**) aSyn PTM antibodies. aSyn = alpha-synuclein; MSA = multiple system atrophy; PTM = post-translational modification

To validate our findings, we aimed to profile the aSyn proteoforms biochemically using the same brain samples. Towards this goal, we chose an optimised sequential extraction protocol that allows for the separation of cytosolic soluble (high-salt [HS] fraction), membrane-bound soluble (Triton [Tx] fraction) and aggregated insoluble (sodium dodecyl sulphate-urea [SDS-urea] fraction) aSyn using small amounts (100-200mg) of starting brain material (Figure 4. 3). The cerebellar tissues of MSA and healthy control brains were then extracted and profiled using a selection of antibodies (9) against non-modified aSyn and aSyn PTMs. In the SDS-urea fractions, specific to MSA samples only, we observed aSyn-positive bands at 15kDa with the non-modified aSyn antibodies LASH-BL 80-96, BD SYN-1 (91-99), BL 4B12 (103-108) and AB 134-

138 (Figure 4. 4A, blue arrows). This band was also detected with the AB MJF-R13 (pS129) antibody, indicating the presence of detergent-insoluble aggregated aSyn phosphorylated at S129 (Figure 4. 4A, blue arrows). In addition to the 15kDa band, we detected 12kDa positivity with the non-modified aSyn antibodies LASH-BL 80-96, BD SYN-1 and BL 4B12 (Figure 4. 4A, green arrows), but not with aSyn pS129 or AB 134-138 antibodies, suggesting that these species at 12kDa may correspond to aSyn truncated in the C-terminus somewhere between residues 110-140. With the HMW species, all of the total aSyn antibodies and also aSyn pS129 antibody revealed a band at around 35kDa, as well as smeared aSyn positivity in the stacking gel (Figure 4. 4A, purple arrows). Unlike the IHC data, we were unable to detect any SDS-urea soluble aSyn pY39, pY133, pY136 or nY39 species, suggesting that higher protein loading may be needed to capture these aSyn PTMs by WB (Figure 4. 4B). We also note that as a significant amount of aSyn did not migrate and remained in the stacking gel, many of the modified aSyn forms may be trapped in this material. Therefore, we are conducting further optimization on this protocol to allow for more disassociation and characterization of these insoluble aSyn species also via mass spectrometry. Interestingly, the aSyn pS129-positive aSyn species were revealed only in the SDS-urea fractions, and not in the Tx or HS fractions, suggesting that this modification is specific to, and enhanced in, insoluble aSyn species. The truncated aSyn at 12kDa, on the other hand, was present both in the HS and Triton fractions in MSA samples, and in the HS fractions in the control samples (Figure 4. 4A, green arrows). This suggests that whilst there are insoluble and C-terminally truncated species specifically in MSA, there are also truncated but non-aggregated aSyn species that are present physiologically both in MSA and healthy control cases. These observations are consistent with previous studies suggesting physiological functions for some truncated forms of aSyn (Anderson et al., 2006; Campbell et al., 2001; Li et al., 2005; Muntane et al., 2012).

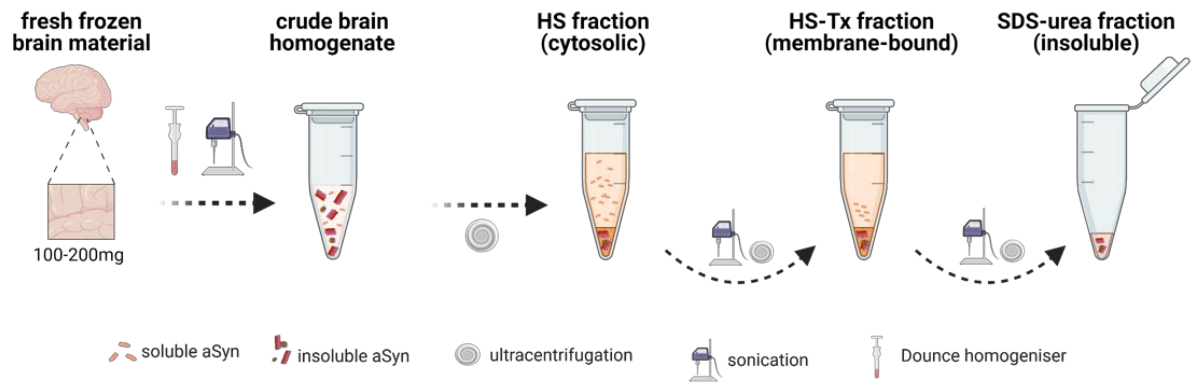

Figure 4. 3 The key steps involved in the sequential extraction protocol that allows for the separation of cytosolic, membrane-bound and insoluble aSyn species from small amounts fresh frozen brain material. Schematic created with Biorender.com (agreement no: *GP23KQP92Q*). aSyn = alpha-synuclein; HS = high salt; SDS = sodium dodecyl sulphate; Tx = Triton X-100

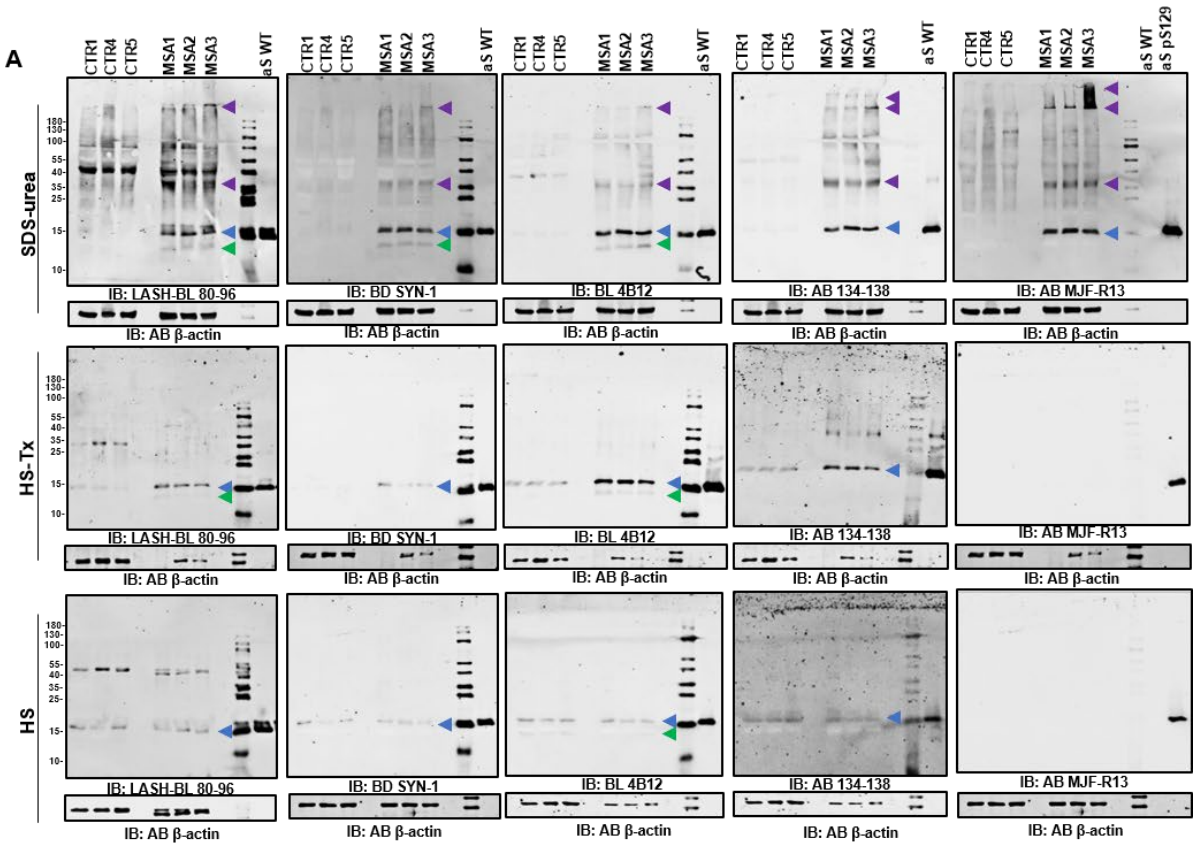
A
CTR1
CTR4
CTR5
MSA1
MSA2
MSA3
aS WT
aS pS129
SDS-urea
HS-Tx
HS
IB: LASH-BL 80-96
IB: BD SYN-1
IB: BL 4B12
IB: AB 134-138
IB: AB MJF-R13
IB: AB β-actin

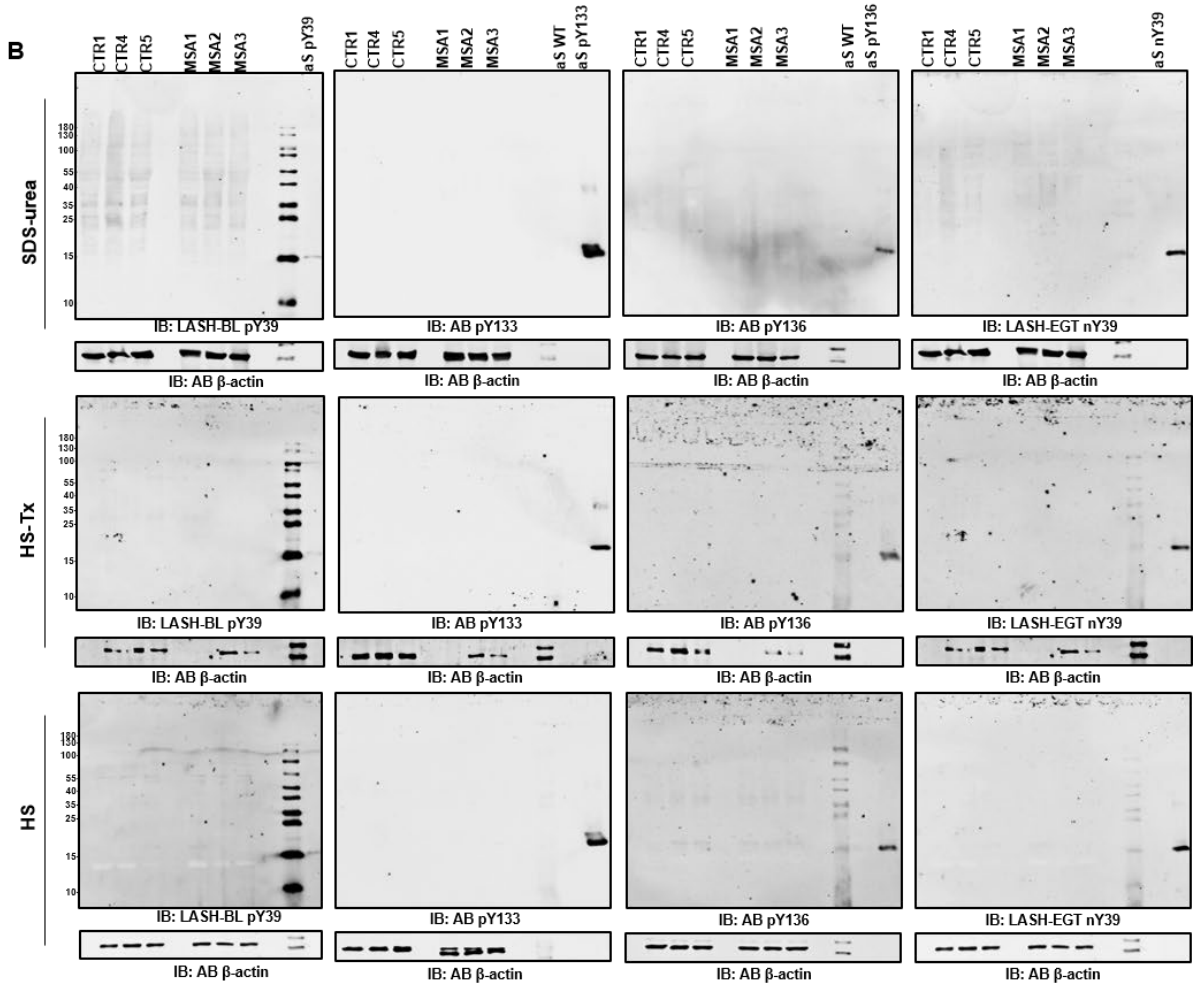
B
CTR1
CTR4
CTR5
MSA1
MSA2
MSA3
aS pY39
aS WT
aS pY133
aS pY136
aS nY39
SDS-urea
HS-Tx
HS
IB: LASH-BL pY39
IB: AB pY133
IB: AB pY136
IB: LASH-EGT nY39
IB: AB β-actin

Figure 4. 4 The biochemical profiling of the aSyn proteoforms in MSA. The cerebellum of three MSA and three healthy control cases were sequentially extracted and profiled by WB. (**A**) The blue arrows show bands positive for aSyn at 15kDa, green arrows for aSyn at 12kDa, and purple arrows for aSyn at 35kDa and in the stacking gel. (**B**) No positivity was revealed by WB for aSyn pY39, pY133, pY136 or aSyn nY39. aSyn = alpha-synuclein; CTR = control; HS = high salt; HS-Tx = high salt-Triton-X100; MSA = multiple system atrophy; SDS= sodium dodecyl sulphate; WB = Western blot

4.3 Discussion

The primary objective of this study is to achieve a comprehensive profiling of aSyn pathology in MSA through deciphering the biochemical signature of aSyn aggregates and the distribution aSyn proteoforms in MSA brains using immunohistochemistry and WB. We report that MSA brain tissues are enriched in insoluble aSyn that is C-terminally truncated or phosphorylated at S129. We also report that GCIs and NCIs in MSA brains are strongly positive for aSyn pS129, but also to aSyn nY39 and aSyn pY136. We also detected moderate positivity to aSyn pY39, pY133 and aSyn truncated at residue 120 in MSA frontal cortex, but found all brain tissues examined to be negative for aSyn pY125 and pS87.

Increasing evidence suggests that aSyn PTMs serve as master regulators of aSyn aggregation, seeding and inclusion maturation processes, yet we have limited knowledge on the exact modifications this protein may undergo in human tissue in health and disease. Whilst the most commonly studied aSyn modifications, namely ubiquitination, phosphorylation at S129 and C-terminal truncations have been frequently reported in LBDs, even these modifications are understudied in MSA human tissues compared to other synucleinopathies. aSyn is ubiquitinated (Arima et al., 1998a; Dickson et al., 1999b; Gai et al., 1999; Kuusisto et al., 2001; Schweighauser et al., 2020; Wakabayashi et al., 1998b) and phosphorylated at S129 (Anderson et al., 2006; Neumann et al., 2002; Nishie et al., 2004). Only two studies reported aSyn nitration in the GCIs and NCIs of MSA (Duda et al., 2000a; Giasson et al., 2000a). In addition, one recent study has reported that aSyn pY39, threonine phosphorylation at T59, T64, T72 and T81, N-terminal acetylation and lysine acetylation at K21, K23, K32, K34, K45, K58, K60, K80 and K96 were found in the aSyn-enriched insoluble fractions from MSA brains (Schweighauser et al., 2020).

However, the authors noted that these modifications were present at low levels and only in a subset of MSA cases studied. Thus, the robustness of these findings and the confidence level for the identification of these PTMs remain unclear. No studies have reported on whether aSyn is phosphorylated at C-terminal tyrosines, and only one recent study has looked at the aSyn nY39-, pS87 and pS129-positive inclusion distribution in PD and MSA brains (Sonustun et al., 2022) using the antibodies we have described in Chapter 2 (p.61). Furthermore, only a handful of studies have investigated the co-existence of multiple aSyn PTMs in MSA tissues, and primarily focused on the interaction of ubiquitination, phosphorylation at S129 and C-terminal truncations (Anderson et al., 2006; Dickson et al., 1999b, p. 19999; Fujiwara et al., 2002; Ishizawa et al., 2008; Schweighauser et al., 2020).

Here, we report, for the first time, that MSA brains, differentially from the healthy control cases, are positive not only for aSyn pS129 but also for C-terminal tyrosine phosphorylations at Y133 and Y136. By IHC, we also detected aSyn nY39, pY39 and aSyn truncated at residue 120 in the glial and neuronal inclusions of MSA brains. In addition, we detected insoluble and S129-phosphorylated 15kDa and HMW species biochemically. The C-terminally truncated aSyn species were present unequivocally in the cytosolic, membrane-bound and insoluble fractions across the MSA cases. The presence of these truncated species in the cytosolic fractions of control cases suggests that C-terminally truncated aSyn species are present in the human brains as part of physiological metabolism, but also in the pathological aSyn aggregates specifically in MSA.

The lack of antibodies specific to ubiquitinated aSyn made it difficult to investigate this modification in relation to other aSyn PTMs. aSyn acetylation has also been reported in MSA tissues recently (Schweighauser et al., 2020), but this modification remained out of the scope of our study due to the lack of antibodies site-specifically targeting this aSyn modification. Further investigations to address these limitations would involve shotgun and targeted proteomics analyses to map all the aSyn proteoforms exactly and comprehensively in MSA. Likewise, further immunohistochemical and biochemical studies to cover other affected brain regions, and to cover a larger cohort of MSA cases to include MSA-C, MSA-P and MSA mixed subtypes would give us clues as to which

aSyn PTMs are universally present across different MSA regions, and which aSyn PTMs may differ between MSA subtypes. Finally, future study could involve comparative mapping of the aSyn PTMs in the neuronal inclusions in brain regions equally affected in LBDs and MSA (e.g. substantia nigra and temporal cortex) to identify any potential differences in the PTM signatures between LBDs and MSA, which may help us understand the role of modifications that may render aSyn strains more aggressive in MSA.

4.4 Materials and methods

4.4.1 Antibodies

A list of antibodies used for this study is presented in Table 4. 1.

Table 4. 1 The primary and secondary antibodies included in this study.

primary antibodies						
antibody	**epitope**	**species/ clonality**	**company / catalogue #**	**IHC: antigen retrieval**	**IHC: dilution**	**WB: dilution**
LASH-EGTNter	aSyn 1-20	rab pc	na	AC+FA	1:15,000	na
LASH-BL 34-45	aSyn 34-45	mus mc	Biolegend #849101	FA	1:30,000	na
LASH-BL 80-96	aSyn 80-96	mus mc	Biolegend #848302	FA	1:20,000	1:1,000
BD SYN-1	aSyn 91-99	mus mc	BD #BD610787	FA	1:5,000	1:2,000
BL 4B12	aSyn 103-108	mus mc	Biolegend #807801	AC+FA	1:100,000	1:1,000
2F10-E12	aSyn 110-115	mus mc	na	AC+FA	1:10,000	na
AB 134-138	aSyn 134-138	rab pc	Abcam #ab131508	AC+FA	1:25,000	1:2,000
LASH-BL pY39	aSyn pY39	mus mc	Biolegend #849201	AC+FA	1:2,000	1:1,000
LASH pS87	aSyn pS87	rab pc	na	FA	1:600	na
AB pY125	aSyn pY125	rab pc	Abcam #ab10789	FA	1:500	na
AB EP1536Y	aSyn pS129	rab mc	Abcam #ab51253	AC+FA	1:60,000	na
AB MJF-R13	aSyn pS129	rab mc	Abcam #ab168381	na	na	1:10,000
AB pY133	aSyn pY133	rab pc	Abcam #ab194910	AC+FA	1:400	1:2,000
AB pY136	aSyn pY136	rab pc	Abcam #ab131491	FA	1:100	1:1,000
LASH-EGT nY39	aSyn nY39	rab pc	na	FA	1:1,000	1:500
6A3-E9	aSyn-120	mus mc	na	AC+FA	1:2,500	na

secondary antibodies				
antibody	**dilution**	**company**	**catalogue #**	**application**
IRDye goat anti-mouse 680	1:20,000	Li-Cor	926-68070	WB
IRDye goat anti-rabbit 800	1:20,000	Li-Cor	926-32211	WB

AC = autoclave; aSyn = alpha-synuclein; FA = formic acid; IHC = immunohistochemistry; mc = monoclonal; mus = mouse; na = not applicable; pc = polyclonal; rab = rabbit; WB = Western blot

4.4.2 Human brain tissue samples

Post-mortem human brains were obtained and selected by the Neurobiobank Muenchen (NBM), Munich, Germany. The samples were collected and stored in accordance with the applicable European Union guidelines as well as the internal guidelines approved by the Ethics Committee of the Ludwig-Maximilians-Universitaet (LMU) Munich upon the written informed consent from donors (#345-13). The ethical approval for research was given by the Ethics Committee of the LMU Munich (#18-851).

4.4.3 Immunohistochemistry with DAB revelation and imaging

3 MSA and 3 healthy control brains were used for the immunohistochemical studies. FFPE sections from prefrontal and occipital cortices were dewaxed in xylene and rehydrated through decreasing concentrations of IDA. AC was run at 121°C for 10 minutes in citrate buffer (pH6.0). For FA pre-treatment, tissues were incubated in 80-100% FA for 15 minutes at RT. The sections were incubated for 30 minutes in 3% hydrogen peroxide in PBS for quenching the endogenous peroxidase activity. Sections were briefly rinsed in distilled water and PBS, blocked in 10% FBS for 30 minutes at RT and left at 4°C overnight for incubation with the primary antibodies. Subsequently, the sections were washed in PBS-T (3x 5 minutes) and incubated in the secondary HRP complex as part of REAL EnVision detection system (Dako #K5007) for 1h at RT. Sections were rinsed in PBS-T (3x 5 minutes) before visualisation with DAB and counterstained with Mayer's haematoxylin. Finally, they were dehydrated in increasing concentrations of IDA, cleared in xylene (3x 5 minutes) and mounted using DPX. Scanning was carried out on the Olympus VS120 microscope.

4.4.4 Sequential extraction and Western blotting

100-200mg of cerebellar frozen tissue from 3 MSA and 3 healthy control brains was disassociated in 4 volumes of ice-cold HS homogenization buffer at pH7.4 (50mM Tris-HCl; 750mM NaCl; 10mM NaF; 5mM EDTA; 1mM EGTA) supplemented with 1% protease and phosphatase inhibitors. Samples were sonicated for further homogenization, left on ice for 30 minutes, and centrifuged at 1,000*g* for 5 minutes at

4°C. The non-homogenised material was discarded, and the supernatant was centrifuged at 160,000*g* for 60 minutes at 4°C. The supernatant was saved as the HS-soluble fraction. The pellet was re-suspended in 4 volumes of homogenization buffer, sonicated until fully homogenized, and spun at 160,000*g* for 60 minutes at 4°C. The supernatant was discarded, and the pellet was re-suspended in 4 volumes of HS homogenization buffer supplemented with protease and phosphatase inhibitors and 1% Triton X-100 (Tx). The sample was sonicated until homogenization and spun at 160,000*g* for 60 minutes at 4°C. The supernatant was saved as the HS-Tx fraction. The pellet was re-suspended in 4 volumes of HS-Tx buffer supplemented with inhibitors and 30% sucrose, and centrifuged at 160,000*g* for 60 minutes at 4°C to float the myelin. The supernatant was discarded and the pellet was re-suspended in HS homogenization buffer supplemented with inhibitors and 5% SDS by sonication. This sample was saved as the SDS-urea fraction. The protein concentration was determined by BCA assay separately for each fraction.

The HS, HS-Tx (10µg) and SDS-urea (80µg) fractions were separated on a 16% Tricine gel, transferred onto a nitrocellulose membrane of pore size 0.22µm using a semi-dry transfer system (BioRad) for 45min at 0.5A and 25V. The membranes were blocked overnight at 4 °C in Odyssey blocking buffer (Li-Cor) and washed three times for 10min in PBS with 0.01% Tween-20 (PBS-T). Membranes were incubated with primary antibodies diluted in PBS for 2h at RT, washed three times for 10min in PBS-T, incubated in dark with secondary antibodies diluted in PBS and washed three times for 10min in PBS-T. The membranes were imaged at 700nm and/or 800nm using the Li-Cor Odyssey CLx imaging system, and the images were processed using Image Studio 5.2.

4.5 Contributions of the authors

Hilal A. Lashuel conceived and conceptualised the study. Viktoria Ruf selected the cases originating the Neurobiobank Muenchen, and contributed to the analysis and interpretation of neuropathological data. Melek Firat Altay designed and performed the experiments, and wrote the chapter.

CHAPTER 5 Conclusion

5.1 Achieved results and future development

Synucleinopathies represent a group of diseases that progressively get worse and lower the life quality of patients. The common neuropathological feature of these ailments is the accumulation of aggregated forms of aSyn in the neurons and glial cells. Despite our knowledge that aSyn plays a key role in the pathogenesis of synucleinopathies, the particular processes linking aSyn aggregation, inclusion formation and maturation, neurodegeneration, and pathology spreading in the periphery and CNS remain unknown. In particular, the sequence and molecular determinants as well as the mechanisms of aSyn aggregation, the biochemical and structural properties of the aggregates and the unique pathological signature that distinguish each disease require new answers. Combined with the lack of a cure, this makes it crucial that we understand the mechanisms of aSyn pathogenesis and spreading to be able to develop and offer new disease-modifying strategies.

Within this context, the goal of the thesis was to develop and validate new tools that would help address these knowledge gaps. Towards this goal, this study focused on three key areas of study: 1) The development, validation and application of aSyn antibodies as a large and well-characterised toolset to capture the pathological diversity in synucleinopathies (Chapter 2); 2) application of these tools for a better understanding of the nature of astrocytic aSyn pathology in LBDs (Chapter 3); and 3) application of these tools to fully profile the aSyn proteoforms and inclusion types in MSA (Chapter 4).

The studies described in Chapter 2 have allowed us to develop 12 novel monoclonal antibodies against different regions and modifications of aSyn. In addition, 31 antibodies of non-modified aSyn and aSyn PTMs were fully characterized and validated through an extensive pipeline that utilizes a combination of biochemical assays, post-mortem human brain tissues of Lewy body diseases and cellular and animal models of pathology formation and spreading, in cells and animals revealed heterogeneous populations of co-existing aSyn species. This enabled us to assemble the most comprehensive antibody toolset. We revealed that aSyn inclusions in LBDs

are not only rich in pS129 and ubiquitination as previously described, but also in tyrosine phosphorylations and N-terminal nitrations, and are distributed across neurons and glial cells. In the neuronal and mouse seeding models, similarly, we discovered aSyn in the newly formed aggregates to be hyperphosphorylated.

The exploration of the LBDs using this battery of antibodies has also opened a new avenue of research related to astrocytic aSyn pathology, described in Chapter 3. The accumulation of aSyn in the astrocytes has previously been reported in the literature as early as the 2000s, but a systematic investigation into the sequence properties, PTMs and aggregation state of these species has not been performed. Using our new panel of antibodies, we have been able to provide the most comprehensive analysis of astrocytic aSyn pathology, detailed in Chapter 3. We were able to investigate the characteristics of these astrocytic accumulations at a single cell level, which also helped us more precisely and methodically map the N- and C-terminal truncation sites of the astrocytic aSyn. We demonstrated that these astrocytic aSyn accumulations are negative for all key markers of LBs, and showed for the first time that they are nitrated and phosphorylated in the N-terminal Tyrosine 39. Our data point at the state of astrocytic aSyn to be non-aggregated oligomeric, but further in-depth structural analysis is needed to understand the exact nature of these accumulations. To the best of our knowledge, this is the first description of aSyn inclusions that are entirely composed of N- and C-terminally cleaved aSyn species. This work paves the way for future studies to decipher the role of these modified astrocytic aSyn species in astrocytic pathology formation, the cell-to-cell spreading of pathology, and also in the immune responses via astrocyte-microglia interactions are key for the identification of therapeutic targets.

Finally, in Chapter 4, we present an additional proof-of-concept study focused on deciphering the diversity of aSyn species in MSA, a rare but a relentless type of synucleinopathy that is less frequently studied in comparison to LBDs. The immunohistochemical screening revealed multiple and also previously under-described aSyn modifications in the MSA brain tissues. We were able to capture some of these modifications by Western blotting, including truncations and phosphorylations, and ongoing work is under way to precisely identify the differentially modified aSyn forms in MSA by proteomics approaches. This work is significant as a detailed insight

into the different types of aSyn species present in MSA versus PD and other LBDs may help us understand the underlying mechanistic, cellular and molecular reasons for the more aggressive nature of MSA pathology, and eventually develop new means and therapeutic approaches to alleviate, stop or even reverse disease progression across all synucleinopathies.

We envision that the work presented here would unfold in two directions: 1) The re-visiting of PD and other LBD staging using this advanced toolset of aSyn antibodies and looking at larger cohorts to have a deeper understanding of the aSyn pathogenesis and the role of aSyn PTMs in the advancement of pathology; and 2) the exploration of the peripheral pathology of aSyn with these antibodies to better determine original sites of aSyn aggregation and pathogenesis.

Acknowledgments

I am very grateful for the continuous help and support I have received throughout my doctoral studies. I would like to start by thanking Hilal Lashuel for accepting to be my thesis supervisor, training me and working with me closely over the past few years. He has been a great inspiration and an exemplary scientist, taught me and challenged me to thrive always for excellence in scientific research. I thank also all of my colleagues at LMNN - Marie, the 'embodiment' of organisational virtues, who makes life easier for everyone in the lab; Anass, Niran, Jean-Christophe, Johannes, Sonia, Iman, Driss, Ramanath, Nadine, Jonathan, Elena, Laura, Alice, Jeremy, Bryan and Andreas, who have now departed LMNN and taken new paths in life; and Anne-Laure, Pedro, Senthil, Yllza, Somanath, Nathan, Galina, Salvatore, Raja, Sergey, Ahmed and Enzo, who still continue their scientific journey at LMNN. Without their help, advice, company and friendship, this journey would not have been the same.

Special thanks to the EPFL BIOP and HCF teams - to Nicolas Chiaruttini, Olivier Burri, Romain Guiet, Jessica Sordet-Dessimoz and Gian-Filippo Mancini for always doing their best to help me advance in my research. I am also very grateful for the help and guidance received from Ralf Schneggenburger, the director of EDNE, and my mentors Brian McCabe and Pascal Steiner. I thank Carmen Sandi, Bernard Schneider, Maria Grazia Spillantini and Erwan Bezard for kindly accepting to be part of the jury panel.

I had the pleasure to be part of several exciting collaborative and international projects during my doctoral studies, and would like to thank Janice Holton, Catherine Strand, Yasuo Miki, Christine Murray and Sandrine Foti at QSBB, UCL, who have been incredibly kind and helpful during my laboratory visit and stay in London. I am also thankful to have worked with Laura Parkkinen, Alan Liu and Selene Lee during my stay (and during the lockdown) in Oxford. It was an absolute privilege especially to be taught by distinguished neuropathologists like Janice Holton, Yasuo Miki, Laura Parkkinen and Alan Liu, who spent hours and hours by the microscope analysing slides with me. I would like to thank also Viktoria Ruf for all the neuropathology insight she has brought to the MSAomics collaborative project. I am very grateful to the brain donors and their families – this work was made possible only thanks to their donations.

Last but not least, friends and family… I am so lucky to have friends and ‘allies’ like Ayah, Silvia, Rita, Aiste, Jane, Aarti and Vivi, who have always been so kind, supportive, perceptive, smart and fun. Although we have been separated by geographical distances, all my friends who live in Turkey, in the UK, in Italy and all around the world have always remained close my heart and shared with me the ups and downs of this journey.

I dedicate this thesis to the brave women and compassionate men (plus the cats and the dogs) of my family – Michele for always being there for me and being a constant source of optimism; my mother and sisters for never doubting my abilities; my father for showing me that it is more valuable to *be* than to *have*; my aunt for the unforgettable and happy childhood memories; my grandmother for the invaluable scientific skills of coffee fortune telling(!); Hasan Baba for passing onto me his passion for Besiktas and for being a second father; and Tuna and now tiny Hazel for being pure epitomes of joy. I am endlessly grateful for your unconditional love and support, and love you back.

Lausanne, 2022

References

Abbott, R.D., Petrovitch, H., White, L.R., Masaki, K.H., Tanner, C.M., Curb, J.D., Grandinetti, A., Blanchette, P.L., Popper, J.S., Ross, G.W., 2001. Frequency of bowel movements and the future risk of Parkinson's disease. Neurology 57, 456–462. https://doi.org/10.1212/WNL.57.3.456

Abbott, R.D., Ross, G.W., White, L.R., Tanner, C.M., Masaki, K.H., Nelson, J.S., Curb, J.D., Petrovitch, H., 2005. Excessive daytime sleepiness and subsequent development of Parkinson disease. Neurology 65, 1442–1446. https://doi.org/10.1212/01.wnl.0000183056.89590.0d

Abdelmotilib, H., Maltbie, T., Delic, V., Liu, Z., Hu, X., Fraser, K.B., Moehle, M.S., Stoyka, L., Anabtawi, N., Krendelchtchikova, V., Volpicelli-Daley, L.A., West, A., 2017. α-Synuclein fibril-induced inclusion spread in rats and mice correlates with dopaminergic Neurodegeneration. Neurobiology of Disease 105, 84–98. https://doi.org/10.1016/j.nbd.2017.05.014

Abe, H., Yagishita, S., Amano, N., Iwabuchi, K., Hasegawa, K., Kowa, K., 1992. Argyrophilic glial intracytoplasmic inclusions in multiple system atrophy: immunocytochemical and ultrastructural study. Acta Neuropathol 84. https://doi.org/10.1007/BF00227820

Abeliovich, A., Schmitz, Y., Fariñas, I., Choi-Lundberg, D., Ho, W.-H., Castillo, P.E., Shinsky, N., Verdugo, J.M.G., Armanini, M., Ryan, A., Hynes, M., Phillips, H., Sulzer, D., Rosenthal, A., 2000. Mice Lacking α-Synuclein Display Functional Deficits in the Nigrostriatal Dopamine System. Neuron 25, 239–252. https://doi.org/10.1016/S0896-6273(00)80886-7

Adler, C.H., Beach, T.G., 2016. Neuropathological basis of nonmotor manifestations of Parkinson's disease. Mov Disord. 31, 1114–1119. https://doi.org/10.1002/mds.26605

Adler, C.H., Beach, T.G., Zhang, N., Shill, H.A., Driver-Dunckley, E., Caviness, J.N., Mehta, S.H., Sabbagh, M.N., Serrano, G.E., Sue, L.I., Belden, C.M., Powell, J., Jacobson, S.A., Zamrini, E., Shprecher, D., Davis, K.J., Dugger, B.N., Hentz, J.G., 2019. Unified Staging System for Lewy Body Disorders: Clinicopathologic Correlations and Comparison to Braak Staging. Journal of Neuropathology & Experimental Neurology 78, 891–899. https://doi.org/10.1093/jnen/nlz080

Adler, C.H., Dugger, B.N., Hentz, J.G., Hinni, M.L., Lott, D.G., Driver-Dunckley, E., Mehta, S., Serrano, G., Sue, L.I., Duffy, A., Intorcia, A., Filon, J., Pullen, J., Walker, D.G., Beach, T.G., 2016. Peripheral Synucleinopathy in Early Parkinson's Disease: Submandibular Gland Needle Biopsy Findings: Submandibular Gland Biopsies in Early PD. Mov Disord. 31, 250–256. https://doi.org/10.1002/mds.26476

Adler, C.H., Dugger, B.N., Hinni, M.L., Lott, D.G., Driver-Dunckley, E., Hidalgo, J., Henry-Watson, J., Serrano, G., Sue, L.I., Nagel, T., Duffy, A., Shill, H.A., Akiyama, H., Walker, D.G., Beach, T.G., 2014. Submandibular gland needle biopsy for the diagnosis of Parkinson disease. Neurology 82, 858–864. https://doi.org/10.1212/WNL.0000000000000204

Agin-Liebes, J., Cortes, E., Vonsattel, J.-P., Marder, K., Alcalay, R.N., 2020. Movement disorders rounds: A case of missing pathology in a patient with LRRK2 Parkinson's disease. Parkinsonism & Related Disorders 74, 76–77. https://doi.org/10.1016/j.parkreldis.2019.11.006

Ahmed, Z., Asi, Y.T., Sailer, A., Lees, A.J., Houlden, H., Revesz, T., Holton, J.L., 2012. The neuropathology, pathophysiology and genetics of multiple system atrophy: Neuropathology, pathophysiology and genetics of MSA. Neuropathology and Applied Neurobiology 38, 4–24. https://doi.org/10.1111/j.1365-2990.2011.01234.x

Alafuzoff, I., Ince, P.G., Arzberger, T., Al-Sarraj, S., Bell, J., Bodi, I., Bogdanovic, N., Bugiani, O., Ferrer, I., Gelpi, E., Gentleman, S., Giaccone, G., Ironside, J.W., Kavantzas, N., King, A., Korkolopoulou, P., Kovács, G.G., Meyronet, D., Monoranu, C., Parchi, P., Parkkinen, L., Patsouris, E., Roggendorf, W., Rozemuller, A., Stadelmann-Nessler, C., Streichenberger, N., Thal, D.R., Kretzschmar, H., 2009. Staging/typing of Lewy body related α-synuclein pathology: a study of the BrainNet Europe Consortium. Acta Neuropathol 117, 635–652. https://doi.org/10.1007/s00401-009-0523-2

Aldecoa, I., Navarro-Otano, J., Stefanova, N., Sprenger, F.S., Seppi, K., Poewe, W., Cuatrecasas, M., Valldeoriola, F., Gelpi, E., Tolosa, E., 2015. Alpha-synuclein immunoreactivity patterns in the enteric nervous system. Neuroscience Letters 602, 145–149. https://doi.org/10.1016/j.neulet.2015.07.005

Alegre-Abarrategui, J., Ansorge, O., Esiri, M., Wade-Martins, R., 2008. LRRK2 is a component of granular alpha-synuclein pathology in the brainstem of Parkinson's disease. Neuropathol Appl Neurobiol 34, 272–283. https://doi.org/10.1111/j.1365-2990.2007.00888.x

Alfaro, J.F., Gong, C.-X., Monroe, M.E., Aldrich, J.T., Clauss, T.R.W., Purvine, S.O., Wang, Z., Camp, D.G., Shabanowitz, J., Stanley, P., Hart, G.W., Hunt, D.F., Yang, F., Smith, R.D., 2012. Tandem mass spectrometry identifies many mouse brain O-GlcNAcylated proteins including EGF domain-specific O-GlcNAc transferase targets. Proceedings of the National Academy of Sciences 109, 7280–7285. https://doi.org/10.1073/pnas.1200425109

Allis, C.D., Berger, S.L., Cote, J., Dent, S., Jenuwien, T., Kouzarides, T., Pillus, L., Reinberg, D., Shi, Y., Shiekhattar, R., Shilatifard, A., Workman, J., Zhang, Y., 2007. New Nomenclature for Chromatin-Modifying Enzymes. Cell 131, 633–636. https://doi.org/10.1016/j.cell.2007.10.039

Almandoz-Gil, L., Lindström, V., Sigvardson, J., Kahle, P.J., Lannfelt, L., Ingelsson, M., Bergström, J., 2017. Mapping of Surface-Exposed Epitopes of In Vitro and In Vivo Aggregated Species of Alpha-Synuclein. Cell Mol Neurobiol 37, 1217–1226. https://doi.org/10.1007/s10571-016-0454-0

Alonso-Canovas, A., Tembl Ferrairó, J.I., Martínez-Torres, I., Lopez-Sendon Moreno, J.L., Parees-Moreno, I., Monreal-Laguillo, E., Pérez-Torre, P., Toledano Delgado, R., García Ribas, G., Sastre Bataller, I., Masjuan, J., Martinez-Castrillo, J.C., Walter, U., 2019. Transcranial sonography in atypical parkinsonism: How reliable is it in real clinical practice? A multicentre comprehensive study. Parkinsonism & Related Disorders 68, 40–45. https://doi.org/10.1016/j.parkreldis.2019.09.032

Anderson, J.P., Walker, D.E., Goldstein, J.M., de Laat, R., Banducci, K., Caccavello, R.J., Barbour, R., Huang, J., Kling, K., Lee, M., Diep, L., Keim, P.S., Shen, X., Chataway, T., Schlossmacher, M.G., Seubert, P., Schenk, D., Sinha, S., Gai, W.P., Chilcote, T.J., 2006. Phosphorylation of Ser-129 Is the Dominant Pathological Modification of α-Synuclein in Familial and Sporadic Lewy Body Disease. J. Biol. Chem. 281, 29739–29752. https://doi.org/10.1074/jbc.M600933200

Andringa, G., Du, F., Chase, T.N., Bennett, M.C., 2003. Mapping of Rat Brain Using the Synuclein-1 Monoclonal Antibody Reveals Somatodendritic Expression of α-Synuclein in Populations of Neurons Homologous to those Vulnerable to Lewy Body Formation in Human Synucleopathies. J Neuropathol Exp Neurol 62, 1060–1075. https://doi.org/10.1093/jnen/62.10.1060

Angot, E., Brundin, P., 2009. Dissecting the potential molecular mechanisms underlying α-synuclein cell-to-cell transfer in Parkinson's disease. Parkinsonism & Related Disorders 15, S143–S147. https://doi.org/10.1016/S1353-8020(09)70802-8

Angot, E., Steiner, J.A., Hansen, C., Li, J.-Y., Brundin, P., 2010. Are synucleinopathies prion-like disorders? The Lancet Neurology 9, 1128–1138. https://doi.org/10.1016/S1474-4422(10)70213-1

Angot, E., Steiner, J.A., Lema Tomé, C.M., Ekström, P., Mattsson, B., Björklund, A., Brundin, P., 2012. Alpha-Synuclein Cell-to-Cell Transfer and Seeding in Grafted Dopaminergic Neurons In Vivo. PLoS ONE 7, e39465. https://doi.org/10.1371/journal.pone.0039465

Annerino, D.M., Arshad, S., Taylor, G.M., Adler, C.H., Beach, T.G., Greene, J.G., 2012. Parkinson's disease is not associated with gastrointestinal myenteric ganglion neuron loss. Acta Neuropathol 124, 665–680. https://doi.org/10.1007/s00401-012-1040-2

Antonini, A., Tolosa, E., Mizuno, Y., Yamamoto, M., Poewe, W.H., 2009. A reassessment of risks and benefits of dopamine agonists in Parkinson's disease. The Lancet Neurology 8, 929–937. https://doi.org/10.1016/S1474-4422(09)70225-X

Antunes, L., Frasquilho, S., Ostaszewski, M., Weber, Jos., Longhino, L., Antony, P., Baumuratov, A., Buttini, M., Shannon, K.M., Balling, R., Diederich, N.J., 2016. Similar α-Synuclein staining in the colon mucosa in patients with Parkinson's disease and controls: PD Mucosa and Synuclein. Mov Disord. 31, 1567–1570. https://doi.org/10.1002/mds.26702

Appel-Cresswell, S., Vilarino-Guell, C., Encarnacion, M., Sherman, H., Yu, I., Shah, B., Weir, D., Thompson, C., Szu-Tu, C., Trinh, J., Aasly, J.O., Rajput, A., Rajput, A.H., Jon Stoessl, A., Farrer, M.J., 2013. Alpha-synuclein p.H50Q, a novel pathogenic mutation for Parkinson's disease: α- Synuclein p.H50q, A Novel Mutation For Pd. Mov Disord. 28, 811–813. https://doi.org/10.1002/mds.25421

Arai, N., Papp, M.I., Lantos, P.L., 1994. New observation on ubiquitinated neurons in the cerebral cortex of multiple system atrophy (MSA). Neuroscience Letters 182, 197–200. https://doi.org/10.1016/0304-3940(94)90796-X

Arai, T., Uéda, K., Ikeda, K., Akiyama, H., Haga, C., Kondo, H., Kuroki, N., Niizato, K., Iritani, S., Tsuchiya, K., 1999. Argyrophilic glial inclusions in the midbrain of patients with Parkinson's disease and diffuse Lewy body disease are immunopositive for NACP/α-synuclein. Neuroscience Letters 259, 83–86. https://doi.org/10.1016/S0304-3940(98)00890-8

Araki, K., Yagi, N., Aoyama, K., Choong, C.-J., Hayakawa, H., Fujimura, H., Nagai, Y., Goto, Y., Mochizuki, H., 2019. Parkinson's disease is a type of amyloidosis featuring accumulation of

amyloid fibrils of α-synuclein. Proc Natl Acad Sci USA 116, 17963–17969. https://doi.org/10.1073/pnas.1906124116
Arima, K., Uéda, K., Sunohara, N., Arakawa, K., Hirai, S., Nakamura, M., Tonozuka-Uehara, H., Kawai, M., 1998a. NACP/α-synuclein immunoreactivity in fibrillary components of neuronal and oligodendroglial cytoplasmic inclusions in the pontine nuclei in multiple system atrophy. Acta Neuropathologica 96, 439–444. https://doi.org/10.1007/s004010050917
Arima, K., Uéda, K., Sunohara, N., Hirai, S., Izumiyama, Y., Tonozuka-Uehara, H., Kawai, M., 1998b. Immunoelectron-microscopic demonstration of NACP/α-synuclein-epitopes on the filamentous component of Lewy bodies in Parkinson's disease and in dementia with Lewy bodies. Brain Research 808, 93–100. https://doi.org/10.1016/S0006-8993(98)00734-3
Arotcarena, M.-L., Dovero, S., Prigent, A., Bourdenx, M., Camus, S., Porras, G., Thiolat, M.-L., Tasselli, M., Aubert, P., Kruse, N., Mollenhauer, B., Trigo Damas, I., Estrada, C., Garcia-Carrillo, N., Vaikath, N.N., El-Agnaf, O.M.A., Herrero, M.T., Vila, M., Obeso, J.A., Derkinderen, P., Dehay, B., Bezard, E., 2020. Bidirectional gut-to-brain and brain-to-gut propagation of synucleinopathy in non-human primates. Brain 143, 1462–1475. https://doi.org/10.1093/brain/awaa096
Asi, Y.T., Simpson, J.E., Heath, P.R., Wharton, S.B., Lees, A.J., Revesz, T., Houlden, H., Holton, J.L., 2014. Alpha-synuclein mRNA expression in oligodendrocytes in MSA: αSyn mRNA Expression in MSA Oligodendrocytes. Glia 62, 964–970. https://doi.org/10.1002/glia.22653
Baba, M., Nakajo, S., Tu, P.H., Tomita, T., Nakaya, K., Lee, V.M., Trojanowski, J.Q., Iwatsubo, T., 1998. Aggregation of alpha-synuclein in Lewy bodies of sporadic Parkinson's disease and dementia with Lewy bodies. Am J Pathol 152, 879–884.
Banati, R.B., Daniel, S.E., Blunt, S.B., 1998. Glial pathology but absence of apoptotic nigral neurons in long-standing Parkinson's disease. Mov Disord. 13, 221–227. https://doi.org/10.1002/mds.870130205
Barbeau, A., Murphy, G.F., Sourkes, T.L., 1961. Excretion of dopamine in diseases of basal ganglia. Science 133, 1706–1707. https://doi.org/10.1126/science.133.3465.1706-a
Barcelo-Coblijn, G., Golovko, M.Y., Weinhofer, I., Berger, J., Murphy, E.J., 2006. Brain neutral lipids mass is increased in α-synuclein gene-ablated mice: α-Synuclein and brain neutral lipid mass. Journal of Neurochemistry 101, 132–141. https://doi.org/10.1111/j.1471-4159.2006.04348.x
Barrenschee, M., Zorenkov, D., Böttner, M., Lange, C., Cossais, F., Scharf, A.B., Deuschl, G., Schneider, S.A., Ellrichmann, M., Fritscher-Ravens, A., Wedel, T., 2017. Distinct pattern of enteric phospho-alpha-synuclein aggregates and gene expression profiles in patients with Parkinson's disease. acta neuropathol commun 5, 1. https://doi.org/10.1186/s40478-016-0408-2
Bartels, T., Choi, J.G., Selkoe, D.J., 2011. α-Synuclein occurs physiologically as a helically folded tetramer that resists aggregation. Nature 477, 107–110. https://doi.org/10.1038/nature10324
Bartels, T., Kim, N.C., Luth, E.S., Selkoe, D.J., 2014. N-Alpha-Acetylation of α-Synuclein Increases Its Helical Folding Propensity, GM1 Binding Specificity and Resistance to Aggregation. PLoS ONE 9, e103727. https://doi.org/10.1371/journal.pone.0103727
Bayer, T.A., Jäkälä, P., Hartmann, T., Egensperger, R., Buslei, R., Falkai, P., Beyreuther, K., 1999. Neural expression profile of α-synuclein in developing human cortex: NeuroReport 10, 2799–2803. https://doi.org/10.1097/00001756-199909090-00019
Beach, T.G., Adler, C.H., Dugger, B.N., Serrano, G., Hidalgo, J., Henry-Watson, J., Shill, H.A., Sue, L.I., Sabbagh, M.N., Akiyama, H., Arizona Parkinson's Disease Consortium, 2013. Submandibular Gland Biopsy for the Diagnosis of Parkinson Disease. J Neuropathol Exp Neurol 72, 130–136. https://doi.org/10.1097/NEN.0b013e3182805c72
Beach, T.G., Adler, C.H., Serrano, G., Sue, L.I., Walker, D.G., Dugger, B.N., Shill, H.A., Driver-Dunckley, E., Caviness, J.N., Intorcia, A., Filon, J., Scott, S., Garcia, A., Hoffman, B., Belden, C.M., Davis, K.J., Sabbagh, M.N., Arizona Parkinson's Disease Consortium, 2016. Prevalence of Submandibular Gland Synucleinopathy in Parkinson's Disease, Dementia with Lewy Bodies and other Lewy Body Disorders. JPD 6, 153–163. https://doi.org/10.3233/JPD-150680
Beach, T.G., Arizona Parkinson's Disease Consortium, Adler, C.H., Sue, L.I., Vedders, L., Lue, L., White III, C.L., Akiyama, H., Caviness, J.N., Shill, H.A., Sabbagh, M.N., Walker, D.G., 2010. Multi-organ distribution of phosphorylated α-synuclein histopathology in subjects with Lewy body disorders. Acta Neuropathol 119, 689–702. https://doi.org/10.1007/s00401-010-0664-3
Beach, T.G., Serrano, G.E., Kremer, T., Canamero, M., Dziadek, S., Sade, H., Derkinderen, P., Corbillé, A.-G., Letournel, F., Munoz, D.G., White, C.L., Schneider, J., Crary, J.F., Sue, L.I., Adler, C.H., Glass, M.J., Intorcia, A.J., Walker, J.E., Foroud, T., Coffey, C.S., Ecklund, D., Riss, H., Goßmann, J., König, F., Kopil, C.M., Arnedo, V., Riley, L., Linder, C., Dave, K.D., Jennings, D., Seibyl, J., Mollenhauer, B., Chahine, L., the Systemic Synuclein Sampling Study (S4),

Guilmette, L., Russell, D., Noyes-Lloyd, C., Mitchell, C., Smith, D., Potter, M., Case, R., Lott, D., Duffy, A., Hogarth, P., Cresswell, M., Akhtar, R., Purri, R., Amara, A., Blair, C., Keshavarzian, A., Marras, C., Visanji, N., Rothberg, B., Oza, V., 2018. Immunohistochemical Method and Histopathology Judging for the Systemic Synuclein Sampling Study (S4). Journal of Neuropathology & Experimental Neurology 77, 793–802. https://doi.org/10.1093/jnen/nly056

Beach, T.G., the Arizona Parkinson's Disease Consortium, Adler, C.H., Lue, L., Sue, L.I., Bachalakuri, J., Henry-Watson, J., Sasse, J., Boyer, S., Shirohi, S., Brooks, R., Eschbacher, J., White, C.L., Akiyama, H., Caviness, J., Shill, H.A., Connor, D.J., Sabbagh, M.N., Walker, D.G., 2009. Unified staging system for Lewy body disorders: correlation with nigrostriatal degeneration, cognitive impairment and motor dysfunction. Acta Neuropathol 117, 613–634. https://doi.org/10.1007/s00401-009-0538-8

Beck, R.O., Betts, C.D., Fowler, C.J., 1994. Genitourinary Dysfunction in Multiple System Atrophy: Clinical Features and Treatment in 62 Cases. Journal of Urology 151, 1336–1341. https://doi.org/10.1016/S0022-5347(17)35246-1

Beckman, J.S., Beckman, T.W., Chen, J., Marshall, P.A., Freeman, B.A., 1990. Apparent hydroxyl radical production by peroxynitrite: implications for endothelial injury from nitric oxide and superoxide. PNAS 87, 1620–1624. https://doi.org/10.1073/pnas.87.4.1620

Beckman, J.S., Ischiropoulos, H., Zhu, L., van der Woerd, M., Smith, C., Chen, J., Harrison, J., Martin, J.C., Tsai, M., 1992. Kinetics of superoxide dismutase- and iron-catalyzed nitration of phenolics by peroxynitrite. Archives of Biochemistry and Biophysics 298, 438–445. https://doi.org/10.1016/0003-9861(92)90432-V

Beckman, J.S., Ye, Y.Z., Anderson, P.G., Chen, J., Accavitti, M.A., Tarpey, M.M., White, C.R., 1994. Extensive Nitration of Protein Tyrosines in Human Atherosclerosis Detected by Immunohistochemistry. Biological Chemistry Hoppe-Seyler 375, 81–88. https://doi.org/10.1515/bchm3.1994.375.2.81

Benabid, A.L., Pollak, P., Louveau, A., Henry, S., de Rougemont, J., 1987. Combined (Thalamotomy and Stimulation) Stereotactic Surgery of the VIM Thalamic Nucleus for Bilateral Parkinson Disease. Stereotact Funct Neurosurg 50, 344–346. https://doi.org/10.1159/000100803

Bensimon, G., Ludolph, A., Agid, Y., Vidailhet, M., Payan, C., Leigh, P.N., 2009. Riluzole treatment, survival and diagnostic criteria in Parkinson plus disorders: The NNIPPS Study. Brain 132, 156–171. https://doi.org/10.1093/brain/awn291

Bernis, M.E., Babila, J.T., Breid, S., Wüsten, K.A., Wüllner, U., Tamgüney, G., 2015. Prion-like propagation of human brain-derived alpha-synuclein in transgenic mice expressing human wild-type alpha-synuclein. acta neuropathol commun 3, 75. https://doi.org/10.1186/s40478-015-0254-7

Beyer, K., Domingo-Sàbat, M., Ariza, A., 2009. Molecular Pathology of Lewy Body Diseases. IJMS 10, 724–745. https://doi.org/10.3390/ijms10030724

Beyer, K., Domingo-Sábat, M., Lao, J.I., Carrato, C., Ferrer, I., Ariza, A., 2008. Identification and characterization of a new alpha-synuclein isoform and its role in Lewy body diseases. Neurogenetics 9, 15–23. https://doi.org/10.1007/s10048-007-0106-0

Beyer, K., Humbert, J., Ferrer, A., Lao, J.I., Carrato, C., L??pez, D., Ferrer, I., Ariza, A., 2006. Low alpha-synuclein 126 mRNA levels in dementia with Lewy bodies and Alzheimer disease: NeuroReport 17, 1327–1330. https://doi.org/10.1097/01.wnr.0000224773.66904.e7

Beyer, K., Lao, J.I., Carrato, C., Mate, J.L., Lopez, D., Ferrer, I., Ariza, A., 2004. Differential expression of alpha-synuclein isoforms in dementia with Lewy bodies. Neuropathol Appl Neurobiol 30, 601–607. https://doi.org/10.1111/j.1365-2990.2004.00572.x

Bhattacharjee, P., Öhrfelt, A., Lashley, T., Blennow, K., Brinkmalm, A., Zetterberg, H., 2019. Mass Spectrometric Analysis of Lewy Body-Enriched α-Synuclein in Parkinson's Disease. J. Proteome Res. 18, 2109–2120. https://doi.org/10.1021/acs.jproteome.8b00982

Bidasee, K.R., Zhang, Y., Shao, C.H., Wang, M., Patel, K.P., Dincer, Ü.D., Besch, H.R., 2004. Diabetes Increases Formation of Advanced Glycation End Products on Sarco(endo)plasmic Reticulum Ca2+-ATPase. Diabetes 53, 463–473. https://doi.org/10.2337/diabetes.53.2.463

Birkmayer, W., Hornykiewicz, O., 1998. The effect of l-3,4-dihydroxyphenylalanine (=DOPA) on akinesia in parkinsonism. Parkinsonism & Related Disorders 4, 59–60. https://doi.org/10.1016/S1353-8020(98)00013-3

Bodles, A.M., Guthrie, D.J.S., Harriott, P., Campbell, P., Irvine, G.B., 2000. Toxicity of non-Aβ component of Alzheimer's disease amyloid, and N-terminal fragments thereof, correlates to formation of β-sheet structure and fibrils: Toxicity of non-Aβ component and fragments thereof. European Journal of Biochemistry 267, 2186–2194. https://doi.org/10.1046/j.1432-1327.2000.01219.x

Boettner, M., Fricke, T., Müller, M., Barrenschee, M., Deuschl, G., Schneider, S.A., Egberts, J.-H., Becker, T., Fritscher-Ravens, A., Ellrichmann, M., Schulz-Schaeffer, W.J., Wedel, T., 2015. Alpha-synuclein is associated with the synaptic vesicle apparatus in the human and rat enteric nervous system. Brain Research 1614, 51–59. https://doi.org/10.1016/j.brainres.2015.04.015

Boettner, M., Zorenkov, D., Hellwig, I., Barrenschee, M., Harde, J., Fricke, T., Deuschl, G., Egberts, J.-H., Becker, T., Fritscher-Ravens, A., Arlt, A., Wedel, T., 2012. Expression pattern and localization of alpha-synuclein in the human enteric nervous system. Neurobiology of Disease 48, 474–480. https://doi.org/10.1016/j.nbd.2012.07.018

Bonifati, V., Rizzu, P., Squitieri, F., Krieger, E., Vanacore, N., van Swieten, J.C., Brice, A., van Duijn, C.M., Oostra, B., Meco, G., Heutink, P., 2003a. DJ-1(PARK7), a novel gene for autosomal recessive, early onset parkinsonism. Neurol Sci 24, 159–160. https://doi.org/10.1007/s10072-003-0108-0

Bonifati, V., Rizzu, P., van Baren, M.J., Schaap, O., Breedveld, G.J., Krieger, E., Dekker, M.C.J., Squitieri, F., Ibanez, P., Joosse, M., van Dongen, J.W., Vanacore, N., van Swieten, J.C., Brice, A., Meco, G., van Duijn, C.M., Oostra, B.A., Heutink, P., 2003b. Mutations in the *DJ-1* Gene Associated with Autosomal Recessive Early-Onset Parkinsonism. Science 299, 256–259. https://doi.org/10.1126/science.1077209

Bousset, L., Pieri, L., Ruiz-Arlandis, G., Gath, J., Jensen, P.H., Habenstein, B., Madiona, K., Olieric, V., Böckmann, A., Meier, B.H., Melki, R., 2013. Structural and functional characterization of two alpha-synuclein strains. Nat Commun 4, 2575. https://doi.org/10.1038/ncomms3575

Bower, J.H., Maraganore, D.M., McDonnell, S.K., Rocca, W.A., 1997. Incidence of progressive supranuclear palsy and multiple system atrophy in Olmsted County, Minnesota, 1976 to 1990. Neurology 49, 1284–1288. https://doi.org/10.1212/WNL.49.5.1284

Boyer, D.R., Li, B., Sun, C., Fan, W., Sawaya, M.R., Jiang, L., Eisenberg, D.S., 2019. Cryo-EM structures of α-synuclein fibrils with the H50Q hereditary mutation reveal new polymorphs. bioRxiv 738450. https://doi.org/10.1101/738450

Boyer, D.R., Li, B., Sun, C., Fan, W., Zhou, K., Hughes, M.P., Sawaya, M.R., Jiang, L., Eisenberg, D.S., 2020. The α-synuclein hereditary mutation E46K unlocks a more stable, pathogenic fibril structure. Proc Natl Acad Sci USA 117, 3592–3602. https://doi.org/10.1073/pnas.1917914117

Braak, E., Sandmann-Keil, D., Rüb, U., Gai, W.P., de Vos, R.A.I., Jansen Steur, E.N.H., Arai, K., Braak, H., 2001. α-Synuclein immunopositive Parkinson's disease-related inclusion bodies in lower brain stem nuclei. Acta Neuropathol 101, 195–201. https://doi.org/10.1007/s004010000247

Braak, H., Braak, E., Yilmazer, D., de Vos, R.A.I., Jansen, E.N.H., Bohl, J., Jellinger, K., 1994. Amygdala pathology in Parkinson's disease. Acta Neuropathol 88, 493–500. https://doi.org/10.1007/BF00296485

Braak, H., de Vos, R.A.I., Bohl, J., Del Tredici, K., 2006. Gastric α-synuclein immunoreactive inclusions in Meissner's and Auerbach's plexuses in cases staged for Parkinson's disease-related brain pathology. Neuroscience Letters 396, 67–72. https://doi.org/10.1016/j.neulet.2005.11.012

Braak, H., Del Tredici, K., Bratzke, H., Hamm-Clement, J., Sandmann-Keil, D., Rüb, U., 2002. Staging of the intracerebral inclusion body pathology associated with idiopathic Parkinson's disease (preclinical and clinical stages). Journal of Neurology 249, 1–1. https://doi.org/10.1007/s00415-002-1301-4

Braak, H., Rueb, U., Gai, W.P., Del Tredici, K., 2003a. Idiopathic Parkinson's disease: possible routes by which vulnerable neuronal types may be subject to neuroinvasion by an unknown pathogen. Journal of Neural Transmission 110, 517–536. https://doi.org/10.1007/s00702-002-0808-2

Braak, H., Rueb, U., Sandmann-Keil, D., Gai, W.P., de Vos, R.A.I., Jansen Steur, E.N.H., Arai, K., Braak, E., 2000. Parkinson's disease: affection of brain stem nuclei controlling premotor and motor neurons of the somatomotor system. Acta Neuropathologica 99, 489–495. https://doi.org/10.1007/s004010051150

Braak, H., Sandmann-Keil, D., Gai, W., Braak, E., 1999. Extensive axonal Lewy neurites in Parkinson's disease: a novel pathological feature revealed by a-synuclein immunocytochemistry. Neuroscience Letters 3.

Braak, H., Sastre, M., Bohl, J.R.E., de Vos, R.A.I., Del Tredici, K., 2007a. Parkinson's disease: lesions in dorsal horn layer I, involvement of parasympathetic and sympathetic pre- and postganglionic neurons. Acta Neuropathol 113, 421–429. https://doi.org/10.1007/s00401-007-0193-x

Braak, H., Sastre, M., Del Tredici, K., 2007b. Development of α-synuclein immunoreactive astrocytes in the forebrain parallels stages of intraneuronal pathology in sporadic Parkinson's disease. Acta Neuropathol 114, 231–241. https://doi.org/10.1007/s00401-007-0244-3

Braak, H., Tredici, K.D., Rüb, U., de Vos, R.A.I., Jansen Steur, E.N.H., Braak, E., 2003b. Staging of brain pathology related to sporadic Parkinson's disease. Neurobiology of Aging 24, 197–211. https://doi.org/10.1016/S0197-4580(02)00065-9

Bradbury, S., Eggleston, C., 1925. Postural hypotension. American Heart Journal 1, 73–86. https://doi.org/10.1016/S0002-8703(25)90007-5

Brahmachari, S., Ge, P., Lee, S.H., Kim, D., Karuppagounder, S.S., Kumar, M., Mao, X., Shin, J.H., Lee, Y., Pletnikova, O., Troncoso, J.C., Dawson, V.L., Dawson, T.M., Ko, H.S., 2016. Activation of tyrosine kinase c-Abl contributes to α-synuclein–induced neurodegeneration. Journal of Clinical Investigation 126, 2970–2988. https://doi.org/10.1172/JCI85456

Braidy, N., Gai, W.-P., Xu, Y.H., Sachdev, P., Guillemin, G.J., Jiang, X.-M., Ballard, J.W.O., Horan, M.P., Fang, Z.M., Chong, B.H., Chan, D.Y., 2013. Uptake and mitochondrial dysfunction of alpha-synuclein in human astrocytes, cortical neurons and fibroblasts. Translational Neurodegeneration 2, 20. https://doi.org/10.1186/2047-9158-2-20

Bras, J.M., Guerreiro, R.J., Ribeiro, M.H., Januario, C., Morgadinho, A., Oliveira, C.R., Cunha, L., Hardy, J., Singleton, A., 2005. G2019S dardarin substitution is a common cause of Parkinson's disease in a Portuguese cohort. Mov. Disord. 20, 1653–1655. https://doi.org/10.1002/mds.20682

Breid, S., Bernis, M.E., Babila, J.T., Garza, M.C., Wille, H., Tamgüney, G., 2016. Neuroinvasion of α-Synuclein Prionoids after Intraperitoneal and Intraglossal Inoculation. J Virol 90, 9182–9193. https://doi.org/10.1128/JVI.01399-16

Brown, D.R., 2009. Metal binding to alpha-synuclein peptides and its contribution to toxicity. Biochemical and Biophysical Research Communications 380, 377–381. https://doi.org/10.1016/j.bbrc.2009.01.103

Buell, A.K., Galvagnion, C., Gaspar, R., Sparr, E., Vendruscolo, M., Knowles, T.P.J., Linse, S., Dobson, C.M., 2014. Solution conditions determine the relative importance of nucleation and growth processes in -synuclein aggregation. Proceedings of the National Academy of Sciences 111, 7671–7676. https://doi.org/10.1073/pnas.1315346111

Burger, D., Fenyi, A., Bousset, L., Stahlberg, H., Melki, R., 2021. Cryo-EM structure of alpha-synuclein fibrils amplified by PMCA from PD and MSA patient brains. bioRxiv. https://doi.org/10.1101/2021.07.08.451588

Burre, J., Sharma, M., Tsetsenis, T., Buchman, V., Etherton, M.R., Sudhof, T.C., 2010. Alpha-synuclein Promotes SNARE-Complex Assembly in Vivo and in Vitro. Science 329, 1663–1667. https://doi.org/10.1126/science.1195227

Burre, J., Vivona, S., Diao, J., Sharma, M., Brunger, A.T., Südhof, T.C., 2013. Properties of native brain α-synuclein. Nature 498, E4–E6. https://doi.org/10.1038/nature12125

Burtscher, J., Copin, J.-C., Rodrigues, J., Kumar, S.T., Chiki, A., Guillot de Suduiraut, I., Sandi, C., Lashuel, H.A., 2019. Chronic corticosterone aggravates behavioral and neuronal symptomatology in a mouse model of alpha-synuclein pathology. Neurobiology of Aging 83, 11–20. https://doi.org/10.1016/j.neurobiolaging.2019.08.007

Calderon-Garciduenas, L., Reynoso-Robles, R., Pérez-Guillé, B., Mukherjee, P.S., Gónzalez-Maciel, A., 2017. Combustion-derived nanoparticles, the neuroenteric system, cervical vagus, hyperphosphorylated alpha synuclein and tau in young Mexico City residents. Environmental Research 159, 186–201. https://doi.org/10.1016/j.envres.2017.08.008

Calne, D.B., Chu, N.-S., Huang, C.-C., Lu, C.-S., Olanow, W., 1994. Manganism and idiopathic parkinsonism: Similarities and differences. Neurology 44, 1583–1583. https://doi.org/10.1212/WNL.44.9.1583

Campbell, B.C.V., McLean, C.A., Culvenor, J.G., Gai, W.P., Blumbergs, P.C., Jakala, P., Beyreuther, K., Masters, C.L., Li, Q.-X., 2001. The solubility of a-synuclein in multiple system atrophy differs from that of dementia with Lewy bodies and Parkinson's disease. Journal of Neurochemistry 10.

Campion, D., Martin, C., Heilig, R., Charbonnier, F., Moreau, V., Flaman, J.M., Petit, J.L., Hannequin, D., Brice, A., Frebourg†, T., 1995. The NACP/synuclein gene: chromosomal assignment and screening for alterations in Alzheimer disease. Genomics 26, 254–257. https://doi.org/10.1016/0888-7543(95)80208-4

Campioni, S., Carret, G., Jordens, S., Nicoud, L., Mezzenga, R., Riek, R., 2014. The Presence of an Air–Water Interface Affects Formation and Elongation of α-Synuclein Fibrils. J. Am. Chem. Soc. 136, 2866–2875. https://doi.org/10.1021/ja412105t

Candelise, N., Schmitz, M., Llorens, F., Villar-Piqué, A., Cramm, M., Thom, T., Silva Correia, S.M., Cunha, J.E.G., Möbius, W., Outeiro, T.F., Álvarez, V.G., Banchelli, M., D'Andrea, C., Angelis, M., Zafar, S., Rabano, A., Matteini, P., Zerr, I., 2019. Seeding variability of different alpha

synuclein strains in synucleinopathies. Ann Neurol 85, 691–703. https://doi.org/10.1002/ana.25446
Cardo, L.F., Coto, E., de Mena, L., Ribacoba, R., Mata, I.F., Menéndez, M., Moris, G., Alvarez, V., 2014. Alpha-synuclein transcript isoforms in three different brain regions from Parkinson's disease and healthy subjects in relation to the SNCA rs356165/rs11931074 polymorphisms. Neuroscience Letters 562, 45–49. https://doi.org/10.1016/j.neulet.2014.01.009
Carletti, R., Campo, F., Fusconi, M., Pellicano, C., De Vincentiis, M., Pontieri, F.E., Di Gioia, C.R., 2017. Phosphorylated α-synuclein immunoreactivity in nerve fibers from minor salivary glands in Parkinson's disease. Parkinsonism & Related Disorders 38, 99–101. https://doi.org/10.1016/j.parkreldis.2017.02.031
Castagnet, P.I., Golovko, M.Y., Barcelo-Coblijn, G.C., Nussbaum, R.L., Murphy, E.J., 2005. Fatty acid incorporation is decreased in astrocytes cultured from α-synuclein gene-ablated mice: α-Synuclein gene-ablation. Journal of Neurochemistry 94, 839–849. https://doi.org/10.1111/j.1471-4159.2005.03247.x
Castellani, R.J., Smith, M.A., Richey, G.L., Perry, G., 1996. Glycoxidation and oxidative stress in Parkinson disease and diffuse Lewy body disease. Brain Research 737, 195–200. https://doi.org/10.1016/0006-8993(96)00729-9
Cavaliere, F., Cerf, L., Dehay, B., Ramos-Gonzalez, P., De Giorgi, F., Bourdenx, M., Bessede, A., Obeso, J.A., Matute, C., Ichas, F., Bezard, E., 2017. In vitro α-synuclein neurotoxicity and spreading among neurons and astrocytes using Lewy body extracts from Parkinson disease brains. Neurobiology of Disease 103, 101–112. https://doi.org/10.1016/j.nbd.2017.04.011
Cavey, J.R., Ralston, S.H., Hocking, L.J., Sheppard, P.W., Ciani, B., Searle, M.S., Layfield, R., 2004. Loss of Ubiquitin-Binding Associated With Paget's Disease of Bone p62 (SQSTM1) Mutations. J Bone Miner Res 20, 619–624. https://doi.org/10.1359/JBMR.041205
Cersosimo, M.G., Perandones, C., Micheli, F.E., Raina, G.B., Beron, A.M., Nasswetter, G., Radrizzani, M., Benarroch, E.E., 2011. Alpha-synuclein immunoreactivity in minor salivary gland biopsies of Parkinson's disease patients. Mov. Disord. 26, 188–190. https://doi.org/10.1002/mds.23344
Chadchankar, H., Ihalainen, J., Tanila, H., Yavich, L., 2011. Decreased reuptake of dopamine in the dorsal striatum in the absence of alpha-synuclein. Brain Research 1382, 37–44. https://doi.org/10.1016/j.brainres.2011.01.064
Chadchankar, H., Yavich, L., 2011. Sub-regional differences and mechanisms of the short-term plasticity of dopamine overflow in striatum in mice lacking alpha-synuclein. Brain Research 1423, 67–76. https://doi.org/10.1016/j.brainres.2011.09.026
Chandra, R., Hiniker, A., Kuo, Y.-M., Nussbaum, R.L., Liddle, R.A., 2017. α-Synuclein in gut endocrine cells and its implications for Parkinson's disease. JCI Insight 2, e92295. https://doi.org/10.1172/jci.insight.92295
Chartier-Harlin, M.-C., Kachergus, J., Roumier, C., Mouroux, V., Douay, X., Lincoln, S., Levecque, C., Larvor, L., Andrieux, J., Hulihan, M., Waucquier, N., Defebvre, L., Amouyel, P., Farrer, M., Destée, A., 2004. α-synuclein locus duplication as a cause of familial Parkinson's disease. The Lancet 364, 1167–1169. https://doi.org/10.1016/S0140-6736(04)17103-1
Chavarria, C., Rodríguez-Bottero, S., Quijano, C., Cassina, P., Souza, J.M., 2018. Impact of monomeric, oligomeric and fibrillar alpha-synuclein on astrocyte reactivity and toxicity to neurons. Biochemical Journal 475, 3153–3169. https://doi.org/10.1042/BCJ20180297
Chen, L., Periquet, M., Wang, X., Negro, A., McLean, P.J., Hyman, B.T., Feany, M.B., 2009. Tyrosine and serine phosphorylation of α-synuclein have opposing effects on neurotoxicity and soluble oligomer formation. J. Clin. Invest. JCI39088. https://doi.org/10.1172/JCI39088
Chen, X., Pettenati, J., George-Hyslop, S., Roses, A.D., Xia, Y., Horsburgh, K., Uda, K., Saitoh, T., 1994. The Human NACP/a-Synuclein Gene: Chromosome Assignment to 4q21.3-q22 and TaqI RFLPAnalysis. Genomics 3.
Choi, D.-H., Kim, Y.-J., Kim, Y.-G., Joh, T.H., Beal, M.F., Kim, Y.-S., 2011. Role of Matrix Metalloproteinase 3-mediated α-Synuclein Cleavage in Dopaminergic Cell Death. J. Biol. Chem. 286, 14168–14177. https://doi.org/10.1074/jbc.M111.222430
Chou, T.-W., Chang, N.P., Krishnagiri, M., Patel, A.P., Lindman, M., Angel, J.P., Kung, P.-L., Atkins, C., Daniels, B.P., 2021. Fibrillar α-synuclein induces neurotoxic astrocyte activation via RIP kinase signaling and NF-κB. Cell Death Dis 12, 756. https://doi.org/10.1038/s41419-021-04049-0
Chung, S.J., Kim, J., Lee, H.J., Ryu, H.-S., Kim, K., Lee, J.H., Jung, K.W., Kim, M.J., Kim, M.-J., Kim, Y.J., Yun, S.-C., Lee, J.-Y., Hong, S.-M., Myung, S.-J., 2016. Alpha-synuclein in gastric and colonic mucosa in Parkinson's disease: Limited role as a biomarker: Enteric Alpha-Synuclein In Parkinson's Disease. Mov Disord. 31, 241–249. https://doi.org/10.1002/mds.26473

Civiero, L., Cogo, S., Biosa, A., Greggio, E., 2018. The role of LRRK2 in cytoskeletal dynamics. Biochemical Society Transactions 46, 1653–1663. https://doi.org/10.1042/BST20180469
Claassen, D.O., Josephs, K.A., Ahlskog, J.E., Silber, M.H., Tippmann-Peikert, M., Boeve, B.F., 2010. REM sleep behavior disorder preceding other aspects of synucleinopathies by up to half a century. Neurology 75, 494–499. https://doi.org/10.1212/WNL.0b013e3181ec7fac
Clairembault, T., Leclair-Visonneau, L., Coron, E., Bourreille, A., Le Dily, S., Vavasseur, F., Heymann, M.-F., Neunlist, M., Derkinderen, P., 2015. Structural alterations of the intestinal epithelial barrier in Parkinson's disease. acta neuropathol commun 3, 12. https://doi.org/10.1186/s40478-015-0196-0
Clayton, D.F., George, J.M., 1999. Synucleins in synaptic plasticity and neurodegenerative disorders. Journal of Neuroscience Research 58, 120–129. https://doi.org/10.1002/(SICI)1097-4547(19991001)58:1<120::AID-JNR12>3.0.CO;2-E
Cole, N.B., DiEuliis, D., Leo, P., Mitchell, D.C., Nussbaum, R.L., 2008. Mitochondrial translocation of α-synuclein is promoted by intracellular acidification. Experimental Cell Research 314, 2076–2089. https://doi.org/10.1016/j.yexcr.2008.03.012
Colom-Cadena, M., Pegueroles, J., Herrmann, A.G., Henstridge, C.M., Muñoz, L., Querol-Vilaseca, M., Martín-Paniello, C.S., Luque-Cabecerans, J., Clarimon, J., Belbin, O., Núñez-Llaves, R., Blesa, R., Smith, C., McKenzie, C.-A., Frosch, M.P., Roe, A., Fortea, J., Andilla, J., Loza-Alvarez, P., Gelpi, E., Hyman, B.T., Spires-Jones, T.L., Lleó, A., 2017. Synaptic phosphorylated α-synuclein in dementia with Lewy bodies. Brain 140, 3204–3214. https://doi.org/10.1093/brain/awx275
Connolly, B.S., Lang, A.E., 2014. Pharmacological Treatment of Parkinson Disease: A Review. JAMA 311, 1670. https://doi.org/10.1001/jama.2014.3654
Conway, K.A., Harper, J.D., Lansbury, P.T., 2000a. Fibrils Formed in Vitro from α-Synuclein and Two Mutant Forms Linked to Parkinson's Disease are Typical Amyloid †. Biochemistry 39, 2552–2563. https://doi.org/10.1021/bi991447r
Conway, K.A., Harper, J.D., Lansbury, P.T., 1998. Accelerated in vitro fibril formation by a mutant α-synuclein linked to early-onset Parkinson disease. Nat Med 4, 1318–1320. https://doi.org/10.1038/3311
Conway, K.A., Lee, S.-J., Rochet, J.-C., Ding, T.T., Harper, J.D., Williamson, R.E., Lansbury, P.T., 2006. Accelerated Oligomerization by Parkinson's Disease Linked α-Synuclein Mutants. Annals of the New York Academy of Sciences 920, 42–45. https://doi.org/10.1111/j.1749-6632.2000.tb06903.x
Conway, K.A., Lee, S.-J., Rochet, J.-C., Ding, T.T., Williamson, R.E., Lansbury, P.T., 2000b. Acceleration of oligomerization, not fibrillization, is a shared property of both alpha -synuclein mutations linked to early-onset Parkinson's disease: Implications for pathogenesis and therapy. Proceedings of the National Academy of Sciences 97, 571–576. https://doi.org/10.1073/pnas.97.2.571
Cook, D.G., Fahn, S., Brait, K.A., 1974. Chronic Manganese Intoxication. Archives of Neurology 30, 59–64. https://doi.org/10.1001/archneur.1974.00490310061010
Corbille, A., Letournel, F., Kordower, J.H., Lee, J., Shanes, E., Neunlist, M., Munoz, D.G., Derkinderen, P., Beach, T.G., 2016a. Evaluation of alpha-synuclein immunohistochemical methods for the detection of Lewy-type synucleinopathy in gastrointestinal biopsies. acta neuropathol commun 4, 35. https://doi.org/10.1186/s40478-016-0305-8
Corbille, A., Neunlist, M., Derkinderen, P., 2016b. Cross-linking for the analysis of α-synuclein in the enteric nervous system. J. Neurochem. 139, 839–847. https://doi.org/10.1111/jnc.13845
Corbille, A., Preterre, C., Rolli-Derkinderen, M., Coron, E., Neunlist, M., Lebouvier, T., Derkinderen, P., 2017. Biochemical analysis of α-synuclein extracted from control and Parkinson's disease colonic biopsies. Neuroscience Letters 641, 81–86. https://doi.org/10.1016/j.neulet.2017.01.050
Cornejo-Olivas, M.R., Torres, L., Mata, I.F., Mazzetti, P., Rivas, D., Cosentino, C., Inca-Martinez, M., Cuba, J.M., Zabetian, C.P., Leverenz, J.B., 2015. A Peruvian family with a novel PARK2 mutation: Clinical and pathological characteristics. Parkinsonism & Related Disorders 21, 444–448. https://doi.org/10.1016/j.parkreldis.2015.01.005
Cotzias, G.C., Papavasiliou, P.S., Gellene, R., 1969. Modification of Parkinsonism — Chronic Treatment with L-Dopa. N Engl J Med 280, 337–345. https://doi.org/10.1056/NEJM196902132800701
Coughlin, D.G., Petrovitch, H., White, L.R., Noorigian, J., Masaki, K.H., Ross, G.W., Duda, J.E., 2019. Most cases with Lewy pathology in a population-based cohort adhere to the Braak progression pattern but 'failure to fit' is highly dependent on staging system applied. Parkinsonism & Related Disorders 64, 124–131. https://doi.org/10.1016/j.parkreldis.2019.03.023

Covell, D.J., Robinson, J.L., Akhtar, R.S., Grossman, M., Weintraub, D., Bucklin, H.M., Pitkin, R.M., Riddle, D., Yousef, A., Trojanowski, J.Q., Lee, V.M.-Y., 2017. Novel conformation-selective alpha-synuclein antibodies raised against different *in vitro* fibril forms show distinct patterns of Lewy pathology in Parkinson's disease. Neuropathol Appl Neurobiol 43, 604–620. https://doi.org/10.1111/nan.12402

Covy, J.P., Van Deerlin, V.M., Giasson, B.I., 2006. Lack of evidence for Lrrk2 in α-synuclein pathological inclusions. Ann Neurol. 60, 618–619. https://doi.org/10.1002/ana.21029

Covy, J.P., Yuan, W., Waxman, E.A., Hurtig, H.I., Van Deerlin, V.M., Giasson, B.I., 2009. Clinical and pathological characteristics of patients with Leucine-rich repeat kinase-2 mutations: Pathological Features of LRRK2 Mutations. Mov. Disord. 24, 32–39. https://doi.org/10.1002/mds.22096

Cremades, N., Cohen, S.I.A., Deas, E., Abramov, A.Y., Chen, A.Y., Orte, A., Sandal, M., Clarke, R.W., Dunne, P., Aprile, F.A., Bertoncini, C.W., Wood, N.W., Knowles, T.P.J., Dobson, C.M., Klenerman, D., 2012. Direct Observation of the Interconversion of Normal and Toxic Forms of α-Synuclein. Cell 149, 1048–1059. https://doi.org/10.1016/j.cell.2012.03.037

Croisier, E., Elfant, D., Deprez, M., Goldring, K., Dexter, D.T., Pearce, R.K.B., Graeber, M.B., Roncaroli, F., 2006. Comparative study of commercially available anti-alpha-synuclein antibodies. Neuropathol Appl Neurobiol 32, 351–356. https://doi.org/10.1111/j.1365-2990.2006.00722.x

Crowther, R.A., Jakes, R., Spillantini, M.G., Goedert, M., 1998. Synthetic filaments assembled from C-terminally truncated α-synuclein. FEBS Letters 436, 309–312. https://doi.org/10.1016/S0014-5793(98)01146-6

Culvenor, J.G., McLean, C.A., Cutt, S., Campbell, B.C.V., Maher, F., Jäkälä, P., Hartmann, T., Beyreuther, K., Masters, C.L., Li, Q.-X., 1999. Non-Aβ Component of Alzheimer's Disease Amyloid (NAC) Revisited. The American Journal of Pathology 155, 1173–1181. https://doi.org/10.1016/S0002-9440(10)65220-0

Dale, G.E., Probst, A., Luthert, P., Martin, J., Anderton, B.H., Leigh, P.N., 1992. Relationships between Lewy bodies and pale bodies in Parkinson's disease. Acta Neuropathol 83, 525–529. https://doi.org/10.1007/BF00310030

Dalfo, E., Martinez, A., Muntané, G., Ferrer, I., 2006. Abnormal α-synuclein solubility, aggregation and nitration in the frontal cortex in Pick's disease. Neuroscience Letters 400, 125–129. https://doi.org/10.1016/j.neulet.2006.02.033

Dalfo, E., Portero-Otin, M., Ayala, V., Martinez, A., Pamplona, R., Ferrer, I., 2005. Evidence of Oxidative Stress in the Neocortex in Incidental Lewy Body Disease. J Neuropathol Exp Neurol 64, 816–830. https://doi.org/10.1097/01.jnen.0000179050.54522.5a

Damier, P., Hirsch, E.C., Agid, Y., Graybiel, A.M., 1999. The substantia nigra of the human brain. Brain 122, 1437–1448. https://doi.org/10.1093/brain/122.8.1437

Danzer, K.M., Haasen, D., Karow, A.R., Moussaud, S., Habeck, M., Giese, A., Kretzschmar, H., Hengerer, B., Kostka, M., 2007. Different Species of -Synuclein Oligomers Induce Calcium Influx and Seeding. Journal of Neuroscience 27, 9220–9232. https://doi.org/10.1523/JNEUROSCI.2617-07.2007

Davidson, W.S., Jonas, A., Clayton, D.F., George, J.M., 1998. Stabilization of Alpha-Synuclein Secondary Structure upon Binding to Synthetic Membranes. Journal of Biological Chemistry 8.

de Oliveira, R.M., Vicente Miranda, H., Francelle, L., Pinho, R., Szegö, É.M., Martinho, R., Munari, F., Lázaro, D.F., Moniot, S., Guerreiro, P., Fonseca, L., Marijanovic, Z., Antas, P., Gerhardt, E., Enguita, F.J., Fauvet, B., Penque, D., Pais, T.F., Tong, Q., Becker, S., Kügler, S., Lashuel, H.A., Steegborn, C., Zweckstetter, M., Outeiro, T.F., 2017. The mechanism of sirtuin 2–mediated exacerbation of alpha-synuclein toxicity in models of Parkinson disease. PLoS Biol 15, e2000374. https://doi.org/10.1371/journal.pbio.2000374

Dehay, B., Bezard, E., 2019. Intrastriatal injection of alpha-synuclein fibrils induces Parkinson-like pathology in macaques. Brain 142, 3321–3322. https://doi.org/10.1093/brain/awz329

Del Tredici, K., Braak, H., 2012. Lewy pathology and neurodegeneration in premotor Parkinson's disease. Mov. Disord. 27, 597–607. https://doi.org/10.1002/mds.24921

Del Tredici, K., Duda, J.E., 2011. Peripheral Lewy body pathology in Parkinson's disease and incidental Lewy body disease: Four cases. Journal of the Neurological Sciences 310, 100–106. https://doi.org/10.1016/j.jns.2011.06.003

Del Tredici, K., Hawkes, C.H., Ghebremedhin, E., Braak, H., 2010. Lewy pathology in the submandibular gland of individuals with incidental Lewy body disease and sporadic Parkinson's disease. Acta Neuropathol 119, 703–713. https://doi.org/10.1007/s00401-010-0665-2

Del Tredici, K., Rüb, U., de Vos, R.A.I., Bohl, J.R.E., Braak, H., 2002. Where Does Parkinson Disease Pathology Begin in the Brain? J Neuropathol Exp Neurol 61, 413–426. https://doi.org/10.1093/jnen/61.5.413

Delamarre, A., Meissner, W.G., 2017. Epidemiology, environmental risk factors and genetics of Parkinson's disease. La Presse Médicale 46, 175–181. https://doi.org/10.1016/j.lpm.2017.01.001

Delic, V., Chandra, S., Abdelmotilib, H., Maltbie, T., Wang, S., Kem, D., Scott, H.J., Underwood, R.N., Liu, Z., Volpicelli-Daley, L.A., West, A.B., 2018. Sensitivity and specificity of phospho-Ser129 α-synuclein monoclonal antibodies. Journal of Comparative Neurology 526, 1978–1990. https://doi.org/10.1002/cne.24468

Deramecourt, V., Bombois, S., Maurage, C.-A., Ghestem, A., Drobecq, H., Vanmechelen, E., Lebert, F., Pasquier, F., Delacourte, A., 2006. Biochemical Staging of Synucleinopathy and Amyloid Deposition in Dementia With Lewy Bodies. J Neuropathol Exp Neurol 65, 278–288. https://doi.org/10.1097/01.jnen.0000205145.54457.ea

Desmet, A.-S., Cirillo, C., Tack, J., Vandenberghe, W., Vanden Berghe, P., 2017. Live calcium and mitochondrial imaging in the enteric nervous system of Parkinson patients and controls. eLife 6, e26850. https://doi.org/10.7554/eLife.26850

Desplats, P., Lee, H.-J., Bae, E.-J., Patrick, C., Rockenstein, E., Crews, L., Spencer, B., Masliah, E., Lee, S.-J., 2009. Inclusion formation and neuronal cell death through neuron-to-neuron transmission of -synuclein. Proceedings of the National Academy of Sciences 106, 13010–13015. https://doi.org/10.1073/pnas.0903691106

Devi, L., Raghavendran, V., Prabhu, B.M., Avadhani, N.G., Anandatheerthavarada, H.K., 2008. Mitochondrial Import and Accumulation of α-Synuclein Impair Complex I in Human Dopaminergic Neuronal Cultures and Parkinson Disease Brain. J. Biol. Chem. 283, 9089–9100. https://doi.org/10.1074/jbc.M710012200

Devos, D., Lebouvier, T., Lardeux, B., Biraud, M., Rouaud, T., Pouclet, H., Coron, E., Bruley des Varannes, S., Naveilhan, P., Nguyen, J.-M., Neunlist, M., Derkinderen, P., 2013. Colonic inflammation in Parkinson's disease. Neurobiology of Disease 50, 42–48. https://doi.org/10.1016/j.nbd.2012.09.007

Dhillon, J.S., Riffe, C., Moore, B.D., Ran, Y., Chakrabarty, P., Golde, T.E., Giasson, B.I., 2017. A novel panel of α-synuclein antibodies reveal distinctive staining profiles in synucleinopathies. PLoS ONE 12, e0184731. https://doi.org/10.1371/journal.pone.0184731

Di Fonzo, A., Chien, H.F., Socal, M., Giraudo, S., Tassorelli, C., Iliceto, G., Fabbrini, G., Marconi, R., Fincati, E., Abbruzzese, G., Marini, P., Squitieri, F., Horstink, M.W., Montagna, P., Libera, A.D., Stocchi, F., Goldwurm, S., Ferreira, J.J., Meco, G., Martignoni, E., Lopiano, L., Jardim, L.B., Oostra, B.A., Barbosa, E.R., The Italian Parkinson Genetics Network, Bonifati, V., 2007. ATP13A2 missense mutations in juvenile parkinsonism and young onset Parkinson disease. Neurology 68, 1557–1562. https://doi.org/10.1212/01.wnl.0000260963.08711.08

Dickson, D.W., Crystal, H., Mattiace, L.A., Kress, Y., Schwagerl, A., Ksiezak-Reding, H., Davies, P., Yen, S.-H., 1989. Diffuse Lewy body disease: light and electron microscopic immunocytochemistry of senile plaques. Acta Neuropathol 78, 572–584. https://doi.org/10.1007/BF00691284

Dickson, D.W., Lin, W., Liu, W.-K., Yen, S.-H., 1999a. Multiple System Atrophy: A Sporadic Synucleinopathy. Brain Pathology 9, 721–732. https://doi.org/10.1111/j.1750-3639.1999.tb00553.x

Dickson, D.W., Liu, W.-K., Hardy, J., Farrer, M., Mehta, N., Uitti, R., Mark, M., Zimmerman, T., Golbe, L., Sage, J., Sima, A., D'Amato, C., Albin, R., Gilman, S., Yen, S.-H., 1999b. Widespread Alterations of α-Synuclein in Multiple System Atrophy. The American Journal of Pathology 155, 1241–1251. https://doi.org/10.1016/S0002-9440(10)65226-1

Dickson, D.W., Schmidt, M.L., Lee, V.M.-Y., Zhao, M.-L., Yen, S.-H., Trojanowski, J.Q., 1994. Immunoreactivity profile of hippocampal CA2/3 neurites in diffuse Lewy body disease. Acta Neuropathol 87, 269–276. https://doi.org/10.1007/BF00296742

Dikiy, I., Eliezer, D., 2014. N-terminal Acetylation Stabilizes N-terminal Helicity in Lipid- and Micelle-bound α-Synuclein and Increases Its Affinity for Physiological Membranes. Journal of Biological Chemistry 289, 3652–3665. https://doi.org/10.1074/jbc.M113.512459

Ding, T.T., Lee, S.-J., Rochet, J.-C., Lansbury, P.T., 2002. Annular α-Synuclein Protofibrils Are Produced When Spherical Protofibrils Are Incubated in Solution or Bound to Brain-Derived Membranes. Biochemistry 41, 10209–10217. https://doi.org/10.1021/bi020139h

Djelloul, M., Holmqvist, S., Boza-Serrano, A., Azevedo, C., Yeung, M.S., Goldwurm, S., Frisén, J., Deierborg, T., Roybon, L., 2015. Alpha-Synuclein Expression in the Oligodendrocyte Lineage:

an In Vitro and In Vivo Study Using Rodent and Human Models. Stem Cell Reports 5, 174–184. https://doi.org/10.1016/j.stemcr.2015.07.002
Doder, M., Jahanshahi, M., Turjanski, N., Moseley, I.F., Lees, A.J., 1999. Parkinson's syndrome after closed head injury: a single case report. Journal of Neurology, Neurosurgery & Psychiatry 66, 380–385. https://doi.org/10.1136/jnnp.66.3.380
Dongmei, H., Jing, L., Mei, X., Ling, Z., Hongmin, Y., Zhidong, W., Li, D., Zikuan, G., Hengxiang, W., 2011. Clinical analysis of the treatment of spinocerebellar ataxia and multiple system atrophy-cerebellar type with umbilical cord mesenchymal stromal cells. Cytotherapy 13, 913–917. https://doi.org/10.3109/14653249.2011.579958
Dorsey, E.R., Elbaz, A., Nichols, E., Abd-Allah, F., Abdelalim, A., Adsuar, J.C., Ansha, M.G., Brayne, C., Choi, J.-Y.J., Collado-Mateo, D., Dahodwala, N., Do, H.P., Edessa, D., Endres, M., Fereshtehnejad, S.-M., Foreman, K.J., Gankpe, F.G., Gupta, R., Hankey, G.J., Hay, S.I., Hegazy, M.I., Hibstu, D.T., Kasaeian, A., Khader, Y., Khalil, I., Khang, Y.-H., Kim, Y.J., Kokubo, Y., Logroscino, G., Massano, J., Mohamed Ibrahim, N., Mohammed, M.A., Mohammadi, A., Moradi-Lakeh, M., Naghavi, M., Nguyen, B.T., Nirayo, Y.L., Ogbo, F.A., Owolabi, M.O., Pereira, D.M., Postma, M.J., Qorbani, M., Rahman, M.A., Roba, K.T., Safari, H., Safiri, S., Satpathy, M., Sawhney, M., Shafieesabet, A., Shiferaw, M.S., Smith, M., Szoeke, C.E.I., Tabarés-Seisdedos, R., Truong, N.T., Ukwaja, K.N., Venketasubramanian, N., Villafaina, S., weldegwergs, K. gidey, Westerman, R., Wijeratne, T., Winkler, A.S., Xuan, B.T., Yonemoto, N., Feigin, V.L., Vos, T., Murray, C.J.L., 2018. Global, regional, and national burden of Parkinson's disease, 1990–2016: a systematic analysis for the Global Burden of Disease Study 2016. The Lancet Neurology 17, 939–953. https://doi.org/10.1016/S1474-4422(18)30295-3
Drazic, A., Myklebust, L.M., Ree, R., Arnesen, T., 2016. The world of protein acetylation. Biochimica et Biophysica Acta (BBA) - Proteins and Proteomics 1864, 1372–1401. https://doi.org/10.1016/j.bbapap.2016.06.007
Duda, J.E., Giasson, B.I., Chen, Q., Gur, T.L., Hurtig, H.I., Stern, M.B., Gollomp, S.M., Ischiropoulos, H., Lee, V.M.-Y., Trojanowski, J.Q., 2000a. Widespread Nitration of Pathological Inclusions in Neurodegenerative Synucleinopathies. The American Journal of Pathology 157, 1439–1445. https://doi.org/10.1016/S0002-9440(10)64781-5
Duda, J.E., Giasson, B.I., Gur, T.L., Montine, T.J., Robertson, D., Biaggioni, I., Hurtig, H.I., Stern, M.B., Gollomp, S.M., Grossman, M., 2000b. Immunohistochemical and Biochemical Studies Demonstrate a Distinct Profile of ␣-Synuclein Permutations in Multiple System Atrophy. J Neuropathol Exp Neurol 59, 12.
Duda, J.E., Giasson, B.I., Mabon, M.E., Lee, V.M.-Y., Trojanowski, J.Q., 2002. Novel antibodies to synuclein show abundant striatal pathology in Lewy body diseases. Ann Neurol. 52, 205–210. https://doi.org/10.1002/ana.10279
Duda, J.E., Shah, U., Arnold, S.E., Lee, V.M.-Y., Trojanowski, J.Q., 1999. The Expression of α-, β-, and γ-Synucleins in Olfactory Mucosa from Patients with and without Neurodegenerative Diseases. Experimental Neurology 160, 515–522. https://doi.org/10.1006/exnr.1999.7228
Duffy, P.E., Tennyson, V.M., 1965. Phase and electron microscopic observations of Lewy bodies and melanin granules in the substantia nigra and locus coeruleus in Parkinson's disease. Journal of Neuropathology and Experimental Neurology 24, 398–414. https://doi.org/10.1097/00005072-196507000-00003
Dufty, B.M., Warner, L.R., Hou, S.T., Jiang, S.X., Gomez-Isla, T., Leenhouts, K.M., Oxford, J.T., Feany, M.B., Masliah, E., Rohn, T.T., 2007. Calpain-Cleavage of α-Synuclein. The American Journal of Pathology 170, 1725–1738. https://doi.org/10.2353/ajpath.2007.061232
El-Agnaf, O.M.A., Jakes, R., Curran, M.D., Wallace, A., 1998. Effects of the mutations Ala ^{30} to Pro and Ala ^{53} to Thr on the physical and morphological properties of α-synuclein protein implicated in Parkinson's disease. FEBS Letters 440, 67–70. https://doi.org/10.1016/S0014-5793(98)01419-7
Elfarrash, S., Jensen, N.M., Ferreira, N., Betzer, C., Thevathasan, J.V., Diekmann, R., Adel, M., Omar, N.M., Boraie, M.Z., Gad, S., Ries, J., Kirik, D., Nabavi, S., Jensen, P.H., 2019. Organotypic slice culture model demonstrates inter-neuronal spreading of alpha-synuclein aggregates. acta neuropathol commun 7, 213. https://doi.org/10.1186/s40478-019-0865-5
Eliezer, D., Kutluay, E., Bussell, R., Browne, G., 2001. Conformational properties of α-synuclein in its free and lipid-associated states 1 1Edited by P. E. Wright. Journal of Molecular Biology 307, 1061–1073. https://doi.org/10.1006/jmbi.2001.4538
Ellis, C.E., Murphy, E.J., Mitchell, D.C., Golovko, M.Y., Scaglia, F., Barcelo-Coblijn, G.C., Nussbaum, R.L., 2005. Mitochondrial Lipid Abnormality and Electron Transport Chain Impairment in Mice Lacking ␣-Synuclein. Mol Cell Biol 25, 12.

Engelhardt, E., 2017. Lafora and Trétiakoff: the naming of the inclusion bodies discovered by Lewy. Arq. Neuro-Psiquiatr. 75, 751–753. https://doi.org/10.1590/0004-282x20170116
Engelhardt, E., Gomes, M. da M., 2017. Lewy and his inclusion bodies: Discovery and rejection. Dement. neuropsychol. 11, 198–201. https://doi.org/10.1590/1980-57642016dn11-020012
Engen, P.A., Dodiya, H.B., Naqib, A., Forsyth, C.B., Green, S.J., Voigt, R.M., Kordower, J.H., Mutlu, E.A., Shannon, K.M., Keshavarzian, A., 2017. The Potential Role of Gut-Derived Inflammation in Multiple System Atrophy. J Parkinsons Dis 7, 331–346. https://doi.org/10.3233/JPD-160991
Eslamboli, A., Romero-Ramos, M., Burger, C., Bjorklund, T., Muzyczka, N., Mandel, R.J., Baker, H., Ridley, R.M., Kirik, D., 2007. Long-term consequences of human alpha-synuclein overexpression in the primate ventral midbrain. Brain 130, 799–815. https://doi.org/10.1093/brain/awl382
Fagerqvist, T., Lindström, V., Nordström, E., Lord, A., Tucker, S.M.E., Su, X., Sahlin, C., Kasrayan, A., Andersson, J., Welander, H., Näsström, T., Holmquist, M., Schell, H., Kahle, P.J., Kalimo, H., Möller, C., Gellerfors, P., Lannfelt, L., Bergström, J., Ingelsson, M., 2013. Monoclonal antibodies selective for α-synuclein oligomers/protofibrils recognize brain pathology in Lewy body disorders and α-synuclein transgenic mice with the disease-causing A30P mutation. J. Neurochem. 126, 131–144. https://doi.org/10.1111/jnc.12175
Fanciulli, A., Wenning, G.K., 2015. Multiple-System Atrophy. N Engl J Med 372, 249–263. https://doi.org/10.1056/NEJMra1311488
Farina, C., Aloisi, F., Meinl, E., 2007. Astrocytes are active players in cerebral innate immunity. Trends in Immunology 28, 138–145. https://doi.org/10.1016/j.it.2007.01.005
Fathy, Y.Y., Jonker, A.J., Oudejans, E., Jong, F.J.J., Dam, A. -M. W., Rozemuller, A.J.M., Berg, W.D.J., 2019. Differential insular cortex subregional vulnerability to α-synuclein pathology in Parkinson's disease and dementia with Lewy bodies. Neuropathol Appl Neurobiol 45, 262–277. https://doi.org/10.1111/nan.12501
Fauvet, B., Fares, M.-B., Samuel, F., Dikiy, I., Tandon, A., Eliezer, D., Lashuel, H.A., 2012a. Characterization of Semisynthetic and Naturally N^{α}-Acetylated α-Synuclein *in Vitro* and in Intact Cells: IMPLICATIONS FOR AGGREGATION AND CELLULAR PROPERTIES OF α-SYNUCLEIN. J. Biol. Chem. 287, 28243–28262. https://doi.org/10.1074/jbc.M112.383711
Fauvet, B., Mbefo, M.K., Fares, M.-B., Desobry, C., Michael, S., Ardah, M.T., Tsika, E., Coune, P., Prudent, M., Lion, N., Eliezer, D., Moore, D.J., Schneider, B., Aebischer, P., El-Agnaf, O.M., Masliah, E., Lashuel, H.A., 2012b. α-Synuclein in Central Nervous System and from Erythrocytes, Mammalian Cells, and *Escherichia coli* Exists Predominantly as Disordered Monomer. J. Biol. Chem. 287, 15345–15364. https://doi.org/10.1074/jbc.M111.318949
Fayyad, M., Erskine, D., Majbour, N.K., Vaikath, N.N., Ghanem, S.S., Sudhakaran, I.P., Abdesselem, H., Lamprokostopoulou, A., Vekrellis, K., Morris, C.M., Attems, J., El-Agnaf, O.M.A., 2020a. Investigating the presence of doubly phosphorylated α-synuclein at tyrosine 125 and serine 129 in idiopathic Lewy body diseases. Brain Pathol bpa.12845. https://doi.org/10.1111/bpa.12845
Fayyad, M., Majbour, N.K., Vaikath, N.N., Erskine, D., El-Tarawneh, H., Sudhakaran, I.P., Abdesselem, H., El-Agnaf, O.M.A., 2020b. Generation of monoclonal antibodies against phosphorylated α-Synuclein at serine 129: Research tools for synucleinopathies. Neuroscience Letters 725, 134899. https://doi.org/10.1016/j.neulet.2020.134899
Fearnley, J.M., Lees, A.J., 1991. Ageing and Parkinson's disease: substantia nigra regional selectivity. Brain 114, 2283–2301. https://doi.org/10.1093/brain/114.5.2283
Federoff, M., Price, T.R., Sailer, A., Scholz, S., Hernandez, D., Nicolas, A., Singleton, A.B., Nalls, M., Houlden, H., 2016. Genome-wide estimate of the heritability of Multiple System Atrophy. Parkinsonism & Related Disorders 22, 35–41. https://doi.org/10.1016/j.parkreldis.2015.11.005
Fellner, L., Irschick, R., Schanda, K., Reindl, M., Klimaschewski, L., Poewe, W., Wenning, G.K., Stefanova, N., 2013. Toll-like receptor 4 is required for α-synuclein dependent activation of microglia and astroglia. Glia 61, 349–360. https://doi.org/10.1002/glia.22437
Fenyi, A., Leclair-Visonneau, L., Clairembault, T., Coron, E., Neunlist, M., Melki, R., Derkinderen, P., Bousset, L., 2019. Detection of alpha-synuclein aggregates in gastrointestinal biopsies by protein misfolding cyclic amplification. Neurobiology of Disease 129, 38–43. https://doi.org/10.1016/j.nbd.2019.05.002
Fernandez-Arcos, A., Vilaseca, I., Aldecoa, I., Serradell, M., Tolosa, E., Santamaría, J., Gelpi, E., Iranzo, A., 2018. Alpha-synuclein aggregates in the parotid gland of idiopathic REM sleep behavior disorder. Sleep Medicine 52, 14–17. https://doi.org/10.1016/j.sleep.2018.08.003
Fevga, C., Park, Y., Lohmann, E., Kievit, A.J., Breedveld, G.J., Ferraro, F., de Boer, L., van Minkelen, R., Hanagasi, H., Boon, A., Wang, W., Petsko, G.A., Hoang, Q.Q., Emre, M., Bonifati, V., 2021. A new alpha-synuclein missense variant (Thr72Met) in two Turkish families with Parkinson's

disease. Parkinsonism & Related Disorders 89, 63–72. https://doi.org/10.1016/j.parkreldis.2021.06.023
Fink, A.L., 2006. The Aggregation and Fibrillation of α-Synuclein. Acc. Chem. Res. 39, 628–634. https://doi.org/10.1021/ar050073t
Folgoas, E., Lebouvier, T., Leclair-Visonneau, L., Cersosimo, M.-G., Barthelaix, A., Derkinderen, P., Letournel, F., 2013. Diagnostic value of minor salivary glands biopsy for the detection of Lewy pathology. Neuroscience Letters 551, 62–64. https://doi.org/10.1016/j.neulet.2013.07.016
Forno, L.S., 1969. Concentric hyalin intraneuronal inclusions of Lewy type in the brains of elderly persons (50 incidental cases): Relationship to Parkinsonism. Journal of the American Geriatrics Society 17, 557–575. https://doi.org/10.1111/j.1532-5415.1969.tb01316.x
Foroud, T., Uniacke, S.K., Liu, L., Pankratz, N., Rudolph, A., Halter, C., Shults, C., Marder, K., Conneally, P.M., Nichols, W.C., the Parkinson Study Group, 2003. Heterozygosity for a mutation in the parkin gene leads to later onset Parkinson disease. Neurology 60, 796–801. https://doi.org/10.1212/01.WNL.0000049470.00180.07
Forsyth, C.B., Shannon, K.M., Kordower, J.H., Voigt, R.M., Shaikh, M., Jaglin, J.A., Estes, J.D., Dodiya, H.B., Keshavarzian, A., 2011. Increased Intestinal Permeability Correlates with Sigmoid Mucosa alpha-Synuclein Staining and Endotoxin Exposure Markers in Early Parkinson's Disease. PLoS ONE 6, e28032. https://doi.org/10.1371/journal.pone.0028032
Fortin, D.L., Troyer, M.D., Nakamura, K., Kubo, S., Anthony, M.D., Edwards, R.H., 2004. Lipid Rafts Mediate the Synaptic Localization of -Synuclein. Journal of Neuroscience 24, 6715–6723. https://doi.org/10.1523/JNEUROSCI.1594-04.2004
Fredenburg, R.A., Rospigliosi, C., Meray, R.K., Kessler, J.C., Lashuel, H.A., Eliezer, D., Lansbury, P.T., 2007. The Impact of the E46K Mutation on the Properties of α-Synuclein in Its Monomeric and Oligomeric States †. Biochemistry 46, 7107–7118. https://doi.org/10.1021/bi7000246
Fujiwara, H., Hasegawa, M., Dohmae, N., Kawashima, A., Masliah, E., Goldberg, M.S., Shen, J., Takio, K., Iwatsubo, T., 2002. α-Synuclein is phosphorylated in synucleinopathy lesions. Nat Cell Biol 4, 160–164. https://doi.org/10.1038/ncb748
Funayama, M., Hasegawa, K., Kowa, H., Saito, M., Tsuji, S., Obata, F., 2002. A new locus for Parkinson's disease (PARK8) maps to chromosome 12p11.2-q13.1. Ann Neurol. 51, 296–301. https://doi.org/10.1002/ana.10113
Funayama, M., Hasegawa, K., Ohta, E., Kawashima, N., Komiyama, M., Kowa, H., Tsuji, S., Obata, F., 2005. An LRRK2 mutation as a cause for the parkinsonism in the original PARK8 family. Ann Neurol. 57, 918–921. https://doi.org/10.1002/ana.20484
Gai, W.P., Power, J.H.T., Blumbergs, P.C., Culvenor, J.G., Jensen, P.H., 1999. Alpha-synuclein Immunoisolation of Glial Inclusions from Multiple System Atrophy Brain Tissue Reveals Multiprotein Components. J. Neurochem. 73, 8. https://doi.org/10.1046/j.1471-4159.1999.02093.x
Gai, W.P., Yuan, H.X., Li, X.Q., Power, J.T.H., Blumbergs, P.C., Jensen, P.H., 2000. In Situ and in Vitro Study of Colocalization and Segregation of α-Synuclein, Ubiquitin, and Lipids in Lewy Bodies. Experimental Neurology 166, 324–333. https://doi.org/10.1006/exnr.2000.7527
Gaig, C., Ezquerra, M., Marti, M.J., Muñoz, E., Valldeoriola, F., Tolosa, E., 2006. LRRK2 Mutations in Spanish Patients With Parkinson Disease: Frequency, Clinical Features, and Incomplete Penetrance. Arch Neurol 63, 377. https://doi.org/10.1001/archneur.63.3.377
Gaig, C., Marti, M.J., Ezquerra, M., Rey, M.J., Cardozo, A., Tolosa, E., 2007. G2019S LRRK2 mutation causing Parkinson's disease without Lewy bodies. Journal of Neurology, Neurosurgery & Psychiatry 78, 626–628. https://doi.org/10.1136/jnnp.2006.107904
Galvagnion, C., Brown, J.W.P., Ouberai, M.M., Flagmeier, P., Vendruscolo, M., Buell, A.K., Sparr, E., Dobson, C.M., 2016. Chemical properties of lipids strongly affect the kinetics of the membrane-induced aggregation of α-synuclein. Proc Natl Acad Sci USA 113, 7065–7070. https://doi.org/10.1073/pnas.1601899113
Galvin, J.E., Giasson, B., Hurtig, H.I., Lee, V.M.-Y., Trojanowski, J.Q., 2000. Neurodegeneration with Brain Iron Accumulation, Type 1 Is Characterized by α-, β-, and γ-Synuclein Neuropathology. The American Journal of Pathology 157, 361–368. https://doi.org/10.1016/S0002-9440(10)64548-8
Gao, L., Chen, H., Li, X., Li, F., Ou-Yang, Q., Feng, T., 2015. The diagnostic value of minor salivary gland biopsy in clinically diagnosed patients with Parkinson's disease: comparison with DAT PET scans. Neurol Sci 36, 1575–1580. https://doi.org/10.1007/s10072-015-2190-5
Gao, X., Chen, H., Fung, T.T., Logroscino, G., Schwarzschild, M.A., Hu, F.B., Ascherio, A., 2007. Prospective study of dietary pattern and risk of Parkinson disease. The American Journal of Clinical Nutrition 86, 1486–1494. https://doi.org/10.1093/ajcn/86.5.1486

Gaspar, R., Meisl, G., Buell, A.K., Young, L., Kaminski, C.F., Knowles, T.P.J., Sparr, E., Linse, S., 2017. Secondary nucleation of monomers on fibril surface dominates *α* -synuclein aggregation and provides autocatalytic amyloid amplification. Quart. Rev. Biophys. 50, e6. https://doi.org/10.1017/S0033583516000172

Gasser, T., 2007. Update on the genetics of Parkinson's disease. Mov Disord. 22, S343–S350. https://doi.org/10.1002/mds.21676

Gelb, D.J., Oliver, E., Gilman, S., 1999. Diagnostic Criteria for Parkinson Disease. Arch Neurol 56, 33. https://doi.org/10.1001/archneur.56.1.33

Gelpi, E., Navarro-Otano, J., Tolosa, E., Gaig, C., Compta, Y., Rey, M.J., Martí, M.J., Hernández, I., Valldeoriola, F., Reñé, R., Ribalta, T., 2014. Multiple organ involvement by alpha-synuclein pathology in Lewy body disorders: Peripheral Alpha-Synuclein In Pd. Mov Disord. 29, 1010–1018. https://doi.org/10.1002/mds.25776

George, J.M., Jin, H., Woods, W.S., Clayton, D.F., 1995. Characterization of a Novel Protein Regulated during the Critical Period for Song Learning in the Zebra Finch. Neuron 12.

Geser, F., Wenning, G.K., Seppi, K., Stampfer-Kountchev, M., Scherfler, C., Sawires, M., Frick, C., Ndayisaba, J.-P., Ulmer, H., Pellecchia, M.T., Barone, P., Kim, H.T., Hooker, J., Quinn, N.P., Cardozo, A., Tolosa, E., Abele, M., Klockgether, T., Østergaard, K., Dupont, E., Schimke, N., Eggert, K.M., Oertel, W., Djaldetti, R., Poewe, W., the European MSA Study Group, 2006. Progression of multiple system atrophy (MSA): A prospective natural history study by the European MSA Study Group (EMSA SG). Mov Disord. 21, 179–186. https://doi.org/10.1002/mds.20678

Ghanem, S.S., Majbour, N.K., Vaikath, N.N., Ardah, M.T., Erskine, D., Jensen, N.M., Fayyad, M., Sudhakaran, I.P., Vasili, E., Melachroinou, K., Abdi, I.Y., Poggiolini, I., Santos, P., Dorn, A., Carloni, P., Vekrellis, K., Attems, J., McKeith, I., Outeiro, T.F., Jensen, P.H., El-Agnaf, O.M.A., 2022. α-Synuclein phosphorylation at serine 129 occurs after initial protein deposition and inhibits seeded fibril formation and toxicity. Proc. Natl. Acad. Sci. U.S.A. 119, e2109617119. https://doi.org/10.1073/pnas.2109617119

Ghosh, D., Mehra, S., Sahay, S., Singh, P.K., Maji, S.K., 2017. α-synuclein aggregation and its modulation. International Journal of Biological Macromolecules 100, 37–54. https://doi.org/10.1016/j.ijbiomac.2016.10.021

Giasson, B.I., Covy, J.P., Bonini, N.M., Hurtig, H.I., Farrer, M.J., Trojanowski, J.Q., Van Deerlin, V.M., 2006. Biochemical and pathological characterization of Lrrk2. Ann Neurol. 59, 315–322. https://doi.org/10.1002/ana.20791

Giasson, B.I., Duda, J.E., Murray, I.V.J., Chen, C., Souza, J.M., Hurtig, H.I., Ischiropoulos, H., Trojanowski, J.Q., Lee, V.M.-Y., 2000a. Oxidative Damage Linked to Neurodegeneration by Selective alpha -Synuclein Nitration in Synucleinopathy Lesions. Science 290, 985–989. https://doi.org/10.1126/science.290.5493.985

Giasson, B.I., Jakes, R., Goedert, M., Duda, J.E., Leight, S., Trojanowski, J.Q., Lee, V.M.Y., 2000b. A Panel of Epitope-Specific Antibodies Detects Protein Domains Distributed Throughout Human ␣ -Synuclein in Lewy Bodies of Parkinson's Disease. Journal of Neuroscience Research 6.

Giasson, B.I., Mabon, M.E., Duda, J.E., Montine, T.J., Robertson, D., Hurtig, H.I., Lee, V.M.-Y., Trojanowski, J.Q., 2003. Tau and 14-3-3 in glial cytoplasmic inclusions of multiple system atrophy. Acta Neuropathologica 106, 243–250. https://doi.org/10.1007/s00401-003-0726-x

Giasson, B.I., Murray, I.V.J., Trojanowski, J.Q., Lee, V.M.-Y., 2001. A Hydrophobic Stretch of 12 Amino Acid Residues in the Middle of α-Synuclein Is Essential for Filament Assembly. J. Biol. Chem. 276, 2380–2386. https://doi.org/10.1074/jbc.M008919200

Gibb, W.R., Lees, A.J., 1988. The relevance of the Lewy body to the pathogenesis of idiopathic Parkinson's disease. Journal of Neurology, Neurosurgery & Psychiatry 51, 745–752. https://doi.org/10.1136/jnnp.51.6.745

Gibb, W.R., Scott, T., Lees, A.J., 1991. Neuronal inclusions of Parkinson's disease. Mov Disord. 6, 2–11. https://doi.org/10.1002/mds.870060103

Gilman, S., Low, P.A., Quinn, N., Albanese, A., Ben-Shlomo, Y., Fowler, C.J., Kaufmann, H., Klockgether, T., Lang, A.E., Lantos, P.L., Litvan, I., Mathias, C.J., Oliver, E., Robertson, D., Schatz, I., Wenning, G.K., 1999. Consensus statement on the diagnosis of multiple system atrophy. Journal of the Neurological Sciences 5.

Gilman, S., Wenning, G.K., Low, P.A., Brooks, D.J., Mathias, C.J., Trojanowski, J.Q., Wood, N.W., Colosimo, C., Durr, A., Fowler, C.J., Kaufmann, H., Klockgether, T., Lees, A., Poewe, W., Quinn, N., Revesz, T., Robertson, D., Sandroni, P., Seppi, K., Vidailhet, M., 2008. Second consensus statement on the diagnosis of multiple system atrophy. Neurology 71, 670–676. https://doi.org/10.1212/01.wnl.0000324625.00404.15

Glozak, M.A., Sengupta, N., Zhang, X., Seto, E., 2005. Acetylation and deacetylation of non-histone proteins. Gene 363, 15–23. https://doi.org/10.1016/j.gene.2005.09.010
Golbe, L.I., Di Iorio, G., Bonavita, V., Miller, D.C., Duvoisin, R.C., 1990. A large kindred with autosomal dominant Parkinson's disease. Ann Neurol. 27, 276–282. https://doi.org/10.1002/ana.410270309
Gold, A., Turkalp, Z.T., Munoz, D.G., 2013. Enteric alpha-synuclein expression is increased in Parkinson's disease but not Alzheimer's disease: Enteric Synuclein in Neurodegenerative Disease. Mov Disord. 28, 237–241. https://doi.org/10.1002/mds.25298
Golovko, M.Y., Faergeman, N.J., Cole, N.B., Castagnet, P.I., Nussbaum, R.L., Murphy, E.J., 2005. α-Synuclein Gene Deletion Decreases Brain Palmitate Uptake and Alters the Palmitate Metabolism in the Absence of α-Synuclein Palmitate Binding †. Biochemistry 44, 8251–8259. https://doi.org/10.1021/bi0502137
Golovko, M.Y., Rosenberger, T.A., Feddersen, S., Cole, N.B., Pribill, I., Berger, J., Nussbaum, R.L., Murphy, E.J., 2006a. Acyl-CoA Synthetase Activity Links Wild-Type but Not Mutant α-Synuclein to Brain Arachidonate Metabolism †. Biochemistry 45, 6956–6966. https://doi.org/10.1021/bi0600289
Golovko, M.Y., Rosenberger, T.A., Feddersen, S., Faergeman, N.J., Murphy, E.J., 2006b. α-Synuclein gene ablation increases docosahexaenoic acid incorporation and turnover in brain phospholipids: α-Synuclein modulates brain 22:6n-3 metabolism. Journal of Neurochemistry 101, 201–211. https://doi.org/10.1111/j.1471-4159.2006.04357.x
Gomez-Tortosa, E., Gonzalo, I., Newell, K., Yébenes, J., Vonsattel, J., Hyman, B., 2002. Patterns of protein nitration in dementia with Lewy bodies and striatonigral degeneration. Acta Neuropathologica 103, 495–500. https://doi.org/10.1007/s00401-001-0495-3
Gomez-Tortosa, E., Newell, K., Irizarry, M.C., Sanders, J.L., Hyman, B.T., 2000. α-Synuclein immunoreactivity in dementia with Lewy bodies: morphological staging and comparison with ubiquitin immunostaining. Acta Neuropathologica 99, 352–357. https://doi.org/10.1007/s004010051135
Gonera, E.G., Hof, M.V., Berger, H.J.C., van Weel, C., Horstink, M.W.I.M., 1997. Symptoms and duration of the prodromal phase in parkinson's disease. Mov Disord. 12, 871–876. https://doi.org/10.1002/mds.870120607
Gonzalez-Rodriguez, P., Zampese, E., Surmeier, D.J., 2020. Selective neuronal vulnerability in Parkinson's disease, in: Progress in Brain Research. Elsevier, pp. 61–89. https://doi.org/10.1016/bs.pbr.2020.02.005
Gorell, J.M., Peterson, E.L., Rybicki, B.A., Johnson, C.C., 2004. Multiple risk factors for Parkinson's disease. Journal of the Neurological Sciences 217, 169–174. https://doi.org/10.1016/j.jns.2003.09.014
Gould, N., Mor, D.E., Lightfoot, R., Malkus, K., Giasson, B., Ischiropoulos, H., 2014. Evidence of Native α-Synuclein Conformers in the Human Brain. J. Biol. Chem. 289, 7929–7934. https://doi.org/10.1074/jbc.C113.538249
Graham, J.G., Oppenheimer, D.R., 1969. Orthostatic hypotension and nicotine sensitivity in a case of multiple system atrophy. Journal of Neurology, Neurosurgery & Psychiatry 32, 28–34. https://doi.org/10.1136/jnnp.32.1.28
Grathwohl, S., Quansah, E., Maroof, N., Steiner, J.A., Spycher, L., Benmansour, F., Duran-Pacheco, G., Siebourg-Polster, J., Oroszlan-Szovik, K., Remy, H., Haenggi, M., Stawiski, M., Sehlhausen, M., Maliver, P., Wolfert, A., Emrich, T., Madaj, Z., Escobar Galvis, M.L., Mueller, C., Herrmann, A., Brundin, P., Britschgi, M., 2019. Experimental colitis drives enteric alpha-synuclein accumulation and Parkinson-like brain pathology. bioRxiv 505164. https://doi.org/10.1101/505164
Gray, M.T., Munoz, D.G., Gray, D.A., Schlossmacher, M.G., Woulfe, J.M., 2014. Alpha-synuclein in the appendiceal mucosa of neurologically intact subjects: α-SYN in the Vermiform Appendix. Mov Disord. 29, 991–998. https://doi.org/10.1002/mds.25779
Greenfield, J.G., Bosanquet, F.D., 1953. The brain-stem lesions in parkinsonism. J Neurol Neurosurg Psychiatry 16, 213–226.
Greffard, S., Verny, M., Bonnet, A.-M., Beinis, J.-Y., Gallinari, C., Meaume, S., Piette, F., Hauw, J.-J., Duyckaerts, C., 2006. Motor Score of the Unified Parkinson Disease Rating Scale as a Good Predictor of Lewy Body–Associated Neuronal Loss in the Substantia Nigra. Arch Neurol 63, 584. https://doi.org/10.1001/archneur.63.4.584
Greggio, E., Jain, S., Kingsbury, A., Bandopadhyay, R., Lewis, P., Kaganovich, A., van der Brug, M.P., Beilina, A., Blackinton, J., Thomas, K.J., Ahmad, R., Miller, D.W., Kesavapany, S., Singleton, A., Lees, A., Harvey, R.J., Harvey, K., Cookson, M.R., 2006. Kinase activity is required for the

toxic effects of mutant LRRK2/dardarin. Neurobiology of Disease 23, 329–341. https://doi.org/10.1016/j.nbd.2006.04.001
Greten-Harrison, B., Polydoro, M., Morimoto-Tomita, M., Diao, L., Williams, A.M., Nie, E.H., Makani, S., Tian, N., Castillo, P.E., Buchman, V.L., Chandra, S.S., 2010. -Synuclein triple knockout mice reveal age-dependent neuronal dysfunction. Proceedings of the National Academy of Sciences 107, 19573–19578. https://doi.org/10.1073/pnas.1005005107
Guardia-Laguarta, C., Area-Gomez, E., Rub, C., Liu, Y., Magrane, J., Becker, D., Voos, W., Schon, E.A., Przedborski, S., 2014. -Synuclein Is Localized to Mitochondria-Associated ER Membranes. Journal of Neuroscience 34, 249–259. https://doi.org/10.1523/JNEUROSCI.2507-13.2014
Guerreiro, P.S., Huang, Y., Gysbers, A., Cheng, D., Gai, W.P., Outeiro, T.F., Halliday, G.M., 2013. LRRK2 interactions with α-synuclein in Parkinson's disease brains and in cell models. J Mol Med 91, 513–522. https://doi.org/10.1007/s00109-012-0984-y
Guerrero-Ferreira, R., Kovacik, L., Ni, D., Stahlberg, H., 2020. New insights on the structure of alpha-synuclein fibrils using cryo-electron microscopy. Current Opinion in Neurobiology 61, 89–95. https://doi.org/10.1016/j.conb.2020.01.014
Guerrero-Ferreira, R., Taylor, N.M., Arteni, A.-A., Kumari, P., Mona, D., Ringler, P., Britschgi, M., Lauer, M.E., Makky, A., Verasdonck, J., Riek, R., Melki, R., Meier, B.H., Böckmann, A., Bousset, L., Stahlberg, H., 2019. Two new polymorphic structures of human full-length alpha-synuclein fibrils solved by cryo-electron microscopy. Elife 8. https://doi.org/10.7554/eLife.48907
Guerrero-Ferreira, R., Taylor, N.M., Mona, D., Ringler, P., Lauer, M.E., Riek, R., Britschgi, M., Stahlberg, H., 2018. Cryo-EM structure of alpha-synuclein fibrils. eLife 7, e36402. https://doi.org/10.7554/eLife.36402
Haebig, K., Gellhaar, S., Heim, B., Djuric, V., Giesert, F., Wurst, W., Walter, C., Hentrich, T., Riess, O., Bonin, M., 2013. LRRK2 guides the actin cytoskeleton at growth cones together with ARHGEF7 and Tropomyosin 4. Biochimica et Biophysica Acta (BBA) - Molecular Basis of Disease 1832, 2352–2367. https://doi.org/10.1016/j.bbadis.2013.09.009
Haehner, A., Boesveldt, S., Berendse, H.W., Mackay-Sim, A., Fleischmann, J., Silburn, P.A., Johnston, A.N., Mellick, G.D., Herting, B., Reichmann, H., Hummel, T., 2009. Prevalence of smell loss in Parkinson's disease – A multicenter study. Parkinsonism & Related Disorders 15, 490–494. https://doi.org/10.1016/j.parkreldis.2008.12.005
Halliday, G.M., Holton, J.L., Revesz, T., Dickson, D.W., 2011. Neuropathology underlying clinical variability in patients with synucleinopathies. Acta Neuropathol 122, 187–204. https://doi.org/10.1007/s00401-011-0852-9
Halliday, G.M., McCann, H., 2010. The progression of pathology in Parkinson's disease: Pathological progression of Parkinson's disease. Annals of the New York Academy of Sciences 1184, 188–195. https://doi.org/10.1111/j.1749-6632.2009.05118.x
Halliday, G.M., Stevens, C.H., 2011. Glia: Initiators and progressors of pathology in Parkinson's disease: Glia in Parkinson's Disease. Mov. Disord. 26, 6–17. https://doi.org/10.1002/mds.23455
Halperin, A., Elstein, D., Zimran, A., 2006. Increased incidence of Parkinson disease among relatives of patients with Gaucher disease. Blood Cells, Molecules, and Diseases 36, 426–428. https://doi.org/10.1016/j.bcmd.2006.02.004
Han, H., Weinreb, P.H., Lansbury, P.T., 1995. The core Alzheimer's peptide NAC forms amyloid fibrils which seed and are seeded by β-amyloid: is NAC a common trigger or target in neurodegenerative disease? Chemistry & Biology 2, 163–169. https://doi.org/10.1016/1074-5521(95)90071-3
Hansen, C., Angot, E., Bergström, A.-L., Steiner, J.A., Pieri, L., Paul, G., Outeiro, T.F., Melki, R., Kallunki, P., Fog, K., Li, J.-Y., Brundin, P., 2011. α-Synuclein propagates from mouse brain to grafted dopaminergic neurons and seeds aggregation in cultured human cells. J. Clin. Invest. 121, 715–725. https://doi.org/10.1172/JCI43366
Hara, K., Momose, Y., Tokiguchi, S., Shimohata, M., Terajima, K., Onodera, O., Kakita, A., Yamada, M., Takahashi, H., Hirasawa, M., Mizuno, Y., Ogata, K., Goto, J., Kanazawa, I., Nishizawa, M., Tsuji, S., 2007. Multiplex Families With Multiple System Atrophy. Arch Neurol 64, 545. https://doi.org/10.1001/archneur.64.4.545
Hart, G.W., Housley, M.P., Slawson, C., 2007. Cycling of O-linked β-N-acetylglucosamine on nucleocytoplasmic proteins. Nature 446, 1017–1022. https://doi.org/10.1038/nature05815
Hart, G.W., Slawson, C., Ramirez-Correa, G., Lagerlof, O., 2011. Cross Talk Between O-GlcNAcylation and Phosphorylation: Roles in Signaling, Transcription, and Chronic Disease. Annu. Rev. Biochem. 80, 825–858. https://doi.org/10.1146/annurev-biochem-060608-102511

Hasegawa, M., Fujiwara, H., Nonaka, T., Wakabayashi, K., Takahashi, H., Lee, V.M.-Y., Trojanowski, J.Q., Mann, D., Iwatsubo, T., 2002. Phosphorylated α-Synuclein Is Ubiquitinated in α-Synucleinopathy Lesions. J. Biol. Chem. 277, 49071–49076. https://doi.org/10.1074/jbc.M208046200

Hatano, Y., Li, Y., Sato, K., Asakawa, S., Yamamura, Y., Tomiyama, H., Yoshino, H., Asahina, M., Kobayashi, S., Hassin-Baer, S., Lu, C.-S., Ng, A.R., Rosales, R.L., Shimizu, N., Toda, T., Mizuno, Y., Hattori, N., 2004. Novel PINK1 mutations in early-onset parkinsonism. Ann Neurol. 56, 424–427. https://doi.org/10.1002/ana.20251

Hawkes, C.H., Del Tredici, K., Braak, H., 2009. Parkinson's Disease: The Dual Hit Theory Revisited. Annals of the New York Academy of Sciences 1170, 615–622. https://doi.org/10.1111/j.1749-6632.2009.04365.x

Hawkes, C.H., Del Tredici, K., Braak, H., 2007. Parkinson's disease: a dual-hit hypothesis. Neuropathol Appl Neurobiol 33, 599–614. https://doi.org/10.1111/j.1365-2990.2007.00874.x

Hayashi, S., Wakabayashi, K., Ishikawa, A., Nagai, H., Saito, M., Maruyama, M., Takahashi, T., Ozawa, T., Tsuji, S., Takahashi, H., 2000. An autopsy case of autosomal-recessive juvenile parkinsonism with a homozygous exon 4 deletion in the parkin gene. Movement Disorders 15, 5.

Hayashida, K., Oyanagi, S., Mizutani, Y., Yokochi, M., 1993. An early cytoplasmic change before Lewy body maturation: an ultrastructural study of the substantia nigra from an autopsy case of juvenile parkinsonism. Acta Neuropathol 85, 445–448. https://doi.org/10.1007/BF00334457

Heintz-Buschart, A., Pandey, U., Wicke, T., Sixel-Döring, F., Janzen, A., Sittig-Wiegand, E., Trenkwalder, C., Oertel, W.H., Mollenhauer, B., Wilmes, P., 2018. The nasal and gut microbiome in Parkinson's disease and idiopathic rapid eye movement sleep behavior disorder: Nose and Gut Microbiome in PD and iRBD. Mov Disord. 33, 88–98. https://doi.org/10.1002/mds.27105

Hejjaoui, M., Butterfield, S., Fauvet, B., Vercruysse, F., Cui, J., Dikiy, I., Prudent, M., Olschewski, D., Zhang, Y., Eliezer, D., Lashuel, H.A., 2012. Elucidating the Role of C-Terminal Post-Translational Modifications Using Protein Semisynthesis Strategies: α-Synuclein Phosphorylation at Tyrosine 125. J. Am. Chem. Soc. 134, 5196–5210. https://doi.org/10.1021/ja210866j

Hejjaoui, M., Haj-Yahya, M., Kumar, K.S.A., Brik, A., Lashuel, H.A., 2011. Towards Elucidation of the Role of Ubiquitination in the Pathogenesis of Parkinson's Disease with Semisynthetic Ubiquitinated α-Synuclein. Angew. Chem. Int. Ed. 50, 405–409. https://doi.org/10.1002/anie.201005546

Helwig, M., Klinkenberg, M., Rusconi, R., Musgrove, R.E., Majbour, N.K., El-Agnaf, O.M.A., Ulusoy, A., Di Monte, D.A., 2016. Brain propagation of transduced α-synuclein involves non-fibrillar protein species and is enhanced in α-synuclein null mice. Brain 139, 856–870. https://doi.org/10.1093/brain/awv376

Henderson, M.X., Covell, D.J., Chung, C.H.-Y., Pitkin, R.M., Sandler, R.M., Decker, S.C., Riddle, D.M., Zhang, B., Gathagan, R.J., James, M.J., Trojanowski, J.Q., Brunden, K.R., Lee, V.M.Y., Luk, K.C., 2020. Characterization of novel conformation-selective α-synuclein antibodies as potential immunotherapeutic agents for Parkinson's disease. Neurobiology of Disease 136, 104712. https://doi.org/10.1016/j.nbd.2019.104712

Henderson, M.X., Sengupta, M., Trojanowski, J.Q., Lee, V.M.Y., 2019. Alzheimer's disease tau is a prominent pathology in LRRK2 Parkinson's disease. acta neuropathol commun 7, 183. https://doi.org/10.1186/s40478-019-0836-x

Hertzman, C., Wiens, M., Bowering, D., Snow, B., Calne, D., 1990. Parkinson's disease: A case-control study of occupational and environmental risk factors. Am. J. Ind. Med. 17, 349–355. https://doi.org/10.1002/ajim.4700170307

Hilton, D., Stephens, M., Kirk, L., Edwards, P., Potter, R., Zajicek, J., Broughton, E., Hagan, H., Carroll, C., 2014. Accumulation of α-synuclein in the bowel of patients in the pre-clinical phase of Parkinson's disease. Acta Neuropathol 127, 235–241. https://doi.org/10.1007/s00401-013-1214-6

Hishikawa, N., Hashizume, Y., Yoshida, M., Sobue, G., 2001. Widespread occurrence of argyrophilic glial inclusions in Parkinson's disease. Neuropathol Appl Neurobiol 27, 362–372. https://doi.org/10.1046/j.1365-2990.2001.00345.x

Holdorff, B., Rodrigues e Silva, A.M., Dodel, R., 2013. Centenary of Lewy bodies (1912–2012). J Neural Transm 120, 509–516. https://doi.org/10.1007/s00702-013-0984-2

Holmberg, B., Johansson, J.-O., Poewe, W., Wenning, G., Quinn, N.P., Mathias, C., Tolosa, E., Cardozo, A., Dizdar, N., Rascol, O., Slaoui, T., Growth-Hormone MSA Study Group, European

MSA Study Group (EMSA-SG), 2007. Safety and tolerability of growth hormone therapy in multiple system atrophy: A double-blind, placebo-controlled study. Mov Disord. 22, 1138–1144. https://doi.org/10.1002/mds.21501

Holmqvist, S., Chutna, O., Bousset, L., Aldrin-Kirk, P., Li, W., Björklund, T., Wang, Z.-Y., Roybon, L., Melki, R., Li, J.-Y., 2014. Direct evidence of Parkinson pathology spread from the gastrointestinal tract to the brain in rats. Acta Neuropathol 128, 805–820. https://doi.org/10.1007/s00401-014-1343-6

Hopfner, F., Künstner, A., Müller, S.H., Künzel, S., Zeuner, K.E., Margraf, N.G., Deuschl, G., Baines, J.F., Kuhlenbäumer, G., 2017. Gut microbiota in Parkinson disease in a northern German cohort. Brain Research 1667, 41–45. https://doi.org/10.1016/j.brainres.2017.04.019

Horsager, J., Andersen, K.B., Knudsen, K., Skjærbæk, C., Fedorova, T.D., Okkels, N., Schaeffer, E., Bonkat, S.K., Geday, J., Otto, M., Sommerauer, M., Danielsen, E.H., Bech, E., Kraft, J., Munk, O.L., Hansen, S.D., Pavese, N., Göder, R., Brooks, D.J., Berg, D., Borghammer, P., 2020. Brain-first versus body-first Parkinson's disease: a multimodal imaging case-control study. Brain 143, 3077–3088. https://doi.org/10.1093/brain/awaa238

Hsu, L.J., Mallory, M., Xia, Y., Veinbergs, I., Hashimoto, M., Yoshimoto, M., Thal, L.J., Saitoh, T., Masliah, E., 1998. Expression Pattern of Synucleins (Non-Aβ Component of Alzheimer's Disease Amyloid Precursor Protein/α-Synuclein) During Murine Brain Development. Journal of Neurochemistry 71, 338–344. https://doi.org/10.1046/j.1471-4159.1998.71010338.x

Hua, J., Yin, N., Xu, S., Chen, Q., Tao, T., Zhang, J., Ding, J., Fan, Y., Hu, G., 2019. Enhancing the Astrocytic Clearance of Extracellular α-Synuclein Aggregates by Ginkgolides Attenuates Neural Cell Injury. Cell Mol Neurobiol 39, 1017–1028. https://doi.org/10.1007/s10571-019-00696-2

Hughes, A.J., Ben-Shlomo, Y., Daniel, S.E., Lees, A.J., 1992a. What features improve the accuracy of clinical diagnosis in Parkinson's disease: A clinicopathologic study. Neurology 42, 1142–1142. https://doi.org/10.1212/WNL.42.6.1142

Hughes, A.J., Colosimo, C., Kleedorfer, B., Daniel, S.E., Lees, A.J., 1992b. The dopaminergic response in multiple system atrophy. Journal of Neurology, Neurosurgery & Psychiatry 55, 1009–1013. https://doi.org/10.1136/jnnp.55.11.1009

Hurtig, H.I., Trojanowski, J.Q., Galvin, J., Ewbank, D., Schmidt, M.L., Lee, V.M.-Y., Clark, C.M., Glosser, G., Stern, M.B., Gollomp, S.M., Arnold, S.E., 2000. Alpha-synuclein cortical Lewy bodies correlate with dementia in Parkinson's disease. Neurology 54, 1916–1921. https://doi.org/10.1212/WNL.54.10.1916

Iacono, D., Geraci-Erck, M., Rabin, M.L., Adler, C.H., Serrano, G., Beach, T.G., Kurlan, R., 2015. Parkinson disease and incidental Lewy body disease: Just a question of time? Neurology 85, 1670–1679. https://doi.org/10.1212/WNL.0000000000002102

Iranzo, A., Borrego, S., Vilaseca, I., Martí, C., Serradell, M., Sánchez-Valle, R., Kovacs, G.G., Valldeoriola, F., Gaig, C., Santamaria, J., Tolosa, E., Gelpi, E., 2018. Alpha-synuclein Aggregates in Labial Salivary Glands of Idiopathic Rapid Eye Movement Sleep Behavior Disorder. Sleep. https://doi.org/10.1093/sleep/zsy101

Iranzo, A., Gelpi, E., Tolosa, E., Molinuevo, J.L., Serradell, M., Gaig, C., Santamaria, J., 2014. Neuropathology of prodromal Lewy body disease: Prodromal Lewy Body Disease. Mov Disord. 29, 410–415. https://doi.org/10.1002/mds.25825

Iranzo, A., Molinuevo, J.L., Santamaría, J., Serradell, M., Martí, M.J., Valldeoriola, F., Tolosa, E., 2006. Rapid-eye-movement sleep behaviour disorder as an early marker for a neurodegenerative disorder: a descriptive study. The Lancet Neurology 5, 572–577. https://doi.org/10.1016/S1474-4422(06)70476-8

Iranzo, A., Santamaria, J., Tolosa, E., 2000. Continuous positive air pressure eliminates nocturnal stridor in multiple system atrophy. The Lancet 356, 1329–1330. https://doi.org/10.1016/S0140-6736(00)02824-5

Irizarry, M.C., Growdon, W., Gomez-isla, T., Newell, K., George, J.M., Clayton, D.F., Hyman, B.T., 1998. Nigral and Cortical Lewy Bodies and Dystrophic Nigral Neurites in Parkinson's Disease and Cortical Lewy Body Disease Contain α-synuclein Immunoreactivity: Journal of Neuropathology and Experimental Neurology 57, 334–337. https://doi.org/10.1097/00005072-199804000-00005

Ischiropoulos, H., Zhu, L., Chen, J., Tsai, M., Martin, J.C., Smith, C.D., Beckman, J.S., 1992. Peroxynitrite-mediated tyrosine nitration catalyzed by superoxide dismutase. Arch. Biochem. Biophys. 298, 431–437. https://doi.org/10.1016/0003-9861(92)90431-u

Ishizawa, K., Komori, T., Arai, N., Mizutani, T., Hirose, T., 2008. Glial cytoplasmic inclusions and tissue injury in multiple system atrophy: A quantitative study in white matter (olivopontocerebellar

system) and gray matter (nigrostriatal system). Neuropathology 28, 249–257. https://doi.org/10.1111/j.1440-1789.2007.00855.x
Issidorides, M.R., Panayotacopoulou, M.T., Tiniacos, G., 1990. Similarities Between Neuronal Lewy Bodies in Parkinsonism and Hepatic Mallory Bodies in Alcoholism. Pathology - Research and Practice 186, 473–478. https://doi.org/10.1016/S0344-0338(11)80466-8
Ito, S., Takao, M., Hatsuta, H., Kanemaru, K., Arai, T., Saito, Y., Murayama, S., 2014. Alpha-synuclein immunohistochemistry of gastrointestinal and biliary surgical specimens for diagnosis of Lewy body disease. Int J Clin Exp Pathol 10.
Iwai, A., Masliah, E., Yoshimoto, M., Ge, N., Flanagan, L., Rohan de Silva, H.A., Kittel, A., Saitoh, T., 1995. The precursor protein of non-Aβ component of Alzheimer's disease amyloid is a presynaptic protein of the central nervous system. Neuron 14, 467–475. https://doi.org/10.1016/0896-6273(95)90302-X
Jakes, R., Crowther, R.A., Lee, V.M.-Y., Trojanowski, J.Q., Iwatsubo, T., Goedert, M., 1999. Epitope mapping of LB509, a monoclonal antibody directed against human α-synuclein. Neuroscience Letters 269, 13–16. https://doi.org/10.1016/S0304-3940(99)00411-5
Jakes, R., Spillantini, M.G., Goedert, M., 1994. Identification of two distinct synucleins from human brain. FEBS Letters 345, 27–32. https://doi.org/10.1016/0014-5793(94)00395-5
Jellinger, K.A., 2009. Formation and development of Lewy pathology: a critical update. J Neurol 256, 270–279. https://doi.org/10.1007/s00415-009-5243-y
Jellinger, K.A., 2004. Lewy body-related alpha-synucleinopathy in the aged human brain. J Neural Transm 111, 1219–1235. https://doi.org/10.1007/s00702-004-0138-7
Jellinger, K.A., 2003. a-Synuclein pathology in Parkinson's and Alzheimer's disease brain: incidence and topographic distribution—a pilot study. Acta Neuropathol 12.
Jellinger, K.A., Lantos, P.L., 2010. Papp–Lantos inclusions and the pathogenesis of multiple system atrophy: an update. Acta Neuropathol 119, 657–667. https://doi.org/10.1007/s00401-010-0672-3
Jenner, P., Olanow, C.W., 1996. Oxidative stress and the pathogenesis of Parkinson's disease. Neurology 47, 161S-170S. https://doi.org/10.1212/WNL.47.6_Suppl_3.161S
Kalaitzakis, M.E., Graeber, M.B., Gentleman, S.M., Pearce, R.K.B., 2008. The dorsal motor nucleus of the vagus is not an obligatory trigger site of Parkinson's disease: a critical analysis of α-synuclein staging. Neuropathol Appl Neurobiol 34, 284–295. https://doi.org/10.1111/j.1365-2990.2007.00923.x
Kalia, L.V., Lang, A.E., Hazrati, L.-N., Fujioka, S., Wszolek, Z.K., Dickson, D.W., Ross, O.A., Van Deerlin, V.M., Trojanowski, J.Q., Hurtig, H.I., Alcalay, R.N., Marder, K.S., Clark, L.N., Gaig, C., Tolosa, E., Ruiz-Martínez, J., Marti-Masso, J.F., Ferrer, I., López de Munain, A., Goldman, S.M., Schüle, B., Langston, J.W., Aasly, J.O., Giordana, M.T., Bonifati, V., Puschmann, A., Canesi, M., Pezzoli, G., Maues De Paula, A., Hasegawa, K., Duyckaerts, C., Brice, A., Stoessl, A.J., Marras, C., 2015. Clinical Correlations With Lewy Body Pathology in *LRRK2* -Related Parkinson Disease. JAMA Neurol 72, 100. https://doi.org/10.1001/jamaneurol.2014.2704
Kann, M., Jacobs, H., Mohrmann, K., Schumacher, K., Hedrich, K., Garrels, J., Wiegers, K., Schwinger, E., Pramstaller, P.P., Breakefield, X.O., Ozelius, L.J., Vieregge, P., Klein, C., 2002. Role of parkin mutations in 111 community-based patients with early-onset parkinsonism. Ann Neurol. 51, 621–625. https://doi.org/10.1002/ana.10179
Kapasi, A., Brosch, J.R., Nudelman, K.N., Agrawal, S., Foroud, T.M., Schneider, J.A., 2020. A novel SNCA E83Q mutation in a case of dementia with Lewy bodies and atypical frontotemporal lobar degeneration. Neuropathology neup.12687. https://doi.org/10.1111/neup.12687
Kato, S., Nakamura, H., 1990. Cytoplasmic argyrophilic inclusions in neurons of pontine nuclei in patients with olivopontocerebellar atrophy: immunohistochemical and ultrastructural studies. Acta Neuropathol 79, 584–594. https://doi.org/10.1007/BF00294235
Kato, S., Nakamura, H., Hirano, A., Ito, H., Llena, J.F., Yen, S.-H., 1991. Argyrophilic ubiquitinated cytoplasmic inclusions of Leu-7-positive glial cells in olivopontocerebellar atrophy (multiple system atrophy). Acta Neuropathol 82, 488–493. https://doi.org/10.1007/BF00293383
Katsuse, O., Iseki, E., Marui, W., Kosaka, K., 2003. Developmental stages of cortical Lewy bodies and their relation to axonal transport blockage in brains of patients with dementia with Lewy bodies. Journal of the Neurological Sciences 211, 29–35. https://doi.org/10.1016/S0022-510X(03)00037-6
Kawamoto, Y., Akiguchi, I., Nakamura, S., Budka, H., 2002. Accumulation of 14-3-3 proteins in glial cytoplasmic inclusions in multiple system atrophy. Ann Neurol. 52, 722–731. https://doi.org/10.1002/ana.10361

Kawamoto, Y., Akiguchi, I., Shirakashi, Y., Honjo, Y., Tomimoto, H., Takahashi, R., Budka, H., 2007. Accumulation of Hsc70 and Hsp70 in glial cytoplasmic inclusions in patients with multiple system atrophy. Brain Research 1136, 219–227. https://doi.org/10.1016/j.brainres.2006.12.049

Kawamoto, Y., Ayaki, T., Urushitani, M., Ito, H., Takahashi, R., 2016. Activated caspase-9 immunoreactivity in glial and neuronal cytoplasmic inclusions in multiple system atrophy. Neuroscience Letters 628, 207–212. https://doi.org/10.1016/j.neulet.2016.06.036

Keck, S., Nitsch, R., Grune, T., Ullrich, O., 2003. Proteasome inhibition by paired helical filament-tau in brains of patients with Alzheimer's disease. Journal of Neurochemistry 85, 115–122. https://doi.org/10.1046/j.1471-4159.2003.01642.x

Keller, J.N., Hanni, K.B., Markesbery, W.R., 2000. Impaired Proteasome Function in Alzheimer's Disease. Journal of Neurochemistry 75, 436–439. https://doi.org/10.1046/j.1471-4159.2000.0750436.x

Kellie, J.F., Higgs, R.E., Ryder, J.W., Major, A., Beach, T.G., Adler, C.H., Merchant, K., Knierman, M.D., 2015. Quantitative Measurement of Intact Alpha-Synuclein Proteoforms from Post-Mortem Control and Parkinson's Disease Brain Tissue by Intact Protein Mass Spectrometry. Sci Rep 4, 5797. https://doi.org/10.1038/srep05797

Kiely, A.P., Asi, Y.T., Kara, E., Limousin, P., Ling, H., Lewis, P., Proukakis, C., Quinn, N., Lees, A.J., Hardy, J., Revesz, T., Houlden, H., Holton, J.L., 2013. α-Synucleinopathy associated with G51D SNCA mutation: a link between Parkinson's disease and multiple system atrophy? Acta Neuropathol 125, 753–769. https://doi.org/10.1007/s00401-013-1096-7

Kiely, A.P., Ling, H., Asi, Y.T., Kara, E., Proukakis, C., Schapira, A.H., Morris, H.R., Roberts, H.C., Lubbe, S., Limousin, P., Lewis, P.A., Lees, A.J., Quinn, N., Hardy, J., Love, S., Revesz, T., Houlden, H., Holton, J.L., 2015. Distinct clinical and neuropathological features of G51D SNCA mutation cases compared with SNCA duplication and H50Q mutation. Mol Neurodegeneration 10, 41. https://doi.org/10.1186/s13024-015-0038-3

Kiely, A.P., Miners, J.S., Courtney, R., Strand, C., Love, S., Holton, J.L., 2019. Exploring the putative role of kallikrein-6, calpain-1 and cathepsin-D in the proteolytic degradation of α-synuclein in multiple system atrophy. Neuropathol Appl Neurobiol 45, 347–360. https://doi.org/10.1111/nan.12512

Killinger, B.A., Madaj, Z., Sikora, J.W., Rey, N., Haas, A.J., Vepa, Y., Lindqvist, D., Chen, H., Thomas, P.M., Brundin, P., Brundin, L., Labrie, V., 2018. The vermiform appendix impacts the risk of developing Parkinson's disease. Science Translational Medicine 10, eaar5280. https://doi.org/10.1126/scitranslmed.aar5280

Kim, H.-J., Jeon, B.S., Jellinger, K.A., 2015. Diagnosis and differential diagnosis of MSA: boundary issues. J Neurol 262, 1801–1813. https://doi.org/10.1007/s00415-015-7654-2

Kim, H.-J., Jeon, B.S., Lee, J.-Y., Yun, J.Y., 2011. Survival of Korean patients with multiple system atrophy. Mov. Disord. 26, 909–912. https://doi.org/10.1002/mds.23580

Kim, J.-S., Park, I.-S., Park, H.-E., Kim, S.-Y., Yun, J.A., Jung, C.K., Sung, H.-Y., Lee, J.-K., Kang, W.-K., 2017. α-Synuclein in the colon and premotor markers of Parkinson disease in neurologically normal subjects. Neurol Sci 38, 171–179. https://doi.org/10.1007/s10072-016-2745-0

Kim, Y.M., Jang, W.H., Quezado, M.M., Oh, Y., Chung, K.C., Junn, E., Mouradian, M.M., 2011. Proteasome inhibition induces α-synuclein SUMOylation and aggregate formation. Journal of the Neurological Sciences 307, 157–161. https://doi.org/10.1016/j.jns.2011.04.015

Kingsbury, A.E., Bandopadhyay, R., Silveira-Moriyama, L., Ayling, H., Kallis, C., Sterlacci, W., Maeir, H., Poewe, W., Lees, A.J., 2010. Brain stem pathology in Parkinson's disease: An evaluation of the Braak staging model: Brain Stem Pathology in Parkinson's Disease. Mov. Disord. 25, 2508–2515. https://doi.org/10.1002/mds.23305

Kirik, D., Annett, L.E., Burger, C., Muzyczka, N., Mandel, R.J., Bjorklund, A., 2003. Nigrostriatal -synucleinopathy induced by viral vector-mediated overexpression of human -synuclein: A new primate model of Parkinson's disease. Proceedings of the National Academy of Sciences 100, 2884–2889. https://doi.org/10.1073/pnas.0536383100

Kirik, D., Rosenblad, C., Burger, C., Lundberg, C., Johansen, T.E., Muzyczka, N., Mandel, R.J., Björklund, A., 2002. Parkinson-Like Neurodegeneration Induced by Targeted Overexpression of α-Synuclein in the Nigrostriatal System. J. Neurosci. 22, 2780–2791. https://doi.org/10.1523/JNEUROSCI.22-07-02780.2002

Klegeris, A., Giasson, B.I., Zhang, H., Maguire, J., Pelech, S., McGeer, P.L., 2006. Alpha-synuclein and its disease-causing mutants induce ICAM-1 and IL-6 in human astrocytes and astrocytoma cells. FASEB j. 20, 2000–2008. https://doi.org/10.1096/fj.06-6183com

Klein, C., Westenberger, A., 2012. Genetics of Parkinson's Disease. Cold Spring Harbor Perspectives in Medicine 2, a008888–a008888. https://doi.org/10.1101/cshperspect.a008888

Kleinknecht, A., Popova, B., Lázaro, D.F., Pinho, R., Valerius, O., Outeiro, T.F., Braus, G.H., 2016. C-Terminal Tyrosine Residue Modifications Modulate the Protective Phosphorylation of Serine 129 of α-Synuclein in a Yeast Model of Parkinson's Disease. PLoS Genet 12, e1006098. https://doi.org/10.1371/journal.pgen.1006098

Klingelhoefer, L., Reichmann, H., 2015. Pathogenesis of Parkinson disease—the gut–brain axis and environmental factors. Nat Rev Neurol 11, 625–636. https://doi.org/10.1038/nrneurol.2015.197

Kobayashi, K., Miyazu, K., Katsukawa, K., Fukutani, Y., Mukai, M., Nakamura, I., Yamaguchi, N., Matsubara, R., Isaki, K., 1992. Cytoskeletal protein abnormalities in patients with olivopontocerebellar atrophy — an immunocytochemical and Gallyas silver impregnation study. Neuropathology and Applied Neurobiology 18, 237–249. https://doi.org/10.1111/j.1365-2990.1992.tb00786.x

Koga, S., Aoki, N., Uitti, R.J., van Gerpen, J.A., Cheshire, W.P., Josephs, K.A., Wszolek, Z.K., Langston, J.W., Dickson, D.W., 2015. When DLB, PD, and PSP masquerade as MSA: An autopsy study of 134 patients. Neurology 85, 404–412. https://doi.org/10.1212/WNL.0000000000001807

Kon, T., Tomiyama, M., Wakabayashi, K., 2020. Neuropathology of Lewy body disease: Clinicopathological crosstalk between typical and atypical cases. Neuropathology 40, 30–39. https://doi.org/10.1111/neup.12597

Kono, S., Shirakawa, K., Ouchi, Y., Sakamoto, M., Ida, H., Sugiura, T., Tomiyama, H., Suzuki, H., Takahashi, Y., Miyajima, H., Hattori, N., Mizuno, Y., 2007. Dopaminergic neuronal dysfunction associated with parkinsonism in both a Gaucher disease patient and a carrier. Journal of the Neurological Sciences 252, 181–184. https://doi.org/10.1016/j.jns.2006.10.019

Kordower, J.H., Chu, Y., Hauser, R.A., Freeman, T.B., Olanow, C.W., 2008. Lewy body–like pathology in long-term embryonic nigral transplants in Parkinson's disease. Nat Med 14, 504–506. https://doi.org/10.1038/nm1747

Kordower, J.H., Dodiya, H.B., Kordower, A.M., Terpstra, B., Paumier, K., Madhavan, L., Sortwell, C., Steece-Collier, K., Collier, T.J., 2011. Transfer of host-derived alpha synuclein to grafted dopaminergic neurons in rat. Neurobiology of Disease 43, 552–557. https://doi.org/10.1016/j.nbd.2011.05.001

Kosaka, K., 1978. Lewy bodies in cerebral cortex. Report of three cases. Acta Neuropathol 42, 127–134. https://doi.org/10.1007/BF00690978

Kovacs, G.G., Breydo, L., Green, R., Kis, V., Puska, G., Lőrincz, P., Perju-Dumbrava, L., Giera, R., Pirker, W., Lutz, M., Lachmann, I., Budka, H., Uversky, V.N., Molnár, K., László, L., 2014. Intracellular processing of disease-associated α-synuclein in the human brain suggests prion-like cell-to-cell spread. Neurobiology of Disease 69, 76–92. https://doi.org/10.1016/j.nbd.2014.05.020

Kovacs, G.G., Wagner, U., Dumont, B., Pikkarainen, M., Osman, A.A., Streichenberger, N., Leisser, I., Verchère, J., Baron, T., Alafuzoff, I., Budka, H., Perret-Liaudet, A., Lachmann, I., 2012. An antibody with high reactivity for disease-associated α-synuclein reveals extensive brain pathology. Acta Neuropathol 124, 37–50. https://doi.org/10.1007/s00401-012-0964-x

Kowal, S.L., Dall, T.M., Chakrabarti, R., Storm, M.V., Jain, A., 2013. The current and projected economic burden of Parkinson's disease in the United States: Economic Burden of PD in The US. Mov Disord. 28, 311–318. https://doi.org/10.1002/mds.25292

Kremer, H.P.H., Bots, G.Th.A.M., 1993. Lewy bodies in the lateral hypothalamus: Do they imply neuronal loss? Mov Disord. 8, 315–320. https://doi.org/10.1002/mds.870080310

Krueger, R., Kuhn, W., Müller, T., Woitalla, D., Graeber, M., Kösel, S., Przuntek, H., Epplen, J.T., Schols, L., Riess, O., 1998. Ala30Pro mutation in the gene encoding α-synuclein in Parkinson's disease. Nat Genet 18, 106–108. https://doi.org/10.1038/ng0298-106

Kumar, S.T., Donzelli, S., Chiki, A., Syed, M.M.K., Lashuel, H.A., 2020a. A simple, versatile and robust centrifugation-based filtration protocol for the isolation and quantification of α-synuclein monomers, oligomers and fibrils: Towards improving experimental reproducibility in α-synuclein research. J. Neurochem. 153, 103–119. https://doi.org/10.1111/jnc.14955

Kumar, S.T., Jagannath, S., Francois, C., Vanderstichele, H., Stoops, E., Lashuel, H.A., 2020b. How specific are the conformation-specific α-synuclein antibodies? Characterization and validation of 16 α-synuclein conformation-specific antibodies using well-characterized preparations of α-synuclein monomers, fibrils and oligomers with distinct structures and morphology. Neurobiology of Disease 146, 105086. https://doi.org/10.1016/j.nbd.2020.105086

Kumar, S.T., Mahul-Mellier, A.-L., Hegde, R.N., Moons, R., Magalhaes, P., Ibanez de Opakua, A., Riviere, G., Rostami, I., Donzelli, S., Zweckstetter, M., Sobott, F., Lashuel, H.A., 2021. A novel mutation (E83Q) unlocks the pathogenicity of human alpha-synuclein fibrils and recapitulates its pathological diversity. bioRxiv. https://doi.org/10.1101/2021.11.21.469421

Kuusisto, E., Parkkinen, L., Alafuzoff, I., 2003. Morphogenesis of Lewy Bodies: Dissimilar Incorporation of ␣-Synuclein, Ubiquitin, and p62. J Neuropathol Exp Neurol 62, 13. https://doi.org/10.1093/jnen/62.12.1241

Kuusisto, E., Salminen, A., Alafuzoff, I., 2001. Ubiquitin-binding protein p62 is present in neuronal and glial inclusions in human tauopathies and synucleinopathies: Neuroreport 12, 2085–2090. https://doi.org/10.1097/00001756-200107200-00009

Landeck, N., Hall, H., Ardah, M.T., Majbour, N.K., El-Agnaf, O.M.A., Halliday, G., Kirik, D., 2016. A novel multiplex assay for simultaneous quantification of total and S129 phosphorylated human alpha-synuclein. Mol Neurodegeneration 11, 61. https://doi.org/10.1186/s13024-016-0125-0

Landureau, M., Redeker, V., Bellande, T., Eyquem, S., Melki, R., 2021. The differential solvent exposure of N-terminal residues provides “fingerprints” of alpha-synuclein fibrillar polymorphs. Journal of Biological Chemistry 296, 100737. https://doi.org/10.1016/j.jbc.2021.100737

Langston, J.W., Ballard, P., Tetrud, J., Irwin, I., 1983. Chronic Parkinsonism in humans due to a product of meperidine-analog synthesis. Science 219, 979–980. https://doi.org/10.1126/science.6823561

Lantos, P.L., 1998. The definition of multiple system atrophy: A review of recent developments. Journal of Neuropathology & Experimental Neurology 57.

Larsen, J.P., Dupont, E., Tandberg, E., 2009. Clinical diagnosis of Parkinson’s disease. Proposal of diagnostic subgroups classified at different levels of confidence. Acta Neurologica Scandinavica 89, 242–251. https://doi.org/10.1111/j.1600-0404.1994.tb01674.x

Lashuel, H.A., Mahul-Mellier, A.-L., Novello, S., Hegde, R.N., Jasiqi, Y., Altay, M.F., Donzelli, S., DeGuire, S.M., Burai, R., Magalhães, P., Chiki, A., Ricci, J., Boussouf, M., Sadek, A., Stoops, E., Iseli, C., Guex, N., 2022. Neighbouring modifications interfere with the detection of phosphorylated alpha-synuclein at Serine 129: Revisiting the specificity of pS129 antibodies. bioRxiv. https://doi.org/10.1101/2022.03.30.486322

Lashuel, H.A., Petre, B.M., Wall, J., Simon, M., Nowak, R.J., Walz, T., Lansbury, P.T., 2002. α-Synuclein, Especially the Parkinson’s Disease-associated Mutants, Forms Pore-like Annular and Tubular Protofibrils. Journal of Molecular Biology 322, 1089–1102. https://doi.org/10.1016/S0022-2836(02)00735-0

Latt, M.D., Lewis, S., Zekry, O., Fung, V.S.C., 2019. Factors to Consider in the Selection of Dopamine Agonists for Older Persons with Parkinson’s Disease. Drugs Aging 36, 189–202. https://doi.org/10.1007/s40266-018-0629-0

Lautenschlaeger, J., Stephens, A.D., Fusco, G., Ströhl, F., Curry, N., Zacharopoulou, M., Michel, C.H., Laine, R., Nespovitaya, N., Fantham, M., Pinotsi, D., Zago, W., Fraser, P., Tandon, A., St George-Hyslop, P., Rees, E., Phillips, J.J., De Simone, A., Kaminski, C.F., Schierle, G.S.K., 2018. C-terminal calcium binding of α-synuclein modulates synaptic vesicle interaction. Nat Commun 9, 712. https://doi.org/10.1038/s41467-018-03111-4

Lauwers, E., Debyser, Z., Dorpe, J., Strooper, B., Nuttin, B., Baekelandt, V., 2006. Neuropathology and Neurodegeneration in Rodent Brain Induced by Lentiviral Vectormediated Overexpression of α-Synuclein. Brain Pathology 13, 364–372. https://doi.org/10.1111/j.1750-3639.2003.tb00035.x

Lebouvier, T., Chaumette, T., Damier, P., Coron, E., Touchefeu, Y., Vrignaud, S., Naveilhan, P., Galmiche, J.-P., Bruley des Varannes, S., Derkinderen, P., Neunlist, M., 2008. Pathological lesions in colonic biopsies during Parkinson’s disease. Gut 57, 1741–1743. https://doi.org/10.1136/gut.2008.162503

Lebouvier, T., Neunlist, M., Bruley des Varannes, S., Coron, E., Drouard, A., N’Guyen, J.-M., Chaumette, T., Tasselli, M., Paillusson, S., Flamand, M., Galmiche, J.-P., Damier, P., Derkinderen, P., 2010. Colonic Biopsies to Assess the Neuropathology of Parkinson’s Disease and Its Relationship with Symptoms. PLoS ONE 5, e12728. https://doi.org/10.1371/journal.pone.0012728

Leclair-Visonneau, L., Clairembault, T., Volteau, C., Chapelet, G., Le Dily, S., Vavasseur, F., Coron, E., Préterre, C., Neunlist, M., Péréon, Y., Derkinderen, P., 2019. Colonic neuropathology is not associated with autonomic dysfunction in Parkinson’s disease. Parkinsonism & Related Disorders 61, 224–227. https://doi.org/10.1016/j.parkreldis.2018.09.021

Lee, E.-J., Woo, M.-S., Moon, P.-G., Baek, M.-C., Choi, I.-Y., Kim, W.-K., Junn, E., Kim, H.-S., 2010. α-Synuclein Activates Microglia by Inducing the Expressions of Matrix Metalloproteinases and the Subsequent Activation of Protease-Activated Receptor-1. J.I. 185, 615–623. https://doi.org/10.4049/jimmunol.0903480

Lee, H.J., Jung, K.W., Chung, S.J., Hong, S.-M., Kim, J., Lee, J.H., Hwang, S.W., Ryu, H.-S., Kim, M.J., Lee, H.-S., Seo, M., Park, S.H., Yang, D.-H., Ye, B.D., Byeon, J.-S., Choe, J., Jung, H.-Y., Yang, S.-K., Myung, S.-J., 2018. Relation of Enteric α-Synuclein to Gastrointestinal Dysfunction in

Patients With Parkinson's Disease and in Neurologically Intact Subjects. J Neurogastroenterol Motil 24, 469–478. https://doi.org/10.5056/jnm17141
Lee, H.-J., Kim, C., Lee, S.-J., 2010a. Alpha-Synuclein Stimulation of Astrocytes: Potential Role for Neuroinflammation and Neuroprotection. Oxidative Medicine and Cellular Longevity 3, 283–287. https://doi.org/10.4161/oxim.3.4.12809
Lee, H.-J., Suk, J.-E., Patrick, C., Bae, E.-J., Cho, J.-H., Rho, S., Hwang, D., Masliah, E., Lee, S.-J., 2010b. Direct Transfer of α-Synuclein from Neuron to Astroglia Causes Inflammatory Responses in Synucleinopathies*. Journal of Biological Chemistry 285, 9262–9272. https://doi.org/10.1074/jbc.M109.081125
Lee, J.T., Wheeler, T.C., Li, L., Chin, L.-S., 2007. Ubiquitination of -synuclein by Siah-1 promotes -synuclein aggregation and apoptotic cell death. Human Molecular Genetics 17, 906–917. https://doi.org/10.1093/hmg/ddm363
Lee, P., Kim, J., Bang, O., Ahn, Y., Joo, I., Huh, K., 2008. Autologous Mesenchymal Stem Cell Therapy Delays the Progression of Neurological Deficits in Patients With Multiple System Atrophy. Clin Pharmacol Ther 83, 723–730. https://doi.org/10.1038/sj.clpt.6100386
Lee, P.H., Lee, J.E., Kim, H.-S., Song, S.K., Lee, H.S., Nam, H.S., Cheong, J.-W., Jeong, Y., Park, H.-J., Kim, D.J., Nam, C.M., Lee, J.D., Kim, H.O., Sohn, Y.H., 2012. A randomized trial of mesenchymal stem cells in multiple system atrophy. Ann Neurol. 72, 32–40. https://doi.org/10.1002/ana.23612
Lee, Y., Weihl, C.C., 2017. Regulation of SQSTM1/p62 via UBA domain ubiquitination and its role in disease. Autophagy 13, 1615–1616. https://doi.org/10.1080/15548627.2017.1339845
Lees, A.J., Selikhova, M., Andrade, L.A., Duyckaerts, C., 2008. The black stuff and Konstantin Nikolaevich Tretiakoff: Black Stuff and Konstantin Nikolaevich Tretiakoff. Mov. Disord. 23, 777–783. https://doi.org/10.1002/mds.21855
Lesage, S., Anheim, M., Letournel, F., Bousset, L., Honoré, A., Rozas, N., Pieri, L., Madiona, K., Dürr, A., Melki, R., Verny, C., Brice, A., for the French Parkinson's Disease Genetics Study Group, 2013. G51D α-synuclein mutation causes a novel Parkinsonian-pyramidal syndrome: SNCA G51D in Parkinsonism. Ann Neurol. 73, 459–471. https://doi.org/10.1002/ana.23894
Lesage, S., Dürr, A., Tazir, M., Lohmann, E., Leutenegger, A.-L., Janin, S., Pollak, P., Brice, A., 2006. *LRRK2* G2019S as a Cause of Parkinson's Disease in North African Arabs. N Engl J Med 354, 422–423. https://doi.org/10.1056/NEJMc055540
Leverenz, J.B., Hamilton, R., Tsuang, D.W., Schantz, A., Vavrek, D., Larson, E.B., Kukull, W.A., Lopez, O., Galasko, D., Masliah, E., Kaye, J., Woltjer, R., Clark, C., Trojanowski, J.Q., Montine, T.J., 2008. Empiric Refinement of the Pathologic Assessment of Lewy-Related Pathology in the Dementia Patient: Pathologic Assessment of Lewy-Related Pathology. Brain Pathology 18, 220–224. https://doi.org/10.1111/j.1750-3639.2007.00117.x
Leverenz, J.B., Umar, I., Wang, Q., Montine, T.J., McMillan, P.J., Tsuang, D.W., Jin, J., Pan, C., Shin, J., Zhu, D., Zhang, J., 2007. Proteomic Identification of Novel Proteins in Cortical Lewy Bodies. Brain Pathology 17, 139–145. https://doi.org/10.1111/j.1750-3639.2007.00048.x
Levine, P.M., Galesic, A., Balana, A.T., Mahul-Mellier, A.-L., Navarro, M.X., De Leon, C.A., Lashuel, H.A., Pratt, M.R., 2019. α-Synuclein O-GlcNAcylation alters aggregation and toxicity, revealing certain residues as potential inhibitors of Parkinson's disease. Proc Natl Acad Sci USA 116, 1511–1519. https://doi.org/10.1073/pnas.1808845116
Lewis, K.A., Su, Y., Jou, O., Ritchie, C., Foong, C., Hynan, L.S., White, C.L., Thomas, P.J., Hatanpaa, K.J., 2010. Abnormal Neurites Containing C-Terminally Truncated α-Synuclein Are Present in Alzheimer's Disease without Conventional Lewy Body Pathology. The American Journal of Pathology 177, 3037–3050. https://doi.org/10.2353/ajpath.2010.100552
Lewis, Y.E., Galesic, A., Levine, P.M., De Leon, C.A., Lamiri, N., Brennan, C.K., Pratt, M.R., 2017. O-GlcNAcylation of α-Synuclein at Serine 87 Reduces Aggregation without Affecting Membrane Binding. ACS Chem. Biol. 12, 1020–1027. https://doi.org/10.1021/acschembio.7b00113
Li, B., Ge, P., Murray, K.A., Sheth, P., Zhang, M., Nair, G., Sawaya, M.R., Shin, W.S., Boyer, D.R., Ye, S., Eisenberg, D.S., Zhou, Z.H., Jiang, L., 2018. Cryo-EM of full-length α-synuclein reveals fibril polymorphs with a common structural kernel. Nature Communications 9, 3609. https://doi.org/10.1038/s41467-018-05971-2
Li, J.-Y., Englund, E., Holton, J.L., Soulet, D., Hagell, P., Lees, A.J., Lashley, T., Quinn, N.P., Rehncrona, S., Björklund, A., Widner, H., Revesz, T., Lindvall, O., Brundin, P., 2008. Lewy bodies in grafted neurons in subjects with Parkinson's disease suggest host-to-graft disease propagation. Nat Med 14, 501–503. https://doi.org/10.1038/nm1746
Li, W., West, N., Colla, E., Pletnikova, O., Troncoso, J.C., Marsh, L., Dawson, T.M., Jakala, P., Hartmann, T., Price, D.L., Lee, M.K., 2005. Aggregation promoting C-terminal truncation of -

synuclein is a normal cellular process and is enhanced by the familial Parkinson's disease-linked mutations. Proceedings of the National Academy of Sciences 102, 2162–2167. https://doi.org/10.1073/pnas.0406976102

Li, W., Wu, X., Hu, X., Wang, T., Liang, S., Duan, Y., Jin, F., Qin, B., 2017. Structural changes of gut microbiota in Parkinson's disease and its correlation with clinical features. Sci. China Life Sci. 60, 1223–1233. https://doi.org/10.1007/s11427-016-9001-4

Li, W.-W., Yang, R., Guo, J.-C., Ren, H.-M., Zha, X.-L., Cheng, J.-S., Cai, D.-F., 2007. Localization of α-synuclein to mitochondria within midbrain of mice. NeuroReport 18, 1543–1546. https://doi.org/10.1097/WNR.0b013e3282f03db4

Li, Y., Zhao, C., Luo, F., Liu, Z., Gui, X., Luo, Z., Zhang, X., Li, D., Liu, C., Li, X., 2018. Amyloid fibril structure of α-synuclein determined by cryo-electron microscopy. Cell Research 28, 897–903. https://doi.org/10.1038/s41422-018-0075-x

Liani, E., Eyal, A., Avraham, E., Shemer, R., Szargel, R., Berg, D., Bornemann, A., Riess, O., Ross, C.A., Rott, R., Engelender, S., 2004. Ubiquitylation of synphilin-1 and -synuclein by SIAH and its presence in cellular inclusions and Lewy bodies imply a role in Parkinson's disease. Proceedings of the National Academy of Sciences 101, 5500–5505. https://doi.org/10.1073/pnas.0401081101

Lin, A., Zheng, W., He, Y., Tang, W., Wei, X., He, R., Huang, W., Su, Y., Huang, Y., Zhou, H., Xie, H., 2018. Gut microbiota in patients with Parkinson's disease in southern China. Parkinsonism & Related Disorders 53, 82–88. https://doi.org/10.1016/j.parkreldis.2018.05.007

Lindstrom, V., Gustafsson, G., Sanders, L.H., Howlett, E.H., Sigvardson, J., Kasrayan, A., Ingelsson, M., Bergström, J., Erlandsson, A., 2017. Extensive uptake of α-synuclein oligomers in astrocytes results in sustained intracellular deposits and mitochondrial damage. Molecular and Cellular Neuroscience 82, 143–156. https://doi.org/10.1016/j.mcn.2017.04.009

Liou, H.H., Tsai, M.C., Chen, C.J., Jeng, J.S., Chang, Y.C., Chen, S.Y., Chen, R.C., 1997. Environmental risk factors and Parkinson's disease: A case-control study in Taiwan. Neurology 48, 1583–1588. https://doi.org/10.1212/WNL.48.6.1583

Lipkin, L.E., 1959. Cytoplasmic inclusions in ganglion cells associated with parkinsonian states: a neurocellular change studied in 53 cases and 206 controls. Am. J. Pathol. 35, 1117–1133.

Liu, B., Fang, F., Pedersen, N.L., Tillander, A., Ludvigsson, J.F., Ekbom, A., Svenningsson, P., Chen, H., Wirdefeldt, K., 2017. Vagotomy and Parkinson disease: A Swedish register–based matched-cohort study. Neurology 88, 1996–2002. https://doi.org/10.1212/WNL.0000000000003961

Liu, C.-W., Giasson, B.I., Lewis, K.A., Lee, V.M., DeMartino, G.N., Thomas, P.J., 2005. A Precipitating Role for Truncated α-Synuclein and the Proteasome in α-Synuclein Aggregation: IMPLICATIONS FOR PATHOGENESIS OF PARKINSON DISEASE. J. Biol. Chem. 280, 22670–22678. https://doi.org/10.1074/jbc.M501508200

Lo Bianco, C., Ridet, J.-L., Schneider, B.L., Deglon, N., Aebischer, P., 2002. Alpha-synucleinopathy and selective dopaminergic neuron loss in a rat lentiviral-based model of Parkinson's disease. Proceedings of the National Academy of Sciences 99, 10813–10818. https://doi.org/10.1073/pnas.152339799

Lopez-Cuina, M., Foubert-Samier, A., Tison, F., Meissner, W.G., 2018. Present and future of disease-modifying therapies in multiple system atrophy. Autonomic Neuroscience 211, 31–38. https://doi.org/10.1016/j.autneu.2017.12.008

Loria, F., Vargas, J.Y., Bousset, L., Syan, S., Salles, A., Melki, R., Zurzolo, C., 2017. α-Synuclein transfer between neurons and astrocytes indicates that astrocytes play a role in degradation rather than in spreading. Acta Neuropathol 134, 789–808. https://doi.org/10.1007/s00401-017-1746-2

Lovestam, S., Schweighauser, M., Matsubara, T., Murayama, S., Tomita, T., Ando, T., Hasegawa, K., Yoshida, M., Tarutani, A., Hasegawa, M., Goedert, M., Scheres, S.H.W., 2021. Seeded assembly *in vitro* does not replicate the structures of α-synuclein filaments from multiple system atrophy. FEBS Open Bio 2211-5463.13110. https://doi.org/10.1002/2211-5463.13110

Lue, L.-F., Walker, D.G., Adler, C.H., Shill, H., Tran, H., Akiyama, H., Sue, L.I., Caviness, J., Sabbagh, M.N., Beach, T.G., 2012. Biochemical Increase in Phosphorylated Alpha-Synuclein Precedes Histopathology of Lewy-Type Synucleinopathies: Phosphorylated α-Synuclein and Lewy Pathology Staging. Brain Pathology 22, 745–756. https://doi.org/10.1111/j.1750-3639.2012.00585.x

Luk, K.C., Kehm, V., Carroll, J., Zhang, B., O'Brien, P., Trojanowski, J.Q., Lee, V.M.-Y., 2012a. Pathological α-Synuclein Transmission Initiates Parkinson-like Neurodegeneration in Nontransgenic Mice. Science 338, 949–953. https://doi.org/10.1126/science.1227157

Luk, K.C., Kehm, V.M., Zhang, B., O'Brien, P., Trojanowski, J.Q., Lee, V.M.Y., 2012b. Intracerebral inoculation of pathological α-synuclein initiates a rapidly progressive neurodegenerative α-synucleinopathy in mice. The Journal of Experimental Medicine 209, 975–986. https://doi.org/10.1084/jem.20112457

Luk, K.C., Song, C., O'Brien, P., Stieber, A., Branch, J.R., Brunden, K.R., Trojanowski, J.Q., Lee, V.M.-Y., 2009. Exogenous -synuclein fibrils seed the formation of Lewy body-like intracellular inclusions in cultured cells. Proceedings of the National Academy of Sciences 106, 20051–20056. https://doi.org/10.1073/pnas.0908005106

Lyras, L., Perry, R.H., Perry, E.K., Ince, P.G., Jenner, A., Jenner, P., Halliwell, B., 2002. Oxidative Damage to Proteins, Lipids, and DNA in Cortical Brain Regions from Patients with Dementia with Lewy Bodies. Journal of Neurochemistry 71, 302–312. https://doi.org/10.1046/j.1471-4159.1998.71010302.x

Ma, L.-Y., Gao, L., Li, X., Ma, H.-Z., Feng, T., 2019. Nitrated alpha-synuclein in minor salivary gland biopsies in Parkinson's disease. Neuroscience Letters 704, 45–49. https://doi.org/10.1016/j.neulet.2019.03.054

MacLeod, D., Dowman, J., Hammond, R., Leete, T., Inoue, K., Abeliovich, A., 2006. The Familial Parkinsonism Gene LRRK2 Regulates Neurite Process Morphology. Neuron 52, 587–593. https://doi.org/10.1016/j.neuron.2006.10.008

Mahul-Mellier, A.-L., Altay, M.F., Burtscher, J., Maharjan, N., Ait-Bouziad, N., Chiki, A., Vingill, S., Wade-Martins, R., Holton, J., Strand, C., Haikal, C., Li, J.-Y., Hamelin, R., Croisier, M., Knott, G., Mairet-Coello, G., Weerens, L., Michel, A., Downey, P., Citron, M., A. Lashuel, H., 2018. The making of a Lewy body: the role of α-synuclein post-fibrillization modifications in regulating the formation and the maturation of pathological inclusions. bioRxiv 500058. https://doi.org/10.1101/500058

Mahul-Mellier, A.-L., Burtscher, J., Maharjan, N., Weerens, L., Croisier, M., Kuttler, F., Leleu, M., Knott, G.W., Lashuel, H.A., 2020. The process of Lewy body formation, rather than simply α-synuclein fibrillization, is one of the major drivers of neurodegeneration. Proc Natl Acad Sci USA 117, 4971. https://doi.org/10.1073/pnas.1913904117

Mahul-Mellier, A.-L., Fauvet, B., Gysbers, A., Dikiy, I., Oueslati, A., Georgeon, S., Lamontanara, A.J., Bisquertt, A., Eliezer, D., Masliah, E., Halliday, G., Hantschel, O., Lashuel, H.A., 2014. c-Abl phosphorylates α-synuclein and regulates its degradation: implication for α-synuclein clearance and contribution to the pathogenesis of Parkinson's disease. Human Molecular Genetics 23, 2858–2879. https://doi.org/10.1093/hmg/ddt674

Mahul-Mellier, A.-L., Vercruysse, F., Maco, B., Ait-Bouziad, N., De Roo, M., Muller, D., Lashuel, H.A., 2015. Fibril growth and seeding capacity play key roles in α-synuclein-mediated apoptotic cell death. Cell Death Differ 22, 2107–2122. https://doi.org/10.1038/cdd.2015.79

Makky, A., Bousset, L., Polesel-Maris, J., Melki, R., 2016. Nanomechanical properties of distinct fibrillar polymorphs of the protein α-synuclein. Sci Rep 6, 37970. https://doi.org/10.1038/srep37970

Mamais, A., Manzoni, C., Nazish, I., Arber, C., Sonustun, B., Wray, S., Warner, T.T., Cookson, M.R., Lewis, P.A., Bandopadhyay, R., 2018. Analysis of macroautophagy related proteins in G2019S LRRK2 Parkinson's disease brains with Lewy body pathology. Brain Research 1701, 75–84. https://doi.org/10.1016/j.brainres.2018.07.023

Mamais, A., Raja, M., Manzoni, C., Dihanich, S., Lees, A., Moore, D., Lewis, P.A., Bandopadhyay, R., 2013. Divergent α-synuclein solubility and aggregation properties in G2019S LRRK2 Parkinson's disease brains with Lewy Body pathology compared to idiopathic cases. Neurobiology of Disease 58, 183–190. https://doi.org/10.1016/j.nbd.2013.05.017

Manetto, V., Perry, G., Tabaton, M., Mulvihill, P., Fried, V.A., Smith, H.T., Gambetti, P., Autilio-Gambetti, L., 1988. Ubiquitin is associated with abnormal cytoplasmic filaments characteristic of neurodegenerative diseases. PNAS 85, 4501–4505. https://doi.org/10.1073/pnas.85.12.4501

Markesbery, W.R., 1997. Oxidative Stress Hypothesis in Alzheimer's Disease. Free Radical Biology and Medicine 23, 134–147. https://doi.org/10.1016/S0891-5849(96)00629-6

Maroteaux, L., Campanelli, J., Scheller, R., 1988. Synuclein: a neuron-specific protein localized to the nucleus and presynaptic nerve terminal. J. Neurosci. 8, 2804–2815. https://doi.org/10.1523/JNEUROSCI.08-08-02804.1988

Maroteaux, L., Scheller, R.H., 1991. The rat brain synucleins; family of proteins transiently associated with neuronal membrane. Molecular Brain Research 11, 335–343. https://doi.org/10.1016/0169-328X(91)90043-W

Marotta, N.P., Lin, Y.H., Lewis, Y.E., Ambroso, M.R., Zaro, B.W., Roth, M.T., Arnold, D.B., Langen, R., Pratt, M.R., 2015. O-GlcNAc modification blocks the aggregation and toxicity of the protein α-

synuclein associated with Parkinson's disease. Nature Chem 7, 913–920. https://doi.org/10.1038/nchem.2361
Marti, M.J., Tolosa, E., Campdelacreu, J., 2003. Clinical overview of the synucleinopathies. Mov Disord. 18, 21–27. https://doi.org/10.1002/mds.10559
Marti-Masso, J.-F., Ruiz-Martínez, J., Bolaño, M.J., Ruiz, I., Gorostidi, A., Moreno, F., Ferrer, I., de Munain, A.L., 2009. Neuropathology of Parkinson's disease with the R1441G mutation in *LRRK2*: Neuropathology of Parkinson's Disease. Mov. Disord. 24, 1998–2001. https://doi.org/10.1002/mds.22677
Martinez-Martin, P., Forjaz, M.J., Frades-Payo, B., Rusiñol, A.B., Fernández-García, J.M., Benito-León, J., Arillo, V.C., Barberá, M.A., Sordo, M.P., Catalán, M.J., 2007. Caregiver burden in Parkinson's disease. Mov. Disord. 22, 924–931. https://doi.org/10.1002/mds.21355
Marui, W., Iseki, E., Nakai, T., Miura, S., Kato, M., Uéda, K., Kosaka, K., 2002. Progression and staging of Lewy pathology in brains from patients with dementia with Lewy bodies. Journal of the Neurological Sciences 195, 153–159. https://doi.org/10.1016/S0022-510X(02)00006-0
Marvian, A.T., Aliakbari, F., Mohammad-Beigi, H., Ahmadi, Z.A., Mehrpooyan, S., Lermyte, F., Nasouti, M., Collingwood, J.F., Otzen, D.E., Morshedi, D., 2020. The status of the terminal regions of α-synuclein in different forms of aggregates during fibrillization. International Journal of Biological Macromolecules 155, 543–550. https://doi.org/10.1016/j.ijbiomac.2020.03.238
Masliah, E., Iwai, A., Mallory, M., Uéda, K., Saitoh, T., 1996. Altered presynaptic protein NACP is associated with plaque formation and neurodegeneration in Alzheimer's disease. Am J Pathol 148, 201–210.
Masuda, H., Asahina, M., Oide, T., Wakita, H., Sekiguchi, Y., Araki, N., Kuwabara, S., 2014. Antemortem detection of colonic α-synuclein pathology in a patient with pure autonomic failure. J Neurol 261, 2451–2452. https://doi.org/10.1007/s00415-014-7529-y
Masuda-Suzukake, M., Nonaka, T., Hosokawa, M., Kubo, M., Shimozawa, A., Akiyama, H., Hasegawa, M., 2014. Pathological alpha-synuclein propagates through neural networks. acta neuropathol commun 2, 88. https://doi.org/10.1186/s40478-014-0088-8
Masuda-Suzukake, M., Nonaka, T., Hosokawa, M., Oikawa, T., Arai, T., Akiyama, H., Mann, D.M.A., Hasegawa, M., 2013. Prion-like spreading of pathological α-synuclein in brain. Brain 136, 1128–1138. https://doi.org/10.1093/brain/awt037
Matsuo, A., Akiguchi, I., Lee, G.C., McGeer, E.G., McGeer, P.L., Kimura, J., 1998. Myelin Degeneration in Multiple System Atrophy Detected by Unique Antibodies. The American Journal of Pathology 153, 735–744. https://doi.org/10.1016/S0002-9440(10)65617-9
Mattila, P.M., Rinne, J.O., Helenius, H., Dickson, D.W., Röyttä, M., Mattila, P.M., 2000. Alpha-synuclein-immunoreactive cortical Lewy bodies are associated with cognitive impairment in Parkinson's disease. Acta Neuropathologica 100, 285–290. https://doi.org/10.1007/s004019900168
May, S., Gilman, S., Sowell, B.B., Thomas, R.G., Stern, M.B., Colcher, A., Tanner, C.M., Huang, N., Novak, P., Reich, S.G., Jankovic, J., Ondo, W.G., Low, P.A., Sandroni, P., Lipp, A., Marshall, F.J., Wooten, F., Shults, C.W., 2007. Potential outcome measures and trial design issues for multiple system atrophy. Mov. Disord. 22, 2371–2377. https://doi.org/10.1002/mds.21734
McCormack, A.L., Mak, S.K., Di Monte, D.A., 2012. Increased α-synuclein phosphorylation and nitration in the aging primate substantia nigra. Cell Death Dis 3, e315–e315. https://doi.org/10.1038/cddis.2012.50
McGeer, P.L., Itagaki, S., Boyes, B.E., McGeer, E.G., 1988. Reactive microglia are positive for HLA-DR in the substantia nigra of Parkinson's and Alzheimer's disease brains. Neurology 38, 1285–1285. https://doi.org/10.1212/WNL.38.8.1285
McKeith, I.G., Boeve, B.F., Dickson, D.W., Halliday, G., Taylor, J.-P., Weintraub, D., Aarsland, D., Galvin, J., Attems, J., Ballard, C.G., Bayston, A., Beach, T.G., Blanc, F., Bohnen, N., Bonanni, L., Bras, J., Brundin, P., Burn, D., Chen-Plotkin, A., Duda, J.E., El-Agnaf, O., Feldman, H., Ferman, T.J., ffytche, D., Fujishiro, H., Galasko, D., Goldman, J.G., Gomperts, S.N., Graff-Radford, N.R., Honig, L.S., Iranzo, A., Kantarci, K., Kaufer, D., Kukull, W., Lee, V.M.Y., Leverenz, J.B., Lewis, S., Lippa, C., Lunde, A., Masellis, M., Masliah, E., McLean, P., Mollenhauer, B., Montine, T.J., Moreno, E., Mori, E., Murray, M., O'Brien, J.T., Orimo, S., Postuma, R.B., Ramaswamy, S., Ross, O.A., Salmon, D.P., Singleton, A., Taylor, A., Thomas, A., Tiraboschi, P., Toledo, J.B., Trojanowski, J.Q., Tsuang, D., Walker, Z., Yamada, M., Kosaka, K., 2017. Diagnosis and management of dementia with Lewy bodies: Fourth consensus report of the DLB Consortium. Neurology 89, 88–100. https://doi.org/10.1212/WNL.0000000000004058
McKeith, I.G., Dickson, D.W., Lowe, J., Emre, M., O'Brien, J.T., Feldman, H., Cummings, J., Duda, J.E., Lippa, C., Perry, E.K., Aarsland, D., Arai, H., Ballard, C.G., Boeve, B., Burn, D.J., Costa, D., Del

Ser, T., Dubois, B., Galasko, D., Gauthier, S., Goetz, C.G., Gomez-Tortosa, E., Halliday, G., Hansen, L.A., Hardy, J., Iwatsubo, T., Kalaria, R.N., Kaufer, D., Kenny, R.A., Korczyn, A., Kosaka, K., Lee, V.M.Y., Lees, A., Litvan, I., Londos, E., Lopez, O.L., Minoshima, S., Mizuno, Y., Molina, J.A., Mukaetova-Ladinska, E.B., Pasquier, F., Perry, R.H., Schulz, J.B., Trojanowski, J.Q., Yamada, M., for the Consortium on DLB, 2005. Diagnosis and management of dementia with Lewy bodies: Third report of the DLB consortium. Neurology 65, 1863–1872. https://doi.org/10.1212/01.wnl.0000187889.17253.b1

McKeith, I.G., Galasko, D., Kosaka, K., Perry, E.K., Dickson, D.W., Hansen, L.A., Salmon, D.P., Lowe, J., Mirra, S.S., Byrne, E.J., Lennox, G., Quinn, N.P., Edwardson, J.A., Ince, P.G., Bergeron, C., Burns, A., Miller, B.L., Lovestone, S., Collerton, D., Jansen, E.N.H., Ballard, C., de Vos, R.A.I., Wilcock, G.K., Jellinger, K.A., Perry, R.H., 1996. Consensus guidelines for the clinical and pathologic diagnosis of dementia with Lewy bodies (DLB): Report of the consortium on DLB international workshop. Neurology 47, 1113–1124. https://doi.org/10.1212/WNL.47.5.1113

McLean, J.R., Hallett, P.J., Cooper, O., Stanley, M., Isacson, O., 2012. Transcript expression levels of full-length alpha-synuclein and its three alternatively spliced variants in Parkinson's disease brain regions and in a transgenic mouse model of alpha-synuclein overexpression. Molecular and Cellular Neuroscience 49, 230–239. https://doi.org/10.1016/j.mcn.2011.11.006

McNaught, K.St.P., Jenner, P., 2001. Proteasomal function is impaired in substantia nigra in Parkinson's disease. Neuroscience Letters 297, 191–194. https://doi.org/10.1016/S0304-3940(00)01701-8

McNaught, K.St.P., Shashidharan, P., Perl, D.P., Jenner, P., Olanow, C.W., 2002. Aggresome-related biogenesis of Lewy bodies: Relationship between aggresomes and Lewy bodies. European Journal of Neuroscience 16, 2136–2148. https://doi.org/10.1046/j.1460-9568.2002.02301.x

Mei, Y.-L., Yang, J., Wu, Z.-R., Yang, Y., Xu, Y.-M., 2021. Transcranial Sonography of the Substantia Nigra for the Differential Diagnosis of Parkinson's Disease and Other Movement Disorders: A Meta-Analysis. Parkinson's Disease 2021, 1–9. https://doi.org/10.1155/2021/8891874

Meixner, A., Boldt, K., Van Troys, M., Askenazi, M., Gloeckner, C.J., Bauer, M., Marto, J.A., Ampe, C., Kinkl, N., Ueffing, M., 2011. A QUICK Screen for Lrrk2 Interaction Partners – Leucine-rich Repeat Kinase 2 is Involved in Actin Cytoskeleton Dynamics. Molecular & Cellular Proteomics 10, M110.001172. https://doi.org/10.1074/mcp.M110.001172

Mezey, E., Dehejia, A.M., Harta, G., Suchy, S.F., Nussbaum, R.L., Brownstein, M.J., Polymeropoulos, M.H., 1998. Alpha synuclein is present in Lewy bodies in sporadic Parkinson's disease. Mol Psychiatry 3, 493–499. https://doi.org/10.1038/sj.mp.4000446

Milber, J.M., Noorigian, J.V., Morley, J.F., Petrovitch, H., White, L., Ross, G.W., Duda, J.E., 2012. Lewy pathology is not the first sign of degeneration in vulnerable neurons in Parkinson disease. Neurology 79, 2307–2314. https://doi.org/10.1212/WNL.0b013e318278fe32

Miller, D.W., Johnson, J.M., Solano, S.M., Hollingsworth, Z.R., Standaert, D.G., Young, A.B., 2005. Absence of α-synuclein mRNA expression in normal and multiple system atrophy oligodendroglia. J Neural Transm 112, 1613–1624. https://doi.org/10.1007/s00702-005-0378-1

Mirza, B., Hadberg, H., Thomsen, P., Moos, T., 1999. The absence of reactive astrocytosis is indicative of a unique inflammatory process in Parkinson's disease. Neuroscience 95, 425–432. https://doi.org/10.1016/S0306-4522(99)00455-8

Moors, T.E., Maat, C.A., Niedieker, D., Mona, D., Petersen, D., Timmermans-Huisman, E., Kole, J., El-Mashtoly, S.F., Spycher, L., Zago, W., Barbour, R., Mundigl, O., Kaluza, K., Huber, S., Hug, M.N., Kremer, T., Ritter, M., Dziadek, S., Geurts, J.J.G., Gerwert, K., Britschgi, M., van de Berg, W.D.J., 2021. The subcellular arrangement of alpha-synuclein proteoforms in the Parkinson's disease brain as revealed by multicolor STED microscopy. Acta Neuropathol. https://doi.org/10.1007/s00401-021-02329-9

Moors, T.E., Maat, C.A., Niedieker, D., Mona, D., Petersen, D., Timmermans-Huisman, E., Kole, J., El-Mashtoly, S.F., Spycher, L., Zago, W., Barbour, R., Mundigl, O., Kaluza, K., Huber, S., Hug, M.N., Kremer, T., Ritter, M., Dziadek, S., Geurts, J.J.G., Gerwert, K., Britschgi, M., van de Berg, W.D.J., 2019. Subcellular orchestration of alpha-synuclein variants in Parkinson's disease brains revealed by 3D multicolor STED microscopy. bioRxiv 470476. https://doi.org/10.1101/470476

Mori, F., Inenaga, C., Yoshimoto, M., Umezu, H., Takahashi, H., Wakabayashi, K., Tanaka, R., 2002. Alpha-synuclein immunoreactivity in normal and neoplastic Schwann cells. Acta Neuropathologica 103, 145–151. https://doi.org/10.1007/s004010100443

Mori, F., Nishie, M., Piao, Y.-S., Kito, K., Kamitani, T., Takahashi, H., Wakabayashi, K., 2005. Accumulation of NEDD8 in neuronal and glial inclusions of neurodegenerative disorders. Neuropathol Appl Neurobiol 31, 53–61. https://doi.org/10.1111/j.1365-2990.2004.00603.x

Mori, F., Tanji, K., Odagiri, S., Toyoshima, Y., Yoshida, M., Ikeda, T., Sasaki, H., Kakita, A., Takahashi, H., Wakabayashi, K., 2012. Ubiquilin immunoreactivity in cytoplasmic and nuclear inclusions in synucleinopathies, polyglutamine diseases and intranuclear inclusion body disease. Acta Neuropathol 124, 149–151. https://doi.org/10.1007/s00401-012-0999-z

Mori, F., Tanji, K., Zhang, H., Kakita, A., Takahashi, H., Wakabayashi, K., 2008. α-Synuclein pathology in the neostriatum in Parkinson's disease. Acta Neuropathol 115, 453–459. https://doi.org/10.1007/s00401-007-0316-4

Mori, H., Kondo, J., Ihara, Y., 1987. Ubiquitin is a component of paired helical filaments in Alzheimer's disease. Science 235, 1641–1644. https://doi.org/10.1126/science.3029875

Mu, L., Chen, J., Sobotka, S., Nyirenda, T., Benson, B., Gupta, F., Sanders, I., Adler, C.H., Caviness, J.N., Shill, H.A., Sabbagh, M., Samanta, J.E., Sue, L.I., Beach, T.G., The Arizona Parkinson's Disease Consortium, 2015. Alpha-Synuclein Pathology in Sensory Nerve Terminals of the Upper Aerodigestive Tract of Parkinson's Disease Patients. Dysphagia 30, 404–417. https://doi.org/10.1007/s00455-015-9612-7

Muench, G., Lueth, H.J., Wong, A., Arendt, Th., Hirsch, E., Ravid, R., Riederer, P., 2000. Crosslinking of α-synuclein by advanced glycation endproducts — an early pathophysiological step in Lewy body formation? Journal of Chemical Neuroanatomy 20, 253–257. https://doi.org/10.1016/S0891-0618(00)00096-X

Muller, C.M., Thal, D.R., Tolnay, M., Braak, H., 2005. Staging of Sporadic Parkinson Disease-Related a-Synuclein Pathology: Inter- and Intra-Rater Reliability. J Neuropathol Exp Neurol 64, 6.

Munishkina, L.A., Henriques, J., Uversky, V.N., Fink, A.L., 2004. Role of Protein−Water Interactions and Electrostatics in α-Synuclein Fibril Formation. Biochemistry 43, 3289–3300. https://doi.org/10.1021/bi034938r

Munishkina, L.A., Phelan, C., Uversky, V.N., Fink, A.L., 2003. Conformational Behavior and Aggregation of α-Synuclein in Organic Solvents: Modeling the Effects of Membranes. Biochemistry 42, 2720–2730. https://doi.org/10.1021/bi027166s

Muntane, G., Ferrer, I., Martinez-Vicente, M., 2012. α-synuclein phosphorylation and truncation are normal events in the adult human brain. Neuroscience 200, 106–119. https://doi.org/10.1016/j.neuroscience.2011.10.042

Murayama, S., Arima, K., Nakazato, Y., Satoh, J., Oda, M., Inose, T., 1992. Immunocytochemical and ultrastructural studies of neuronal and oligodendroglial cytoplasmic inclusions in multiple system atrophy. Acta Neuropathol 84, 32–38. https://doi.org/10.1007/BF00427212

Nakamura, K., Mori, F., Kon, T., Tanji, K., Miki, Y., Tomiyama, M., Kurotaki, H., Toyoshima, Y., Kakita, A., Takahashi, H., Yamada, M., Wakabayashi, K., 2016. Accumulation of phosphorylated α-synuclein in subpial and periventricular astrocytes in multiple system atrophy of long duration: Phosphorylated α-synuclein in MSA astrocytes. Neuropathology 36, 157–167. https://doi.org/10.1111/neup.12243

Nakamura, K., Mori, F., Kon, T., Tanji, K., Miki, Y., Tomiyama, M., Kurotaki, H., Toyoshima, Y., Kakita, A., Takahashi, H., Yamada, M., Wakabayashi, K., 2015. Filamentous aggregations of phosphorylated α-synuclein in Schwann cells (Schwann cell cytoplasmic inclusions) in multiple system atrophy. acta neuropathol commun 3, 29. https://doi.org/10.1186/s40478-015-0208-0

Nayernouri, T., 1985. Posttraumatic Parkinsonism. Surgical Neurology 24, 263–264. https://doi.org/10.1016/0090-3019(85)90035-7

Nee, L.E., Gomez, M.R., Dambrosia, J., Bale, S., Eldridge, R., Polinsky, R.J., 1991. Environmental-occupational risk factors and familial associations in multiple system atrophy: a preliminary investigation. Clinical Autonomic Research 1, 9–13.

Negro, A., Brunati, A.M., Donella-Deana, A., Massimino, M.L., Pinna, L.A., 2002. Multiple phosphorylation of α-synuclein by protein tyrosine kinase Syk prevents eosin-induced aggregation. FASEB j. 16, 1–22. https://doi.org/10.1096/fj.01-0517fje

Nemani, V.M., Lu, W., Berge, V., Nakamura, K., Onoa, B., Lee, M.K., Chaudhry, F.A., Nicoll, R.A., Edwards, R.H., 2010. Increased Expression of α-Synuclein Reduces Neurotransmitter Release by Inhibiting Synaptic Vesicle Reclustering after Endocytosis. Neuron 65, 66–79. https://doi.org/10.1016/j.neuron.2009.12.023

Neumann, M., Kahle, P.J., Giasson, B.I., Ozmen, L., Borroni, E., Spooren, W., Müller, V., Odoy, S., Fujiwara, H., Hasegawa, M., Iwatsubo, T., Trojanowski, J.Q., Kretzschmar, H.A., Haass, C., 2002. Misfolded proteinase K–resistant hyperphosphorylated α-synuclein in aged transgenic mice with locomotor deterioration and in human α-synucleinopathies. J. Clin. Invest. 110, 1429–1439. https://doi.org/10.1172/JCI200215777

Neumann, M., Müller, V., Kretzschmar, H.A., Haass, C., Kahle, P.J., 2004. Regional Distribution of Proteinase K-Resistant α-Synuclein Correlates with Lewy Body Disease Stage. J Neuropathol Exp Neurol 63, 1225–1235. https://doi.org/10.1093/jnen/63.12.1225

Ninkina, N.N., Alimova-Kost, M.V., Paterson, J.W.E., Delaney, L., Cohen, B.B., Imreh, S., Gnuchev, N.V., Davies, A.M., Buchman, V.L., 1998. Organization, expression and polymorphism of the human persyn gene. Human Molecular Genetics 7, 1417–1424. https://doi.org/10.1093/hmg/7.9.1417

Nirenberg, M.J., Libien, J., Vonsattel, J.-P., Fahn, S., 2007. Multiple system atrophy in a patient with the spinocerebellar ataxia 3 gene mutation. Mov Disord. 22, 251–253. https://doi.org/10.1002/mds.21231

Nishie, M., Mori, F., Fujiwara, H., Hasegawa, M., Yoshimoto, M., Iwatsubo, T., Takahashi, H., Wakabayashi, K., 2004. Accumulation of phosphorylated a-synuclein in the brain and peripheral ganglia of patients with multiple system atrophy. Acta Neuropathologica 107, 292–298. https://doi.org/10.1007/s00401-003-0811-1

Nonnekes, J., Post, B., Tetrud, J.W., Langston, J.W., Bloem, B.R., 2018. MPTP-induced parkinsonism: an historical case series. The Lancet Neurology 17, 300–301. https://doi.org/10.1016/S1474-4422(18)30072-3

Ohlsson, B., Englund, E., 2019. Atrophic Myenteric and Submucosal Neurons Are Observed in Parkinson's Disease. Parkinson's Disease 2019, 1–5. https://doi.org/10.1155/2019/7935820

Ohrfelt, A., Zetterberg, H., Andersson, K., Persson, R., Secic, D., Brinkmalm, G., Wallin, A., Mulugeta, E., Francis, P.T., Vanmechelen, E., Aarsland, D., Ballard, C., Blennow, K., Westman-Brinkmalm, A., 2011. Identification of Novel α-Synuclein Isoforms in Human Brain Tissue by using an Online NanoLC-ESI-FTICR-MS Method. Neurochem Res 36, 2029–2042. https://doi.org/10.1007/s11064-011-0527-x

Olanow, C.W., Perl, D.P., DeMartino, G.N., McNaught, K.S.P., 2004. Lewy-body formation is an aggresome-related process: a hypothesis. The Lancet Neurology 3, 496–503. https://doi.org/10.1016/S1474-4422(04)00827-0

Osterberg, V.R., Spinelli, K.J., Weston, L.J., Luk, K.C., Woltjer, R.L., Unni, V.K., 2015. Progressive Aggregation of Alpha-Synuclein and Selective Degeneration of Lewy Inclusion-Bearing Neurons in a Mouse Model of Parkinsonism. Cell Reports 10, 1252–1260. https://doi.org/10.1016/j.celrep.2015.01.060

O'Sullivan, S.S., Massey, L.A., Williams, D.R., Silveira-Moriyama, L., Kempster, P.A., Holton, J.L., Revesz, T., Lees, A.J., 2008. Clinical outcomes of progressive supranuclear palsy and multiple system atrophy. Brain 131, 1362–1372. https://doi.org/10.1093/brain/awn065

Ozelius, L.J., Senthil, G., Saunders-Pullman, R., Ohmann, E., Deligtisch, A., Tagliati, M., Hunt, A.L., Klein, C., Henick, B., Hailpern, S.M., Lipton, R.B., Soto-Valencia, J., Risch, N., Bressman, S.B., 2006. *LRRK2* G2019S as a Cause of Parkinson's Disease in Ashkenazi Jews. N Engl J Med 354, 424–425. https://doi.org/10.1056/NEJMc055509

Paillusson, S., Gomez-Suaga, P., Stoica, R., Little, D., Gissen, P., Devine, M.J., Noble, W., Hanger, D.P., Miller, C.C.J., 2017. α-Synuclein binds to the ER–mitochondria tethering protein VAPB to disrupt Ca2+ homeostasis and mitochondrial ATP production. Acta Neuropathol 134, 129–149. https://doi.org/10.1007/s00401-017-1704-z

Paisan-Ruiz, C., Jain, S., Evans, E.W., Gilks, W.P., Simón, J., van der Brug, M., de Munain, A.L., Aparicio, S., Gil, A.M., Khan, N., Johnson, J., Martinez, J.R., Nicholl, D., Carrera, I.M., Peňa, A.S., de Silva, R., Lees, A., Martí-Massó, J.F., Pérez-Tur, J., Wood, N.W., Singleton, A.B., 2004. Cloning of the Gene Containing Mutations that Cause PARK8-Linked Parkinson's Disease. Neuron 44, 595–600. https://doi.org/10.1016/j.neuron.2004.10.023

Paisan-Ruiz, C., Sàenz, A., de Munain, A.L., Martì, I., Martìnez Gil, A., Martì-Massò, J.F., Pèrez-Tur, J., 2005. Familial Parkinson's disease: Clinical and genetic analysis of four Basque families: PARK8 Linked Basque PD. Ann Neurol. 57, 365–372. https://doi.org/10.1002/ana.20391

Paleologou, K.E., Oueslati, A., Shakked, G., Rospigliosi, C.C., Kim, H.-Y., Lamberto, G.R., Fernandez, C.O., Schmid, A., Chegini, F., Gai, W.P., Chiappe, D., Moniatte, M., Schneider, B.L., Aebischer, P., Eliezer, D., Zweckstetter, M., Masliah, E., Lashuel, H.A., 2010. Phosphorylation at S87 Is Enhanced in Synucleinopathies, Inhibits -Synuclein Oligomerization, and Influences Synuclein-Membrane Interactions. Journal of Neuroscience 30, 3184–3198. https://doi.org/10.1523/JNEUROSCI.5922-09.2010

Pamphlett, R., Bishop, D.P., 2022. Mercury is present in neurons and oligodendrocytes in regions of the brain affected by Parkinson's disease and co-localises with Lewy bodies. PLoS ONE 17, e0262464. https://doi.org/10.1371/journal.pone.0262464

Papp, M.I., Kahn, J.E., Lantos, P.L., 1989. Glial cytoplasmic inclusions in the CNS of patients with multiple system atrophy (striatonigral degeneration, olivopontocerebellar atrophy and Shy-Drager syndrome). Journal of the Neurological Sciences 94, 79–100. https://doi.org/10.1016/0022-510X(89)90219-0

Papp, M.I., Lantos, P.L., 1994. The distribution of oligodendroglial inclusions in multiple system atrophy and its relevance to clinical symptomatology. Brain 117, 235–243. https://doi.org/10.1093/brain/117.2.235

Papp, M.I., Lantos, P.L., 1992. Accumulation of tubular structures in oligodendroglial and neuronal cells as the basic alteration in multiple system atrophy. Journal of the Neurological Sciences 107, 172–182. https://doi.org/10.1016/0022-510X(92)90286-T

Parihar, M.S., Parihar, A., Fujita, M., Hashimoto, M., Ghafourifar, P., 2008. Mitochondrial association of alpha-synuclein causes oxidative stress. Cell. Mol. Life Sci. 65, 1272–1284. https://doi.org/10.1007/s00018-008-7589-1

Parkinson, J., 2002. An Essay on the Shaking Palsy. J Neuropsychiatry Clin Neurosci 14.

Parkkinen, L., Hartikainen, P., Alafuzoff, I., 2007. Abundant glial a-synuclein pathology in a case without overt clinical symptoms. Clinical Neuropathology 8.

Parkkinen, L., Pirttilä, T., Alafuzoff, I., 2008. Applicability of current staging/categorization of α-synuclein pathology and their clinical relevance. Acta Neuropathol 115, 399–407. https://doi.org/10.1007/s00401-008-0346-6

Parkkinen, L., Soininen, H., Laakso, M., Alafuzoff, I., 2001. alpha-Synuclein pathology is highly dependent on the case selection. Neuropathol Appl Neurobiol 27, 314–325. https://doi.org/10.1046/j.0305-1846.2001.00342.x

Pasanen, P., Myllykangas, L., Siitonen, M., Raunio, A., Kaakkola, S., Lyytinen, J., Tienari, P.J., Pöyhönen, M., Paetau, A., 2014. A novel α-synuclein mutation A53E associated with atypical multiple system atrophy and Parkinson's disease-type pathology. Neurobiology of Aging 35, 2180.e1-2180.e5. https://doi.org/10.1016/j.neurobiolaging.2014.03.024

Paumier, K.L., Luk, K.C., Manfredsson, F.P., Kanaan, N.M., Lipton, J.W., Collier, T.J., Steece-Collier, K., Kemp, C.J., Celano, S., Schulz, E., Sandoval, I.M., Fleming, S., Dirr, E., Polinski, N.K., Trojanowski, J.Q., Lee, V.M., Sortwell, C.E., 2015. Intrastriatal injection of pre-formed mouse α-synuclein fibrils into rats triggers α-synuclein pathology and bilateral nigrostriatal degeneration. Neurobiology of Disease 82, 185–199. https://doi.org/10.1016/j.nbd.2015.06.003

Payton, J.E., Perrin, R.J., Clayton, D.F., George, J.M., 2001. Protein–protein interactions of alpha-synuclein in brain homogenates and transfected cells. Molecular Brain Research 95, 138–145. https://doi.org/10.1016/S0169-328X(01)00257-1

Peelaerts, W., Bousset, L., Van der Perren, A., Moskalyuk, A., Pulizzi, R., Giugliano, M., Van den Haute, C., Melki, R., Baekelandt, V., 2015. α-Synuclein strains cause distinct synucleinopathies after local and systemic administration. Nature 522, 340–344. https://doi.org/10.1038/nature14547

Peng, C., Gathagan, R.J., Covell, D.J., Medellin, C., Stieber, A., Robinson, J.L., Zhang, B., Pitkin, R.M., Olufemi, M.F., Luk, K.C., Trojanowski, J.Q., Lee, V.M.-Y., 2018. Cellular milieu imparts distinct pathological α-synuclein strains in α-synucleinopathies. Nature 557, 558–563. https://doi.org/10.1038/s41586-018-0104-4

Perez, R.G., Waymire, J.C., Lin, E., Liu, J.J., Guo, F., Zigmond, M.J., 2002. A Role for α-Synuclein in the Regulation of Dopamine Biosynthesis. J. Neurosci. 22, 3090–3099. https://doi.org/10.1523/JNEUROSCI.22-08-03090.2002

Perkin, G.D., 1998. An Atlas of Parkinson's Disease and Related Disorders, 0 ed. CRC Press. https://doi.org/10.1201/NOE1850709435

Perry, G., Friedman, R., Shaw, G., Chau, V., 1987. Ubiquitin is detected in neurofibrillary tangles and senile plaque neurites of Alzheimer disease brains. PNAS 84, 3033–3036. https://doi.org/10.1073/pnas.84.9.3033

Perry, R.H., Irving, D., Tomlinson, B.E., 1990. Lewy body prevalence in the aging brain: relationship to neuropsychiatric disorders, Alzheimer-type pathology and catecholaminergic nuclei. Journal of the Neurological Sciences 100, 223–233. https://doi.org/10.1016/0022-510X(90)90037-N

Petrov, V.A., Saltykova, I.V., Zhukova, I.A., Alifirova, V.M., Zhukova, N.G., Dorofeeva, Yu.B., Tyakht, A.V., Kovarsky, B.A., Alekseev, D.G., Kostryukova, E.S., Mironova, Yu.S., Izhboldina, O.P., Nikitina, M.A., Perevozchikova, T.V., Fait, E.A., Babenko, V.V., Vakhitova, M.T., Govorun, V.M., Sazonov, A.E., 2017. Analysis of Gut Microbiota in Patients with Parkinson's Disease. Bull Exp Biol Med 162, 734–737. https://doi.org/10.1007/s10517-017-3700-7

Polymeropoulos, M.H., Higgins, J.J., Golbe, L.I., Johnson, W.G., Ide, S.E., Di Iorio, G., Sanges, G., Stenroos, E.S., Pho, L.T., Schaffer, A.A., Lazzarini, A.M., Nussbaum, R.L., Duvoisin, R.C.,

1996. Mapping of a Gene for Parkinson's Disease to Chromosome 4q21-q23. Science 274, 1197–1199. https://doi.org/10.1126/science.274.5290.1197
Polymeropoulos, M.H., Lavedan, C., Leroy, E., Ide, S.E., Dehejia, A., Dutra, A., Pike, B., Root, H., Rubenstein, J., Boyer, R., Stenroos, E.S., Chandrasekharappa, S., Athanassiadou, A., Papapetropoulos, T., Johnson, W.G., Lazzarini, A.M., Duvoisin, R.C., Di Iorio, G., Golbe, L.I., Nussbaum, R.L., 1997. Mutation in the -Synuclein Gene Identified in Families with Parkinson's Disease. Science 276, 2045–2047. https://doi.org/10.1126/science.276.5321.2045
Pouclet, H., Lebouvier, T., Coron, E., Bruley des Varannes, S., Rouaud, T., Roy, M., Neunlist, M., Derkinderen, P., 2012a. A comparison between rectal and colonic biopsies to detect Lewy pathology in Parkinson's disease. Neurobiology of Disease 45, 305–309. https://doi.org/10.1016/j.nbd.2011.08.014
Pouclet, H., Lebouvier, T., Coron, E., Des Varannes, S.B., Neunlist, M., Derkinderen, P., 2012b. A comparison between colonic submucosa and mucosa to detect Lewy pathology in Parkinson's disease: Colonic mucosa in Parkinson's disease. Neurogastroenterology & Motility 24, e202–e205. https://doi.org/10.1111/j.1365-2982.2012.01887.x
Pouclet, H., Lebouvier, T., Coron, E., Rouaud, T., Flamant, M., Toulgoat, F., Roy, M., Vavasseur, F., Bruley des Varannes, S., Neunlist, M., Derkinderen, P., 2012c. Analysis of colonic alpha-synuclein pathology in multiple system atrophy. Parkinsonism & Related Disorders 18, 893–895. https://doi.org/10.1016/j.parkreldis.2012.04.020
Pountney, D.L., Chegini, F., Shen, X., Blumbergs, P.C., Gai, W.P., 2005a. SUMO-1 marks subdomains within glial cytoplasmic inclusions of multiple system atrophy. Neuroscience Letters 381, 74–79. https://doi.org/10.1016/j.neulet.2005.02.013
Pountney, D.L., Lowe, R., Quilty, M., Vickers, J.C., Voelcker, N.H., Gai, W.P., 2004. Annular alpha-synuclein species from purified multiple system atrophy inclusions. J Neurochem 90, 502–512. https://doi.org/10.1111/j.1471-4159.2004.02533.x
Pountney, D.L., Treweek, T.M., Chataway, T., Huang, Y., Chegini, F., Blumbergs, P.C., Raftery, M.J., Gai, W.P., 2005b. αB-Crystallin is a major component of glial cytoplasmic inclusions in multiple system atrophy. neurotox res 7, 77–85. https://doi.org/10.1007/BF03033778
Pramstaller, P.P., Schlossmacher, M.G., Jacques, T.S., Scaravilli, F., Eskelson, C., Pepivani, I., Hedrich, K., Adel, S., Gonzales-McNeal, M., Hilker, R., Kramer, P.L., Klein, C., 2005. Lewy body Parkinson's disease in a large pedigree with 77 Parkin mutation carriers. Ann Neurol. 58, 411–422. https://doi.org/10.1002/ana.20587
Prasad, K., Beach, T.G., Hedreen, J., Richfield, E.K., 2012. Critical Role of Truncated α-Synuclein and Aggregates in Parkinson's Disease and Incidental Lewy Body Disease: Role of Truncated α-Synuclein. Brain Pathology 22, 811–825. https://doi.org/10.1111/j.1750-3639.2012.00597.x
Probst-Cousin, S., Bergmann, M., Kuchelmeister, K., Schröder, R., Schmid, K.W., 1996. Ubiquitin-positive Inclusions in Different Types of Multiple System Atrophy: Distribution and Specificity. Pathology - Research and Practice 192, 453–461. https://doi.org/10.1016/S0344-0338(96)80007-0
Proukakis, C., Dudzik, C.G., Brier, T., MacKay, D.S., Cooper, J.M., Millhauser, G.L., Houlden, H., Schapira, A.H., 2013. A novel -synuclein missense mutation in Parkinson disease. Neurology 80, 1062–1064. https://doi.org/10.1212/WNL.0b013e31828727ba
Prusiner, S.B., Woerman, A.L., Mordes, D.A., Watts, J.C., Rampersaud, R., Berry, D.B., Patel, S., Oehler, A., Lowe, J.K., Kravitz, S.N., Geschwind, D.H., Glidden, D.V., Halliday, G.M., Middleton, L.T., Gentleman, S.M., Grinberg, L.T., Giles, K., 2015. Evidence for α-synuclein prions causing multiple system atrophy in humans with parkinsonism. Proc Natl Acad Sci USA 112, E5308–E5317. https://doi.org/10.1073/pnas.1514475112
Przedborski, S., Dawson, T.M., 2001. The Role of Nitric Oxide in Parkinson's Disease, in: Parkinson's Disease. Humana Press, New Jersey, pp. 113–136. https://doi.org/10.1385/1-59259-142-6:113
Punsoni, M., Friedman, J.H., Resnick, M., Donahue, J.E., Yang, D.F., Stopa, E.G., 2019. Enteric Pathologic Manifestations of Alpha-Synucleinopathies: Applied Immunohistochemistry & Molecular Morphology 27, 543–548. https://doi.org/10.1097/PAI.0000000000000613
Qian, Y., Yang, X., Xu, S., Wu, C., Song, Y., Qin, N., Chen, S.-D., Xiao, Q., 2018. Alteration of the fecal microbiota in Chinese patients with Parkinson's disease. Brain, Behavior, and Immunity 70, 194–202. https://doi.org/10.1016/j.bbi.2018.02.016
Qing, H., Wong, W., McGeer, E.G., McGeer, P.L., 2009a. Lrrk2 phosphorylates alpha synuclein at serine 129: Parkinson disease implications. Biochemical and Biophysical Research Communications 387, 149–152. https://doi.org/10.1016/j.bbrc.2009.06.142

Qing, H., Zhang, Y., Deng, Y., McGeer, E.G., McGeer, P.L., 2009b. Lrrk2 interaction with α-synuclein in diffuse Lewy body disease. Biochemical and Biophysical Research Communications 390, 1229–1234. https://doi.org/10.1016/j.bbrc.2009.10.126

Raasi, S., Varadan, R., Fushman, D., Pickart, C.M., 2005. Diverse polyubiquitin interaction properties of ubiquitin-associated domains. Nat Struct Mol Biol 12, 708–714. https://doi.org/10.1038/nsmb962

Rajput, A.H., Dickson, D.W., Robinson, C.A., Ross, O.A., Dachsel, J.C., Lincoln, S.J., Cobb, S.A., Rajput, M.L., Farrer, M.J., 2006. Parkinsonism, Lrrk2 G2019S, and tau neuropathology. Neurology 67, 1506–1508. https://doi.org/10.1212/01.wnl.0000240220.33950.0c

Rajput, A.H., Rozdilsky, B., Rajput, A., Ang, L., 1990. Levodopa Efficacy and Pathological Basis of Parkinson Syndrome: Clinical Neuropharmacology 13, 553–558. https://doi.org/10.1097/00002826-199012000-00007

Ramirez, A., Heimbach, A., Gründemann, J., Stiller, B., Hampshire, D., Cid, L.P., Goebel, I., Mubaidin, A.F., Wriekat, A.-L., Roeper, J., Al-Din, A., Hillmer, A.M., Karsak, M., Liss, B., Woods, C.G., Behrens, M.I., Kubisch, C., 2006. Hereditary parkinsonism with dementia is caused by mutations in ATP13A2, encoding a lysosomal type 5 P-type ATPase. Nat Genet 38, 1184–1191. https://doi.org/10.1038/ng1884

Recasens, A., Dehay, B., Bové, J., Carballo-Carbajal, I., Dovero, S., Pérez-Villalba, A., Fernagut, P.-O., Blesa, J., Parent, A., Perier, C., Fariñas, I., Obeso, J.A., Bezard, E., Vila, M., 2014. Lewy body extracts from Parkinson disease brains trigger α-synuclein pathology and neurodegeneration in mice and monkeys: LB-Induced Pathology. Ann Neurol. 75, 351–362. https://doi.org/10.1002/ana.24066

Ree, R., Varland, S., Arnesen, T., 2018. Spotlight on protein N-terminal acetylation. Exp Mol Med 50, 1–13. https://doi.org/10.1038/s12276-018-0116-z

Rey, N.L., Petit, G.H., Bousset, L., Melki, R., Brundin, P., 2013. Transfer of human α-synuclein from the olfactory bulb to interconnected brain regions in mice. Acta Neuropathol 126, 555–573. https://doi.org/10.1007/s00401-013-1160-3

Rey, N.L., Steiner, J.A., Maroof, N., Luk, K.C., Madaj, Z., Trojanowski, J.Q., Lee, V.M.-Y., Brundin, P., 2016. Widespread transneuronal propagation of α-synucleinopathy triggered in olfactory bulb mimics prodromal Parkinson's disease. The Journal of Experimental Medicine 213, 1759–1778. https://doi.org/10.1084/jem.20160368

Reyes, J.F., Rey, N.L., Bousset, L., Melki, R., Brundin, P., Angot, E., 2014. Alpha-synuclein transfers from neurons to oligodendrocytes: α-Synuclein Neuron-to-Oligodendrocyte Spread. Glia 62, 387–398. https://doi.org/10.1002/glia.22611

Reynolds, A.D., Glanzer, J.G., Kadiu, I., Ricardo-Dukelow, M., Chaudhuri, A., Ciborowski, P., Cerny, R., Gelman, B., Thomas, M.P., Mosley, R.L., Gendelman, H.E., 2008a. Nitrated alpha-synuclein-activated microglial profiling for Parkinson's disease: Synuclein-induced microglia activation. Journal of Neurochemistry 104, 1504–1525. https://doi.org/10.1111/j.1471-4159.2007.05087.x

Reynolds, A.D., Kadiu, I., Garg, S.K., Glanzer, J.G., Nordgren, T., Ciborowski, P., Banerjee, R., Gendelman, H.E., 2008b. Nitrated Alpha-Synuclein and Microglial Neuroregulatory Activities. J Neuroimmune Pharmacol 3, 59–74. https://doi.org/10.1007/s11481-008-9100-z

Reynolds, A.D., Stone, D.K., Mosley, R.L., Gendelman, H.E., 2009. Nitrated α-Synuclein-Induced Alterations in Microglial Immunity Are Regulated by CD4+ T Cell Subsets. The Journal of Immunology 182, 4137–4149. https://doi.org/10.4049/jimmunol.0803982

Richter-Landsberg, C., Gorath, M., Trojanowski, J.Q., Lee, V.M.-Y., 2000. α-synuclein is developmentally expressed in cultured rat brain oligodendrocytes. Journal of Neuroscience Research 62, 9–14. https://doi.org/10.1002/1097-4547(20001001)62:1<9::AID-JNR2>3.0.CO;2-U

Robotta, M., Gerding, H.R., Vogel, A., Hauser, K., Schildknecht, S., Karreman, C., Leist, M., Subramaniam, V., Drescher, M., 2014. Alpha-Synuclein Binds to the Inner Membrane of Mitochondria in an α-Helical Conformation. ChemBioChem 15, 2499–2502. https://doi.org/10.1002/cbic.201402281

Roeters, S.J., Iyer, A., Pletikapić, G., Kogan, V., Subramaniam, V., Woutersen, S., 2017. Evidence for Intramolecular Antiparallel Beta-Sheet Structure in Alpha-Synuclein Fibrils from a Combination of Two-Dimensional Infrared Spectroscopy and Atomic Force Microscopy. Sci Rep 7, 41051. https://doi.org/10.1038/srep41051

Ross, O.A., Toft, M., Whittle, A.J., Johnson, J.L., Papapetropoulos, S., Mash, D.C., Litvan, I., Gordon, M.F., Wszolek, Z.K., Farrer, M.J., Dickson, D.W., 2006. Lrrk2 and Lewy body disease. Ann Neurol. 59, 388–393. https://doi.org/10.1002/ana.20731

Rostami, J., Holmqvist, S., Lindström, V., Sigvardson, J., Westermark, G.T., Ingelsson, M., Bergström, J., Roybon, L., Erlandsson, A., 2017. Human Astrocytes Transfer Aggregated Alpha-Synuclein via Tunneling Nanotubes. J. Neurosci. 37, 11835–11853. https://doi.org/10.1523/JNEUROSCI.0983-17.2017

Rott, R., Szargel, R., Haskin, J., Bandopadhyay, R., Lees, A.J., Shani, V., Engelender, S., 2011. α-Synuclein fate is determined by USP9X-regulated monoubiquitination. Proc Natl Acad Sci USA 108, 18666. https://doi.org/10.1073/pnas.1105725108

Rott, R., Szargel, R., Haskin, J., Shani, V., Shainskaya, A., Manov, I., Liani, E., Avraham, E., Engelender, S., 2008. Monoubiquitylation of α-Synuclein by Seven in Absentia Homolog (SIAH) Promotes Its Aggregation in Dopaminergic Cells. J. Biol. Chem. 283, 3316–3328. https://doi.org/10.1074/jbc.M704809200

Rott, R., Szargel, R., Shani, V., Hamza, H., Savyon, M., Abd Elghani, F., Bandopadhyay, R., Engelender, S., 2017. SUMOylation and ubiquitination reciprocally regulate α-synuclein degradation and pathological aggregation. Proc Natl Acad Sci USA 114, 13176–13181. https://doi.org/10.1073/pnas.1704351114

Rouaud, T., Clairembault, T., Coron, E., Neunlist, M., Anheim, M., Derkinderen, P., 2017. Enteric alpha-synuclein pathology in LRRK2-G2019S Parkinson's disease. Parkinsonism & Related Disorders 40, 83–84. https://doi.org/10.1016/j.parkreldis.2017.05.001

Ruffmann, C., Bengoa-Vergniory, N., Poggiolini, I., Ritchie, D., Hu, M.T., Alegre-Abarrategui, J., Parkkinen, L., 2018. Detection of alpha-synuclein conformational variants from gastro-intestinal biopsy tissue as a potential biomarker for Parkinson's disease. Neuropathol Appl Neurobiol 44, 722–736. https://doi.org/10.1111/nan.12486

Sacino, A.N., Brooks, M., McGarvey, N.H., McKinney, A.B., Thomas, M.A., Levites, Y., Ran, Y., Golde, T.E., Giasson, B.I., 2013. Induction of CNS α-synuclein pathology by fibrillar and non-amyloidogenic recombinant α-synuclein. acta neuropathol commun 1, 38. https://doi.org/10.1186/2051-5960-1-38

Sacino, A.N., Brooks, M., McKinney, A.B., Thomas, M.A., Shaw, G., Golde, T.E., Giasson, B.I., 2014a. Brain Injection of α-Synuclein Induces Multiple Proteinopathies, Gliosis, and a Neuronal Injury Marker. J. Neurosci. 34, 12368–12378. https://doi.org/10.1523/JNEUROSCI.2102-14.2014

Sacino, A.N., Brooks, M., Thomas, M.A., McKinney, A.B., Lee, S., Regenhardt, R.W., McGarvey, N.H., Ayers, J.I., Notterpek, L., Borchelt, D.R., Golde, T.E., Giasson, B.I., 2014b. Intramuscular injection of -synuclein induces CNS -synuclein pathology and a rapid-onset motor phenotype in transgenic mice. Proceedings of the National Academy of Sciences 111, 10732–10737. https://doi.org/10.1073/pnas.1321785111

Saito, Y., Kawashima, A., Ruberu, N.N., Fujiwara, H., Koyama, S., Sawabe, M., Arai, T., Nagura, H., Yamanouchi, H., Hasegawa, M., Iwatsubo, T., Murayama, S., 2003. Accumulation of Phosphorylated α-Synuclein in Aging Human Brain. J Neuropathol Exp Neurol 62, 644–654. https://doi.org/10.1093/jnen/62.6.644

Saito, Y., Ruberu, N.N., Sawabe, M., Arai, T., Kazama, H., Hosoi, T., Yamanouchi, H., Murayama, S., 2004. Lewy Body-Related α-Synucleinopathy in Aging. J Neuropathol Exp Neurol 63, 742–749. https://doi.org/10.1093/jnen/63.7.742

Sakamoto, M., Uchihara, T., Hayashi, M., Nakamura, A., Kikuchi, E., Mizutani, T., Mizusawa, H., Hirai, S., 2002. Heterogeneity of Nigral and Cortical Lewy Bodies Differentiated by Amplified Triple-Labeling for Alpha-Synuclein, Ubiquitin, and Thiazin Red. Experimental Neurology 177, 88–94. https://doi.org/10.1006/exnr.2002.7961

Sakamoto, M., Uchihara, T., Nakamura, A., Mizutani, T., Mizusawa, H., 2005. Progressive accumulation of ubiquitin and disappearance of α-synuclein epitope in multiple system atrophy-associated glial cytoplasmic inclusions: triple fluorescence study combined with Gallyas-Braak method. Acta Neuropathol 110, 417–425. https://doi.org/10.1007/s00401-005-1066-9

Sampathu, D.M., Giasson, B.I., Pawlyk, A.C., Trojanowski, J.Q., Lee, V.M.-Y., 2003. Ubiquitination of α-Synuclein Is Not Required for Formation of Pathological Inclusions in α-Synucleinopathies. The American Journal of Pathology 163, 91–100. https://doi.org/10.1016/S0002-9440(10)63633-4

Sanchez-Ferro, Á., Rábano, A., Catalán, M.J., Rodríguez-Valcárcel, F.C., Díez, S.F., Herreros-Rodríguez, J., García-Cobos, E., Álvarez-Santullano, M.M., López-Manzanares, L., Mosqueira, A.J., Desojo, L.V., López-Lozano, J.J., López-Valdés, E., Sánchez-Sánchez, R., Molina-Arjona, J.A., 2015. In vivo gastric detection of α-synuclein inclusions in Parkinson's disease: Gastric Detection ofα-Synuclein Inclusions. Mov Disord. 30, 517–524. https://doi.org/10.1002/mds.25988

Sano, K., Atarashi, R., Satoh, K., Ishibashi, D., Nakagaki, T., Iwasaki, Y., Yoshida, M., Murayama, S., Mishima, K., Nishida, N., 2017. Prion-Like Seeding of Misfolded α-Synuclein in the Brains of Dementia with Lewy Body Patients in RT-QUIC. Mol Neurobiol. https://doi.org/10.1007/s12035-017-0624-1

Sano, K., Iwasaki, Y., Yamashita, Y., Irie, K., Hosokawa, M., Satoh, K., Mishima, K., 2021. Tyrosine 136 phosphorylation of α-synuclein aggregates in the Lewy body dementia brain: involvement of serine 129 phosphorylation by casein kinase 2. acta neuropathol commun 9, 182. https://doi.org/10.1186/s40478-021-01281-9

Schapira, A.H.V., Chaudhuri, K.R., Jenner, P., 2017. Non-motor features of Parkinson disease. Nat Rev Neurosci 18, 435–450. https://doi.org/10.1038/nrn.2017.62

Schaser, A.J., Osterberg, V.R., Dent, S.E., Stackhouse, T.L., Wakeham, C.M., Boutros, S.W., Weston, L.J., Owen, N., Weissman, T.A., Luna, E., Raber, J., Luk, K.C., McCullough, A.K., Woltjer, R.L., Unni, V.K., 2019. Alpha-synuclein is a DNA binding protein that modulates DNA repair with implications for Lewy body disorders. Scientific Reports 9, 10919. https://doi.org/10.1038/s41598-019-47227-z

Schenck, C.H., Bundlie, S.R., Mahowald, M.W., 1996. Delayed emergence of a parkinsonian disorder in 38% of 29 older men initially diagnosed with idiopathic rapid eye movement sleep behavior disorder. Neurology 46, 388–393. https://doi.org/10.1212/WNL.46.2.388

Schiesling, C., Kieper, N., Seidel, K., Krüger, R., 2008. Review: Familial Parkinson's disease – genetics, clinical phenotype and neuropathology in relation to the common sporadic form of the disease. Neuropathol Appl Neurobiol 34, 255–271. https://doi.org/10.1111/j.1365-2990.2008.00952.x

Schrag, A., Kingsley, D., Phatouros, C., Mathias, C.J., Lees, A.J., Daniel, S.E., Quinn, N.P., 1998. Clinical usefulness of magnetic resonance imaging in multiple system atrophy. Journal of Neurology, Neurosurgery & Psychiatry 65, 65–71. https://doi.org/10.1136/jnnp.65.1.65

Schrag, A., Wenning, G.K., Quinn, N., Ben-Shlomo, Y., 2008. Survival in multiple system atrophy: Survival in MSA. Mov. Disord. 23, 294–296. https://doi.org/10.1002/mds.21839

Schweighauser, M., Shi, Y., Tarutani, A., Kametani, F., Murzin, A.G., Ghetti, B., Matsubara, T., Tomita, T., Ando, T., Hasegawa, K., Murayama, S., Yoshida, M., Hasegawa, M., Scheres, S.H.W., Goedert, M., 2020. Structures of α-synuclein filaments from multiple system atrophy. Nature 1–6. https://doi.org/10.1038/s41586-020-2317-6

Schwiertz, A., Spiegel, J., Dillmann, U., Grundmann, D., Bürmann, J., Faßbender, K., Schäfer, K.-H., Unger, M.M., 2018. Fecal markers of intestinal inflammation and intestinal permeability are elevated in Parkinson's disease. Parkinsonism & Related Disorders 50, 104–107. https://doi.org/10.1016/j.parkreldis.2018.02.022

Seppi, K., Yekhlef, F., Diem, A., Luginger Wolf, E., Mueller, J., Tison, F., Quinn, N.P., Poewe, W., Wenning, G.K., 2005. Progression of parkinsonism in multiple system atrophy. J Neurol 252, 91–96. https://doi.org/10.1007/s00415-005-0617-2

Shahmoradian, S.H., Lewis, A.J., Genoud, C., Hench, J., Moors, T.E., Navarro, P.P., Castaño-Díez, D., Schweighauser, G., Graff-Meyer, A., Goldie, K.N., Sütterlin, R., Huisman, E., Ingrassia, A., Gier, Y. de, Rozemuller, A.J.M., Wang, J., Paepe, A.D., Erny, J., Staempfli, A., Hoernschemeyer, J., Großerüschkamp, F., Niedieker, D., El-Mashtoly, S.F., Quadri, M., Van IJcken, W.F.J., Bonifati, V., Gerwert, K., Bohrmann, B., Frank, S., Britschgi, M., Stahlberg, H., Van de Berg, W.D.J., Lauer, M.E., 2019. Lewy pathology in Parkinson's disease consists of crowded organelles and lipid membranes. Nat Neurosci 22, 1099–1109. https://doi.org/10.1038/s41593-019-0423-2

Shahnawaz, M., Mukherjee, A., Pritzkow, S., Mendez, N., Rabadia, P., Liu, X., Hu, B., Schmeichel, A., Singer, W., Wu, G., Tsai, A.-L., Shirani, H., Nilsson, K.P.R., Low, P.A., Soto, C., 2020. Discriminating α-synuclein strains in Parkinson's disease and multiple system atrophy. Nature 578, 273–277. https://doi.org/10.1038/s41586-020-1984-7

Shannon, K.M., Keshavarzian, A., Dodiya, H.B., Jakate, S., Kordower, J.H., 2012a. Is alpha-synuclein in the colon a biomarker for premotor Parkinson's Disease? Evidence from 3 cases: Is Alpha-Synuclein a Biomarker for Premotor PD? Mov. Disord. 27, 716–719. https://doi.org/10.1002/mds.25020

Shannon, K.M., Keshavarzian, A., Mutlu, E., Dodiya, H.B., Daian, D., Jaglin, J.A., Kordower, J.H., 2012b. Alpha-synuclein in colonic submucosa in early untreated Parkinson's disease: Colonic α-Synuclein in Parkinson's Disease. Mov. Disord. 27, 709–715. https://doi.org/10.1002/mds.23838

Sharrad, D.F., de Vries, E., Brookes, S.J.H., 2013. Selective expression of α-synuclein-immunoreactivity in vesicular acetylcholine transporter-immunoreactive axons in the guinea pig rectum and human colon. J. Comp. Neurol. 521, 657–676. https://doi.org/10.1002/cne.23198

Shiba, M., Bower, J.H., Maraganore, D.M., McDonnell, S.K., Peterson, B.J., Ahlskog, J.E., Schaid, D.J., Rocca, W.A., 2000. Anxiety disorders and depressive disorders preceding Parkinson's disease: A case-control study. Mov. Disord. 15, 669–677. https://doi.org/10.1002/1531-8257(200007)15:4<669::AID-MDS1011>3.0.CO;2-5

Shin, C., Park, S.-H., Yun, J.Y., Shin, J.H., Yang, H.-K., Lee, H.-J., Kong, S.-H., Suh, Y.-S., Kim, H.-J., Jeon, B., 2018. Alpha-synuclein staining in non-neural structures of the gastrointestinal tract is non-specific in Parkinson disease. Parkinsonism & Related Disorders 55, 15–17. https://doi.org/10.1016/j.parkreldis.2018.09.026

Shin, C., Park, S.-H., Yun, J.Y., Shin, J.H., Yang, H.-K., Lee, H.-J., Kong, S.-H., Suh, Y.-S., Shen, G., Kim, Y., Kim, H.-J., Jeon, B., 2017. Fundamental limit of alpha-synuclein pathology in gastrointestinal biopsy as a pathologic biomarker of Parkinson's disease: Comparison with surgical specimens. Parkinsonism & Related Disorders 44, 73–78. https://doi.org/10.1016/j.parkreldis.2017.09.001

Shin, E.C., Cho, S.E., Lee, D.-K., Hur, M.-W., Paik, S.R., Park, J.H., Kim, J., 2000. Expression Patterns of Alpha-synuclein in Human Hematopoietic Cells and in Drosophila at Different Developmental Stages. Molecules and Cells 6.

Shin, J., Park, S.-H., Shin, C., Kim, J., Yun, T.J., Kim, H.-J., Jeon, B., 2019. Submandibular gland is a suitable site for alpha synuclein pathology in Parkinson disease. Parkinsonism & Related Disorders 58, 35–39. https://doi.org/10.1016/j.parkreldis.2018.04.019

Shoji, M., Harigaya, Yasuo, Sasaki, A., Ueda, K., Ishiguro, K., Matsubara, E., Watanabe, M., Ikeda, M., Kanai, M., Tomidokoro, Y., Shizuka, M., Amari, M., Kosaka, K., Nakazato, Y., Okamoto, K., Hirai, S., 2000. Accumulation of NACP/alpha -synuclein in Lewy body disease and multiple system atrophy. Journal of Neurology, Neurosurgery & Psychiatry 68, 605–608. https://doi.org/10.1136/jnnp.68.5.605

Shrivastava, A.N., Bousset, L., Renner, M., Redeker, V., Savistchenko, J., Triller, A., Melki, R., 2020. Differential Membrane Binding and Seeding of Distinct α-Synuclein Fibrillar Polymorphs. Biophysical Journal 118, 1301–1320. https://doi.org/10.1016/j.bpj.2020.01.022

Shy, G.M., Drager, G.A., 1960. A Neurological Syndrome Associated with Orthostatic Hypotension: A Clinical-Pathologic Study. AMA Arch Neurol 2, 511. https://doi.org/10.1001/archneur.1960.03840110025004

Singleton, A.B., Farrer, M., Johnson, J., Singleton, A., Hague, S., Kachergus, J., Hulihan, M., Peuralinna, T., Dutra, A., Nussbaum, R., Lincoln, S., Crawley, A., Hanson, M., Maraganore, D., Adler, C., Cookson, M.R., Muenter, M., Baptista, M., Miller, D., Blancato, J., Hardy, J., Gwinn-Hardy, K., 2003. Alpha-synuclein Locus Triplication Causes Parkinson's Disease. Science 302, 841–841. https://doi.org/10.1126/science.1090278

Skorvanek, M., Gelpi, E., Mechirova, E., Ladomirjakova, Z., Han, V., Lesko, N., Feketeova, E., Repkova, B., Urbancikova, Z., Vargova, A., Spisak, P., Ribeiro Ventosa, J., Kudela, F., Kulcsarova, K., Babinska, S., Toth, S., Gombosova, L., Zakuciova, M., Veseliny, E., Trebuna, F., Lutz, M.I., Gdovinova, Z., Kovacs, G.G., the PARCAS studygroup, 2018. α-Synuclein antibody 5G4 identifies manifest and prodromal Parkinson's disease in colonic mucosa: LETTERS: NEWOBSERVATIONS. Mov Disord. 33, 1366–1368. https://doi.org/10.1002/mds.27380

Sofroniew, M.V., Vinters, H.V., 2010. Astrocytes: biology and pathology. Acta Neuropathologica 29.

Soma, H., Yabe, I., Takei, A., Fujiki, N., Yanagihara, T., Sasaki, H., 2006. Heredity in multiple system atrophy. Journal of the Neurological Sciences 240, 107–110. https://doi.org/10.1016/j.jns.2005.09.003

Song, Y.J.C., Halliday, G.M., Holton, J.L., Lashley, T., O'Sullivan, S.S., McCann, H., Lees, A.J., Ozawa, T., Williams, D.R., Lockhart, P.J., Revesz, T.R., 2009. Degeneration in Different Parkinsonian Syndromes Relates to Astrocyte Type and Astrocyte Protein Expression. J Neuropathol Exp Neurol 68, 1073–1083. https://doi.org/10.1097/NEN.0b013e3181b66f1b

Sonustun, B., Altay, M.F., Strand, C., Hondhamuni, G., Warner, T.T., Lashuel, H.A., Bandopadhyay, R., 2022. Pathological relevance of post-translationally modified alpha-synuclein (pSer87, pSer129, nTyr39) in idiopathic Parkinson's disease and Multiple System Atrophy. bioRxiv. https://doi.org/10.1101/2022.01.11.475823

Sorrentino, Z.A., Goodwin, M.S., Riffe, C.J., Dhillon, J.-K.S., Xia, Y., Gorion, K.-M., Vijayaraghavan, N., McFarland, K.N., Golbe, L.I., Yachnis, A.T., Giasson, B.I., 2019. Unique α-synuclein pathology within the amygdala in Lewy body dementia: implications for disease initiation and progression. acta neuropathol commun 7, 142. https://doi.org/10.1186/s40478-019-0787-2

Spillantini, M.G., Crowther, R.A., Jakes, R., Cairns, N.J., Lantos, P.L., Goedert, M., 1998a. Filamentous a-synuclein inclusions link multiple system atrophy with Parkinson's disease and dementia with Lewy bodies. Neuroscience Letters 4.

Spillantini, M.G., Crowther, R.A., Jakes, R., Hasegawa, M., Goedert, M., 1998b. Alpha-synuclein in filamentous inclusions of Lewy bodies from Parkinson's disease and dementia with Lewy bodies. Proceedings of the National Academy of Sciences 95, 6469–6473. https://doi.org/10.1073/pnas.95.11.6469

Spillantini, M.G., Divane, A., Goedert, M., 1995. Assignment of Human α-Synuclein (SNCA) and β-Synuclein (SNCB) Genes to Chromosomes 4q21 and 5q35. Genomics 27, 379–381. https://doi.org/10.1006/geno.1995.1063

Spillantini, M.G., Schmidt, M.L., Lee, V.M.-Y., Trojanowski, J.Q., Jakes, R., Goedert, M., 1997. α-Synuclein in Lewy bodies. Nature 388, 839–840. https://doi.org/10.1038/42166

Spira, P.J., Sharpe, D.M., Halliday, G., Cavanagh, J., Nicholson, G.A., 2001. Clinical and pathological features of a parkinsonian syndrome in a family with an Ala53Thr ?-synuclein mutation. Ann Neurol. 49, 313–319. https://doi.org/10.1002/ana.67

Sprenger, F.S., Stefanova, N., Gelpi, E., Seppi, K., Navarro-Otano, J., Offner, F., Vilas, D., Valldeoriola, F., Pont-Sunyer, C., Aldecoa, I., Gaig, C., Gines, A., Cuatrecasas, M., Högl, B., Frauscher, B., Iranzo, A., Wenning, G.K., Vogel, W., Tolosa, E., Poewe, W., 2015. Enteric nervous system α-synuclein immunoreactivity in idiopathic REM sleep behavior disorder. Neurology 85, 1761–1768. https://doi.org/10.1212/WNL.0000000000002126

St Martin, J.L., Klucken, J., Outeiro, T.F., Nguyen, P., Keller-McGandy, C., Cantuti-Castelvetri, I., Grammatopoulos, T.N., Standaert, D.G., Hyman, B.T., McLean, P.J., 2007. Dopaminergic neuron loss and up-regulation of chaperone protein mRNA induced by targeted over-expression of alpha-synuclein in mouse substantia nigra. J Neurochem 0, 070214184024010-??? https://doi.org/10.1111/j.1471-4159.2006.04310.x

Steiner, J.A., Quansah, E., Brundin, P., 2018. The concept of alpha-synuclein as a prion-like protein: ten years after. Cell Tissue Res 373, 161–173. https://doi.org/10.1007/s00441-018-2814-1

Steiner, P., Sarria, J.-C.F., Glauser, L., Magnin, S., Catsicas, S., Hirling, H., 2002. Modulation of receptor cycling by neuron-enriched endosomal protein of 21 kD. Journal of Cell Biology 157, 1197–1209. https://doi.org/10.1083/jcb.200202022

Stewart, T., Sui, Y.-T., Gonzalez-Cuyar, L.F., Wong, D.T.W., Akin, D.M., Tumas, V., Aasly, J., Ashmore, E., Aro, P., Ginghina, C., Korff, A., Zabetian, C.P., Leverenz, J.B., Shi, M., Zhang, J., 2014. Cheek cell–derived α-synuclein and DJ-1 do not differentiate Parkinson's disease from control. Neurobiology of Aging 35, 418–420. https://doi.org/10.1016/j.neurobiolaging.2013.08.008

Stokholm, M.G., Danielsen, E.H., Hamilton-Dutoit, S.J., Borghammer, P., 2016. Pathological α-synuclein in gastrointestinal tissues from prodromal Parkinson disease patients: α-Synuclein in Prodromal PD. Ann Neurol. 79, 940–949. https://doi.org/10.1002/ana.24648

Stolzenberg, E., Berry, D., Yang, D., Lee, E.Y., Kroemer, A., Kaufman, S., Wong, G.C.L., Oppenheim, J.J., Sen, S., Fishbein, T., Bax, A., Harris, B., Barbut, D., Zasloff, M.A., 2017. A Role for Neuronal Alpha-Synuclein in Gastrointestinal Immunity. J Innate Immun 9, 456–463. https://doi.org/10.1159/000477990

Strohaeker, T., Jung, B.C., Liou, S.-H., Fernandez, C.O., Riedel, D., Becker, S., Halliday, G.M., Bennati, M., Kim, W.S., Lee, S.-J., Zweckstetter, M., 2019. Structural heterogeneity of α-synuclein fibrils amplified from patient brain extracts. Nat Commun 10, 5535. https://doi.org/10.1038/s41467-019-13564-w

Sultana, R., Poon, H.F., Cai, J., Pierce, W.M., Merchant, M., Klein, J.B., Markesbery, W.R., Butterfield, D.A., 2006. Identification of nitrated proteins in Alzheimer's disease brain using a redox proteomics approach. Neurobiology of Disease 22, 76–87. https://doi.org/10.1016/j.nbd.2005.10.004

Suwijn, S.R., van Boheemen, C.J., de Haan, R.J., Tissingh, G., Booij, J., de Bie, R.M., 2015. The diagnostic accuracy of dopamine transporter SPECT imaging to detect nigrostriatal cell loss in patients with Parkinson's disease or clinically uncertain parkinsonism: a systematic review. EJNMMI Res 5, 12. https://doi.org/10.1186/s13550-015-0087-1

Svensson, E., Horváth-Puhó, E., Thomsen, R.W., Djurhuus, J.C., Pedersen, L., Borghammer, P., Sørensen, H.T., 2015. Vagotomy and subsequent risk of Parkinson's disease: Vagotomy and Risk of PD. Ann Neurol. 78, 522–529. https://doi.org/10.1002/ana.24448

Tagliafierro, L., Chiba-Falek, O., 2016. Up-regulation of SNCA gene expression: implications to synucleinopathies. Neurogenetics 17, 145–157. https://doi.org/10.1007/s10048-016-0478-0

Taguchi, K., Watanabe, Y., Tsujimura, A., Tanaka, M., 2016. Brain region-dependent differential expression of alpha-synuclein. Journal of Comparative Neurology 524, 1236–1258. https://doi.org/10.1002/cne.23901

Takahashi, H., Iwanaga, K., Egawa, S., Ikuta, F., 1994. Ultrastructural Relationship between Lewy Bodies and Pale Bodies Studied in Locus Ceruleus Neurons of a Non-Parkinsonian Patient. Neuropathology 14, 73–80. https://doi.org/10.1111/j.1440-1789.1994.tb00242.x

Takanashi, M., Funayama, M., Matsuura, E., Yoshino, H., Li, Y., Tsuyama, S., Takashima, H., Nishioka, K., Hattori, N., 2018. Isolated nigral degeneration without pathological protein aggregation in autopsied brains with LRRK2 p.R1441H homozygous and heterozygous mutations. acta neuropathol commun 6, 105. https://doi.org/10.1186/s40478-018-0617-y

Takao, M., Ghetti, B., Yoshida, H., Piccardo, P., Narain, Y., Murrell, J.R., Vidal, R., Glazier, B.S., Jakes, R., Tsutsui, M., Spillantini, M.G., Crowther, R.A., Goedert, M., Koto, A., 2004. Early-onset Dementia with Lewy Bodies. Brain Pathology 14, 137–147. https://doi.org/10.1111/j.1750-3639.2004.tb00046.x

Takeda, A., Arai, N., Komori, T., Kato, S., Oda, M., 1997. Neuronal inclusions in the dentate fascia in patients with multiple system atrophy. Neuroscience Letters 227, 157–160. https://doi.org/10.1016/S0304-3940(97)00336-4

Takeda, A., Hashimoto, M., Mallory, M., Sundsumo, M., Hansen, L., Masliah, E., 2000. C-terminal α-synuclein immunoreactivity in structures other than Lewy bodies in neurodegenerative disorders. Acta Neuropathol 99, 296–304. https://doi.org/10.1007/PL00007441

Tamaoka, A., Mizusawa, H., Mori, H., Shoji, S., 1995. Ubiquitinated αB-crystallin in glial cytoplasmic inclusions from the brain of a patient with multiple system atrophy. Journal of the Neurological Sciences 129, 192–198. https://doi.org/10.1016/0022-510X(94)00275-S

Tamura, T., Yoshida, M., Hashizume, Y., Sobue, G., 2012. Lewy body-related α-synucleinopathy in the spinal cord of cases with incidental Lewy body disease: The spinal cord pathology of ILBD. Neuropathology 32, 13–22. https://doi.org/10.1111/j.1440-1789.2011.01211.x

Tan, A.H., Chong, C.W., Song, S.L., Teh, C.S.J., Yap, I.K.S., Loke, M.F., Tan, Y.Q., Yong, H.S., Mahadeva, S., Lang, A.E., Lim, S.-Y., 2018. Altered gut microbiome and metabolome in patients with multiple system atrophy: Gut Microbiome and Metabolome In MSA. Mov Disord. 33, 174–176. https://doi.org/10.1002/mds.27203

Tanji, K., Mori, F., Mimura, J., Itoh, K., Kakita, A., Takahashi, H., Wakabayashi, K., 2010. Proteinase K-resistant α-synuclein is deposited in presynapses in human Lewy body disease and A53T α-synuclein transgenic mice. Acta Neuropathol 120, 145–154. https://doi.org/10.1007/s00401-010-0676-z

Tanji, K., Mori, F., Nakajo, S., Imaizumi, T., Yoshida, H., Hirabayashi, T., Yoshimoto, M., Satoh, K., Takahashi, H., Wakabayashi, K., 2001. Expression of β-synuclein in normal human astrocytes. NeuroReport 12, 2845–2848.

Tanner, C.M., Kamel, F., Ross, G.W., Hoppin, J.A., Goldman, S.M., Korell, M., Marras, C., Bhudhikanok, G.S., Kasten, M., Chade, A.R., Comyns, K., Richards, M.B., Meng, C., Priestley, B., Fernandez, H.H., Cambi, F., Umbach, D.M., Blair, A., Sandler, D.P., Langston, J.W., 2011. Rotenone, Paraquat, and Parkinson's Disease. Environmental Health Perspectives 119, 866–872. https://doi.org/10.1289/ehp.1002839

Tanudjojo, B., Shaikh, S.S., Fenyi, A., Bousset, L., Agarwal, D., Marsh, J., Zois, C., Heman-Ackah, S., Fischer, R., Sims, D., Melki, R., Tofaris, G.K., 2021. Phenotypic manifestation of α-synuclein strains derived from Parkinson's disease and multiple system atrophy in human dopaminergic neurons. Nat Commun 12, 3817. https://doi.org/10.1038/s41467-021-23682-z

Tarutani, A., Suzuki, G., Shimozawa, A., Nonaka, T., Akiyama, H., Hisanaga, S., Hasegawa, M., 2016. The Effect of Fragmented Pathogenic α-Synuclein Seeds on Prion-like Propagation. J. Biol. Chem. 291, 18675–18688. https://doi.org/10.1074/jbc.M116.734707

Tayebi, N., Walker, J., Stubblefield, B., Orvisky, E., LaMarca, M.E., Wong, K., Rosenbaum, H., Schiffmann, R., Bembi, B., Sidransky, E., 2003. Gaucher disease with parkinsonian manifestations: does glucocerebrosidase deficiency contribute to a vulnerability to parkinsonism? Molecular Genetics and Metabolism 79, 104–109. https://doi.org/10.1016/S1096-7192(03)00071-4

Terada, S., Ishizu, H., Haraguchi, T., Takehisa, Y., Tanabe, Y., Kawai, K., Kuroda, S., 2000. Tau-negative astrocytic star-like inclusions and coiled bodies in dementia with Lewy bodies. Acta Neuropathologica 100, 464–468. https://doi.org/10.1007/s004010000213

Terada, S., Ishizu, H., Yokota, O., Tsuchiya, K., Nakashima, H., Ishihara, T., Fujita, D., Uéda, K., Ikeda, K., Kuroda, S., 2003. Glial involvement in diffuse Lewy body disease. Acta Neuropathol 105, 163–169. https://doi.org/10.1007/s00401-002-0622-9

Testa, D., Filippini, G., Farinotti, M., Palazzini, E., Caraceni, T., 1996. Survival in multiple system atrophy: a study of prognostic factors in 59 cases. J Neurol 243, 401–404. https://doi.org/10.1007/BF00868999

Theillet, F.-X., Binolfi, A., Bekei, B., Martorana, A., Rose, H.M., Stuiver, M., Verzini, S., Lorenz, D., van Rossum, M., Goldfarb, D., Selenko, P., 2016. Structural disorder of monomeric α-synuclein persists in mammalian cells. Nature 530, 45–50. https://doi.org/10.1038/nature16531

Thomas, M.P., Chartrand, K., Reynolds, A., Vitvitsky, V., Banerjee, R., Gendelman, H.E., 2007. Ion channel blockade attenuates aggregated alpha synuclein induction of microglial reactive oxygen species: relevance for the pathogenesis of Parkinson's disease. J Neurochem 100, 503–519. https://doi.org/10.1111/j.1471-4159.2006.04315.x

Thomzig, A., Wagenführ, K., Pinder, P., Joncic, M., Schulz-Schaeffer, W.J., Beekes, M., 2021. Transmissible α-synuclein seeding activity in brain and stomach of patients with Parkinson's disease. Acta Neuropathol 141, 861–879. https://doi.org/10.1007/s00401-021-02312-4

Thornalley, P.J., 2008. Protein and nucleotide damage by glyoxal and methylglyoxal in physiological systems - role in ageing and disease. Drug Metabolism and Drug Interactions 23. https://doi.org/10.1515/DMDI.2008.23.1-2.125

Tofaris, G.K., Razzaq, A., Ghetti, B., Lilley, K.S., Spillantini, M.G., 2003. Ubiquitination of α-Synuclein in Lewy Bodies Is a Pathological Event Not Associated with Impairment of Proteasome Function. J. Biol. Chem. 278, 44405–44411. https://doi.org/10.1074/jbc.M308041200

Tolosa, E., Borght, T.V., Moreno, E., 2007. Accuracy of DaTSCAN (123I-ioflupane) SPECT in diagnosis of patients with clinically uncertain parkinsonism: 2-Year follow-up of an open-label study. Mov. Disord. 22, 2346–2351. https://doi.org/10.1002/mds.21710

Tong, J., Wong, H., Guttman, M., Ang, L.C., Forno, L.S., Shimadzu, M., Rajput, A.H., Muenter, M.D., Kish, S.J., Hornykiewicz, O., Furukawa, Y., 2010. Brain α-synuclein accumulation in multiple system atrophy, Parkinson's disease and progressive supranuclear palsy: a comparative investigation. Brain 133, 172–188. https://doi.org/10.1093/brain/awp282

Touchman, J.W., Dehejia, A., Chiba-Falek, O., Cabin, D.E., Schwartz, J.R., Orrison, B.M., Polymeropoulos, M.H., Nussbaum, R.L., 2001. Human and Mouse alpha -Synuclein Genes: Comparative Genomic Sequence Analysis and Identification of a Novel Gene Regulatory Element. Genome Research 11, 78–86. https://doi.org/10.1101/gr.165801

Trexler, A.J., Rhoades, E., 2012. N-terminal acetylation is critical for forming α-helical oligomer of α-synuclein. Protein Science 21, 601–605. https://doi.org/10.1002/pro.2056

Trojanowski, J.Q., Goedert, M., Iwatsubo, T., Lee, V.M.-Y., 1998. Fatal attractions: abnormal protein aggregation and neuron death in Parkinson's disease and Lewy body dementia. Cell Death Differ 5, 832–837. https://doi.org/10.1038/sj.cdd.4400432

Trojanowski, J.Q., Revesz, T., 2007. Proposed neuropathological criteria for the post mortem diagnosis of multiple system atrophy. Neuropathol Appl Neurobiol 33, 615–620. https://doi.org/10.1111/j.1365-2990.2007.00907.x

Tu, P., Galvin, J.E., Baba, M., Giasson, B., Tomita, T., Leight, S., Nakajo, S., Iwatsubo, T., Trojanowski, J.Q., Lee, V.M.-Y., 1998. Glial cytoplasmic inclusions in white matter oligodendrocytes of multiple system atrophy brains contain insoluble ?-synuclein. Ann Neurol. 44, 415–422. https://doi.org/10.1002/ana.410440324

Ueda, K., Fukushima, H., Masliah, E., Xia, Y., Iwai, A., Yoshimoto, M., Otero, D.A., Kondo, J., Ihara, Y., Saitoh, T., 1993. Molecular cloning of cDNA encoding an unrecognized component of amyloid in Alzheimer disease. PNAS 90, 11282–11286. https://doi.org/10.1073/pnas.90.23.11282

Ueda, K., Saitoh, T., Mori, H., 1994. Tissue-Dependent Alternative Splicing of mRNA for NACP, the Precursor of Non-Aβ Component of Alzheimer's Disease Amyloid. Biochemical and Biophysical Research Communications 205, 1366–1372. https://doi.org/10.1006/bbrc.1994.2816

Uhlen, M., Fagerberg, L., Hallstrom, B.M., Lindskog, C., Oksvold, P., Mardinoglu, A., Sivertsson, A., Kampf, C., Sjostedt, E., Asplund, A., Olsson, I., Edlund, K., Lundberg, E., Navani, S., Szigyarto, C.A.-K., Odeberg, J., Djureinovic, D., Takanen, J.O., Hober, S., Alm, T., Edqvist, P.-H., Berling, H., Tegel, H., Mulder, J., Rockberg, J., Nilsson, P., Schwenk, J.M., Hamsten, M., von Feilitzen, K., Forsberg, M., Persson, L., Johansson, F., Zwahlen, M., von Heijne, G., Nielsen, J., Ponten, F., 2015. Tissue-based map of the human proteome. Science 347, 1260419–1260419. https://doi.org/10.1126/science.1260419

Ulusoy, A., Musgrove, R.E., Rusconi, R., Klinkenberg, M., Helwig, M., Schneider, A., Di Monte, D.A., 2015. Neuron-to-neuron α-synuclein propagation in vivo is independent of neuronal injury. acta neuropathol commun 3, 13. https://doi.org/10.1186/s40478-015-0198-y

Ulusoy, A., Phillips, R.J., Helwig, M., Klinkenberg, M., Powley, T.L., Di Monte, D.A., 2017. Brain-to-stomach transfer of α-synuclein via vagal preganglionic projections. Acta Neuropathol 133, 381–393. https://doi.org/10.1007/s00401-016-1661-y

Ulusoy, A., Rusconi, R., Pérez-Revuelta, B.I., Musgrove, R.E., Helwig, M., Winzen-Reichert, B., Monte, D.A.D., 2013. Caudo-rostral brain spreading of α-synuclein through vagal connections. EMBO Mol Med 5, 1119–1127. https://doi.org/10.1002/emmm.201302475

Uryu, K., Richter-Landsberg, C., Welch, W., Sun, E., Goldbaum, O., Norris, E.H., Pham, C.-T., Yazawa, I., Hilburger, K., Micsenyi, M., Giasson, B.I., Bonini, N.M., Lee, V.M.-Y., Trojanowski, J.Q., 2006. Convergence of Heat Shock Protein 90 with Ubiquitin in Filamentous α-Synuclein Inclusions of α-Synucleinopathies. The American Journal of Pathology 168, 947–961. https://doi.org/10.2353/ajpath.2006.050770

Uversky, V.N., Li, J., Fink, A.L., 2001a. Evidence for a Partially Folded Intermediate in α-Synuclein Fibril Formation. Journal of Biological Chemistry 276, 10737–10744. https://doi.org/10.1074/jbc.M010907200

Uversky, V.N., Li, J., Fink, A.L., 2001b. Metal-triggered Structural Transformations, Aggregation, and Fibrillation of Human α-Synuclein. Journal of Biological Chemistry 276, 44284–44296. https://doi.org/10.1074/jbc.M105343200

Uversky, V.N., Li, J., Souillac, P., Millett, I.S., Doniach, S., Jakes, R., Goedert, M., Fink, A.L., 2002. Biophysical Properties of the Synucleins and Their Propensities to Fibrillate: INHIBITION OF α-SYNUCLEIN ASSEMBLY BY β- AND γ-SYNUCLEINS. J. Biol. Chem. 277, 11970–11978. https://doi.org/10.1074/jbc.M109541200

Vaikath, N.N., Erskine, D., Morris, C.M., Majbour, N.K., Vekrellis, K., Li, J. -Y., El-Agnaf, O.M.A., 2019. Heterogeneity in α-synuclein subtypes and their expression in cortical brain tissue lysates from Lewy body diseases and Alzheimer's disease. Neuropathol Appl Neurobiol 45, 597–608. https://doi.org/10.1111/nan.12531

Vaikath, N.N., Majbour, N.K., Paleologou, K.E., Ardah, M.T., van Dam, E., van de Berg, W.D.J., Forrest, S.L., Parkkinen, L., Gai, W.-P., Hattori, N., Takanashi, M., Lee, S.-J., Mann, D.M.A., Imai, Y., Halliday, G.M., Li, J.-Yi., El-Agnaf, O.M.A., 2015. Generation and characterization of novel conformation-specific monoclonal antibodies for α-synuclein pathology. Neurobiology of Disease 79, 81–99. https://doi.org/10.1016/j.nbd.2015.04.009

Valente, E.M., Abou-Sleiman, P.M., Caputo, V., Muqit, M.M.K., Harvey, K., Gispert, S., Ali, Z., Turco, D.D., Bentivoglio, A.R., Healy, D.G., Albanese, A., Nussbaum, R., González-Maldonado, R., Deller, T., Salvi, S., Cortelli, P., Gilks, W.P., Latchman, D.S., Harvey, R.J., Dallapiccola, B., Auburger, G., Wood, N.W., 2004a. Hereditary Early-Onset Parkinson's Disease Caused by Mutations in PINK1. Science 304, 1158–1160. https://doi.org/10.1126/science.1096284

Valente, E.M., Salvi, S., Ialongo, T., Marongiu, R., Elia, A.E., Caputo, V., Romito, L., Albanese, A., Dallapiccola, B., Bentivoglio, A.R., 2004b. PINK1 mutations are associated with sporadic early-onset parkinsonism. Ann Neurol. 56, 336–341. https://doi.org/10.1002/ana.20256

Van der Perren, A., Gelders, G., Fenyi, A., Bousset, L., Brito, F., Peelaerts, W., Van den Haute, C., Gentleman, S., Melki, R., Baekelandt, V., 2020. The structural differences between patient-derived α-synuclein strains dictate characteristics of Parkinson's disease, multiple system atrophy and dementia with Lewy bodies. Acta Neuropathol 139, 977–1000. https://doi.org/10.1007/s00401-020-02157-3

Varkonyi, J., Rosenbaum, H., Baumann, N., MacKenzie, J.J., Simon, Z., Aharon-Peretz, J., Walker, J.M., Tayebi, N., Sidransky, E., 2003. Gaucher disease associated with parkinsonism: Four further case reports: Gaucher Disease and Parkinsonism. Am. J. Med. Genet. 116A, 348–351. https://doi.org/10.1002/ajmg.a.10028

Varland, S., Osberg, C., Arnesen, T., 2015. N-terminal modifications of cellular proteins: The enzymes involved, their substrate specificities and biological effects. Proteomics 15, 2385–2401. https://doi.org/10.1002/pmic.201400619

Vicente Miranda, H., Szegő, É.M., Oliveira, L.M.A., Breda, C., Darendelioglu, E., de Oliveira, R.M., Ferreira, D.G., Gomes, M.A., Rott, R., Oliveira, M., Munari, F., Enguita, F.J., Simões, T., Rodrigues, E.F., Heinrich, M., Martins, I.C., Zamolo, I., Riess, O., Cordeiro, C., Ponces-Freire, A., Lashuel, H.A., Santos, N.C., Lopes, L.V., Xiang, W., Jovin, T.M., Penque, D., Engelender, S., Zweckstetter, M., Klucken, J., Giorgini, F., Quintas, A., Outeiro, T.F., 2017. Glycation potentiates α-synuclein-associated neurodegeneration in synucleinopathies. Brain 140, 1399–1419. https://doi.org/10.1093/brain/awx056

Vilas, D., Gelpi, E., Aldecoa, I., Grau, O., Rodriguez-Diehl, R., Jaumà, S., Martí, M.J., Tolosa, E., 2019. Lack of central and peripheral nervous system synuclein pathology in R1441G *LRRK2* -associated Parkinson's disease. J Neurol Neurosurg Psychiatry 90, 832–833. https://doi.org/10.1136/jnnp-2018-318473

Vilas, D., Iranzo, A., Tolosa, E., Aldecoa, I., Berenguer, J., Vilaseca, I., Martí, C., Serradell, M., Lomeña, F., Alós, L., Gaig, C., Santamaria, J., Gelpi, E., 2016. Assessment of α-synuclein in

submandibular glands of patients with idiopathic rapid-eye-movement sleep behaviour disorder: a case-control study. The Lancet Neurology 15, 708–718. https://doi.org/10.1016/S1474-4422(16)00080-6
Visanji, N.P., Marras, C., Kern, D.S., Al Dakheel, A., Gao, A., Liu, L.W.C., Lang, A.E., Hazrati, L.-N., 2015. Colonic mucosal -synuclein lacks specificity as a biomarker for Parkinson disease. Neurology 84, 609–616. https://doi.org/10.1212/WNL.0000000000001240
Volpicelli-Daley, L.A., Luk, K.C., Lee, V.M.-Y., 2014. Addition of exogenous α-synuclein preformed fibrils to primary neuronal cultures to seed recruitment of endogenous α-synuclein to Lewy body and Lewy neurite–like aggregates. Nat Protoc 9, 2135–2146. https://doi.org/10.1038/nprot.2014.143
Volpicelli-Daley, L.A., Luk, K.C., Patel, T.P., Tanik, S.A., Riddle, D.M., Stieber, A., Meaney, D.F., Trojanowski, J.Q., Lee, V.M.-Y., 2011. Exogenous α-Synuclein Fibrils Induce Lewy Body Pathology Leading to Synaptic Dysfunction and Neuron Death. Neuron 72, 57–71. https://doi.org/10.1016/j.neuron.2011.08.033
Wakabayashi, K., Hayashi, S., Kakita, A., Yamada, M., Toyoshima, Y., Yoshimoto, M., Takahashi, H., 1998a. Accumulation of α-synuclein/NACP is a cytopathological feature common to Lewy body disease and multiple system atrophy. Acta Neuropathologica 96, 445–452. https://doi.org/10.1007/s004010050918
Wakabayashi, K., Hayashi, S., Yoshimoto, M., Kudo, H., Takahashi, H., 2000. NACP/α-synuclein-positive filamentous inclusions in astrocytes and oligodendrocytes of Parkinson's disease brains. Acta Neuropathol 99, 14–20. https://doi.org/10.1007/PL00007400
Wakabayashi, K., Mori, F., Nishie, M., Oyama, Y., Kurihara, A., Yoshimoto, M., Kuroda, N., 2005. An autopsy case of early ("minimal change") olivopontocerebellar atrophy (multiple system atrophy-cerebellar). Acta Neuropathol 110, 185–190. https://doi.org/10.1007/s00401-005-1029-1
Wakabayashi, K., Takahashi, H., 1996. Gallyas-positive, tau-negative glial inclusions in Parkinson's disease midbrain. Neuroscience Letters 217, 133–136. https://doi.org/10.1016/0304-3940(96)13080-9
Wakabayashi, K., Tanji, K., Mori, F., Takahashi, H., 2007. The Lewy body in Parkinson's disease: Molecules implicated in the formation and degradation of α-synuclein aggregates: Molecular components of Lewy body. Neuropathology 27, 494–506. https://doi.org/10.1111/j.1440-1789.2007.00803.x
Wakabayashi, K., Tanji, K., Odagiri, S., Miki, Y., Mori, F., Takahashi, H., 2013. The Lewy Body in Parkinson's Disease and Related Neurodegenerative Disorders. Mol Neurobiol 47, 495–508. https://doi.org/10.1007/s12035-012-8280-y
Wakabayashi, K., Yoshimoto, M., Tsuji, S., Takahashi, H., 1998b. α-Synuclein immunoreactivity in glial cytoplasmic inclusions in multiple system atrophy. Neuroscience Letters 249, 180–182. https://doi.org/10.1016/S0304-3940(98)00407-8
Walker, D.G., Lue, L.-F., Adler, C.H., Shill, H.A., Caviness, J.N., Sabbagh, M.N., Akiyama, H., Serrano, G.E., Sue, L.I., Beach, T.G., 2013. Changes in properties of serine 129 phosphorylated α-synuclein with progression of Lewy-type histopathology in human brains. Experimental Neurology 240, 190–204. https://doi.org/10.1016/j.expneurol.2012.11.020
Wan, L., Zhou, X., Wang, C., Chen, Z., Peng, H., Hou, Xuan, Peng, Y., Wang, P., Li, T., Yuan, H., Shi, Y., Hou, Xiaocan, Xu, K., Xie, Y., He, L., Xia, K., Tang, B., Jiang, H., 2019. Alterations of the Gut Microbiota in Multiple System Atrophy Patients. Front. Neurosci. 13, 1102. https://doi.org/10.3389/fnins.2019.01102
Wang, W., Nguyen, L.T.T., Burlak, C., Chegini, F., Guo, F., Chataway, T., Ju, S., Fisher, O.S., Miller, D.W., Datta, D., Wu, F., Wu, C.-X., Landeru, A., Wells, J.A., Cookson, M.R., Boxer, M.B., Thomas, C.J., Gai, W.P., Ringe, D., Petsko, G.A., Hoang, Q.Q., 2016. Caspase-1 causes truncation and aggregation of the Parkinson's disease-associated protein α-synuclein. Proc Natl Acad Sci USA 113, 9587–9592. https://doi.org/10.1073/pnas.1610099113
Wang, Z., Park, K., Comer, F., Hsieh-Wilson, L.C., Saudek, C.D., Hart, G.W., 2009. Site-Specific GlcNAcylation of Human Erythrocyte Proteins. Diabetes 58, 309–317. https://doi.org/10.2337/db08-0994
Wang, Z., Udeshi, N.D., O'Malley, M., Shabanowitz, J., Hunt, D.F., Hart, G.W., 2010. Enrichment and Site Mapping of O-Linked N-Acetylglucosamine by a Combination of Chemical/Enzymatic Tagging, Photochemical Cleavage, and Electron Transfer Dissociation Mass Spectrometry. Molecular & Cellular Proteomics 9, 153–160. https://doi.org/10.1074/mcp.M900268-MCP200
Watanabe, H., Saito, Y., Terao, S., Ando, T., Kachi, T., Mukai, E., Aiba, I., Abe, Y., Tamakoshi, A., Doyu, M., Hirayama, M., Sobue, G., 2002. Progression and prognosis in multiple system atrophy. Brain 125, 1070–1083. https://doi.org/10.1093/brain/awf117

Watanabe, I., Vachal, E., Tomita, T., 1977. Dense core vesicles around the Lewy body in incidental Parkinson's disease: an electron microscopic study. Acta Neuropathol 39, 173–175. https://doi.org/10.1007/BF00703325

Watts, J.C., Giles, K., Oehler, A., Middleton, L., Dexter, D.T., Gentleman, S.M., DeArmond, S.J., Prusiner, S.B., 2013. Transmission of multiple system atrophy prions to transgenic mice. Proceedings of the National Academy of Sciences 110, 19555–19560. https://doi.org/10.1073/pnas.1318268110

Waxman, E.A., Duda, J.E., Giasson, B.I., 2008. Characterization of antibodies that selectively detect α-synuclein in pathological inclusions. Acta Neuropathol 116, 37–46. https://doi.org/10.1007/s00401-008-0375-1

Waxman, E.A., Giasson, B.I., 2008. Specificity and Regulation of Casein Kinase-Mediated Phosphorylation of Alpha-Synuclein: Journal of Neuropathology and Experimental Neurology PAP. https://doi.org/10.1097/NEN.0b013e31816fc995

Weinreb, P.H., Zhen, W., Poon, A.W., Conway, K.A., Lansbury, P.T., 1996. NACP, A Protein Implicated in Alzheimer's Disease and Learning, Is Natively Unfolded †. Biochemistry 35, 13709–13715. https://doi.org/10.1021/bi961799n

Wenning, G.K., Colosimo, C., Geser, F., Poewe, W., 2004a. Multiple system atrophy. The Lancet Neurology 3, 93–103. https://doi.org/10.1016/S1474-4422(03)00662-8

Wenning, G.K., Geser, F., Krismer, F., Seppi, K., Duerr, S., Boesch, S., Köllensperger, M., Goebel, G., Pfeiffer, K.P., Barone, P., Pellecchia, M.T., Quinn, N.P., Koukouni, V., Fowler, C.J., Schrag, A., Mathias, C.J., Giladi, N., Gurevich, T., Dupont, E., Ostergaard, K., Nilsson, C.F., Widner, H., Oertel, W., Eggert, K.M., Albanese, A., del Sorbo, F., Tolosa, E., Cardozo, A., Deuschl, G., Hellriegel, H., Klockgether, T., Dodel, R., Sampaio, C., Coelho, M., Djaldetti, R., Melamed, E., Gasser, T., Kamm, C., Meco, G., Colosimo, C., Rascol, O., Meissner, W.G., Tison, F., Poewe, W., 2013. The natural history of multiple system atrophy: a prospective European cohort study. The Lancet Neurology 12, 264–274. https://doi.org/10.1016/S1474-4422(12)70327-7

Wenning, G.K., Shlomo, Y.B., Magalhães, M., Danie, S.E., Quinn, N.P., 1994. Clinical features and natural history of multiple system atrophy: An analysis of 100 cases. Brain 117, 835–845. https://doi.org/10.1093/brain/117.4.835

Wenning, G.K., Tison, F., Seppi, K., Sampaio, C., Diem, A., Yekhlef, F., Ghorayeb, I., Ory, F., Galitzky, M., Scaravilli, T., Bozi, M., Colosimo, C., Gilman, S., Shults, C.W., Quinn, N.P., Rascol, O., Poewe, W., and the Multiple System Atrophy Study Group, 2004b. Development and validation of the Unified Multiple System Atrophy Rating Scale (UMSARS). Mov Disord. 19, 1391–1402. https://doi.org/10.1002/mds.20255

Wersinger, C., Sidhu, A., 2003. Attenuation of dopamine transporter activity by α-synuclein. Neuroscience Letters 340, 189–192. https://doi.org/10.1016/S0304-3940(03)00097-1

Whetten-Goldstein, K., Sloan, F., Kulas, E., Cutson, T., Schenkman, M., 1997. The Burden of Parkinson's Disease on Society, Family, and the Individual. Journal of the American Geriatrics Society 45, 844–849. https://doi.org/10.1111/j.1532-5415.1997.tb01512.x

Wilhelmsson, U., Bushong, E.A., Price, D.L., Smarr, B.L., Phung, V., Terada, M., Ellisman, M.H., Pekny, M., 2006. Redefining the concept of reactive astrocytes as cells that remain within their unique domains upon reaction to injury. Proceedings of the National Academy of Sciences 103, 17513–17518. https://doi.org/10.1073/pnas.0602841103

Willis, A.W., Evanoff, B.A., Lian, M., Galarza, A., Wegrzyn, A., Schootman, M., Racette, B.A., 2010. Metal Emissions and Urban Incident Parkinson Disease: A Community Health Study of Medicare Beneficiaries by Using Geographic Information Systems. American Journal of Epidemiology 172, 1357–1363. https://doi.org/10.1093/aje/kwq303

Withers, G.S., George, J.M., Banker, G.A., Clayton, D.F., 1997. Delayed localization of synelfin (synuclein, NACP) to presynaptic terminals in cultured rat hippocampal neurons. Developmental Brain Research 99, 87–94. https://doi.org/10.1016/S0165-3806(96)00210-6

Witze, E.S., Old, W.M., Resing, K.A., Ahn, N.G., 2007. Mapping protein post-translational modifications with mass spectrometry. Nat Methods 4, 798–806. https://doi.org/10.1038/nmeth1100

Wong, M.B., Goodwin, J., Norazit, A., Meedeniya, A.C.B., Richter-Landsberg, C., Gai, W.P., Pountney, D.L., 2013. SUMO-1 is Associated with a Subset of Lysosomes in Glial Protein Aggregate Diseases. Neurotox Res 23, 1–21. https://doi.org/10.1007/s12640-012-9358-z

Wood, S.J., Wypych, J., Steavenson, S., Louis, J.-C., Citron, M., Biere, A.L., 1999. α-Synuclein Fibrillogenesis Is Nucleation-dependent. Journal of Biological Chemistry 274, 19509–19512. https://doi.org/10.1074/jbc.274.28.19509

Woodard, J.S., 1962. Concentric hyaline inclusion body formation in mental disease analysis of twenty-seven cases. Journal of Neuropathology and Experimental Neurology 21, 442–449. https://doi.org/10.1097/00005072-196207000-00012

Wszolek, Z.K., Pfeiffer, R.F., Tsuboi, Y., Uitti, R.J., McComb, R.D., Stoessl, A.J., Strongosky, A.J., Zimprich, A., Müller-Myhsok, B., Farrer, M.J., Gasser, T., Calne, D.B., Dickson, D.W., 2004. Autosomal dominant parkinsonism associated with variable synuclein and tau pathology. Neurology 62, 1619–1622. https://doi.org/10.1212/01.WNL.0000125015.06989.DB

Wullner, U., Schmitt, I., Kammal, M., Kretzschmar, H.A., Neumann, M., 2008. Definite multiple system atrophy in a German family. Journal of Neurology, Neurosurgery & Psychiatry 80, 449–450. https://doi.org/10.1136/jnnp.2008.158949

Xia, Q., Liao, L., Cheng, D., Duong, D.M., Gearing, M., Lah, J.J., Levey, A.I., Peng, J., 2008. Proteomic identification of novel proteins associated with Lewy bodies. Front. Biosci. 13, 3850–3856. https://doi.org/10.2741/2973

Xuan, Q., Zhang, Y.-X., Liu, D.-G., Chan, P., Xu, S.-L., Cui, Y.-Q., 2016. Post-translational modifications of α-synuclein contribute to neurodegeneration in the colon of elderly individuals. Molecular Medicine Reports 13, 5077–5083. https://doi.org/10.3892/mmr.2016.5166

Yamada, M., Iwatsubo, T., Mizuno, Y., Mochizuki, H., 2004. Overexpression of alpha-synuclein in rat substantia nigra results in loss of dopaminergic neurons, phosphorylation of alpha-synuclein and activation of caspase-9: resemblance to pathogenetic changes in Parkinson's disease. J Neurochem 91, 451–461. https://doi.org/10.1111/j.1471-4159.2004.02728.x

Yamanaka, K., Chun, S.J., Boillee, S., Fujimori-Tonou, N., Yamashita, H., Gutmann, D.H., Takahashi, R., Misawa, H., Cleveland, D.W., 2008. Astrocytes as determinants of disease progression in inherited amyotrophic lateral sclerosis. Nat Neurosci 11, 251–253. https://doi.org/10.1038/nn2047

Yan, F., Chen, Y., Li, M., Wang, Y., Zhang, W., Chen, X., Ye, Q., 2018. Gastrointestinal nervous system α-synuclein as a potential biomarker of Parkinson disease: Medicine 97, e11337. https://doi.org/10.1097/MD.0000000000011337

Yang, X., Qian, K., 2017. Protein O-GlcNAcylation: emerging mechanisms and functions. Nat Rev Mol Cell Biol 18, 452–465. https://doi.org/10.1038/nrm.2017.22

Yavich, L., Tanila, H., Vepsalainen, S., Jakala, P., 2004. Role of -Synuclein in Presynaptic Dopamine Recruitment. Journal of Neuroscience 24, 11165–11170. https://doi.org/10.1523/JNEUROSCI.2559-04.2004

Yoshimoto, M., Iwai, A., Kang, D., Otero, D.A., Xia, Y., Saitoh, T., 1995. NACP, the precursor protein of the non-amyloid beta/A4 protein (A beta) component of Alzheimer disease amyloid, binds A beta and stimulates A beta aggregation. PNAS 92, 9141–9145. https://doi.org/10.1073/pnas.92.20.9141

Yoshinaga, S., Yamanaka, T., Miyazaki, H., Okuzumi, A., Hiyama, A., Murayama, S., Nukina, N., 2020. Preserved proteinase K-resistant core after amplification of alpha-synuclein aggregates: Implication to disease-related structural study. Biochemical and Biophysical Research Communications 522, 655–661. https://doi.org/10.1016/j.bbrc.2019.11.142

Yu, S., Li, X., Liu, G., Han, J., Zhang, C., Li, Y., Xu, S., Liu, C., Gao, Y., Yang, H., Uéda, K., Chan, P., 2007. Extensive nuclear localization of α-synuclein in normal rat brain neurons revealed by a novel monoclonal antibody. Neuroscience 145, 539–555. https://doi.org/10.1016/j.neuroscience.2006.12.028

Zarranz, J.J., Alegre, J., Gómez-Esteban, J.C., Lezcano, E., Ros, R., Ampuero, I., Vidal, L., Hoenicka, J., Rodriguez, O., Atarés, B., Llorens, V., Tortosa, E.G., del Ser, T., Muñoz, D.G., de Yebenes, J.G., 2004. The new mutation, E46K, of α-synuclein causes parkinson and Lewy body dementia: New α-Synuclein Gene Mutation. Ann Neurol. 55, 164–173. https://doi.org/10.1002/ana.10795

Zhang, L., Zhang, C., Zhu, Y., Cai, Q., Chan, P., Uéda, K., Yu, S., Yang, H., 2008. Semi-quantitative analysis of α-synuclein in subcellular pools of rat brain neurons: An immunogold electron microscopic study using a C-terminal specific monoclonal antibody. Brain Research 1244, 40–52. https://doi.org/10.1016/j.brainres.2008.08.067

Zhang, Wei, Wang, T., Pei, Z., Miller, D.S., Wu, X., Block, M.L., Wilson, B., Zhang, Wanqin, Zhou, Y., Hong, J.-S., Zhang, J., 2005. Aggregated α-synuclein activates microglia: a process leading to disease progression in Parkinson's disease. The FASEB Journal 19, 533–542. https://doi.org/10.1096/fj.04-2751com

Zhang, Zhentao, Kang, S.S., Liu, X., Ahn, E.H., Zhang, Zhaohui, He, L., Iuvone, P.M., Duong, D.M., Seyfried, N.T., Benskey, M.J., Manfredsson, F.P., Jin, L., Sun, Y.E., Wang, J.-Z., Ye, K., 2017. Asparagine endopeptidase cleaves α-synuclein and mediates pathologic activities in Parkinson's disease. Nat Struct Mol Biol 24, 632–642. https://doi.org/10.1038/nsmb.3433

Zhu, X., Babar, A., Siedlak, S.L., Yang, Q., Ito, G., Iwatsubo, T., Smith, M.A., Perry, G., Chen, S.G., 2006a. LRRK2 in Parkinson's disease and dementia with Lewy bodies. Mol Neurodegeneration 1, 17. https://doi.org/10.1186/1750-1326-1-17

Zhu, X., Siedlak, S.L., Smith, M.A., Perry, G., Chen, S.G., 2006b. LRRK2 protein is a component of Lewy bodies. Ann Neurol. 60, 617–618. https://doi.org/10.1002/ana.20928

Zigoneanu, I.G., Yang, Y.J., Krois, A.S., Haque, Md.E., Pielak, G.J., 2012. Interaction of α-synuclein with vesicles that mimic mitochondrial membranes. Biochimica et Biophysica Acta (BBA) - Biomembranes 1818, 512–519. https://doi.org/10.1016/j.bbamem.2011.11.024

Zimprich, A., Biskup, S., Leitner, P., Lichtner, P., Farrer, M., Lincoln, S., Kachergus, J., Hulihan, M., Uitti, R.J., Calne, D.B., Stoessl, A.J., Pfeiffer, R.F., Patenge, N., Carbajal, I.C., Vieregge, P., Asmus, F., Müller-Myhsok, B., Dickson, D.W., Meitinger, T., Strom, T.M., Wszolek, Z.K., Gasser, T., 2004. Mutations in LRRK2 Cause Autosomal-Dominant Parkinsonism with Pleomorphic Pathology. Neuron 44, 601–607. https://doi.org/10.1016/j.neuron.2004.11.005

Zis, P., Martinez-Martin, P., Sauerbier, A., Rizos, A., Sharma, J.C., Worth, P.F., Sophia, R., Silverdale, M., Chaudhuri, K.R., 2015. Non-motor symptoms burden in treated and untreated early Parkinson's disease patients: argument for non-motor subtypes. Eur J Neurol 22, 1145–1150. https://doi.org/10.1111/ene.12733

Curriculum vitae

MELEK FIRAT ALTAY

E-mail: altay.mf@gmail.com
Phone: 0041 76 690 3469
LinkedIn: linkedin.com/in/melek-firat-altay
Skype: firat.altay
ORCID ID: 0000-0002-8174-5631

EDUCATION

PhD Neuroscience **2016 - 2022**
LMNN-BMI-SV, Ecole Polytechnique Fédérale de Lausanne (EPFL, Switzerland)
Nominated for the Brain Mind Institute (BMI) thesis award.

MSc Neuroscience (1st) **2015 - 2016**
King's College London, University of London (UK)
Specialisation on neural stem cells and nervous system repair.

BSc Hons Natural Sciences (1st): Biology **2011 - 2015**
The Open University (UK)

BMus Hons Classical Performance (1st): Piano and Composition **2007 - 2010**
Trinity College of Music (UK)
Awarded with the Keyboard Department medal.

PROFESSIONAL AND RESEARCH EXPERIENCE

Doctoral research assistant **2016-2022**
Hilal Lashuel Lab (LMNN-BMI-SV), Ecole Polytechnique Fédérale de Lausanne (EPFL, Switzerland)
Capturing the heterogeneity of alpha-synuclein pathology in synucleinopathies.

Visiting researcher **2019-2020**
Laura Parkkinen Lab, Nuffield Department of Clinical Neurosciences, University of Oxford (UK)
Re-visiting the staging of PD and other Lewy body diseases.

Visiting researcher **2018-2020**
Janice Holton Lab, UCL Queen Square Institute of Neurology, University College London (UK)
Unmasking the pathological heterogeneity of alpha-synuclein in human post-mortem brain tissues.

Teaching assistant **2017-2018**
Faculté des sciences de la vie, Ecole Polytechnique Fédérale de Lausanne (EPFL, Switzerland)
Selected Topics in Biotechnology (Fall 2017), master level
Laboratoire Intégré en Sciences de la Vie (Fall 2017), bachelor level
Biologie I (Fall 2017) and Biologie II (Spring 2017), bachelor level

Research intern for MSc dissertation **2016**
Jack Price Lab, Maurice Wohl Clinical Neuroscience Institute, King's College London (UK)
Modelling effects of maternal immune activation on neuronal development using iPSCs.

Research intern **2015**
Hulusi Kafaligonul Lab, UMRAM, Bilkent University (Turkey)
Neural mechanisms underlying multisensory perception of speed.

Freelance interpreter and translator (Turkish <-> English) (UK) **2010 - 2016**

Piano and music theory tutor, London School of Arts (UK) **2008 – 2016**

KEY SKILLS

Technical skills: mammalian, stem and primary cell culture, immunocytochemistry, immunohistochemistry, immunofluorescence, RNA extraction and quantitative PCR, cell lysis and protein extraction, SDS-PAGE, dot/slot blotting, Western blotting, recombinant DNA manipulation and cloning, purification and analysis of plasmid DNA, high throughput screening (INCellAnalyser/ CellInsight), image analysis with Fiji and QuPath, confocal microscopy, transmission electron microscopy, protein expression and purification

Administrative skills: data entry and analysis, document and lab notebook management, reporting, ethical permit application, grant application, scientific writing

Soft skills: problem solving, attention to detail, reliability, adaptability, team work, planning, communication, proactivity, project management

ADDITIONAL SKILLS, ROLES AND DUTIES

Languages: English (C2+), Turkish (C2+), French (B2), German (B1), Spanish (A2). **Language qualifications:** French DALF C1 (2013), German Zertifikat deutsch/ Goethe-Zertifikat B1 (2012).

Institutional responsibilities: Scientific staff representative for the Life Sciences/ SV School Council (EPFL, Switzerland, 2018-2022), internal affairs co-ordinator and committee member of the Association of Doctoral Students in the Life Sciences/ ADSV (EPFL, Switzerland, 2018-2021).

Leadership roles: Participant in the FLP-funded peer-to-peer mentoring group project 'Stepping up the ladder: Mutual help in career development and work-life balance' (Switzerland, 2020-2021). Co-organiser of the *FutureUp* Neuroscience Symposium for PhD students (EPFL, Switzerland, 2018).

Professional training: EPFL Research Office course 'How to prepare successful grant proposals' (Lausanne, Switzerland, 2021-2022). EPFL-FLP course 'Leadership & how to succeed in a scientific community' (Lausanne, Switzerland, 2020). REGARD workshop 'Project management for successful researchers' (Fribourg, Switzerland, 2019). EPFL Teaching Support Centre workshop 'Teaching assistants in the lab' (Lausanne, Switzerland, 2019). EPFL-DSPS course 'Working in a P2&P3 environment (Lausanne, Switzerland, 2018). FELASA Category B course 'RESAL module 1: Introductory course in laboratory animals' (Lausanne, Switzerland, 2018). University of Warwick course 'Laboratory Skills' (Warwick, UK, 2015),

Other accredited courses: Introduction to Philosophy and Metaphysics (University of Oxford, UK, 2013), Philosophy of Mind (University of Oxford, UK, 2012), Economics and Economic Change (The Open University, UK, 2011).

Scholarships: ICV postgraduate study scholarship (2015), Goethe Institut Language Scholarship (2013), Trinity College London Scholarship (2008-2010). **Prizes:** Finalist - The Cavatina Chamber Music Competition (2009), First Prize - Gladys Puttick Extemporisation Competition (2009), First Prize - John Halford Piano Competition (2008).

PUBLICATIONS

Altay, M.F., Liu, A.K.L, Holton, J.L., Parkkinen, L., Lashuel, H.A. Prominent astrocytic alpha-synuclein pathology with unique post-translational modification signatures unveiled across Lewy body diseases. *Manuscript in preparation*.

Altay, M.F., Kumar, S.T., Burtscher, J., Jagannath, S., Strand, C., Miki, Y., Parkkinen, L., Holton, J.L., Lashuel, H.A. Development and validation of an expanded antibody toolset that captures alpha-synuclein pathological diversity in Lewy body diseases. *Manuscript in preparation.*

Sonustun, B., **Altay, M.F.,** Strand, C., Ebanks, K., Hondhamuni, G., Warner, T.T., Lashuel, H.A., Bandopadhyay, R., 2022. Pathological relevance of post-translationally modified alpha-synuclein (pSer87, pSer129, nTyr39) in idiopathic Parkinson's disease and multiple system atrophy. Cells 11, 906. https://doi.org/10.3390/cells11050906

Lashuel, H.A., Mahul-Mellier, A.-L., Novello, S., Hegde, R.N., Jasiqi, Y., **Altay, M.F.,** Donzelli, S., DeGuire, S.M., Burai, R., Magalhães, P., Chiki, A., Ricci, J., Boussouf, M., Sadek, A., Stoops, E., Iseli, C., Guex, N., 2022. Neighbouring modifications interfere with the detection of phosphorylated alpha-synuclein at Serine 129: Revisiting the specificity of pS129 antibodies. bioRxiv. https://doi.org/10.1101/2022.03.30.486322

Miki, Y., Tanji, K., Tanaka, M., **Altay, M.F.,** Foti, S.C., Strand, C.M, Kon, T., Shimoyama, S., Furukawa, T., Nishijima, H., Asi Y.T., Betterncourt, C., Jaunmuktane, Z., Tada, M., Mori, F., Tomiyama, M., Lashuel, H.A, Lashley, T., Kakita, A., Ling, H., Lees, A.J., Quinn, N.P., Holton, J.L., Warner, T.T., Wakabayashi, K. The pathological substrate of memory impairment in multiple system atrophy. Neuropathology and Applied Neurobiology (submitted).

Mahul-Mellier, A.L., **Altay, M.F.**, Burtscher, J., Maharjan, N., Ait-Bouziad, N., Chiki, A., Vingill, S., Wade-Martins, R., Holton, J., Strand, C., Haikal, C., Lashuel, H.A., 2018. The making of a Lewy body: the role of alpha-synuclein post-fibrillization modifications in regulating the formation and the maturation of pathological inclusions. *bioRxiv*, p.500058.

PRESENTATIONS

Altay, M.F., Strand, C., Miki, Y., Kumar, S.T., Mahul-Mellier, A.L., Jagannath, S., Donzelli, S., Holton, J.L., Lashuel, H.A. Generation, screening and validation of an antibody-based toolbox that enables capturing the diversity of alpha-synuclein proteoforms and pathology. Poster presentation at the Synuclein Meeting: Where we are and where we need to go (Porto, Portugal, September 2019).

Altay, M.F. Deciphering the seeding mechanisms of alpha-synuclein fibrils, and Lewy body formation and maturation in mouse primary neurons. Oral presentation at the European Meeting of Neuroscience, GIN (Grenoble, France, May 2018).

Altay, M.F., Mahul-Mellier, A.L, Chiki, A., Aumedes, J.R., Lashuel, H.A. Deciphering the seeding mechanism of alpha-synuclein fibrils in HeLa cells. Poster and oral presentation at the Gut Matters EPFL-ETHZ Winter School: Human Health, Microbiome & Nutrition (Fiesch, Switzerland, March 2017).